School of Engineering and Science

Developing magnetic functionalized multi-walled carbon nanotubes-based buckypaper for the removal of Furazolidone

Fahad Saleem Ahmed Khan

0000-0002-3483-3241

This thesis is presented for the Degree of
Doctor of Philosophy
of
Curtin University

March 2023

DECLARATION

To the best of my knowledge and belief, this thesis contains no material previously published by anyone except where due acknowledgment has been made.

This thesis contains no material accepted for the award of any other degree or diploma in any university.

Name FAHAD SALEEM AHMED KHAN

Signature Fahad

Date 6th March 2023

ACKNOWLEDGEMENT

First and foremost, I would like to thank Almighty Allah, who has bestowed upon me countless blessings for which I can never be grateful enough. Through His providence, I have come so far, and without which, I would not have been able to reach this stage of my life.

I would like to express my deepest appreciation to all my supervisors, Dr. Tan Yie Hua, Assoc. Prof. Dr. Mubarak Mujawar, and Prof. Mohammad Khalid, for their constructive and valuable suggestions and guidance throughout the planning and development of this research. Their willingness to help at all times is exemplary and is very much appreciated. Their mentorship will be cherished for the rest of my life.

I would also like to express my sincere thanks to Prof. Dr. Agus Saptoro, Deputy Dean of Research and Development and Director of Graduate Studies Committee, for always being a source of light during the challenging stages of the studies.

My special thanks also go to all my colleagues and friends for their moral support, insightful suggestions, and motivation. Additionally, I am particularly grateful to all the laboratory technicians for their thoughtfulness and kind assistance in my experimental research work.

Lastly, I would like to take this opportunity to express my heartfelt gratitude to my parents, and my wife, Maria Fahad, who have been unwavering in their support and encouragement. It would have been impossible without their unconditional love and support.

LIST OF PUBLICATIONS

JOURNAL PAPERS

i. **Fahad Saleem Ahmed Khan**, N.M. Mubarak, Mohammad Khalid, Yie Hua Tan, Ezzat Chan Abdullah, Ekhlasur Rahman, Rama Rao Kari (2021). A comprehensive review on micropollutant removal using carbon nanotubes-based adsorbents and membrane. *Environmental Chemical Engineering*. 106647. Q1; IF 5.9 (ISI-Cited Publication).

ii. **Fahad Saleem Ahmed Khan**, N.M. Mubarak, Mohammad Khalid, Yie Hua Tan, Ezzat Chan Abdullah, Ekhlasur Rahman, Rama Rao Kari (2021). Comprehensive review on carbon nanotubes embedded in different metal and polymer matrix: fabrications and applications. *Critical Reviews in Solid State and Materials Sciences*. 1-28, Q1; IF 10.36

iii. **Fahad Saleem Ahmed Khan**, N.M. Mubarak, Yie Hua Tan, Mohammad Khalid, Rama Rao Karri, Rashmi Walvekar, E.C. Abdullah, Sabzoi Nizamuddin, Shaukat Ali Mazari (2021). A comprehensive review on magnetic carbon nanotubes and carbon nanotube-based buckypaper- heavy metal and dyes removal. *Journal of Hazardous Materials* (413) 125375. Q1; IF 9.3 (ISI-Cited Publication).

iv. **Fahad Saleem Ahmed Khan**, Nabisab Mujawar Mubarak, Yie Hua Tan, Rama Rao Karri, Mohammad Khalid, Rashmi Walvekar, Ezzat Chan Abdullah, Shaukat Ali Mazari, Sabzoi Nizamuddin (2020). Magnetic nanoparticles incorporation into different substrates for dyes and heavy metals removal-A Review. *Environmental Science and Pollution Research*, 27, 43526-43541 Q2; IF 3.2 (ISI-Cited Publication)

v. **Fahad Saleem Ahmed Khan**, Nabisab Mujawar Mubarak, Mohammad

Khalid, Rashmi Walvekar, Ezzat Chan Abdullah, Shaukat A. Mazari, Sabzoi Nizamuddin, Rama Rao Karri (2020). Magnetic nano adsorbents potential route for heavy metals removal—a review. *Environmental Science and Pollution Research*, 27, 24342-24356 Q2: IF 3.2 (ISI-Cited Publication)

AWARDS

i. **Silver Medal** – The international Conference and Exposition on Inventions by Institutions of Higher Learning Pecipta 2022 (2-3 November), for poster title "Developing magnetic functionalized carbon nanotube-based buckypaper for micropollutant removal"

ii. **Gold Medal** – The UNIMAS innovation and technology exposition (InTEX22) (15-16 June), for innovation title "Developing magnetic functionalized carbon nanotube-based buckypaper for micropollutant removal"

iii. **Best Project** – Bionanotechnology Research Seminar and Conference (BioNanoSem 2022) (4 August), for poster title "Developing magnetic functionalized carbon nanotube-based buckypaper for micropollutant removal"

ABSTRACT

Furazolidone (FZD) is a widely used anti-microbial agent in aquaculture and animal husbandry, but its use poses severe adverse effects, including mutagenicity, genotoxicity and carcinogenicity, making it harmful to various life forms on the planet. As existing water and wastewater treatment methods struggle to cope with this pollutant, providing safe and clean water becomes challenging. Therefore, the removal of FZD micropollutant is crucial to reduce environmental toxicity. Various methods like biodegradation, adsorption, photolysis, oxidation and ozonation have been explored for FZD treatment, but their efficiency, cost, production of toxic by-products and operation stability limit their consideration. To address these challenges, this study introduces a novel approach by incorporating magnetic nanoparticles (magnetite) into functionalized multi-walled carbon nanotubes (f-MWCNTs) to form a magnetic nanocomposite. This nanocomposite is then utilized to fabricate buckypaper (BP) with the aid of vacuum filtration technique. Characterization of the magnetic BP membrane was performed using Fourier transform infrared spectroscopy (FT-IR), Energy dispersive X-ray (EDX), vibrating sample magnetometer (VSM), field emission scanning electron microscope (FE-SEM), and thermogravimetric analysis (TGA). The adsorption efficiency of the developed magnetic BP membrane was evaluated in batch-mode using response surface methodology (RSM) and adaptive neuro-fuzzy inference system (ANFIS) model to examine the uptake of FZD micropollutant from aqueous solution (pH 4-6, agitation speed 100-200 rpm, and contact time 20-350 min). The results showed that the maximum removal efficiency of FZD micropollutant was achieved at 10 mg/L, pH 6, agitation speed 200 rpm and a contact time of 350 min., with a remarkable removal efficiency of 98.74% The adsorption mechanism was described by the Langmuir isotherm model with a maximum FZD uptake of 29.67 mg/g, and the kinetic data followed a pseudo-second order kinetic models. Thermodynamic parameters indicated the

spontaneous and exothermic nature of FZD micropollutant adsorption over the magnetic f-MWCNTs-based BP/ polyvinyl alcohol. Moreover, the reusability study demonstrated that the magnetic f-MWCNTs-based BP/PVA membrane can retain up to 88% of its FZD micropollutant removal efficiency even after five successive cycles using ethanol as a desorption solvent. Comparing the RSM and ANFIS models, the ANFIS model proved to be more accurate in predicting the removal of FZD micropollutant with a correlation coefficient of 0.985. The statistical indices confirmed ANFIS as the best predictive model for FZD micropollutant removal. In conclusion, the research study demonstrated that the fabricated magnetic f-MWCNTs-based BP/PVA membrane efficiently removes FZD micropollutant without any additional separation stage, making it suitable for practical applications.

Keywords:

Micropollutant, magnetic buckypaper, carbon nanotubes, furazolidone removal, aquatic environment, wastewater, water treatment

TABLE OF CONTENTS

LIST OF TABLES

LIST OF FIGURES

LIST OF ABBREVIATIONS

SWCNT	Single-walled carbon nanotube
MWCNTs	Multi-walled carbon nanotubes
CNTs	Carbon nanotubes
PVA	Poly vinyl alcohol
BP	Buckypaper
f-MWCNTs	Functionalized multi-walled carbon nanotubes
ANOVA	Analysis of variance
DOE	Design of experiment
FCCCD	Face-centred central composite design
ANFIS	Adaptive neuro-fuzzy interference system
TSK	Takagi Sugeno Kang
FZD	Furazolidone
CVD	Chemical vapour deposition
FE-SEM	Field emission scanning electron microscope
FT-IR	Fourier transform infrared
TGA	Thermogravimetric analysis
EDX	Energy dispersive X-ray spectroscopy
PTFE	Polytetrafluoroethylene
RSM	Response surface methodology
UV-Vis	Ultraviolet-visible

NOMENCLATURE

A_T	Temkin isotherm equilibrium binding constant
C_i	Initial concentration of FZD MP solution
C_o	Final concentration of FZD MP solution
C_e	Concentration of dye at equilibrium
D	Desorption efficiency
k_F	Freundlich constant
k_a	Langmuir constant
k_T	Temkin constant
M	Mass of membrane
q_d	Amount of micropollutant desorbed
q_e	Equilibrium adsorption capacity
q_{max}	Maximum adsorption capacity
R	Universal gas constant
R^2	Coefficient of determination
R^2_{adj}	Adjusted coefficient of determination
V	Volume of micropollutant solution
Y	Predicted response
λ_{max}	Maximum absorption wavelength
ΔG^o	Gibbs free energy
ΔH^o	Activation enthalpy

ΔS^o	Activation entropy
K_D	Thermodynamic equilibrium constant
B	Dubinin-Radushkevich isotherm constant
β_i	Linear coefficient
β_{ii}	Quadratic coefficient

LIST OF APPENDICES

CHAPTER I

INTRODUCTION

A significant global consumption of chemical products has led to an inclining chemical contamination of ground and surface waters, with still unknown influence on the human and aquatic health (Richardson et al. 2019, Tetreault et al. 2012). The pollution of natural water through a numerous amount of chemical components, despite most of them being present in extreme minor concentrations (ng- µg), causes substantial ecological concerns and is a foremost concern globally (Schwarzenbach et al. 2006, Buxton et al. 2005, Diamanti-Kandarakis et al. 2009). These components are labelled as 'trace pollutants' or 'micropollutant'. In general, micropollutants are ascribed as chemical components exist at low concentrations, i.e., ng/L in the environment, and which, regardless of their low intensity, can have severe impacts on living species (Clara et al. 2004). This comprises various hydrophobic and hydrophilic contaminants such as flame retardants, heavy metals, polychlorinated biphenyl, pharmaceuticals, and pesticides. Most of these micropollutants, for instance, pharmaceuticals, detergents or biocides products, are mainly discarded into municipal sewer systems, and only limited elimination in the traditional wastewater treatment plants, which can reach the aquatic environment (Benner et al. 2013). Thus, wastewater treatment plants discharges are considered as the most important vector of these micropollutants into the ecosystems. The pathways through which micropollutants infiltrate the environment have been delineated and elucidated in ***Fig. 1.1***, providing a comprehensive visual representation of the intricate routes by which these pollutants enter the ecological systems.

***Fig. 1.1**:* Pathways of micropollutant into environment (Metz et al. 2014)

1.1 Influence of micropollutant

1.1.1 Drinking water

Contamination of surface waters through micropollutants discharged from wastewater treatment plants has raised concerns about drinking water pollution, since surface waters are one of the primary sources of drinking water universally (Benner et al. 2013). Different micropollutants in wastewater sources have been found in drinking waters in numerous countries. To assess the possible human health risk, life-long human exposure to micropollutants through drinking water was measured in a few studies. The dose of micropollutants ingested during 70 years of life through drinking 2 liters of water per day ranges between < 5 µg to 4 mg, corresponding, for most of 58 pharmaceuticals examined, to <10% of single defined daily dose prescribed to a patient in a day (Houtman et al. 2014).

Due to the low intensity of micropollutants in drinking waters, all analyzed studies had determined that noticeable adverse effects on human health were doubtful at the present level of contact, even if the possible influence of low level chronic exposure to chemical blends is still predominantly unidentified (Sanderson 2011, Kosek et al. 2020). Nonetheless, even if human health effects are unlikely, drinking water reserves are valuable and have to be safeguard and well-preserved to provide high quality water in the future.

1.1.2 Aquatic life

If the worldwide issue of persistent, toxic and bio-accumulative components is already partially controlled through international legislations, the influence on wildlife associated with less persistent but continuously discharged elements, such as pharmaceuticals, personal care products, endocrine disrupters and biocides, has been lately reported worldwide. For example, intercourse and reproduction disorder in marine species were reported in many rivers downstream of wastewater treatment plant channels, almost certainly linked to the release of estrogenic endocrine disrupters (nonyl-phenol, ethinyl-estradiol) (Tetreault et al. 2012, Gagné et al. 2011). Although it is extremely difficult to associate these adverse effects with specific micropollutants, there is evidence that these effects were primarily due to the toxicity of micropollutants and not due to other macropollutants detected in wastewaters (Gillis et al. 2014). Certainly, it was also reported that a few of these harmful effects clearly declined after the degradation of most micropollutant through ozonation (which did not impact the macropollutants' concentration) (Bundschuh et al. 2011, Peschke et al. 2014). Besides, numerous studies had revealed that micropollutant can possess noxious effects already at the intensities detected in wastewater treatment plant effluents. ***Fig. 1.2*** illustrates the descriptive impact of micropollutants on the environmental and biological system.

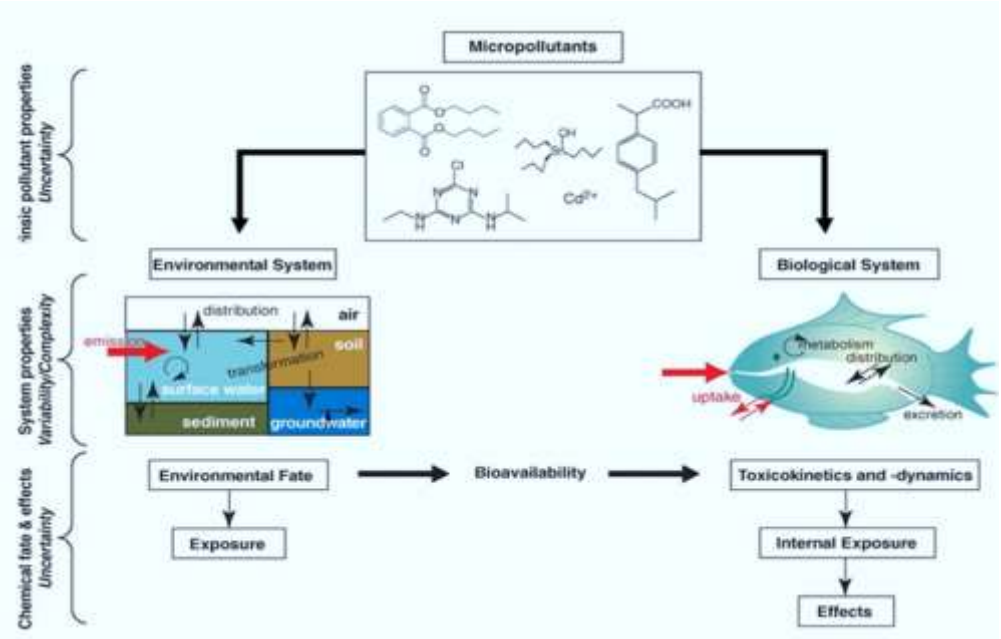

Fig. 1.2: Impact of micropollutant (Schwarzenbach et al. 2006)

For example, the anti-inflammatory drug diclofenac was reported to introduce cytological disruption in fish kidney, gills and liver at 0.5 to 1 µg/l, concentration detected in wastewater treatment plant effluents (Triebskorn et al. 2004). Indeed, diclofenac is known for its potential noxiousness to wildlife and was related to the decline of the vulture population in Pakistan, affected to renal malfunction associated with the intake of diclofenac-treated livestock (Oaks et al. 2004).

1.2 Global statistic usage of micropollutant

European Union has marked more than 100,000 chemicals as micropollutants, and around 30,000-70,000 chemicals, are intaken daily for various purposes (Rogowska et al. 2020). In contrast to other Asian countries, only limited data for the Malaysian aquatic environment is available (Prabhakaran et al. 2017). Significantly limited published papers reported that the concentration of micropollutants in Malaysian water sources. A research article was published by Universiti Putra Malaysia (UPM) in 2003, detecting the average concentration (ng/L) of micropollutants' existence in the Malaysian river and sewage and wastewater treatment plant using an analytical approach

(Vedamanikam et al. 2008, Yang et al. 2022). It was observed that a high concentration of pharmaceuticals and steroid hormones micropollutants were present in different water sources; for instance, diclofenac concentration in the article was reported as 105 ng/L (Dehkordi et al. 2021). It reflects that the traditional water and wastewater treatment processes are ineffective to remove several polar and semi-polar micropollutants (Sayadi et al. 2010). One of the steroids that have been extensively used in the Asian continent is nitrofurans. This steroid is an anti-microbial agent, including nitrofurazone, furaltadone, furazolidone, and nitrofurantoin. Nitrofurans are employed to kill a range of gram-positive /harmful bacteria and fungi (Bock et al. 2007). In Malaysia, they are extensively applied in aquaculture and animal husbandry. Nevertheless, there are signs that nitrofurans have significant toxicity and adverse effects on life, such as carcinogenicity and mutagenicity (Ferreira et al. 2020, Heravi et al. 2020). Several countries have restricted their use in recent years. However, due to high efficiency and economic price, they are still employed in farms and aquafarms in many countries, such as Malaysia, Thailand, and China (Cooper et al. 2008). Consequently, untreated sewage consisting of nitrofurans is often released unintentionally into the waters, which may be brought about potential severe effects on human life and aquatic species (Vinas et al. 2007). Thus, an appropriate and efficient approach or material is required to treat nitrofurans and other micropollutant contents in different water sources. The total water pollution detected in various aquatic environment worldwide reported by WHO is presented in ***Fig. 1.3***.

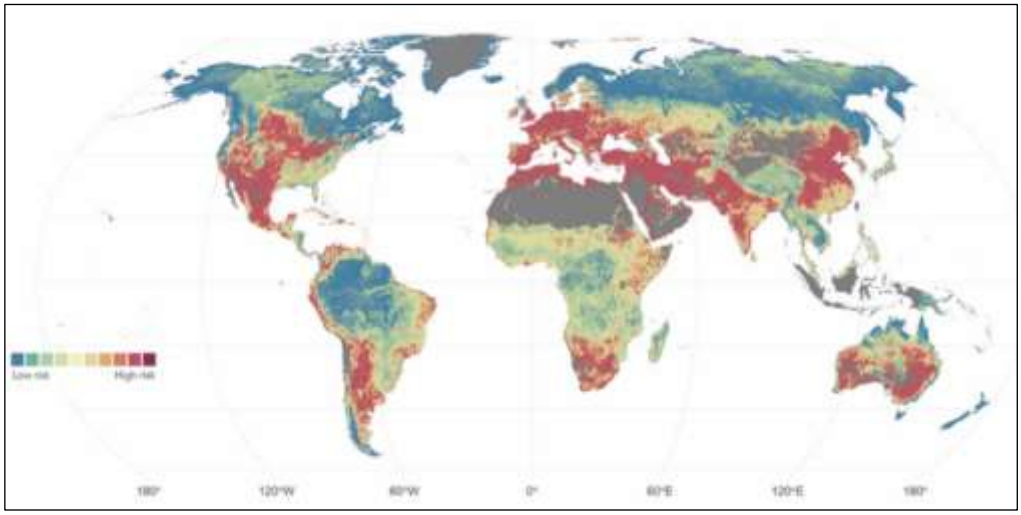

Fig. 1.3: Total water pollution worldwide (Omer et al. 2022)

1.3 Carbon nanotube-based nanocomposites and membranes for the removal of micropollutant

The high content of emerging micropollutants, especially pharmaceuticals and steroid hormones, has been observed in wastewater effluents. Even if many volatile, biodegradable, and hydrophobic compounds can be treated through traditional wastewater, most micropollutants are not removed. Therefore, clean and safe water quality is endangered due to various micropollutants in different water sources.

Scientific researchers have designed and fabricated different approaches and materials to deal with the emerging pollutants that occur in the aquatic medium. Advanced oxidation processes, reverse osmosis, adsorption, and nanofiltration are some known examples designed for removing emerging pollutants (Alizadeh Fard et al. 2013). Nanotechnology has played a vital role in many industrial applications in the present era, including water and wastewater treatment (Palani et al. 2021). Besides, nanotechnology helps to introduce nanocomposites to the real world, a material comprising an inorganic element in the form of fiber or particles, reinforced in an organic component, measured on the nano-scale (Khan et al. 2020). An extensive range of nanocomposites has been reported in the literature, for instance, polymer-based nanocomposites (Nagy et al. 2014). In terms of environmental remediation,

carbon-based nanocomposites are often recommended. Carbon is one of the most researched materials, and there are various forms available, such as graphene, carbon nanotubes, carbon fibers, and fullerene. Carbon nanotubes (CNTs), especially multi-walled CNTs (MWCNTs), possess unique properties that can be considered in a broad range of fields. Research has demonstrated that MWCNTs possess high adsorption for heavy metal ions, dyes, and micropollutants, indicating their wide spectrum applications in water and wastewater treatment (Qu et al. 2013). Based on their countless benefits, these materials have a few drawbacks, for example, they are very small and lightweight to separate from the aqueous phase (Mohmood et al. 2013). Raw MWCNTs are functionalized and embedded with magnetic nanoparticles for water purification and remediation applications (Mailler et al. 2016). Recent studies show that magnetic f-MWCNTs have shown high adsorption capacity towards different contaminants, including micropollutants (Shukla, Khan, et al. 2021). Magnetic f-MWCNTs facilitate only small-scale removal as an external magnetic field is necessary to complete the separation process.

Like magnetic f-MWCNTs, another carbon-based material, called buckypaper (BP), has gained substantial attention in many applications due to its environmentally friendly, lightweight, flexible, and high chemical strength characteristics (Chen et al. 2016). Several studies have demonstrated the capability and feasibility of BP to be utilized as catalyst support and filter membranes. The development of BP is simple and easy as it requires vacuum filtration of f-MWCNTs solution through microporous membrane material, i.e., poly-tetra- fluoro-ethylene (PTFE) and polycarbonate (PC). Studies have revealed that BP can be used for water purification and environmental remediation, as its pores support 60-70% of its overall volume (Chapartegui et al. 2013).

As mentioned above, magnetic nanoparticles incorporated in MWCNTs have attained significant interest among scientific researchers, especially for water cleaning and remediation. Nevertheless, due to an external magnetic field requirement, magnetic-based nanocomposite materials are restricted in real-world industries. In contrast, BP membrane applications are limited due to low

mechanical strength; however, the BP membranes have demonstrated high adsorption capability towards various pollutants in water and wastewater effluents. This research aims to develop an innovative membrane that has the characteristics of magnetic f-MWCNTs and BP and is acceptable to be utilized for micropollutant removal from the aqueous phase without the use of an external magnetic field for separation. In addition, a mathematical modeling framework will also be designed to predict the feasibility and adsorption capacity of the membrane for treating a high volume of furazolidone (FZD) micropollutants.

1.4 Research Questions

The research questions linked with this research topic are listed below:

i. How do the operational parameters such as the initial pH of the FZD micropollutant, agitation speed and contact time affect the elimination of FZD by the magnetic f-MWCNTs-based BP/PVA membrane?
ii. How does surface modification alter the chemical, thermal, morphological, functional and magnetic properties of the magnetic f-MWCNTs-based BP/PVA membrane?
iii. Is the adsorption efficiency of the fabricated membrane comparable with the conventional adsorbents?
iv. Which approach, i.e., statistical and machine learning techniques, predicts the removal efficiency of FZD micropollutant on the magnetic f-MWCNTs-based BP/PVA membrane more effectively?

1.5 Aim & Objectives

This study aims to develop a magnetic f-MWCNTs-based BP/ PVA using functionalized MWCNTs for FZD micropollutant removal. The following steps are required to achieve the goal.

i. To optimize the operational parameters (pH 4-8, contact time 20-350 min., and agitation speed 100-200 rpm) for the optimum removal of FZD micropollutant from the aqueous solution.

ii. To determine the properties such as thermal stability, chemical composition, surface topology, and magnetic strength of the magnetic f-MWCNTs-based BP/PVA membrane through advanced characterization techniques.

iii. To determine and compare the adsorption capacity of the magnetic f-MWCNTs-based BP/PVA membrane with the conventional adsorbents.

iv. To compare the modeling of RSM-CCD and ANFIS for the percentage removal of FZD micropollutant on the magnetic f-MWCNTs-based BP/PVA membrane

1.6 Novelty

Carbon nanotubes, a nanotechnology product, exhibit substantial properties that have gained researchers' interest in using it for various applications, including water purification, remediation, and desalination. However, its usage are impractical because of their nano-size, formation of bundles, low solubility and dispersibility, difficulty in being difficult to separate, and low reusability and recovery. Therefore, researchers have discovered various approaches to modify the surface of CNTs to overcome the aforementioned drawbacks. They are modifying the surface of CNTs and incorporating them with metal/ metal oxide to transform CNT into magnetic CNT as nano-adsorbents have sparked rapid interest in environmental protection applications. Many research studies have shown that magnetic CNTs exhibited excellent adsorption of contaminants such as heavy metal ions, organic and inorganic compounds, and dyes. However, these nano-adsorbents also have a few disadvantages, for instance, requiring an additional external magnet to sweep off magnetic CNTs covered with pollutants from an aqueous medium.

Furthermore, some studies have revealed that magnetic CNTs, after absorbing pollutants from an aqueous medium, are not entirely swept off using an external magnet. Due to this, magnetic CNTs as nano-adsorbent materials are restricted for heavy metals and dye removal applications. Like magnetic CNTs, CNT-based membranes, especially BP, have also displayed great interest in the current era and have shown excellent potential for water purification and desalination. Enhancing the mechanical properties of the BP membrane is essential as it offers to create a break-free membrane, which restricts the risks that arise from CNT as individuals in the environment. Based on the literature, the mechanical properties of BP membranes can be improved through infiltration with polymers, such as polystyrene, PVA, etc. In addition, most polymer infiltration studies have been conducted on single-walled CNTs (SWCNTs), and limited studies on multi-walled CNTs (MWCNTs).

Individually, both magnetic CNTs and CNT-based BP membranes have been extensively researched. However, no study has been conducted where properties of magnetic CNT-based BP membranes are combined to form a magnetic membrane. The novelty of this study is the development of a membrane that has high efficiency in adsorption, separation, and reusability. Moreover, the successful development of this membrane will not require any additional separation stage like magnetic-CNTs nano-adsorbents material. Besides, no study on magnetic CNT-based BP membrane infiltration with PVA has been conducted for micropollutant removal. Lastly, statistical and mathematical modeling are compared to predict the removal efficiency of FZD micropollutant using magnetic BP membrane.

1.7 Significance of the Study

No research has considered magnetic f-MWCNTs-based BP/PVA membranes for micropollutant removal from water sources. The use of magnetic f-MWCNTs-based BP/PVA membranes for micropollutant removal may improve the overall economic feasibility. It can improve the adsorption

capability, mechanical strength, long life-cycle, and reusability. Besides, it can also reduce environmental concerns, such as reducing effluent growth and energy consumption. Moreover, the findings of this study may provide an opportunity for developing wastewater treatment approaches that are feasible in real-life industrial applications. This proposed study is expected to have considerable breakthroughs and impact on the future research studies associated with different pharmaceuticals and steroid hormones micropollutant removal applications using a novel membrane, magnetic f-MWCNTs-based BP/PVA.

1.8 Scope of the Study

The research scope of this study is to examine the magnetic f-MWCNTs-based BP/ PVA membrane and its use as an aquatic micropollutant removal membrane comprehensively. f-MWCNTs will be prepared and reinforced with magnetic nanoparticles to fabricate magnetic f-MWCNTs nanocomposite, which will later be used to develop the BP membrane. To strengthen the mechanical stability of the membrane, the developed membrane will be infiltrated with PVA. Then, characterization analysis will be conducted using different analysis approaches, including FE-SEM, TGA, EDX, FT-IR, and VSM. Furthermore, process parameters such as concentration and pH of micropollutant solution, temperature, and time will be investigated to evaluate their relationship with the developed magnetic f-MWCNTs-based BP/PVA membrane. Also, adsorption studies will be performed using the adsorption isotherm models, thermodynamics, and kinetics for a better understanding of the adsorption phenomenon of the developed membrane. Additionally, an assessment of the prepared membrane is conducted in comparison to conventional absorbents, focusing on parameters such as removal efficiency, adsorption capacity, and reusability. To capture the inherent characteristics and better predict the adsorption efficiency and feasibility of the developed membrane for treating a large volume of micropollutant, RSM-CCD and ANFIS mathematical modeling will be used and evaluated. Besides, it will also

help to understand the relationship between process parameters and optimize the performance.

1.9 Outline of the Thesis

The thesis report is comprised of five chapters, as summarized below. The structure of the thesis report is graphically presented in ***Fig. 1.4***

i. ***Chapter 1:*** States the occurrence of micropollutant in different water sources and their environmental effects and risk. Furthermore, problem statements, research gaps, and questions are discovered, through which the specific objectives of this study are designed. Moreover, the novelty significance of this study is also comprised.

ii. ***Chapter 2:*** Describes the current water contaminants' overview, emphasizing micropollutant existence in different water sources. Besides, discuss their environmental risks and effects-furthermore, the current role of magnetic separation and membrane technology in water and wastewater treatment applications.

iii. ***Chapter 3:*** Comprises the study's chemicals, materials, and methodology. The comprehensive description for each step is described in this chapter, which includes the surface modification of MWCNTs, synthesis of magnetic f-MWCNTs and magnetic f-MWCNTs-based BP, infiltration of PVA on magnetic f-MWCNTs-based BP, and its characterization analysis. The optimization analyses for micropollutant removal using magnetic f-MWCNTs-based BP/PVA under batch treatment were also included.

iv. ***Chapter 4:*** Interpret the results and broad discussions of this study, which consist of:

- Surface modification and characterization analyses of f-MWCNTs, and magnetic f-MWCNTs.

- Optimization analysis of FZD micropollutant removal under batch treatment.
- Characterization analyses of magnetic f-MWCNTs-based BP/PVA membrane.
- Adsorption analysis of magnetic f-MWCNTs-based BP/PVA membrane for MP removal.
- Optimization of FZD MP removal using magnetic f-MWCNTs-based BP/PVA via artificial neural network.

v. ***Chapter 5:*** Shows a conclusion summarizing all significant findings from this research study. Furthermore, future research prospective of magnetic f-MWCNTs-based BP/PVA membranes also are presented.

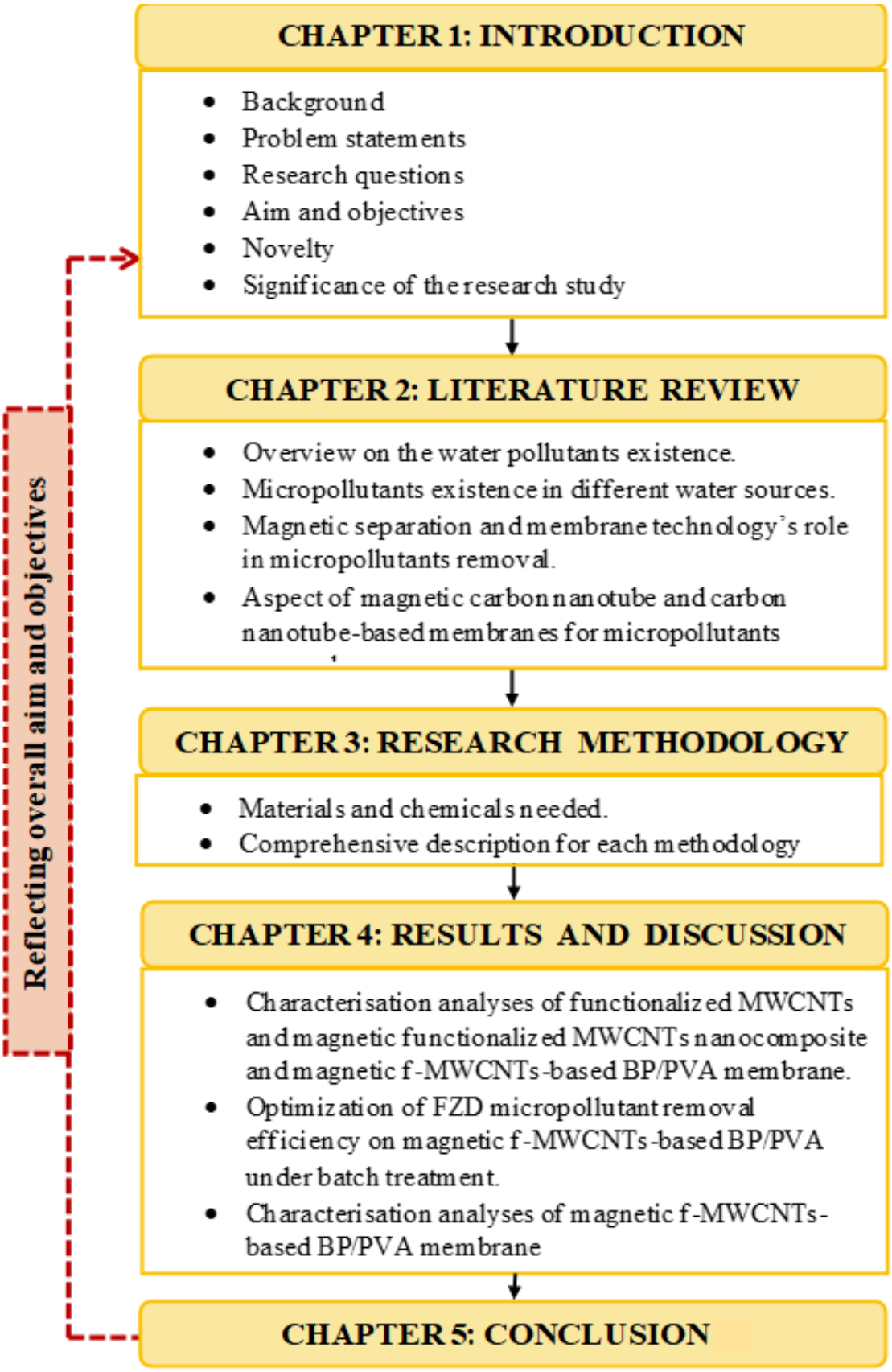

Fig. 1.4: Thesis schematic flowchart

CHAPTER II

LITERATURE REVIEW

This chapter is a literature review. An adapted version has been published in ***J. Environ. Chem. Eng.****, with the name "****A comprehensive review on micropollutant removal using carbon nanotubes-based adsorbent and membranes****", by Fahad Saleem Ahmed Khan, Nabisab Mujawar Mubarak, Mohammad Khalid, Yie Hua Tan, Ezzat Chan, Muhammad Ekhlasur Rahman, and Rama Rao Karri.*

2.1 Introduction

Water-associated issues are a persistent global problem. Different factors have frequently stressed hydrological resources, including urbanization, industrialization, and population growth (Amprako 2016). Furthermore, increasing use of fertilizers and chemical materials have also contributed to the eutrophication of rivers and the development of dead zones in various habitats. Moreover, mishandling of wastewater and lack of public strategies have compounded the situation (Guner 2011, Olvera et al. 2017). ***Fig. 2.1*** illustrates the various pathways of contamination into the aquatic environment.

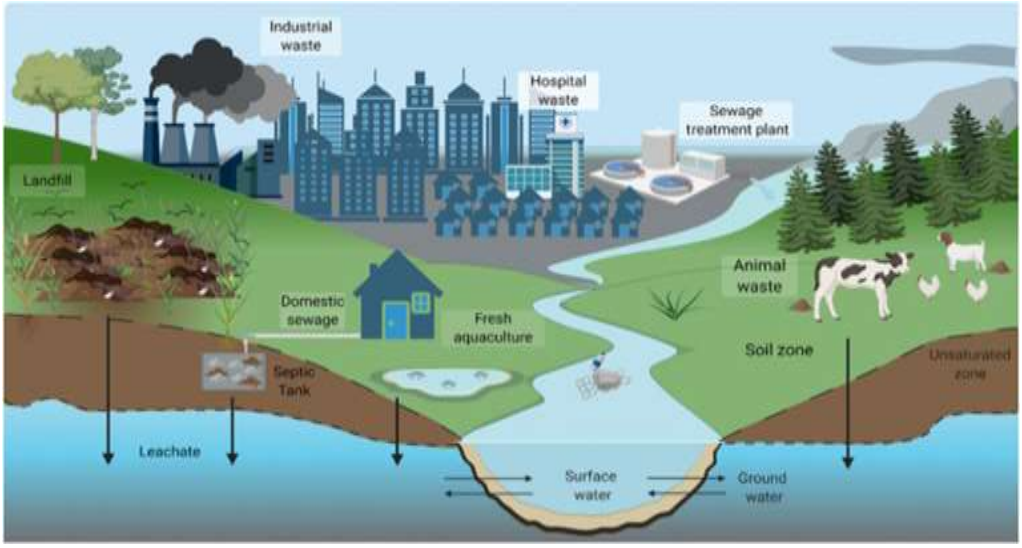

Fig. 2.1: Pathways of pollutants into the aquatic environment (Kosek et al. 2020)

For several decades, the health of global waterways and natural bodies of clean water has been in the state of deterioration (Sweetman et al. 2017). Clean water is essential for both wildlife and human life, and the accessibility of fresh drinking water is critical for maintaining a healthy life. Many researchers have stated that the impacts of climate change will worsen these water problems and hypothetically result in more severe droughts, flooding, and increased toxicity of chemical pollutants in the environment (Noyes et al. 2009). Contaminated water sources can injure humans due to possible exposure to pathogens, harmful chemicals through plant irrigation with polluted water, toxins consumption in aquatic creatures, or polluted surface water use for recreational purposes such as swimming (Akhtar et al. 2021). Thus, for people living in developing countries, human health is most generally affected through direct consumption of polluted water.

Water pollution consists of natural and artificial components, and each species affects human health to different degrees. A considerable share of contamination and impurities in water comes from naturally occurring resources (Komatsu et al. 2020). Allochthonous pollution were derived from the interruption of terrestrial animal and plant matter transported into waterways. Allochthonous pollutants originate from within each channel, resulting from natural actions of micro-organisms and water vegetation breakdown (Lozovik et al. 2007). Moreover, individual chemical compounds that constitute of natural organic matter include micro-organisms such as viruses and bacteria are mainly categorized as biological water pollutants. Whereas usually organic compounds are measured to be comparatively benign to human health, some micro-organisms may have substantial and extensive health effects (King et al. 2016).

An extensive increase in the concentration and variety of artificial chemical species has recently penetrated global waterways. Growth in agriculture, industry, and the disposal nature of an advanced society has led to the introduction of a significant range of synthetic organic and inorganic pollutants into the water system (Kong et al. 2015). Industrial pollutants include heavy

metals, dyes, pigments, and plasticizers (Alahmadi 2022). Due to the substantial diversity of artificially introduced organic and inorganic pollutants, there are perhaps the most challenging ways to efficiently remove from water. Contaminants derived from agriculture include pesticides and fertilizers that usually exist in waterways, resulting in the discharge of nitrogen and phosphorous, potentially causing microorganisms (Akhtar et al. 2021). In addition, pharmaceuticals and personal care products are two new growing sources of artificial water pollution. Although the discharge of particular therapeutics and hormonal mixtures is distressing, the release of antibiotics is of grave concern because of the likelihood of the growth of resistant bacteria (Jovanovic et al. 2021). ***Tab. 2.1*** summarizes different pollutant types in the aquatic environment, and their removal approaches.

Tab. 2.1: Summary of different pollutants detected in the aquatic environment

Pollutant Class	Contaminants	Removal Approaches	References
Micro-organism	• Viruses • Bacteria • Protozoa	Size-exclusion filtration, chlorine disinfection	(Ma et al. 2012)
Synthetic organics	• Solvents • Dyes • Perfluorinated compounds	Filtration, adsorption	(Forgacs et al. 2004)
Natural organic	• Fulvic acids • Humic acids		(Sharpe et al. 2004)
Heavy metals	• Mercury • Chromium • Arsenic • Lead	Reverse osmosis, ion-exchange, sedimentation, adsorption	(Rasheed et al. 2016)
Agricultural	• Fertilizer • Pesticides • Animal waste	Filtration, flocculation, reverse osmosis, adsorption	(Karimi et al. 2016)
Pharmaceuticals	• Personal care products • Anti-biotics • Steroids	Filtration, adsorption, degradation	(Rivera-Utrilla et al. 2013)

A broad-range of the above-mentioned contaminated classes are utilized daily in workplaces, homes or in urban environment and deposits in the sewers. This is generally the issue for “down the drain” products, such as personal care products, detergents, pharmaceuticals and their additives and metabolites which are excreted in faeces and urine; moreover, various plastics and food additives are comprised in textiles (Warner et al. 2019). Besides, municipal wastewaters are also polluted with non-domestic contaminants such as pesticides, heavy metals and hydro-carbons, which are stripped during rain runoff from streets, urban gardens and buildings (Margot et al. 2015). In wastewater treatment, the fate of these contaminants mainly depends on their physicochemical features, such as volatility, biodegradability, hydrophobicity, and also treatment route (Lalwani et al. 2020). Regarding the reduction of these pollutants into the aquatic environment, improvement of the removal processes is necessary. This chapter aims to bridge the gap in the literature by providing an overview of current magnetic carbon nanotube-based nanocomposites and carbon nanotube-based membrane, especially buckypaper; moreover, their applications for the elimination of micropollutants, particularly pharmaceuticals. Furthermore, it focuses on removing the pharmaceutical micropollutant through magnetic carbon nanotube-based nanocomposites and carbon nanotube-based membrane rather than conventional nanocomposites and membranes, such as activated alumina, silica gel, or membrane bioreactors (Sher et al. 2021, Guardado et al. 2021, Gutiérrez et al. 2022). In addition, statistical and machine learning techniques are also reviewed under this chapter and are employed for the elimination of pharmaceutical micropollutants from various water sources.

2.2 Micropollutant

Most surface water forms display a high number of anthropogenically generated compounds; moreover, only 10% of European lakes are labeled ‘very clean’ based on their chemical grade (Loos et al. 2009). Besides, the United Nations resolution in 2010 designated water as the ‘new gold of the 21st century’. There is currently an agreement in place that provides a long-

term source of enhanced water quality, which is inextricably linked to marine eco-health and the surrounding territory by providing essential eco-services. Furthermore, water pollution can cause a variety of problems, including the extinction of marine species, reduced biodiversity, and pathogenic eruptions, and it can harm marine species even at low quantities (Gerbersdorf et al. 2015). As a result, environmental concerns, including improving water quality, are one of the most pressing issues for present and future generations. By recognizing and eliminating contamination sources, water quality could be improved in a sustainable and effective manner.

To date, the Chemical Abstract Service (CAS) has labeled around 89,000,000 chemical compounds (Fantke et al. 2020, Yang et al. 2021). Because of the introduction of new items, the number of anthropogenic substances in water continues to rise daily, and this frightening situation becomes increasingly obvious with improved analytics. One of the rising fears is the ‘emerging pollutants’ or micropollutants (Fawell et al. 2012). The term micropollutants is described as anthropogenic chemicals found in the aquatic environment at more than the usual natural level due to human action, with trace concentrations i.e., ng/L. Hence, micropollutants are described by their anthropogenic source and their existence at low concentrations. Most often, micropollutants are mentioned as anthropogenic trace compounds (ATC) (Loos et al. 2013). Micropollutants may comprise uncontaminated synthetic chemicals, natural compounds, or even estrogens. Micropollutants source include agriculture, pharmaceuticals, steroid hormones, food products, and pesticides (Lim et al. 2017). They are primarily introduced into the environment by effluents from wastewater treatment plants and agricultural wastes. Micropollutants have been found in large quantities in water sources used to produce drinking water in the past (Luo et al. 2014).

The existence of micropollutants in various water sources has been reported widely (Luo et al. 2014). It has been estimated that nearly 70% of the pharmaceuticals in the wastewater come from domestic households, 5% from hospital discharge, 20% from livestock farming, and the remaining derives

from unspecified sources; nevertheless, geographical and seasonal variations are average occurrences (Zdarta et al. 2022). The concentration of micropollutants in different water sources is very much dependent on their physiochemical properties, for instance, octanol-water partition coefficient (LogP), dissociation constant (pKa), and water-solubility (Sithamparanathan et al. 2021). LogP and pKa are essential properties of micropollutants influencing their sorption affinity and charge. According to Rogers, sorption potential is determined by the value of LogP, i.e., the value of LogP less than 2.5 a shows low sorption potentials while the LogP value greater than 4 shows a high sorption potential (Venegas et al. 2021). A list of well-known micropollutants found in different water sources and their physiochemical aspects are listed in ***Tab. 2.2***:

Tab. 2.2: Physicochemical features of the known micropollutants

Compound	Molecular weight (g/mol)	Density (g/cm^3) at 25ºC	Water solubility (mg/L) at 25ºC	pKa	LogP	References
Tylosin, Antibiotics ($C_{46}H_{77}NO_{17}$)	920	~1.1	210	7.7	1.6	(Ashraf et al. 2018)
Ibuprofen, Anti-inflammatory ($C_{13}H_{18}O_2$)	210	1	21	4.5	3.8	(Caliskan Salihi et al. 2022)
Furazolidone, Antibacterial ($C_{15}H_{12}N_2O$)	230	1.5	40	2.4	0	(Amalraj et al. 2021)
Pravastatin, Lipid ($C_{23}H_{36}O_7$)	420	~4.2	6.1	4.2	3.1	(Althanoon et al. 2020)
Atenolol, β-blockers ($C_{14}H_{22}N_2O_3$)	270	260	13000	9.6	0.2	(Kumar et al. 2018)
Triclosan, Antibacterial ($C_{12}H_7Cl_3O_2$)	290	1.5	10	7.9	4.8	(Wang et al. 2017)
Methyl-paraben, Preservatives ($C_8H_8O_3$)	150	1.2	2500	-	2	(Bernal et al. 2021)
17-β ethinylestradiol, Hormones ($C_{20}H_{24}O_2$)	300	-	11	10	3.7	(Khan et al. 2021)
Diazinon, Insecticides ($C_{12}H_{21}N_2O_3PS$)	300	1.1	40	2.6	3.8	(Rad et al. 2022)
Butylhydroxytoluene, Food additives ($C_{20}H_{12}$)	220	1.1	0.6	-	5.1	(Ribeiro et al. 2021)
Bisphenol A, Plasticizers ($C_{15}H_{16}O_2$)	230	1.2	300	10	3.3	(Choi et al. 2019)
Tri(chloropropyl) phosphate, Flame retardants ($C_9H_{18}C_{13}O_4P$)	330	1.4	7000	-	2.8	(Truong et al. 2020)

Compound	Molecular weight (g/mol)	Density (g/cm^3) at 25ºC	Water solubility (mg/L) at 25ºC	pKa	LogP	References
Oxybenzone, Sunscreen ($C_{14}H_{12}O_3$)	230	1.2	3.7	7.6	3.8	(Hopkins et al. 2017)
Homosalate, UV filters ($C_{16}H_{22}O_3$)	260	1	<1	-	6.2	(Mitchelmore et al. 2021)
Tonalide, Cosmetics ($C_{18}H_{26}O_2$)	260	1	1.30	-	5.7	(Ehiguese et al. 2021)

Since micropollutants can be found everywhere and are usually used to enhance human life, it is not easy to control the release of these compounds' sources in the water environment (Ebele et al. 2017). Many studies have testified that micropollutants' availability is significant in drinking, ground, surface, and wastewater (Chen et al. 2006). The available conventional methods employed at wastewater treatment plants are not designed to eliminate micropollutants; thus, these compounds remain in the processed water and wastewater run-off. ***Tab. 2.3*** provides the list of known micropollutants which has been comprehensively studied and detected in different aquatic sources globally:

Tab. 2.3: Micropollutant detected in different water sources based on country

Micropollutant	Aquatic compartments	Research country	Concentration (mg/L)	References
17-α- Ethinylestradiol	Surface-water Wastewater	China Germany South Africa Korea	0.2-1.9 <1-8	(Vulliet et al. 2011, Manickum et al. 2014)
Diclofenac	Grey-water Surface-water	France Spain Greece United Kingdom	1.2-380 0.8-1000 0.5-260	(López-Serna et al. 2013, Stasinakis et al. 2012, Spongberg et al. 2011)
2- ethylhexyl-4-methoxycinnamate	Wastewater Surface-water	Norway Japan	4.7-510 12-1000	(Tsui et al. 2014, Amin et al. 2014)
Methylparaben	Sewage-water	Spain	290-1000	(González-Mariño et al. 2011)
Butyl-paraben	Tap-water	Spain	28	(Zhao et al. 2014)
Neonicotinoids	Surface-water	United States of America Spain Australia	1.1-110	(Papadakis et al. 2015, Campo et al. 2013)
Macrolide	Surface-water Wastewater	Spain United States of America	0-780 54-1900	(Birošová et al. 2014, Lara-Martín et al. 2014)
Butyl-methoxy-di-benzoylo-methane	Sewage-water	Hong Kong	290	(Tsui et al. 2014)

Micropollutant	Aquatic compartments	Research country	Concentration (mg/L)	References
17-β- Estradiol	Wastewater	Sweden	<1-88	(Nie et al. 2012, Zorita et al. 2009)
		China		
	Grey-water	United States of America	0.3-150	
		France		
Ibuprofen	Surface-water	Costa Rica	5	(Spongberg et al. 2011, Kim et al. 2009, Lin et al. 2011)
		South Korea	15	
		Taiwan	5-280	
	Groundwater	Spain	190	
Oxybenzone	Tap-water	United States of America	14	(Subedi et al. 2015)
Carbamazepine	Surface-water	Canada	3	(Kleywegt et al. 2011, Spongberg et al. 2011, Stepien et al. 2013)
		United Kingdom	5-680	
		South Korea	4-600	
	Groundwater	United States of America	40	
		France	10	
Triclosan	Sewage-water	India	890	(Subedi et al. 2017)
		United States of America	540	
Gemfibrozil	Surface-water	Costa Rica	41	(Lin et al. 2011)
		Taiwan	1.9-3.5	
	Groundwater	Spain	170	
Sulfamethoxazole	Groundwater	Spain	48	(Fram et al. 2011)
		United States of America	160	

Micropollutant	Aquatic compartments	Research country	Concentration (mg/L)	References
Trimethoprim	Surface-water	Taiwan	1	(Wang et al. 2011)
		United Kingdom	7-120	
		United States of America	9.1	
Triclocarban	Tap-water	United States of America	54	(Subedi et al. 2015, Carmona et al. 2014)
		Spain	13	

2.2.1 Present Legislation and normative strategies

In early days, there was a belief that the existence of micropollutants in the ecosystem induces a threat primarily for the natural water sources and the related marine species rather than for human beings' health. As a result, the primary concern with micropollutants is that the vast majority of them are not controlled or recognized by national or international legislation (Włodarczyk-Makuła et al. 2018). Consequently, regulation and normative strategies through various organizations emphasize traditional pollutants to protect the quality of environmental systems, particularly associated with waters (Tosun et al. 2020). On the other hand, several institutions periodically create vital rules on various legislations and proposals features of substances with particular concerns "priority contaminants," for instance joint FAO/WHO expert committee on food additives (JECFA), all focusing on micropollutants due to their risk based on the analyzed or potential effects (Aidonojie 2023).

Till to date, a limited number of countries have implemented regulations on specific micropollutants; for instance, environmental quality standards (EQS) for nonylphenol and diiron (micropollutants) have been recognized by the EU Parliament (Bennion et al. 2007). Micropollutants, i.e., steroid hormones, pharmaceuticals, and personal care products (PPCs), are not stated on the controlled substance list. More research on micropollutant' effects on ecological and human health is required to create supervisory benchmarks for micropollutant. Many review papers have been issued concerning micropollutants occurrence in various water bodies; more comprehensive studies on micropollutants occurrence are still needed (Lapworth et al. 2012).

Even though no defined standard is available to determine the limits of the release of micropollutants, few regulations have been issued. The first regulation marked in the EU water policy was Directive 2000/ 60/ EC (Čížková et al. 2013). This regulation mainly focuses on defining the high-risk substances as well as prioritized them. Directive 2008/ 105/ EC and EQS endorsed thirty-three priority substances (PSs) (Directive 2008). Furthermore,

Directive 2013/ 39/ EU in 2013 suggested having a closer look at the monitorization and treatment options for 45 PSs, meeting the safeguard of the human health and aquatic compartment (Commission 2013). In the same Directive, two pharmaceuticals and natural hormones were suggested in the initial watch-list of ten substances for EU monitoring, introduced within 2 years. On March 20' 2015, the watch-list of EU monitoring substances (Directive 2008/ 105/ EC) was revised in Decision 2015/ 495/ EU. The regular rate of pollutants of the emerging issue in the surrounding, helped the revision of the outline to cover a vast number of toxic compounds, besides endorsements for wastewater treatment phases or even innovative treatment states (Bolong et al. 2009, Gibs et al. 2013, Nie et al. 2012). ***Tab. 2.4*** lists the various European regulations stated for the legal bases of micropollutant handling:

Tab. 2.4: Legal bases for the handling of micropollutant

Regulations	Description	Aim	References
Water Framework Moreover, the risk to living species is contingent upon Directive (2000/60/ EC)	The Directive was adopted on 23rd October'2000. A European directive promises that all European Union (EU) must attain all water bodies' good quantitative and qualitative rank. The completion date for the plan is 2027.	• Safeguard the transitional, in-land surface, ground, and coastal waters. • Secure 'Good Status' for all kinds of waters at the targeted deadline. • Water management regarding River Basins. • 'Combined Approach' of discharge limit values as well as quality standards. • Measures for decreasing the relevant contaminants/ contaminant group (VIII of WFD) • Adequate water costing.	(Parliament et al. 2000, Cabezas 2012)
Plant Protection Product Legislation (1107/2009)	The legislation was published on 21st October '2009. The legislation states guidelines for the plant protection products (PPPs) authorization in marketable form and their setting on the market, use, and maintain within the community. Moreover, set regulations for active substances, synergists, and safeners approval, which PPPs comprise, and co-formulants and adjuvants rules. In short, it is legislation about PPPs that place in the EU	• Support high-level safeguard of the environment and human health. • Improve operation of the internal market. • Control as well as improve the competitiveness of the EU chemical market.	(House et al. 2008, Matyjaszczyk 2018)

Regulations	Description	Aim	References
	market.		
Groundwater Directive (2000/118/EC)	The Conciliation Committee accepted the Directive on 28th November 2006.	• Description of suitable groundwater chemical conditions. • The sustained upward and significant reversal trend in contaminants concentration. • EQS for pesticides as well as parameters for threshold values. • Measure for controlling good water status and avoid/ decrease the pollutants input.	(Nieto et al. 2005)
Marine Strategy Framework Directive (2008/ 56/ EU)	The Directive became official on 17th July 2008. It is established as a legal framework for safeguarding and managing EU seas and guarantees their long-standing, sustainable use. The legislation plan is to attain the excellent status of the EU's marine water by 2020.	• Achieve good status of the marine water. • Measures for controlling or decreasing relevant contaminants or contaminant groups.	(Fung et al. 2012)
Regulation on Detergent (648/ 2004)	The regulation was officially presented on 31st March 2004. The regulation updates and merges the current Directive on detergent. The regulation executes a two-tier testing rule on the active detergent ingredient's bio-degradability,	• Launch free movement of detergent and surfactants for detergents on the inner market, guaranteeing a high degree of safeguard of human health and environment. • Bans on surfactants in terms of the bio-	(Pedrazzani et al. 2012, Wind 2007)

Regulations	Description	Aim	References
	referred to as surfactants. Furthermore, the regulation introduces stricter labeling requirements on detergent producers.	degradability two-tier testing rule.	
Directive on Industrial Emissions (2010/ 75/ EU)	The Directive was officially presented on 24th November'2010. This EU Directive which pledges EU member state to maintain and reduce the industrial emission impact on the environment.	• Establish guidelines on integrated prevention and pollution control are rising from industrial actions. • Design rules to stop or decrease emissions into water, air, and land. Moreover, limit waste generation to attain a high level of safeguard of the environment.	(Bachmann et al. 2014, Kim et al. 2022, Abdelkareem et al. 2021)
Regulation on Biocidal Products (528/ 2012/ EU)	The regulation was adopted on 22nd May'2012. The regulation relates to biocidal product use and place in the market, which is used to shield animals, humans, articles, or materials against toxic organisms such as bacteria or pests by the action of active constituents contained in the biocidal product.	• Biocidal products authorization regarding environmental risk valuation of active biocidal products and substances.	(Backhaus et al. 2013, Union 2012)

2.2.2 Environmental risks and effects of micropollutant

Environmental risk induced through substances mainly depends on their chemical and physical affinity and speciation for water and solid matter, which substantially impacts their bio-availability (Zamora-Ledezma et al. 2021). Moreover, the danger to various forms of life also hinges on the movement of substances and their capacity to be conveyed into the food chain. In tissues of aquatic species, pollutants can be ingested or mixed with suspended matter or water (Rathi et al. 2021). Consequently, contaminants concentration in the tissues of marine species may be present at levels equivalent to or higher than to the environment's concentration. The wide deviation in environmental conditions in different water sectors can also be an essential factor affecting bioavailability (Cheng et al. 2020). Temperature, salinity, turbidity, or pH can be prominent among these conditions (Xu et al. 2020, Yang et al. 2021).

Moreover, the physicochemical aspects and sensitivity (trophic level, feeding behavior, life stage, habitat conditions, genetic adaptions, and contaminant interactions) are also competent to affect the ability of organisms to bio-accumulate contaminants (Rogowska et al. 2020). Various organisms have different potentials to bio-accumulate elements, even when introduced to similar levels of particular pollutants. Even individuals of a single species exposed to a similar concentration of pollutants for the same duration may not accumulate elements at an equal rate. It is also linked with several other factors, for instance, size, sex, age, and physiological condition of the species (Ghirardini et al. 2020).

Data on the chemical concentration levels in different water sources is insufficient to investigate the environmental risk. The results of chemical studies only offer specific information about the potential endangerment to human beings and ecology. The environmental risk assessment to study the effects of micropollutant on plants, human health, ground/surface water quality, and aquatic species reported a broad spectrum of disorders posed by the exposure of micropollutant (Kim et al. 2016). These chemical elements in drinking water may cause serious, long-lasting effects and produce irreversible

mutations in humans and wildlife (Fang et al. 2017). Research performed on 24 individual post-mortem brain materials detected the accumulation of methyl-paraben, n-propyl paraben, triclocarban, bisphenol, and methylparaben in their white-matter brain tissues (Van der Meer et al. 2017). A survey conducted in the US on 20 teenage girls, age 14-19, also found the accumulation of 16 noxious chemical compounds related to personal care products use, for instance, cosmetic products (Cohen et al. 2019). ***Fig. 2.2*** depicts the known or suspected effect of micropollutant on human's health and the environment:

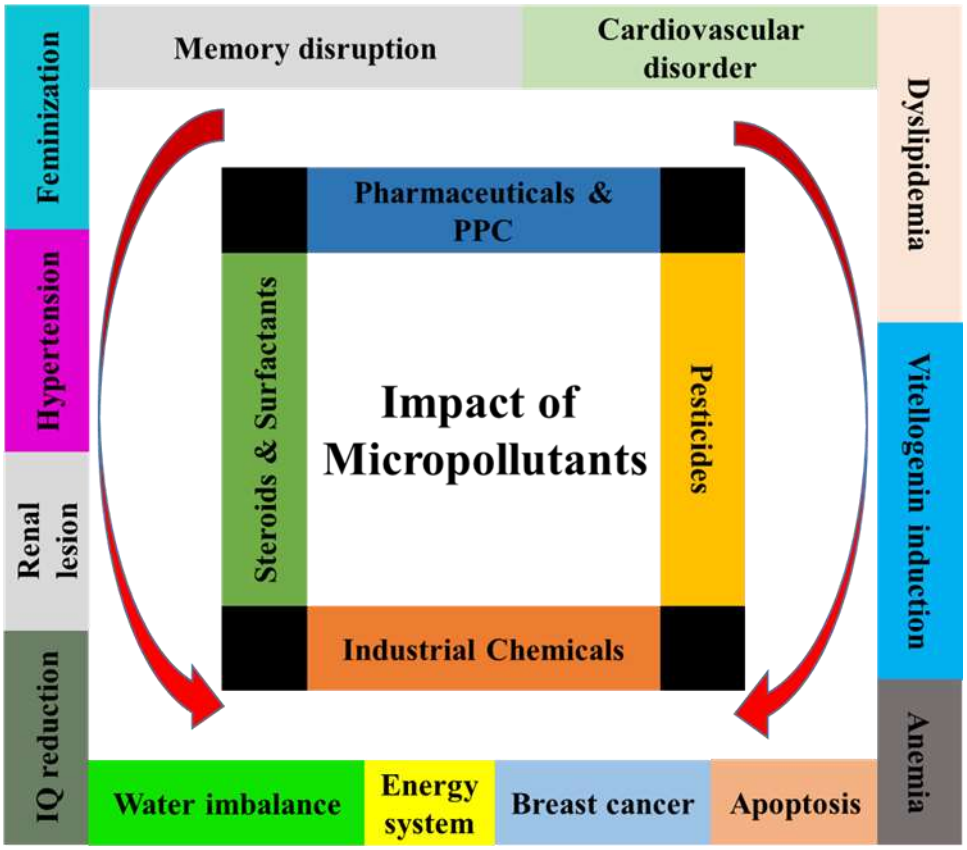

Fig. 2.2: Effects of micropollutant on human's health and the environment (Vasilachi et al. 2021)

The organic compounds found in aquatic ecosystems affect the reproductive networks can damage in marine species (Bainbridge et al. 2018). Aromatic micropollutants can react with chlorine to form chlorine by-products that are extremely harmful and cause severe effects on living species (Younis et al. 2017). Antibacterial triclosan disturbs the hormonal functions, affecting to human beings' metabolism and reproductive systems (Maksymowicz et al.

2021). Studies performed by Sattar and associates had discovered that the micropollutant, specifically endocrine-disrupting compounds, can modulate endocrine functioning, i.e., damage fertility, menstrual cycle malfunctions, and endometriosis (Ratnasari et al. 2022). Besides, Desai and co-associates' explained the role of endocrine-disrupting compounds in metabolic illnesses, for instance, dyslipidemia, cardiovascular diseases, obesity and insulin resistance in human beings (Desai et al. 2015). A separate study performed by Giulio and his co-associates elucidated the ability of endocrine-disrupting compounds on the pathogenesis of breast disease even at minor concentrations (Giulivo et al. 2016). The effect of chronic and acute exposure on the reproductive system, histopathological changes, and body organs of fishes, mammals, snails, and birds had also been described (Overturf et al. 2015).

Antibiotic FZD has been widely utilized as an antibacterial and antiprotozoal feed additive for poultry, cattle, and farmed fish as well as in human medicine for the eradication of helicobacter pylori (Liu et al. 2017, Mund et al. 2017). Researchers have found evidence that FZD and its metabolite 3-amino-2-oxazolidinone (AOZ) can cause mutations and harm the genome in test animals (Beliatskaya et al. 2020). It has also been found to cause cancer and teratogenic consequences in humans at low concentrations, bacterial resistance, and organ failure in animals (Balasubramanian et al. 2019). DNA damage and cell growth inhibition are additionally possible side effects of FZD in humans (Feitosa et al. 2021). The long-term impact of FZD exposure includes aplastic anaemia, granular leukocyte deficiency, grey baby syndrome, neurotoxic responses, and hypersensitivity (Seyedmajidi et al. 2021, Anh et al. 2022). There were several instances in which the hazardous biological metabolite AOZ and its FZD-derived residues were found in a variety of aquatic species as well as in pond water and silt (Sousa et al. 2020). Consequently, in polluted areas or municipal wastewaters, it is important to detoxify FZD and AOZ. Previous study showed that FZD and furaltadone tartrate were the most poisonous to *Selenastrum capricornutum* and *Daphnia magna*, followed by *furaltadone chlorohydrate* (Kim et al. 2012). FZD toxicity to Culex pipiens and Daphnia magna was subsequently discovered to be significant. Furthermore, FZD is very poisonous to microalgae like Ulva lactuca and Aliivibrio fischeri, and to bacteria like

Heterocypris incongruens and Aliivibrio fischeri (crustaceans) (Leston et al. 2013). ***Tab. 2.5*** shows the ecotoxicological impact of various micropollutants on aquatic organisms.

Tab. 2.5: Ecotoxicological impact of pharmaceutical contaminants residues on aquatic organisms

Micropollutant	Usages	Concentration (µg/L)	Species	Effects	References
Estradiol	help reduce symptoms of menopause	0.80	Pimephales, promelas	Reduction in reproductive output	(Santen 2015)
Estrone	treat abnormalities related to gonadotropin hormone dysfunction	–	Daniorerio	Reproduction/secondary sexual characteristics	(Niranjan et al. 2019)
Tamoxifen	treat breast cancer	5.6	Pimephales promelas	Inhibition of Reproductive output/VTG/Gonadal histology	(Owumi et al. 2021)
Fadrozole	treatment of estrogen-dependent disease, including breast cancer.	24	Pimephales promelas	GSI/VTG	(Brixius-Anderko et al. 2019)
Letrozole	treat early breast cancer	5	Oryziaslatipes	Fecundity/fertility/VTG	(Masri et al. 2010)
5α-Dihydrotestosterone	triggers the development of male characteristics	6	Pimephales promelas	Masculinization of females/Vtg induction in females	(Ornostay et al. 2016)
Cyproterone	relieve the symptoms of a tumor of the prostate gland	-	Fundulus heteroclitus	plasma and 11-KT reduction in males	(Sharpe et al. 2004)
Flutamide	treat men with prostate cancer	500- 651	Gasterosteus Aculeatus,	Behavioral problems in male, Testis histopathology	(Ankley et al. 2004)

Micropollutant	Usages	Concentration (µg/L)	Species	Effects	References
			Pimephales promelas	/ Ovary histopathology, VTG induction in males and Females, fecundity/ hatching	
Norethindrone	Birth control to prevent pregnancy	25–10	Oryziaslatipes Pimephales promelas	Inhibition of reproduction/ masculinization of females/steroid levels	(Vilk Ayalon et al. 2022)
Levonorgestrel	Prevention of pregnancy after the confirmed or suspected failure of contraception	-	Pimephales promelas	Prolonged time for reproduction	(Zhang et al. 2009)
Diclofenac	used to treat pain and inflammatory diseases such as gout	0.5–50	Brown trout Rainbow trout Carp	Hinders prostaglandin synthesis, histological alterations in kidney and gills, cytological alterations in liver and kidney, inhibition of CYP_2M	(Mehinto et al. 2010)
Furazolidone	relieve pain, such as muscle aches, or arthritis	1–100 1000 >10 206-280	Medaka Rainbow trout Zebrafish Carp	Change of reproduction pattern, impairment of ion regulation, cardio abnormalities, inhibition of	(Yu et al. 2014)

Micropollutant	Usages	Concentration (µg/L)	Species	Effects	References
				CYP_2M	
Indomethacin	relieve moderate to severe pain, tenderness, and swelling	100000	Zebrafish	Disruption of oocyte maturation/ovulation	(Magalhães et al. 2017)
Naproxen	Arthritis, degenerative type, spondylitis, acute gout skeleton disorder	230260	Carp	Inhibition of CYP_2M	(Kean et al. 2005)
Fluoxetine	treat depression, obsessive-compulsive disorder	6 23–100 51–170 0.1–0.5 51–53 0.1–5	Bluehead wrasse Striped bass Fathead minnow Medaka	Decreased territorial aggression and ability to catch prey, reduced feeding rate in Fathead minnow	(Weinberger II et al. 2014)
Ketoconazole	treat skin infections	25 30 3.2 8000	Fathead minnow Flounder	Decrease in egg production, morphological changes to gonads, increased levels of CYP17 and CYP11A, inhibition of testosterone	(Monteiro et al. 2000)

2.3 Advancement in the application of nanotechnology for micropollutant removal

Improving wastewater quality and management is one of the primary focuses of nanotechnology. As a result, nanotechnology has been reported in the literature as the most advanced process for wastewater treatment. Several major nanotechnology techniques for water treatments are membrane filters with nanoparticles, nano-adsorption, and photocatalysis using nanoparticles (Cheriyamundath et al. 2021). Das and his co-associates studied the trends in nanomaterials usages in environmental remediation and monitoring and highlighted the effectiveness of these nano-tools and the requirement to restrict environmental pollution caused by their use (Das et al. 2015). Likewise, Karn and his co-associates described nanomaterials' advantages and possible risks and stated that nanotechnology must be customarily seen as more advantageous than harmful (Karn et al. 2009). Several nano-scale materials have been introduced for environmental applications, such as metal oxides, carbon nanotubes, zeolites, and different noble metals. In contrast to all, CNT-based composites/ membranes have received substantial consideration for water and wastewater treatment applications; therefore, numerous researches have been conducted by the scientific community over the past few years. The popularity of CNT-based composites/ membrane for water-related applications can be revealed by the number of articles that have been published till now which continues to increasing each year, according to the search engine Web of Science database as depicted in ***Fig.2.3***:

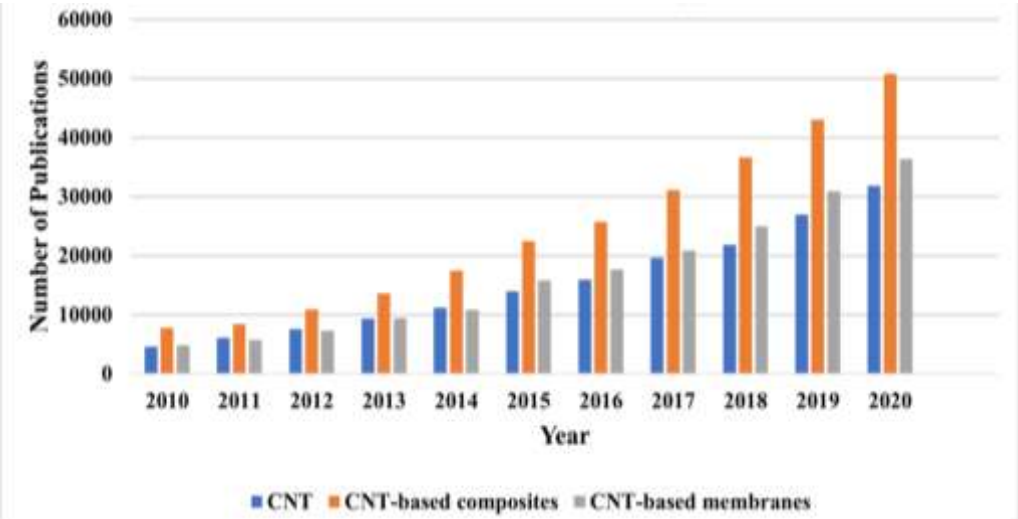

***Fig. 2.3**:* Scientific publication period of 2010-2020 (Vilardi et al. 2018, Barrejón et al. 2022)

The above graph (***Fig.*** 2.3) is constructed based on the use of CNT and CNT-based composites/ membranes for water and wastewater treatment applications such as heavy metal, dyes, salt, and micropollutants removal between 2010 and 2020. It is apparent that there have been substantial studies conducted on CNT, CNT-based composites and CNT-based membranes. Given the popularity of CNT, CNT-based composites and CNT-based membranes, the later section (Section 2.4 and Section 2.5) mainly focuses on them, specifically micropollutants removal.

2.4 Carbon nanotubes

With the rapid interest in nanotechnology, nano-structured materials have gained substantial applications in several sectors, especially environmental remediation and wastewater treatment. They have been introduced in different forms, such as nanotubes, nanofibers, nanoparticles, and nanowires (Farghali et al. 2013). These nanomaterials have demonstrated a higher adsorption capacity for most water pollutants than other bulk materials (Muhamad et al. 2017). Among different nanostructured materials, carbon-based nanomaterials have shown remarkable attention as future-generation materials for different applications because of their unique physicochemical features, excellent mechanical, electrical conductivity, and thermal properties (Cha et al. 2013).

The outstanding properties of carbon-based nanomaterials lead them to a revolutionary technological breakthrough towards a diverse range of applications, such as electrically conductive materials, biomedical fields, catalyst supports, and biosensors (Kwon et al. 2017, Ioniță et al. 2018). Furthermore, carbon-based nanomaterials are well-known as excellent adsorbents for pollutants removal from wastewater.

Amongst carbon-based nanomaterials, CNTs have been observed to have a higher adsorption capacity for organic compounds because of their characteristic morphology, which offers durable interaction of CNTs with organic compound through non-covalent forces, including π-π stacking, van der Walls forces, hydrophobic interactions, hydrogen bonding, and electrostatic forces (Gupta et al. 2013). The mechanisms are based on the features of the compound of interest. The prognosticate of adsorption of organic contaminants on CNTs is not straightforward since it depends upon the nature of interaction among pollutants and CNTs (Aslam et al. 2021). Features such as surface area, functional groups, purity, and adsorption sites play a crucial part in the adsorption of organic contaminants onto CNTs (***Fig.2.4***). CNTs consist of high surface activity sites and controlled pore size, resulting in tremendous sorption efficiency (Madhura et al. 2019).

Besides, CNTs tend to aggregate in an aqueous phase after the growth of several interstitial grooves and space, which results in high adsorption sites and assists in an elevation in adsorption capabilities of organic contaminants (Thines et al. 2017). Recently, single-walled CNTs have been observed to have great adsorption features of organic contaminants because of their large micropore volume and surface area. A factor that determines the cost-effectiveness of CNTs is regeneration. It is recommended that CNTs can be recycled by decreasing the pH of the solution using an acid, for instance, nitric acid (HNO_3) (Xue et al. 2017, Zhang et al. 2011).

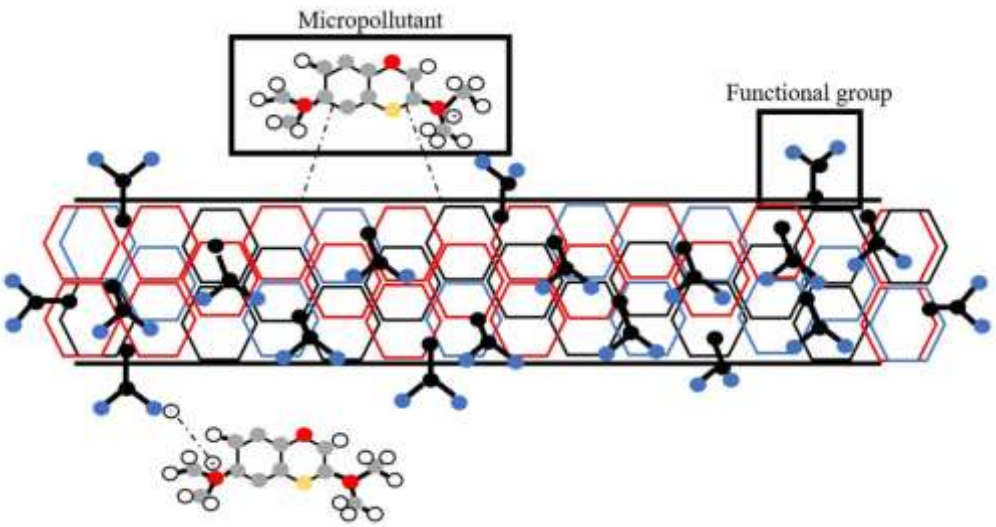

Fig. 2.4: Adsorption of aquatic micropollutant using CNTs (Lee et al. 2018)

The popularity of CNTs has rapidly increased in the scientific society due to numerous aspects such as controlled nano-size and shapes, mass production, economical feasibility, and potential to be employed for various applications (De Volder et al. 2013). Fabrication of these materials through suitable techniques will dictate their efficiency. Various studies have been performed to discover effective fabrication routes to attain the finest, highly stable, and shape-controlled carbon nanotube-based nanocomposites, for instance, filling, hydrothermal, arc-discharge, chemical vapor deposition, and pyrolysis methods (Rao et al. 2018, Deng et al. 2019). In our previous work, a comprehensive discussion has been presented along with their merits and demerits (Khan et al. 2020).

2.4.1 Functionalization of carbon nanotubes

Despite the unique physical and chemical properties of CNTs, the implementation of CNTs in various applications is still hindered. This occurs because pure CNTs have a tendency to form aggregates along the CNT tubules owing to the relatively weak Van der Waals interactions (Dubey et al. 2021). Besides, CNTs have low solubility, making them difficult to disperse and dissolve in most solvents (Krishna et al. 2018). Moreover, the impurities produced during the synthesis of CNTs can significantly alter the performance

of CNTs as these impurities limit the available adsorption sites of contaminants onto the surface of CNTs. To overcome these barriers, surface modification of CNTs can be performed to take advantage of CNTs' unique properties.

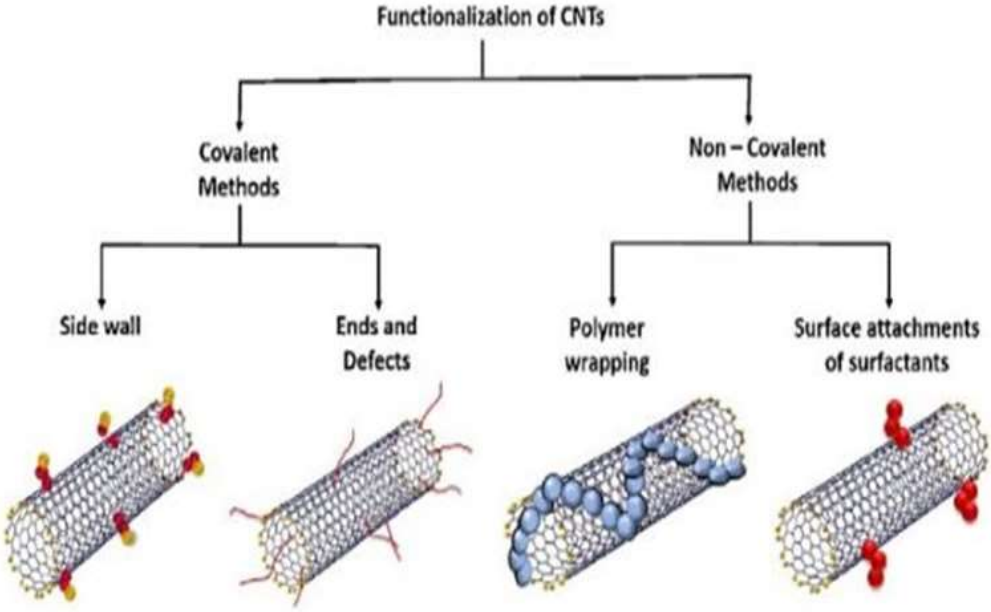

***Fig. 2.5**:* Functionalization routes of carbon nanotubes (Meng et al. 2009)

Previous researchers had reported numerous surface modification techniques of CNTs, such as acid oxidation, air oxidation, grafting of functional molecules/groups, and impregnation with metal/metal oxides. Acid oxidation treatment can be achieved by chemical treatment of CNTs with various acidic and alkaline solutions, such as potassium permanganate ($KMNO_4$), nitric acid (HNO_3), hydrochloric acid (HCl), and sulphuric acid (H_2SO_4) (Gupta et al. 2016). Besides, the functionalization of CNTs can alter the surface of CNTs by attaching different functional groups on the surface of CNTs, such as –OH, -C=O, and –COOH onto the surfaces of CNTs. These functional groups make CNTs more hydrophilic and suitable for the adsorption of relatively low molecular weight and polar contaminants, such as dye and phenol. Besides, some studies had reported the grafting of functional groups, such as carboxyl and amino groups, on the surface of CNTs, to remove pollutants from effluents (Mohammadi et al. 2018). Furthermore, studies have demonstrated that functionalized CNTs have improved solubility and dispersibility, stabilization of CNTs against agglomeration, and enhancement in adsorption efficiency

(Karkeh-Abadi et al. 2016, Azevedo et al. 2015). Oxidized CNTs can be further functionalized via esterification of oxidized-CNTs with pentaerythritol (PER) stated by Yang and co-associates, to form oxidized-CNTs-PER, which was used for organic dyes removal (alizarin red S), and the result displayed good adsorption capacity, i.e., 257.73 mg/g (Yang et al. 2018). Doping hetero-atoms in CNT is an effective technique to improve CNTs' exterior electronic polarization, which can be advantageous for adsorptive interaction of organic pollutants. Yi and co-associates successfully fabricated nitrogen-doped CNTs to adsorb tylosin, tetracycline, and bisphenol-A. In contrast to non-doped CNTs, nitrogen-doped CNTs possess significantly higher adsorption capacity, credited to their electron-exhaustion and remarkably uniform π- electron acceptor sites (Yi et al. 2014).

Additionally, the functionalization of CNTs by metal oxide is another effective technique to improve the characteristics of CNTs. Several studies reported that the CNTs impregnated with iron oxide, aluminum oxide, and manganese oxide showed promising results for removing wastewater contaminants (Mallakpour et al. 2016, Liang et al. 2015).

2.4.2 Functionalized carbon nanotubes for micropollutants removal

Concerning micropollutants, CNT and functionalized CNTs have been used by several researchers to explore their adsorption efficiency. Ji and co-associates employed f-MWCNTs to remove tylosin from synthetic water; good adsorption properties were observed with a maximum adsorption capacity of 85 mg/g (Ji et al. 2010). Using f-MWCNTs, a high adsorption capacity of 162 mg/g was achieved for bisphenol AP removal from the synthetic water sample (Bohdziewicz et al. 2013). Another antiepileptic, Triclosan, was also analyzed by Raoof and co-associates using f-MWCNTs, and the result showed the maximum adsorption of 106 mg/g (Raoof et al. 2012). Besides, research performed by Al-Shaalan and co-associates to remove diuron, a pesticide displayed a maximum adsorption efficiency of 110 mg/g (Al-Shaalan et al. 2019). The research work performed by different researchers reflects that

modified CNTs, particularly MWCNTs, have shown substantial potential adsorption capacity to remove various water pollutants, including various micropollutants. ***Tab. 2.6*** shows the recent research studies on CNTs and functionalized CNTs for the removal of micropollutants from various water sources.

Tab. 2.6: Publications on pristine and surface modified CNTs for the treatment of micropollutant

Carbon nanotubes	Target micropollutant	Removal percentage (%)	Adsorption capacity/efficiency (mg/g)	Remarks	References
Pristine SWCNTs	Carbamazepine	80	130	▪ Freundlich isotherm model was well fit. ▪ Increasing pH may have an adverse effect.	(Cai et al. 2014)
	Atrazine	n/a	33	▪ Thermodynamic parameters observed that the reaction was exothermic. ▪ Desorption studies noticed that no significant desorption hysteresis happened.	(Machado et al. 2016)
	17β- estradiol	99	27	▪ Calculated data from the model revealed that the Pseudo-second-order kinetic model was the best fit.	(Zaib et al. 2012)
	Tetracycline	96.2	100	▪ Lower adsorption reversibility was observed. ▪ Specific surface area elevated from 410.7 to 652.8 $m^2.g^{-1}$; moreover, extensive pore volume was developed during activation. ▪ It was improved in adsorption up to 2-3 times.	(Kim et al. 2014)
	Sulfamethoxazole	94	1000		
	Tylosin	98	10000		
	Ibuprofen	99	231	▪ Polanyi-Manes model was the best-fitted isotherm model. ▪ Stronger sorption was observed due to the high specific surface area. ▪ Sorption was directly affected by the electrostatic repulsive interactions among the SWCNT	(Zhou et al. 2013)

Carbon nanotubes	Target micropollutant	Removal percentage (%)	Adsorption capacity/efficiency (mg/g)	Remarks	References
				surface and compound.	
	17α-ethinyl estradiol	99	120	▪ Experimental studies observed that both Freundlich and Langmuir models are suitable ▪ Variation in pH did not affect the adsorption capacity ▪ Observed higher log K_{ow} value, i.e., ~10.5	(Joseph et al. 2013)
	Oxytetracycline	98.4	554	▪ An increase in adsorption capacity was noticed at pH ranges from 3 to 7. ▪ Brouers-Sotolongo was considered the best adsorption model.	(Ncibi et al. 2015)
	Ciprofloxacin	97.3	724		
		98.5	475		
	Olaquindox	99.7	133	▪ Adsorption kinetics of olaquindox was extremely fast, reached at equilibrium within 2 min. ▪ Langmuir isotherm model display maximum adsorption capacity of olaquindox on pristine MWCNTs	(Awad et al. 2020)
	Tetracycline	90.2	190	▪ Pseudo-second and Langmuir isotherm model was the best-fitted system ▪ Desorption efficiencies were reasonable	(Álvarez-Torrellas et al. 2016)
	Oxytetracycline	96.5	391	▪ The temperature effect causes a slight variation in adsorption capacity ▪ The removal efficiency began to decline after pH 7	(Ncibi et al. 2015)

Carbon nanotubes	Target micropollutant	Removal percentage (%)	Adsorption capacity/efficiency (mg/g)	Remarks	References
Pristine MWCNTs	ASulfapyridine	80	1000	▪ The pollutant possesses low hydrophobicity but is still strongly adsorbed to MWCNTs. ▪ The pH effect on adsorption was almost insignificant. ▪ The pollutant possesses low hydrophobicity but is still strongly adsorbed to MWCNTs. ▪ The pH effect on adsorption was almost insignificant. ▪ The experimental studies concluded that MWCNTs are an appropriate candidate for removing given micropollutant from the aqueous phase.	(Ji et al. 2009)
	Sulfadimethoxine	85	600	▪ Pseudo-second-order kinetic model explained the kinetic data, and the Langmuir isotherm offered the best fit for all experimental data.	(Xia et al. 2013)
		90	1300		
	Tylosin	98	300		
	Atrazine	n/a	36	▪ Experimental data was well-described by the dual Langmuir model for low concentration; hence, the Polanyi-Manes model is suitable for the lowest concentration. ▪ Atrazine sorption stayed unchanged from pH 3 to 9,	(Chen et al. 2008)

Carbon nanotubes	Target micropollutant	Removal percentage (%)	Adsorption capacity/efficiency (mg/g)	Remarks	References
				whereas, after pH-6, no decrease in sorption was observed.	
	Ibuprofen	n/a	81	▪ The experimental result analyzed that the adsorption capability of SWCNTs is comparatively higher than MWCNTs, whereas, in comparison to acid-treated MWCNTs, MWCNTs display higher adsorption capacity. ▪ Experimental data was well-described by the Polanyi-Manes model.	(Cho et al. 2011)
	Diclofenac	96	41	▪ Based on the isotherm model, it can be reflected that a temperature rise will lower the adsorption capacity. ▪ The Freundlich model well-presented experimental data ▪ Efficient enough to be used for other emerging pollutants, such as caffeine, Isoproturon, and atenolol.	(Sotelo et al. 2012)
	Ciprofloxacin	88	1.8	▪ Research studies concluded that the adsorption capacity inclined with the increasing time. ▪ Studies revealed that adsorption of ciprofloxacin on MWCNTs. is a chemisorption process ▪ Pseudo-second model and Freundlich isotherm were	(Avcı et al. 2020)

Carbon nanotubes	Target micropollutant	Removal percentage (%)	Adsorption capacity/efficiency (mg/g)	Remarks	References
				favorable.	
	Diuron	>97	50	▪ Polanyi-Manes model well-described the experimental data. ▪ The adsorption of micropollutant was directly correlated with the SSA and micropore volume of MWCNTs.	(Chen et al. 2011)
	17α-ethinyl estradiol	93.4	0.5	▪ A high amount of MWCNTs was used in this study, i.e., 100 mg. ▪ A Pseudo-second model was suggested ▪ Thermodynamics studies revealed that the removal process is enthalpy-driven. ▪ The removal rate was inclined with the rising amount of MWCNTs used. ▪ Adsorption capacity decreased at higher solution temperature, observed through kinetic studies.	(Al-Khateeb et al. 2014)
	Estrone	85.6	0.4		
	17β- estradiol	93.3	0.5		
	Triclosan	n/a	435	▪ Polanyi-Manes model was well-fit to represent the kinetic model. ▪ Stronger sorption of triclosan was observed due to high specific surface area. ▪ Sorption was directly affected by the electrostatic repulsive interactions among the MWCNT surface and compound	(Cho et al. 2011)
	Isoproturon	>96	16	▪ The adsorption capacity of the micropollutant decreased in the	(Sotelo et al.

Carbon nanotubes	Target micropollutant	Removal percentage (%)	Adsorption capacity/efficiency (mg/g)	Remarks	References
				multi-pollutant solution. ▪ Experimental data were the best fit by Freundlich isotherm; however, equilibrium adsorption data demonstrated that Langmuir data was well-represented. ▪ Temperature influenced the adsorption process with MWCNTs	2012)
$(NH_4)_2S_2O_8$-H_2SO_4-SWCNTs	17β- estradiol	99	27	▪ There is a slight elevate in SWCNTs diameter after acid treatment, noticed through Raman spectroscopy. ▪ The pseudo-second-order kinetic model was the best fit, noticed from the R^2 value.	(Zaib et al. 2012)
COOH-SWCNTs	Ethidium bromide	38.42	200	▪ Pseudo-second order kinetic model well-defined the kinetic model study ▪ Isotherm's study observed that Langmuir better-defined adsorption.	(Moradi et al. 2012)
COOH-MWCNTs	Carbamazepine	93	14	▪ Freundlich isotherm model well-defined experimental data. ▪ The pseudo-second-order kinetic model represented the kinetic data successfully.	(Cai et al. 2014)
	Alkylphenoletoxilates	94	18	▪ Freundlich isotherm model well-described experimental data. ▪ COOH-MWCNTs show extremely -ve surface charge at	(Patiño et al. 2015)

Carbon nanotubes	Target micropollutant	Removal percentage (%)	Adsorption capacity/efficiency (mg/g)	Remarks	References
				the operation parameters.	
Hydroxylated-MWCNTs	Norfloxacin	>94	72	▪ Freundlich isotherm well-presented the experimental data. ▪ The higher temperature is more likely favorable for the micropollutant sorption. ▪ The sorption process was thermodynamically favorable, predicted by noticing the -ve value of ΔG^o	(Wang et al. 2010)
O-MWCNTs	Triclosan	n/a	106	▪ Polanyi-Manes model was well-fit to represent the kinetic model. ▪ Sorption isotherm analysis with O-MWCNTs revealed that the chemical features of triclosan, MWCNTs' surface chemistry, and aqueous solution chemistry play a vital role in triclosan adsorption onto O-MWCNTs	(Cho et al. 2011)
NH_2-MWCNTs	Quinolone	93	160	▪ Freundlich isotherm model described the experimental data well. ▪ The highest adsorption was noticed, compared to other pollutants used in the research.	(Patiño et al. 2015)

2.5 Carbon nanotube-based magnetic nanocomposites

Carbon has been the most studied material for countless reasons, such as superior mechanical strength, high chemical stability and anisotropy, and conductivity. The scientific society has explored various morphologies of carbon, for instance, carbon nanofiber, buckminsterfullerene, activated carbon, graphene, and CNTs (Yu et al. 2012). Unique magnetic features are revealed when these materials are combined with magnetic nanoparticles. Magnetic carbon-based materials are very proficient materials that can introduce beneficial advancements in various operational areas (Kaiser et al. 2008). Researchers have merged the magnetic features with carbonaceous materials, resulting in porous and stable elements possessing magnetic properties (Poudel et al. 2018). Furthermore, the porous structure of carbon-based magnetic materials facilitates their applications in disciplines such as catalysis materials, electrode, and environmental remediation (Yee et al. 2014). Hence, it can be projected that carbon-based magnetic materials may have the capability as an innovative magnetic element by combining the magnetic features of nanoparticles and the remarkable mechanical strength of CNTs (Yu et al. 2016).

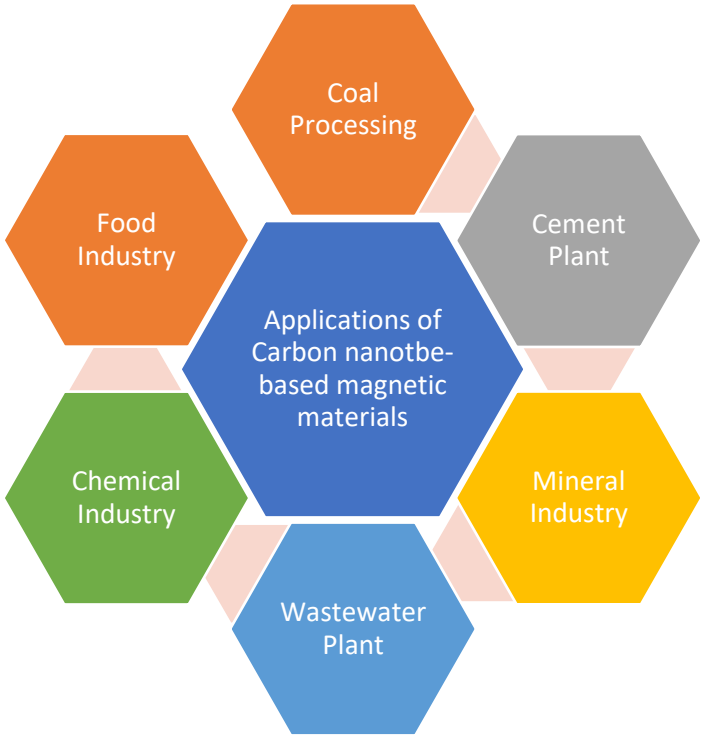

Fig. 2.6: Application of magnetic nanoparticles in different industrial sectors (Igwegbe et al. 2021)

Regarding water and wastewater treatment, magnetic nanoparticles, particularly maghemite, magnetite, ferrite collides, and hematite, are gaining considerable attention in research. Maghemite and magnetite are exceptional nanoscale materials applied in the biomedical field as adsorbents (Mamani et al. 2013). Particularly, magnetite nanoparticles possess a high surface area and adsorption capacity, which allow them to remove various impurities, such as heavy metal ions. Pristine magnetite nanoparticles have a few drawbacks; they tend to oxidize and rust in an acidic atmosphere. Moreover, disposal of aggregation through magnetic forces, will eventually decline its magnetic strength and adsorption capacity (Morel et al. 2013).

Consequently, surface modification of magnetic nanoparticles is required to restrict the aggregation. Therefore, oxides, polymeric compounds, and surfactants are generally used to enhance the strength of magnetic nanoparticles. Lately, magnetic nanoparticles' modification using organic molecules is getting significant attention and is employed in different industrial applications such as hyperthermia, drug delivery, and cell separation (Mohammad et al. 2015). However, modification of magnetic nanoparticles with suitable coating such as polymers, silica, chitosan, and various functional

groups, has been proven to be the most effective route. In an approach where magnetic separation and bio-sorption are merged, the efficient adsorption capability of aquatic pollutants can be observed with several advantages, such as cost-effective operation, environmentally friendly, and flexibility (Meng et al. 2018). Hence, it is more suitable for the magnetic nanoparticles to be mixed with contaminants efficiently and stored carefully due to their maximum ferromagnetism since water pollutants generally have non-magnetic characteristics. The utilization of magnetic nanoparticles for efficient contaminant removal is enhanced by their heightened ferromagnetic properties, allowing facile separation from the aqueous environment. To ensure optimal performance, proper storage is essential, involving measures such as maintaining a dry and controlled environment, stable temperature, protection from light, preventing aggregation, and regular inspection to sustain their efficacy and utility in environmental remediation.

2.5.1 Synthesis techniques

The popularity of magnetic CNTs has rapidly increased in the scientific society due to numerous aspects such as mass production, economics, and the potential to be employed for various applications (Samadishadlou et al. 2018). Fabrication of these nanocomposites through suitable techniques will dictate their efficiency. Multiple studies had been performed to discover effective fabrication routes to attain the finest, highly stable, and shape-controlled magnetic CNTs nanocomposites, for instance, filling, hydrothermal, arc-discharge, chemical vapor deposition, and pyrolysis methods. The advantages and limitations of a few well-known approaches for magnetic CNTs synthesis are summarized in ***Tab. 2.7***.

Tab. 2.7: Synthesis techniques for carbon nanotube-based magnetic nanocomposites

Approach	Advantages	Limitations	References
Hydrothermal	• Potential to maintain the nano-size structure • Crystalline phases can be developed	• Required extremely high temperature and pressure for operation	(Guo et al. 2021)
Pyrolysis	• Suitable for mass-production • Demonstrate good magnetic and mechanical features • Display ferromagnetic properties at ambient condition	• Difficult for magnetic nanostructure to be controlled • Not suitable in terms of process safety	(Chu et al. 2009)
Chemical vapor deposition	• Suitable for mass-production • Ease to control the nanostructure	• Required high consumption of energy • High operation cost • Complex equipment	(Amara et al. 2013)
Sol-gel	• The quality of the product can be adjusted • Recommended especially for carbon-based magnetic materials	• Raw material cost is very high • High permeability • Weak bonding	(Mahdiani et al. 2017)
Template-based	• Produce a good quality product • Nanostructure size and shape can be varied • Convenient and simple	• Required more than one stage to attain the product • Product quality is based on the template structure used	(Zhang et al. 2001)
Arc-discharge	• Cost-saving approach • The required product size can quickly be produced.	• Not categorized as a time-saving approach • Difficult to extract the product from the arc chamber • The requirement of the inert condition is	(Samadishadlou et al. 2018)

Approach	Advantages	Limitations	References
		must	
Self-assembly	• Efficient enough to control the properties of the produced material	• Challenging task to maintain the produced materials uniformity	(Whitelam et al. 2015)
Electro-spinning	• Ease operation approach • Suitable for mass-production • Time-saving • Cost-effective	• Required extremely high temperature	(Zhu et al. 2008)
Capillary-action	• Mostly employed for 3-D nanodevices	• Not suitable when substrate thickness is less than 100nm	(Bulmer et al. 2021)
Sono-chemical	• Convenient and simple • Particle size can be adjusted • Also suitable for metal oxide production	• Required extremely high temperature	(Theerthagiri et al. 2022)

2.5.2 Carbon nanotubes-based magnetic nanocomposites for micropollutants removal

In contrast to SWCNT, MWCNTs are more often used in research studies. Magnetic nanoparticles embedded with MWCNTs are usually produced using the chemical deposition of λ-Fe_2O_3 or Fe_2O_3 onto covalently modified MWCNTs; however, several other approaches are also designed for their production (Huang et al. 2015, Nasrollahzadeh et al. 2021). Currently, scientific researchers are more often considering magnetic modified CNTs for different contaminants in water sources. Yet, limited studies have reported the interaction between magnetic modified CNTs and pollutants in the aqueous environment (Bhatia et al. 2019, Peng et al. 2021).

Duman and co-associates compared the morphology and surface features of magnetic oxidized MWCNTs/ Fe_3O_4 and non-magnetic oxidized MWCNTs (Duman et al. 2019). The study demonstrated that magnetic oxidized MWCNTs displayed better adsorption capacity than non-magnetic oxidized MWCNTs/Fe_3O_4. Donghai and associates prepared magnetic ferrite (Fe_2O_4) modified MWCNTs that can be utilized to remove organic toxins from wastewater (Wu et al. 2017). While introducing Fe_2O_4 with MWCNTs was not very helpful for bezafibrate adsorption, it could be conveniently isolated magnetically and regenerated. Besides, MWCNTs loaded with iron metal-organic framework (MIL-53 (Fe)) composite had displayed high adsorption capacity, particularly for tetracycline antibiotics (Xiong et al. 2018). These research works reflected that CNTs-based adsorption materials could efficiently remove organic pollutants from different water sources. ***Tab. 2.8*** reviews selected publications on CNT-based magnetic nanocomposites for the treatment of micropollutants:

Tab. 2.8: Removal of aquatic micropollutant using different CNTs-based magnetic nanocomposites

CNT-based nanomaterial	Target micropollutant	Adsorption model	Max. adsorption capacity/ efficiency (mg/g)	Removal efficiency (%)	References
f-MWCNTs/ FeCl	Bisphenol-A Ketoprofen	Langmuir	2.7	>92	(Fard et al. 2018)
f-MWCNTs/ $(NH_4)_2.FeSO_4.6H_2O$	Nitrofurazone Furaltadone		7.5-14	92~94	(Zhen-Yuan et al. 2015)
f-CNTs/ Fe^{2+}/ $SrTiO_3$	Progesterone	-	2.5~7.5	97.19	(Razmkhah et al. 2018)
f-MWCNTs/ $FeCl_3$. $4H_2O$	Ibuprofen	Langmuir	1.2~12	>93	(Oba et al. 2021)
f-MWCNTs/ $FeCl_3$. $6H_2O$	Nicosulfuron	-	-	87.3	(Ma et al. 2016)
	Metsulfuron methyl			97.7	
	Chlorimuron ethyl			96	
f-MWCNTs/ $FeCl_2$	Carbamazepine	Redlich-Peterson	65	80	(Deng et al. 2019)
f-MWCNTs/ $CoFe_2O_4$	Sulfamethoxazole	Freundlich	7.4	>95	(Wang et al. 2015)
	17β- estradiol		19	70	
f-MWCNTs/ $FeCl_3$	Tonalide	Langmuir	2.6-2.9	>94	(Fard et al. 2018)
f-SWCNTs/ Fe^{2+} or Fe^{3+}	17β- estradiol Progesterone	-	-	>94	(Razmkhah et al. 2018)
f-MWCNTs/ $(NH_4)_2.FeSO_4.12H_2O$	Diclofenac	Langmuir	33	91	(Xiong et al. 2018)

CNT-based nanomaterial	Target micropollutant	Adsorption model	Max. adsorption capacity/ efficiency (mg/g)	Removal efficiency (%)	References
f-MWCNTs/ PAN/ TiO_2/NH_2	Naproxen	-	-	99	(Uheida et al. 2019)
	Cetirizine			96	
COOH-SWCNT/ Fe_3O_4	Paraquat		2.8	92.89	(Ruan et al. 2014)

2.6 Membrane technology for water-treatment

There was no membrane industry until the early twenties. The preliminary study on membrane separation phenomena was meant to explain the process physiochemical principles, and the diffusion mechanism (Samsami et al. 2020). Thomas Graham was the first to research gas separation using porous and dense membranes (Peydayesh et al. 2021). Moreover, he found that rubber showed selective permeability to various gases and discovered substances with lower molecular weight to be concentrated in the permeated gas when the membrane pore size is near to gas molecules' mean free path. Graham's research was further extended in 1856 by Schmidt, where bovine heart membranes were used for soluble Acacia separation (Kamali et al. 2019). However, the first membrane-based technique was introduced in 1970 for treating Cu (II), Zn (II), and Ni (II) found in electroplating water (Abdullah et al. 2019). The technique was successful as it was discovered that all the metals were removed. Since then, microporous structure membranes were made. Later, with advancement in polymer chemistry, many synthetic membranes were produced that were mainly used for polymeric membrane development. Such growth allowed researchers to produce a wide range of membranes with fundamental properties (Yang et al. 2020). In 1950, membrane technologies were first used for effluents treatment and considered suitable for polymer membranes' application for salt separation from water (Davenport et al. 2020).

In the late 1960s, the membrane processes entered industrial applications as feasible alternatives to conventional extraction, evaporation, or distillation methods (Sumida et al. 2012). Membranes can be categorized according to their surface chemistry, morphology, bulk structure, and production technique. However, asymmetric, dense, and porous membranes are well-known membranes widely used in separation industries (Yampolskii et al. 2020).

Several membrane processes have been discovered, for instance, pressure-driven membrane processes that include ultra-filtration, nanofiltration, microfiltration, and reverse osmosis. Pressure-driven membrane processes are vital to global water remediation and purification systems (Van der Bruggen et

al. 2003). Generally, the operating cost of membrane systems is linked with the high pressure required to remove dissolved pollutants, such as minor organic molecules (Le et al. 2016).

To remove organic solutes and dissolved ions, reverse osmosis and nanofiltration are mostly recommended; hence, high pressure is needed to operate these membranes, i.e., 600~7000 kPa. On the other hand, micro and ultra-filtration can be performed at much lower pressure, i.e., 34~400 kPa (Warsinger et al. 2018). Such approaches are currently an established part of many industrial processes. Membrane processes include nanofiltration and reverse osmosis for water purification and desalination, hemodialysis for artificial kidneys, and electro-dialysis in a caustic chlorine cell. Ultra-filtration is used in the food sector for protein separation from milk whey, genetic engineering, pervaporation for de-hydration of ethanol, etc. (Yan et al. 2020, Bernardo et al. 2020).

2.6.1 Carbon nanotube-based membranes

Carbon nanotubes (CNTs) play an essential role in membrane technology, especially for water purification, supporting low-energy explanations for water treatment. CNT-based membranes offer near-frictionless or frictionless water transports to retain a range of water pollutants such as dyes, desalination, heavy metal ions, and micropollutants (Al-Tohamy et al. 2022). Their high aspect ratio and even hydrophobic walls allow ultra-effective transportation of water molecules. CNT-based membranes can improve or change the membrane performance of reverse/ forward osmosis, micro-filtration, and nano-filtration in water cleaning and remediation (Ahn et al. 2012). It permits the CNT-based membranes to replace ultra-filtration and reverse osmosis with low energy consumption (Barrejón et al. 2022). One of the essential benefits of CNT-based membranes is that they do not require any pre or post-treatment when employed for water-related applications (Rashed et al. 2021, Das et al. 2014). A brief comparison between CNT-based and conventional membranes is presented in ***Tab. 2.9***:

Tab. 2.9: Comparison between CNT-based and other form of membranes

Membrane	Materials	Thickness (µm)	Operating Pressure (bar)	Permeability (m/Pa.s)	Advantages	References
CNT-based	CNTs, ceramics, or polymers	Depend on type	Varied with application	~$7x10^{-7}$	• Low consumption of energy • Operate in challenging environmental situations • Cost-effective • Resistance to fouling • High performance and durability	(Thamaraiselvan et al. 2018)
Nanofiltration	Organic polymers	~0.1	20 to 40	~ $40x10^{-12}$	• Low resistance to the problematic environmental situation • Low durability • Fouling susceptible • Not cost-saving as CNT-based membranes. • Good performance • High consumption of energy	(Oatley-Radcliffe et al. 2017)
Microfiltration	Polysulfone, polypropylene, polyurethane and so forth	50-100	<1	~$5x10^{-12}$	• Energy usage is moderate • Low performance and durability • Resistance is less to the severe environmental situation • Fouling susceptible	(Julian et al. 2022, Cheng et al. 2022)

Membrane	Materials	Thickness (µm)	Operating Pressure (bar)	Permeability (m/Pa.s)	Advantages	References
					• Cost is comparatively higher than CNT-based membranes	
Reverse osmosis	Organic polymer, for instance, polyether sulfone	~0.1 to 0.2	30 to 60	~$3x10^{-12}$	• Energy consumption is relatively higher • Good performance and low durability • Operate in serve environmental situation is same as micro and nano-filtration membrane • Fouling susceptible • Not economical as CNT-based membranes	(Abascal et al. 2022, Jiang et al. 2018)

Membrane	Materials	Thickness (µm)	Operating Pressure (bar)	Permeability (m/Pa.s)	Advantages	References
Ultrafiltration	Cellulose, acrylic, Polysulfone, and so forth.	150 to 300	1 to 10	~$0.5x10^{-10}$	• Energy consumption is moderate • Operate in serve environmental situation is low • Fouling susceptible • Performance is moderate • Durability is the same as micro, nano, and reverse osmosis filtration • Not cost-effective as CNT-based membranes	(Awad et al. 2021, Ahmad et al. 2020)

2.6.2 Types of carbon nanotube-based membranes

Carbon nanotube-based membranes are generally categorized according to the development approach; however, the two known classes based on literature are mixed matrix and free-standing CNT membranes. The two primary types of free-standing CNT-based membranes that are broadly employed for water-related applications are vertically aligned CNT and CNT-based BP membranes (Ali et al. 2019). Vertically aligned CNT membranes (VA-CNT) are distinct micro-structures of well-assembled cylindrical pores made from available CNTs arrays on a non-permeable substance that form a well-disciplined anisotropic structure to be employed in a range of applications (Ali et al. 2019). Since 1998 when aligned CNTs were fabricated using the CVD approach, VA-CNT membranes have been investigated (Das et al. 2014). These membranes have captivated an interest because of their steady mesoporous morphology, allowing them to be utilized in various filtration membrane applications (Hong et al. 2019).

Conversely, BP membranes hold macroscopic morphology consisting of CNTs with pristine thermal, physiochemical, and electrical strengths. The strength of CNT-based BP membranes is provided by π-π interaction and Van der Waals forces among the attached nanotubes (Sweetman et al. 2017, Selvaraj et al. 2020). CNT-based BP membranes provide an extremely porous 3-D framework created by interstitial gaps among the nanotubes, making them promising for catalysis and adsorption in addition to separation applications (Yang et al. 2013, Bhol et al. 2021).

The mixed matrix CNT membranes possess a morphology analogous to the fine-film composite reverse osmosis membranes, where the upper layer is hybrid polymer and CNTs (Bounos et al. 2017). All of the mentioned types of CNT-based membranes have their own merits and demerits. For instance, fabrication techniques of CNT-based BP and mixed matrix CNT are simple compared to VA-CNT membrane (Vatanpour et al. 2017, Zhao et al. 2021). ***Tab. 2.10*** lists the different research works that has been published based on CNT-based membranes for various applications:

Tab. 2.10: Few of the recent publications on CNT-based membranes for various applications

Carbon nanotube membranes	Synthesis route	Functionalization technique	Application	Remarks	References
Vertically aligned carbon nanotube membrane	Encapsulation+ plasma etching	Carboxyl groups	CO_2 separation	• The prepared membrane approach has the potential to be commercialized • Displayed gas permeability with purified SWCNT greater than pristine SWCNT	(Surapathi et al. 2011)
	CVD+ polymer infiltration	-	Water contamination	• The research results concluded that water flux is 3 times more significant on the developed membrane than the ultra-filtration membrane; moreover, water transport is 70000 times higher. • The rejection property is the same as ultra-filtration membranes. • Good bio-fouling resistance, i.e., 15% less permeate flux drop.	(Baek et al. 2014)
	CVD+ vapor phase infiltration	Air plasma	Protective fabrics for both domestic and military settings	• Allow elimination of $\geq$5nm analyze via size exclusion. • Study results confirmed that the membrane offers adequate safeguard from the biological threat.	(Bui et al. 2016)

Carbon nanotube membranes	Synthesis route	Functionalization technique	Application	Remarks	References
Carbon nanotube-based buckypaper membrane	Shear pressing	-	Sensors, filters or bio-scaffolds	• Tensile analysis showed good tensile and mechanical strengths, >400 MPa. • Produced millimeter-long CNT film with high CNT alignment.	(Zhang et al. 2020)
	Vacuum filtration	Nitric acid-treated	Structural material for developing high volume fraction nanocomposites	• The study results revealed that the CNT-based BP membrane's mechanical strength increased by improving the power of oxidation agents. • The porosity of the membrane is affected by increasing the density of polar functional groups.	(Zehua et al. 2012)
	Vacuum filtration	Carboxyl groups	Organic pollutant removal	• The prepared film was employed to remove organic pollutants from the aqueous phase, and it showed the removal of 93% of humic acid. • The attachment of functional support the hydrophilicity aspect of CNT	(Thamaraiselvan et al. 2020)
	Vacuum filtration	Propane-2-ol	Salt removal	• The prepared film is exceptionally hydrophobic (113^0) and porous (90%) • The film displayed a 99% salt removal and flux rate of approximately 12 $kg.m^{-2}.h^{-1}$.	(Drioli et al. 2015)

Carbon nanotube membranes	Synthesis route	Functionalization technique	Application	Remarks	References
Mixed matrix CNT membrane	Phase inversion	Carboxyl groups	Water pollutants removal	• Displayed good hydrophilic aspect • The pore size of the membrane increased up to 1.5% wt. Content of MWCNTs, and declined after 4% wt. content of MWCNTs • The membrane displayed high flux demonstrates low rejection, and vice versa	(Cong et al. 2007)
	Phase inversion through immersion precipitation	Carboxyl groups	Organic pollutants removal	• The result showed improved anti-fouling properties • Adequate egg albumin (protein) removal from the aqueous phase, i.e., 88% • Hydrophilicity properties enhanced due to the use of modified MWCNTs.	(Khalid et al. 2015)
	Interfacial polymerization	Carboxyl groups	Salt removal	• The analysis result showed a 51.5% higher flux rate in comparison to raw MWCNTs/ PP film • An incline in the mass transfer coefficient, i.e., 1.5 times higher • Obtained high salt removal rate, i.e., 99.9%	(Roy et al. 2014)
	Blending	Carboxyl groups	Salt removal	• The result showed an increase of 54% in permeate flux and salt removal of 99.9%	(Bhadra et al. 2016b)

Carbon nanotube membranes	Synthesis route	Functionalization technique	Application	Remarks	References
				• Mass transfer coefficient is comparatively higher pristine MWCNTs/ PTFE film • Also displayed good stability without wetting and anti-fouling problems	

2.6.3 Carbon nanotube-based membranes for micropollutant removal

The primary aim of water treatment is to get rid of undesired components. Membranes offer a physical obstacle for such components based on their size, allowing them to employ unconventional water sources (Shen et al. 2011). As the vital part of water cleaning and purification, they provide superior-level automation, reduce the use of chemicals and land, and their modular structure gives flexible design (Rodrigues et al. 2019).

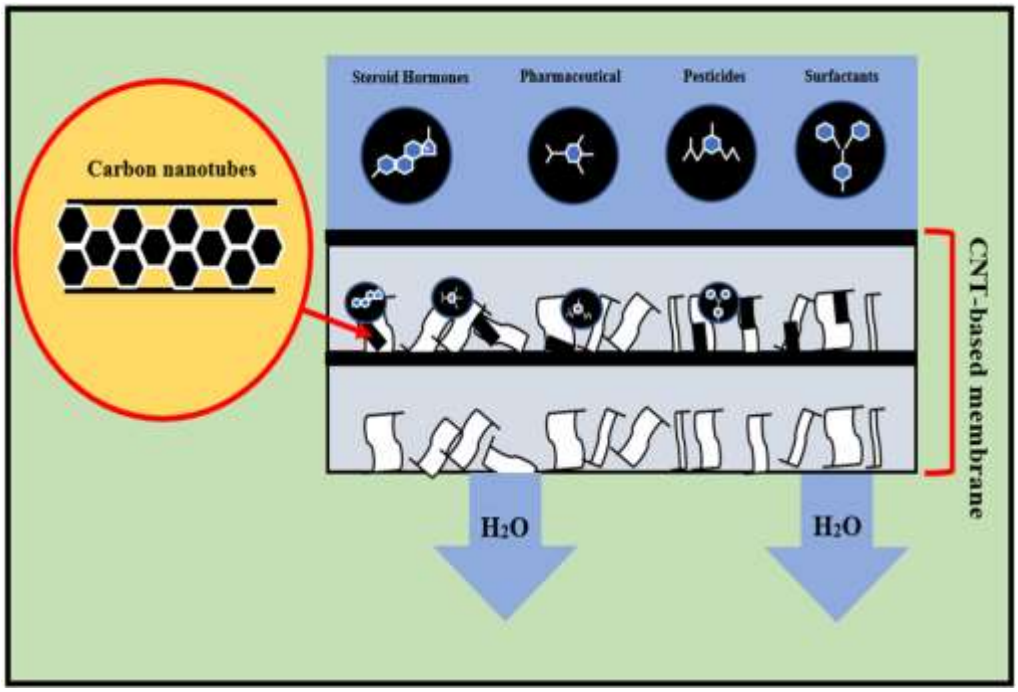

Fig. 2.7: Adsorption mechanism of CNT-based membrane (Khan et al. 2021)

A significant barrier of membrane technology is the fundamental trade-off between membrane permeability and selectivity. The consumption of excess energy is an imperative barrier to the wide-spectrum applications of pressure-driven membrane processes (Jafari et al. 2015). Membrane fouling combines the energy utilization and difficulty of the process design and operation. Moreover, it reduces the modules and lifespan of membranes (Westerhoff et al. 2016). The efficiency of the membrane system is mainly determined by the material used for the membrane. Reinforcement in functional nanomaterials into membranes offers great potential to enhance their fouling resistance, permeability, thermal and mechanical strength, moreover, providing modern

functions for pollutant degradation and self-cleaning (Fan et al. 2016, Yan et al. 2018).

Recently, there is an immediate concern in developing novel materials for water cleaning and remediation, desalination, and many other membrane technology applications. They have received considerable attention from the scientific community regarding pollutant-free safe, clean water, specifically CNTs, and CNT-based membranes (Pendergast et al. 2011). Notably, the application of CNT-based membranes was acknowledged a long time ago, but their use as filtration has been introduced lately. Several research studies have been performed on the feasibility and potential of CNT-based membranes for wastewater treatment due to their exclusive features, such as a high range of water flux and fouling resistance (Lu et al. 2020). CNT-based membranes have been employed in membrane distillation, capacitive deionization, and pressure-driven filtration for water purification. Moreover, CNT-based membranes, particularly BP membranes, have been recommended as self-heating and supercapacitor materials for de-icing applications (Mpatani et al. 2021). The schematic representation of the adsorption mechanism of CNT-based membranes is illustrated in ***Fig.2.7***.

Micropollutants, organic pollutants, are generally referred to as endocrine-disrupting chemicals that have been typically found in water and wastewater. Most CNT-based membranes with water and wastewater treatments are focused on salt rejection, heavy metal ions, and dye removal (Santhosh et al. 2016). ***Tab. 2.11*** lists information on the removal of selected micropollutants by CNT-based membranes technology based on literature studies.

Tab. 2.11: CNT-based membranes employed for micropollutants removal

CNT-based membrane	Target micropollutant	Removal efficiencies	Remarks	References
Polyvinylidene fluoride/ f-MWCNTs/ laccase	Diclofenac	95	• The highest removal efficiency was received within 4 hrs. • The results displayed adequate operational and thermal strength due to the immobilized laccase. • The findings suggested that the fabricated PVDF/ f-MWCNT/ laccase membrane is appropriate for water and wastewater treatment applications. • Self-cleaning and re-coating presenting new opportunities towards sustainability and long-term applications	(Masjoudi et al. 2021, Ji et al. 2016)
	Bisphenol-A	85		
	Ibuprofen	63		
	Clofibric acid	52		
f-SWCNTs/ Fenton	Amoxicillin	97	• Studies displayed a high removal rate and water permeability (19.6 L/m^2.h.bar). • It can be predicted to be used for various aquatic micropollutant. • Reliability was further observed by comparing experimental and predicted results analyzed by ORIGIN software.	(Jiang et al. 2021)
	Ampicillin	94		
	Florfenicol	91		
	Carbamazepine	85		
Polyethersulfone/ f-SWCNTs	17β-estradiol	72	• Demonstrated high permeability and removal efficiency within the range of 50- 75% from 100 ng/L feed solution. • Adsorption kinetics were rapid, and adsorption was independent of retention time, ranging from 0.08-7.1. • Displayed poor adsorption, ranging from pH 11 to 12. • The prepared membrane could not meet the European guidelines, i.e., 99% removal.	(Mpatani et al. 2021)
	Progesterone	75		
f-MWCNTs	Caffeine	93	• Filtration of pharmaceuticals and PPCs by the prepared membrane is an essential pre-treatment approach.	
	Carbendazim	97		

CNT-based membrane	Target micropollutant	Removal efficiencies	Remarks	References
Sodium dodecyl sulfate/f-MWCNTs/ polypropylene	Cortisone	97	• The fabricated membrane was reliable and effective in removing various glucocorticoids • Linearity range from 0.2 to 100, and the limit of quantification (LOQ) from 0.065 to 0.326 ng/mL. • Results showed high time efficiency, good reproducibility, low consumption of solvent, and high precision with RSDs of <10%.	(Fallah et al. 2021)
	Hydrocortisone	71		
	Prednisolone	78		
	Hydrocortisone butyrate	64		
	Budesonide	88		
Nickle-Cobalt/ f-MWCNTs	Ibuprofen	80	• Removal efficiency decreased with increasing pH to 11. • Displayed high performance and stability.	(Goh et al. 2021)
Polyethersulfone/ f-SWCNTs	Bisphenol A	80	• Removal efficiency increased with an increase in the %wt. content of f-SWCNT, however, too high %wt. content of f-SWCNT leads to saturation and probably declines the removal rate. • Fouling of membrane also showed favorable outcomes with the increase in the %wt. content of f-SWCNT • Due to the hydrophobic nature of the organic micropollutant, it can be understood that high adsorption leads to an increase of removal for increasing the %wt. content of f-SWCNT	(Kang et al. 2019)
	4-Nonylphenol	84		

CNT-based membrane	Target micropollutant	Removal efficiencies	Remarks	References
Polyethersulfone/ nitrogen-doped SWCNTs	Carbamazepine 4-Nonylephenol Bisphenol A Galaxolide Tonalide Caffeine	89 99 99 99 99 87	• Results show the potential to employ the prepared membrane for various organic micropollutant • Water flux improved with the addition of nitrogen-doped SWCNTs to raw PES • The prepared membrane displayed good porosity and a large specific area, i.e., 0.37±0.03 cm^3/g^1 and 94.3±0.06 m^2/g, respectively. • Findings displayed good chemical, mechanical, and fouling resistance properties	(Kaminska et al. 2015)
Polyethersulfone/f-SWCNTs	17β estradiol	>75	• In most studies, the complete breakthrough was not attained due to the high adsorption capacity of SWCNTs • Results demonstrated the ambitious drink water target; however, European regulations were not met.	(İlyasoglu et al. 2022)
Polyvinyl chloride/ f-MWCNTs/ Fe_3O_4	Norfloxacin Bisphenol A	23 65	• Retentions for both pollutants decrease with the increase in pressure • Findings showed minor effects of ionic strength and initial concentration on retentions	(Wu et al. 2016)
f-MWCNTs	Ciprofloxacin	>99	• Results concluded that the prepared membrane is a promising candidate for antibiotics removal from the aqueous phase. • Finding also revealed that f-MWCNTs showed higher filtration efficiency compared to pristine or modified SWCNTs	(Dong et al. 2018)
Polyethersulfone/ f-SWCNTs	B-endosulfan	>99	• Results confirmed that the prepared membrane has the potential to be employed for micro-contaminants • Pristine SWCNTs show lower adsorption efficiency than modified SWCNTs	(Adamczak et al. 2021)

CNT-based membrane	Target micropollutant	Removal efficiencies	Remarks	References
MWCNTs	Ibuprofen Bisphenol	>90	• Satisfactory sorption performance • Findings revealed that cross-flow configuration display great potential in removing the organic micropollutant • Excellent antifouling resistance, efficient solute transport under hydrodynamic flow, and higher retention time in eliminating organic pollutants compared to previously researched work	(Bakr et al. 2019)
SWCNTs	17β estradiol	70	• Findings discovered that the prepared membrane is a promising material. • High adsorption determined	(Lu et al. 2022)
TiO_2/MWCNTs	Carbamazepine Acetaminophen	80 24	• Higher reusability of the membrane • Findings displayed that the effect of pH on adsorption of pharmaceutical micropollutant achieved the maximum loading on the sorbent at equilibrium saturation	(Zaib et al. 2013)

2.7 Carbon nanotube-based buckypaper membrane

The filtration process is restricted due to issues associated with the currently available membrane, including low solute selectivity, limited lifetime, and fouling (Wang, Zhang, et al. 2020). Currently, extensive attention has been given to developing innovative materials for gas separation, water purification, desalination, and several other membrane filtration applications. Concerning water purification from various pollutants, CNTs have gained substantial attention as a membrane. Therefore, molecular dynamic simulations have demonstrated that CNT-based BP membranes are remarkably permeable to gases and liquids. Even though the scientific community has acknowledged BP membrane for an extended period, its filtration-associated uses were only explored lately (Werber et al. 2016). Consequently, BP membranes can be an appropriate candidate for water purification at the commercial level (Goh et al. 2019). Furthermore, several research studies have observed their potential to filter solute and nanoparticles selectivity depending on different sizes. For instance, Wang and co-associates had demonstrated that graphene oxide membranes exhibited preferential permeation of smaller ions while effectively blocking larger molecules (Wang et al. 2019).

2.7.1 Fabrication routes

The enhancement of preparation methods that improve the yield and properties of CNT-based BP membranes has gained attention in the scientific society. Based on the preparation conditions, the development method of CNT-based BP membranes can be categorized as dry and wet approaches. Compared to the dry process, the wet approach is convenient and straightforward (Luo et al. 2017). Moreover, the CNT-based BP membrane developed using a wet method displays good properties due to the fact the product quality can be controlled. Currently, the wet approach is typically limited to laboratory scale. The dry process is utilized for commercial fabrication and can produce mass production at an economical cost (Wang et al. 2021, Zhu et al. 2022). Nevertheless, the

dry approach requires complicated reaction conditions and the properties of the developed membrane, which cannot be maintained or controlled.

Dry Approach: The primary principle of the dry approach is to consider micro-molecular hydro-carbons as raw materials and constant reaction with catalysis and high pressure to produce CNTs (Xia et al. 2020, Lee et al. 2016). The pristine CNTs are constantly gathered on the deposited panel to develop compact BP directly (El-Aswar et al. 2022). Different hydro-carbon materials can be used in the fabrication method as carbon precursors such as tri-chloro-benzene with nickel, iron, or any other transition metal used as a catalyst (Ramezani et al. 2022). The membrane produced using this approach is quantify. The process has several limitations, such as its complex approach and composition, which involves intricate steps and precise controls over various parameters. Besides, this process may generate high amounts of residual catalyst that need to be carefully managed and disposed of. However, economic and mass production are the essential advantages of using this approach for commercial purposes. It has been noted in the literature that 20 g/m^2 of CNT-based BP membrane using tri-chloro-benzene costs about 3 to 50 $\$/m^2$ (Hou et al. 2022, Liu et al. 2022). To enhance the homogeneity of the CNT-based BP membrane, CNT arrays were compressed or filtered to develop an aligned CNT-based BP membrane. However, the BP produced was small in size because of the CNT array size. Furthermore, CNT-based BP membrane developed using CNT arrays is not cost-effective; it costs around 5000 to 12000 $\$/m^2$ depending on the CNT array cost (Sakurai et al. 2013, Gross et al. 2018).

Wet Approach: This approach is the most recommended for developing CNT-based BP membranes. The underlying principle of this approach aligns with paper technology, involving two distinct stages: synthesis and filtration of CNT suspension (Amjadi et al. 2016). The specific content of CNTs and surfactants are combined using mechanical stirring and sonication to attain uniform suspension. Later, the suspension is washed and filtered until the mat form materializes without any residual traces of the mixed solvent (Zhang et al. 2019, Sharma et al. 2020). The most known surfactants are Triton X-100 and

poly-vinyl-pyrrolidone. The membrane developed using this approach needs to be even smaller than 1 µm (Jun et al. 2019, Gao et al. 2022).

In this approach, suspension and filter mat are the primary factors directly affecting the CNT-based BP membrane quality in the preparation method. To enhance the preparation method and characteristics of CNT-based BP membranes, the scientific community has directed its attention towards enhancing the wet process. For instance, efforts have been made to reinforce the van der Waals interaction between hydrogen bonds and CNTs (Azam et al. 2018). One of the disadvantages of this approach is that the BP membrane developed is small (µm) and expensive, limiting its application for commercial purposes (Schneider et al. 2015). Accordingly, a CNT-based BP membrane of 20 g/m^2 costs around $3 to $500 and $1000 to $6000 for MWCNTs and SWCNT, respectively (Schneider et al. 2021). ***Tab. 2.12*** lists the various methods falls under the category of dry and wet approach that have been employed for the fabrication of CNT-based BP membranes along with their advantages and disadvantages:

Tab. 2.12: Advantages and disadvantages of preparation approaches for CNT-based BP membranes

Preparation Approaches	**Advantages**	**Disadvantages**	**References**
Domino Pushing	Adequate and convenient approach, high electrical and thermal properties	Time-consuming, high pressure required	(Oh et al. 2015)
Shear Pressing	Time-saving, satisfactory volume fraction, stiffness, strength, and degree of alignment	Unpredicted thickness, high pressure required	(Li et al. 2015)
CNT Drawing	Lengthy sheet, display density, and thickness of 0.5 g/cm^3 and 50 nm, respectively	Inappropriate for CNT forest, can form bundles	(Chitranshi et al. 2020)
Drop Casting	Fast and straightforward approach, cost-effective, large-scale production	Low solubility and CNTs' properties, difficulty to control the thickness, and no uniform coating	(Nardecchia et al. 2013)
Electrophoretic	Display satisfactory macroscopic homogeneity, economical and straightforward approach	Low yield, a specific range of particles are required for good deposition, display more cracks<0.06 nm	(Besra et al. 2007)
Rod-coating	Economical, thickness adjustable, simple approach	Coating viscosity is an issue; optimal speed needs to attain membrane	(Wang and Guo 2020)
Tape-casting	Range of membrane geometry, foldable and mass-scale production, adequate thickness, and density	Required mechanical pressing, limited application due to the width	(Susantyoko et al. 2017)
Ink-jet Printing	Fast production, dimensions can be adjusted	Employ for specific CNTs' diameter, restricted to commercial applications, low mechanical strength	(Chatzikomis et al. 2012)

Preparation Approaches	Advantages	Disadvantages	References
Vacuum Filtration	Wettability can be controlled, the potential to produce the thinnest membrane	Lengthy fabrication procedure, limited to lab-scale, low thickness, high pressure required	(Zhou et al. 2018)
Air Spraying	Can produce long and thickness membrane, potential to be used for large range devices	Surfactant and high temperature is must, surfactant challenging to extract	(Abdelhalim et al. 2013)
Vapor Deposition	Fabricate at room temperature, adequate gap-filling, leakage free	Not suitable for mass-scale production, high cost	(Zhang et al. 2015)
Non-filling	Filter nano-scale poliovirus and bacteria, high porosity, simple approach	Low mechanical stability, suitable for specific applications only	(Saraswathi et al. 2019)
Polymer Injection	Simple approach, mechanical durability, produces a thin membrane	Interstitial filler required may cause air bubbles between CNTs	(Park et al. 2017)
Densification	High pore density, classified as capillary and mechanical compression densification	Not suitable with smaller CNT diameters, difficult to separate the substrate, difficult to manipulate	(Lee et al. 2017)

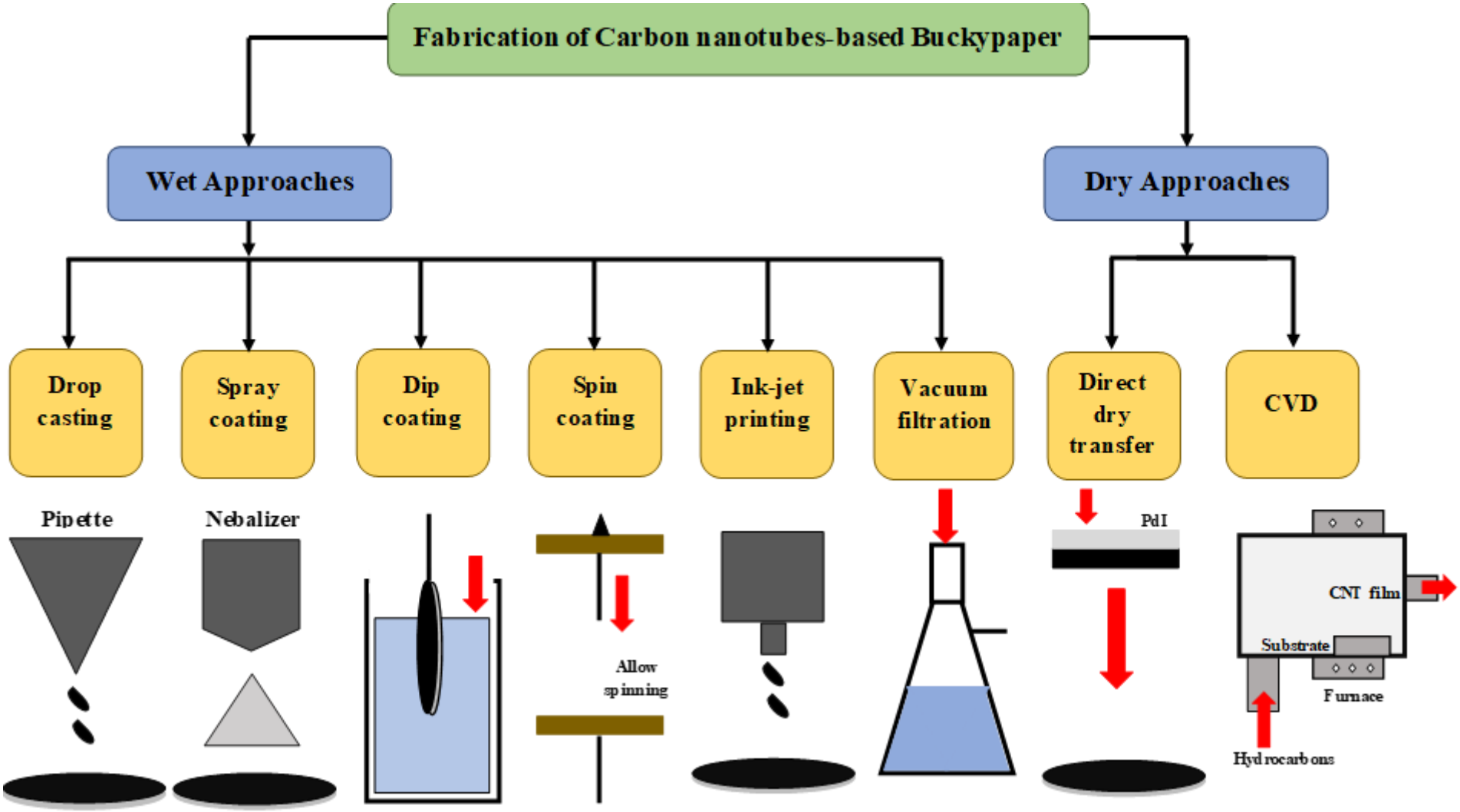

Fig. 2.8: Simplified illustration of few known fabrication approaches of CNT-based BP (Rathanasamy et al. 2021)

2.7.2 Carbon nanotube-based buckypaper for micropollutant removal

Recently, there has been an immediate concern in developing novel materials for water cleaning and remediation, desalination, and many other membrane technology applications. These materials have received considerable attention from the scientific community regarding pollutant-free safe, clean water, CNTs, and CNT-based membranes (Saraswathi et al. 2019). Notably, the application of CNT-based membranes was acknowledged long ago, but their use as filtration has only been introduced lately. Several researches have been performed on the feasibility and potential of CNT-based BP membranes for wastewater treatment due to their exclusive features, such as a high range of water flux and fouling resistance (Adeleye et al. 2016). CNT-based BP membranes have been employed in membrane distillation, capacitive deionization, and pressure-driven filtration for water purification (Gasim et al. 2022, Shukla, Giri, et al. 2021).

Based on a literature review, it has been observed that energy consumption via CNT-based BP membrane, particularly for desalination, can be exceedingly lower than that of a reverse osmosis system because the molecules of water passing through nanotubes are around double to five times greater than the hypothetical prediction via the equation introduced by Haggen Poiseuille (Park et al. 2017). A study performed by Dumee and co-associates analyzed the performance of CNT-based BP membrane in direct contact membrane distillation. The result revealed that the CNT-based BP membrane is highly porous, thermally conductive and hydrophobic (Dumée et al. 2011, Bhadra et al. 2016a). The prepared membrane was used for salt rejection from synthetic water, and it showed 99% rejection, making it a suitable candidate for desalination.

Regarding micropollutant removal, limited studies have been found in literature, as most research works have been performed for salt, heavy metals, and dye removal using CNT- based BP membranes. Fontananova and co-associates employed a CNT-PVDF membrane to remove ibuprofen and acetaminophen, and the result showed a removal of 95% for both

pharmaceutical micropollutants (Fontananova et al. 2015). The removal mechanism of CNT-based membranes for micropollutants generally occurs because of hydrogen bonding, Van der Waals interactions, π-π interactions, and chemical adsorption between the micropollutants and CNT-based materials.

Likewise, for the elimination of inorganic pollutants, the competition among various organic chemicals in water may appear on the CNT surface, which effectively declines the adsorption of organic pollutants. Thus, tailoring the surface features of CNT for selective adsorption of various organic pollutants is an essential study task for improved water treatment (Shanmuganathan et al. 2017, Parida et al. 2021).

2.8 Mathematical modelling

2.8.1 Adaptive neuro-fuzzy inference system (ANFIS)

Interpretation of the dynamics of non-linear systems based on conventional mathematical tools is problematic due to the unavailability of systematic tools to deal with uncertain and ill-defined systems. Using a fuzzy if-then strategy, a fuzzy interference system can model the qualitative aspects of human knowledge and reasoning procedures but lacks a standard design approach to utilize detailed quantitative analyses. Neural networks (NN) detect data patterns, understand relationships, and adapt to them. This knowledge can then be used to forecast the aftermath for new combinations of data (Baghbani et al. 2022, Mohan et al. 2021). The control approach in fuzzy identification was initially introduced by Takagi-Sugeno-Kang and has been extensively employed in several fuzzy-control applications for decision making, medical diagnosis, and problem-solving based on data mining (Badnjevic et al. 2018, Precup et al. 2020). Hence, a few elementary features of this approach are required for comprehensive understanding. More precisely, the lack of a standard design approach and the optimization process to convert human knowledge into a fuzzy interference system's rule base and database (Karaboga et al. 2019, Haznedar et al. 2018). It is difficult to understand the tuning of the

membership function, lessen output error-index, and select a suitable network structure.

Owing to the salient features of NN and its embedding with the rule-based fuzzy logic, the adaptive neuro-fuzzy interference system (ANFIS) has been developed and significantly considered to represent a non-linear system. This system, which is the combination of NN with fuzzy systems, has the benefit of offering a straightforward interpretation of the final system into if-then set rules, and the fuzzy system can be observed as a neural network structure with the information distributed throughout the connection strengths (Dastjerd et al. 2019, Khashei et al. 2012). The research on ANFIS by scientific community has stated that the neural and fuzzy systems are supportive in the sectors such as the applicability of the current algorithm for ANNs, and the adaption of information articulated as a set of fuzzy linguistic rules (Arab et al. 2021). The system can be learned in a forward and backward phase. In the forward phase, learn the algorithm, subsequently identify the minimum squares estimate, whereas, in the back step, the error signals, which are the derivate of squared error with respect to every node output, propagate backward from the output to the input layer (Jiang et al. 2022, Ahmadi et al. 2018). The premise parameters are updated via the gradient descent algorithm in the backward pass. The primary advantage of this system is that it converges too fast, as it reduces the search space dimensions of the back-propagation technique employed in neural networks (Arrieta et al. 2020). In general, ANFIS is the fuzzy Sugeno model in the adaptive system framework, which helps model building and justifies the developed model to facilitate training and adaptation. One of the primary benefits of ANFIS is that it has the smoothness features from the fuzzy principle and adaptability from neural networks training structure. It has been extensively employed in the engineering sector (Choi et al. 2015, Kampouropoulos et al. 2014).

2.8.1.1 Designing the ANFIS model

An adaptive framework is a multi-layer feed-forward network consisting of nodes joined via a direct link. Every node plays a specific function on the node input, besides a set of parameters that refer to this node. Every link in the adaptive network indicates the direction of signal flow from one another node; no weights are connected with the connection (Marani et al. 2020, Sarıkaya et al. 2021). The primary objective of ANFIS is to determine the optimum values of the equivalent fuzzy interference system parameter by using a learning algorithm. The optimization of parameters must be done to minimize the error between the target and the actual output. ANFIS employs a hybrid algorithm for optimization, combining gradient descent and the most minor square estimate techniques (Selimefendigil et al. 2018). The parameters that are optimized in ANFIS are the premise parameters. These parameters reflect the member functions' shape. Several optimization strategies can be used later to reduce the error, constituting the member functions (Sehgal et al. 2014). The parameter set of an adaptive framework offers fuzzy systems to learn from the data they are modeling.

While designing the ANFIS model, the number of member functions, fuzzy rules, and training epochs must be tuned accurately (Tung et al. 2020). Mapping those parameters is crucial for the system as it may follow the system to over-fit or enable it to fit the data. This adjustment can be made via a hybrid algorithm (Nishant et al. 2020, Collins et al. 2021). A lower difference between the ANFIS output and desired objective, describes a more accurate ANFIS system. ***Fig. 2.9*** illustrates the basic design of the ANFIS system

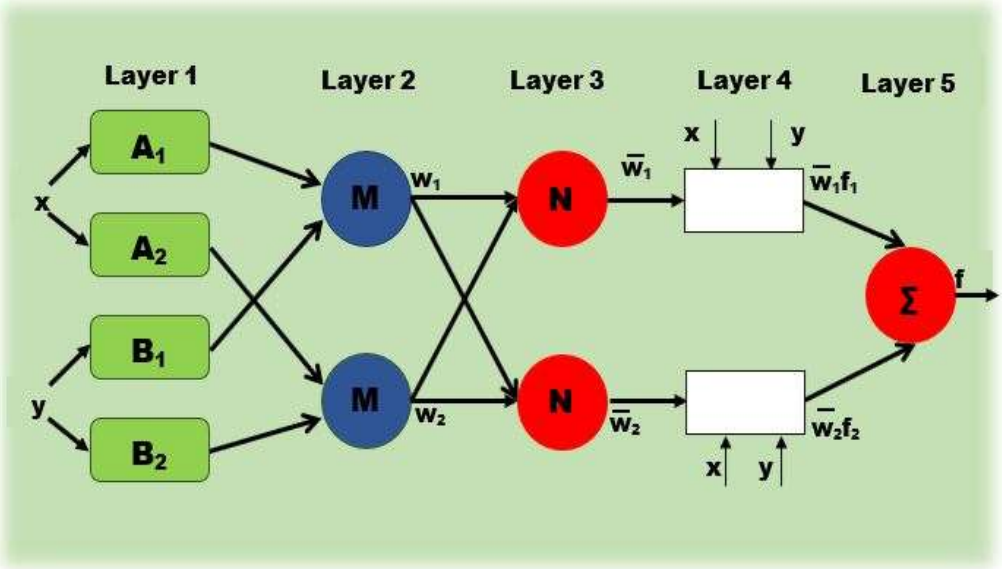

Fig. 2.9: ANFIS structure (Pae et al. 2018)

A brief description of each layer along with its mathematical expression is described in ***Tab. 2.13***:

Tab. 2.13: Layers of the ANFIS (Merabet et al. 2017, Djamila et al. 2018)

Layer	Description	Equation
1	• It is known as the fuzzy layer • Each node in this layer is a square node with a node function • In this layer, parameters are labeled as premise parameters	$O_i^1 = \mu_{Ai}(x)_i$ O_i^1= member function of A_i A_i= linguistic label linked with node function μ_{Ai}= member function x =input to node i
2	• The primary purpose of this layer is to identify the weight of member functions and label as M • It gets the input value from the first layer and acts as a member function. • Each node is a fixed node, and output is determined through the product of all incoming signals	$O_i^2 = w_i = \mu_{Ai}(x).\mu_{Bi}(y)$ i= 1,2,….
3	• Each node is marked as N, expressing normalization to the firing strength from the prior layer • This layer performs pre-condition matching of fuzzy rules • The ith determines the ith rule's firing strength to the addition of all the firing strength rules. • The output of the third layer is known as normalized firing strength	$O_i^3 = \overline{w_i} = \frac{w_i}{w_1 + w_2}$ i= 1,2,…...
4	• Each node in this layer is a square node with a node function • The parameter in the fourth layer is called consequent parameters	$O_i^4 = \overline{w_i}\, f_i = \overline{w_i}(p_i x + q_i y + r_i)$ p_i,q_i, r_i = consequent parameters i= 1,2,….

Layer	Description	Equation
5	• This layer comprises of single fixed node and is marked as Σ • This layer offers the summation of all the input generated from the fourth layer and transforms fuzzy classification results into crisp values	$O_i^5 = overall = \Sigma \overline{w_i}\, f_i = \Sigma \frac{w_i f_i}{w_i}$

Hence, it is noticed that when the premise parameters' values are fixed, the overall output of the adaptive network is known as a linear combination of consequent parameters (Ho et al. 2002, Svalina et al. 2013). Besides, it can also be observed that the ANFIS architecture comprises two adaptive layers, namely the first and fourth layers.

2.8.1.2 Applications of the ANFIS model

It is crystal clear that conducting an experimental study on various aspects is expensive and time-consuming. Therefore, it would be essential to have a tool to predict, such as artificial intelligence. In this regard, Kumar and co-associates used the ANFIS system to predict the surface roughness in turning operations (Kumar et al. 2015). Different parameters were used as input to encode the problem, such as feed rate and cutting speed. The experimental data and ANFIS values showed that the ANFIS system displays satisfactory prediction accuracy.

Tamer and co-associates initially introduced the use of ANFIS in medical diagnosis. They used the Takagi Sugeno Kang (TSK) model to predict the presence of mycobacterium tuberculosis. The ANFIS model was developed based on 250 records (Uçar et al. 2013). The proposed model indicated the instance with the exactness of 97%; however, the rough algorithm showed 92% accuracy. This learning has played an essential role in predicting the patients even before the medical examination. Marzi and co-associates utilized this model as a temperature water controller system (Marzi et al. 2017). The study concluded that ANFIS is a more suitable controller than the PID controller. Bahrami and co-associates used the ANFIS to predict the thermo-physical properties of nano-fluids (Bahrami et al. 2019). Alrashed and co-associates used the thermo-physical properties experimental data of Cu-water nanofluids and used the ANFIS approach to prognosticate (Alrashed et al. 2018). The research revealed that the ANFIS has a good capacity for predicting the thermos-physical features of nano-fluids.

The ANFIS model has also been employed in water and wastewater treatment research studies to predict the quality of effluent and adsorption efficiency of the material. Muhammad and co-associates proposed this model for the removal of nitrogen and carbon removal in the sewage treatment plant (Gaya et al. 2014). The simulation results showed better prognosticate in all the considered variables, i.e., COD and ammonium nitrogen. Thus, the study concluded that the proposed ANFIS model was suitable for the wastewater treatment plant. In another study, the ANFIS model was proposed to forecast anaerobic digestion discharge quality. The model was compared with mean absolute percent error (MAPE) and root mean square error (RMSE); hence, results obtained from the ANFIS model displayed higher model feasibility on the anaerobic system (Erdirencelebi et al. 2011). The ANFIS model has been proposed to predict the membranes' adsorption capacity towards dye removal, methylene blue (Lau et al. 2020, Rashed et al. 2021). Experimental studies showed that methylene blue removal efficiency mainly depended on process parameters such as pH, rotation speed, and reaction time. Therefore, the same process parameters were used in the ANFIS model as input to predict. The simulation results displayed higher dye removal efficiency, i.e., 99.7%. The RSM model was also used; however, the ANFIS model showed higher removal prediction efficiency. This study thus demonstrated that the prepared membrane could be employed for practical application, particularly for industrial dye effluent.

Based on the above published scientific literature, it is well understood that the ANFIS has the potential to be employed for modeling, predicting and controlling studies in chemical engineering processes, likewise other machine learning methods (Emembolu et al. 2022, Hanumanthu et al. 2021). In this proposed work, ANFIS is used as a primary source for the prediction of FZD micropollutant elimination using the prepared membrane for large-scale applications (Karaboga et al. 2019, Zhou et al. 2022). Once the model is successfully built on ANFIS, the model can be utilized for predicting the removal efficiency of FZD micropollutant using an appropriate prediction approach.

CHAPTER III
RESEARCH METHODOLOGY

3.1 Introduction

This chapter includes the list of materials and chemicals utilized in this experimental study. The experimental methodology for the fabrication and characterization of functionalized MWCNTs, magnetic functionalized MWCNTs nanocomposite, and magnetic functionalized MWCNTs-based BP/PVA membrane was described. Besides, the experimental approach for examining the performance of magnetic functionalized MWCNTs-based BP/PVA membrane for FZD micropollutant removal was also prepared in this chapter. Furthermore, the characterization and analytical methods were also discussed in this research study.

3.2 Materials

MWCNTs (99.99%) were obtained from the previous study (Siddiqui et al. 2019). The specification of MWCNTs is listed in ***Tab. 3.1***. For functionalization of MWCNTs, sulphuric acid (H_2SO_4); MW= 98 g/mol; 98 wt. %) and nitric acid (HNO_3; MW= 63 g/mol; 68 wt. %) were purchased from Merck (Germany).

Tab. 3.1: Specification of MWCNTs

MWCNTs specification	
Purity	>95 wt.%
Outer Diameter	10-20 nm
Length	10-30 µm
Specific surface area	>121 m^2/g

Iron chloride hexahydrate ($FeCl_3.6H_2O$; MW= 270 g/mol; purity 97%), ethylene glycol ($C_2H_8O_2$; MW= 62 g/mol; purity >99%), sodium acetate ($C_2H_3NaO_2$; MW= 82 g/mol; purity 99%), polyvinyl alcohol (PVA; MW= 31000-50000 g/mol) and absolute ethanol (C_2H_5OH; MW= 46 g/mol; purity 99.9%) in the reagent grade were supplied by Sigma-Aldrich, were used in the synthesis of magnetic MWCNTs. Polytetrafluoroethylene (PTFE) membrane (47 mm, 0.45 µm), procured by Merck Millipore (Germany), was used as a filter in the preparation of magnetic BP membrane.

Furazolidone ($C_8H_7N_3O_5$; MW= 230 g/mol; purity 98%) was supplied by Merck (Germany); the chemical structure is illustrated in ***Fig. 3.1***. Besides, the molecular structure and physicochemical properties of FZD micropollutant is displayed in ***Tab. 3.2***. Distilled and ultra-pure water were employed throughout the research study.

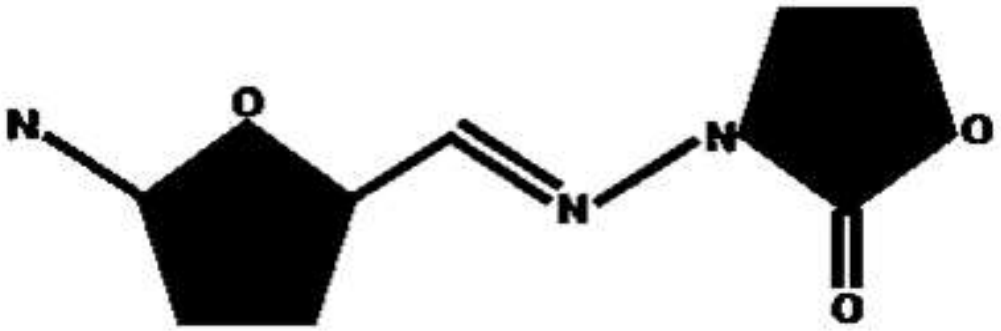

Fig. 3.1: Chemical structure of furazolidone (FZD) (Amalraj et al. 2021)

Tab. 3.2: Physicochemical properties of FZD micropollutant

Property	Furazolidone
Molecular formula	$C_8H_7N_3O_5$
Synonyms	Nitrofuroxon, furazolidine, nitrofurazolidone
Molar mass (g/mol)	230
Color	Yellow odorless solid
Solubility in water	40 mg/L at 25 ^oC

3.3 Methodology

The flowchart of the research methodology of the present study is illustrated in ***Fig. 3.2***. The fabrication of magnetic f-MWCNTs-based BP/PVA membrane involves several stages. In the first stage, raw MWCNTs were treated with strong acids to modify their hydrophobic surface into hydrophilic. In the second stage, magnetic f-MWNCTs nanocomposite was prepared using reflux approach with a Liebeg condenser and hot-plate support. In the last stage, the prepared magnetic f-MWCNTs nanocomposite was used to prepare a film, known as buckypaper (BP), using a vacuum filtration technique, followed by poly vinyl alcohol (PVA) infiltration. Several characterization analyses were conducted on each synthesis stage material to determine various aspects, such as dispersion capability, element and chemical compositions, functional groups existence, and magnetic strength. Moreover, an optimization study of FZD micropollutant removal efficiency under batch-mode using magnetic f-MWCNTs-based BP/PVA membrane was also conducted. Besides, a reusability study was also performed using a desorption solvent i.e., ethanol. Lastly, critical comparison of the predictive abilities of the two models employed was also described.

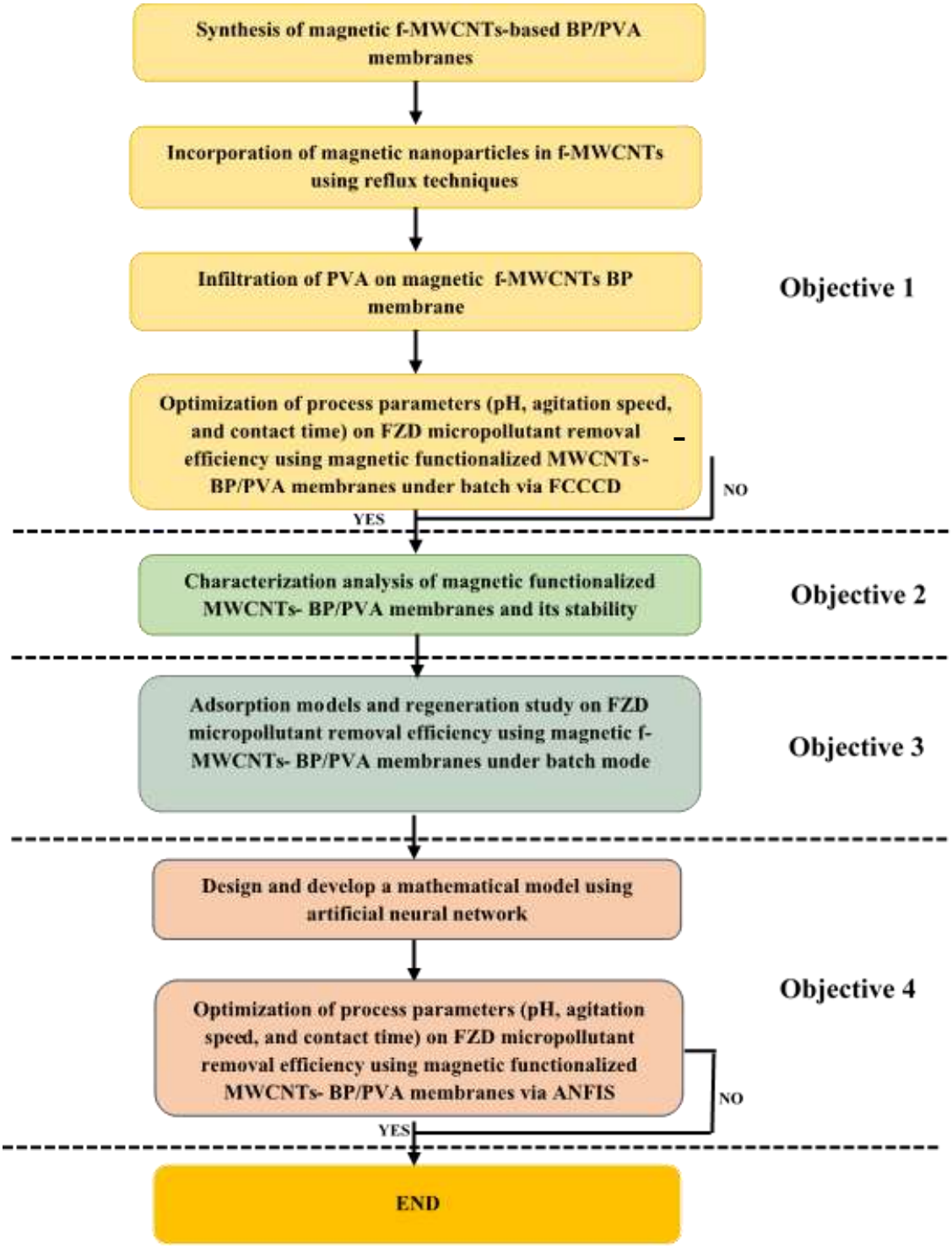

Fig. 3.2: Summary of experiment flowchart

3.4 Synthesis of Magnetic f-MWCNTs-based BP/ PVA Membrane

3.4.1 Acid treatment of MWCNTs

Rigid acid treatment is needed to change the hydrophobic characteristic of MWCNTs to hydrophilic. The acid treatment on the MWCNTs helps to improve the solubility and reactivity, as well as offers an avenue for further chemical modification of MWCNTs such as metal deposition, ion adsorption, and many others (Liew et al. 2016). In the present study, acid treatment on 0.3 g of MWCNTs was performed using sulphuric acid (H_2SO_4) and nitric acid (HNO_3) with a ratio of 1:3 (v/v). Once the raw MWCNTs and acids were finely mixed, the mixture was sonicated using an ultra-sonication bath (Tech- Lab Scientific, S-60) for 2.5 hrs. at room temperature. Later, the mixture was washed with ultra-pure water until the solution was neutralized (pH 7). Subsequently, a vacuum filter filtered the solution through a PTFE membrane (Tech- Lab Scientific, DTC-41). The filtered sample was frozen for 48 hrs. before keeping it in a freeze dryer (Fisher-Labconco. 1.5L) for 24 hrs., 40 ^{o}C, and 0.1 bar to attain a powder form material, i.e., hydrophilic MWCNTs. The current methodology used is based on previous studies (Jun et al. 2020) with minor improvisation.

3.4.2 Preparation of magnetic f-MWCNTs nanocomposites

The incorporation of iron oxide with f-MWNCTs can be conducted by several routes such as solvo-thermal, blending, sol-gel, flow injection, gas-phase deposition, and many others (Sadegh et al. 2014, Kobyliukh et al. 2020, Moazzen et al. 2019, Neto et al. 2019). Most of these methods require highly complex equipment, are time-consuming or involve extreme operating conditions. In the present study, reinforced f-MWCNTs with iron oxide using reflux approach and an aqueous bath. In the preparation process, 0.5 g of f-MWCNTs was added to a 100 mL round bottom flask along with $FeCl_3.6H_2O$ (3 g), $C_2H_3Na_2$ (3.5 g), and C_2H_5OH (100 mL). With the help of the orbital shaker (Tech- Lab Scientific, KS-501), the prepared mixture was shaken at 180 rpm for 30 min. The homogenous mixture was left to settle, subsequently refluxed using a Liebeg condenser distillation tube. As the reaction completed,

the colour of the solution commuted from dark yellow to greyish. Later, the reflux solution was washed with ultra-pure water (100 mL) and ethanol (50 mL) and left to dry in the oven (Binder, ED-24) overnight at 80 ^{o}C. Five samples were prepared using the aforementioned methods and labeled as samples A, B, C, D and E. The operating conditions were varied for each sample and are described in detail in ***Tab. 3.3***.

Tab. 3.3: Operation conditions for the preparation of magnetic f-MWCNTS

Sample	f-MWCNTs (gm)	Amount of chemicals used	Time (hrs.)	Temperature (^{o}C)
A	0.5		16	300
B	0.5	$FeCl_3.6H_2O$=3 gm	16	330
C	0.5	$C_2H_3Na_2$ =3.5 gm	16	350
D	0.5	C_2H_5OH=100 mL	18.5	300
E	0.5		18.5	350

3.4.3 Preparation of Magnetic f-MWCNTs-based BP/PVA

Due to the simple and ease approach, vacuum filtration was employed to prepare the magnetic f-MWCNT-based BP. 100 mg of magnetic f-MWCNTs was mixed with 50 mL of C_2H_5OH in a polypropylene beaker, and sonicated using an ultra-sonication bath (Sonorex, S-60H) for 30 min. at 40°C. Next, the sonicated solution was transferred to probe sonication for 10 min. with 10 second interval, to attain finely disperse magnetic f-MWCNTs solution (Sono Mechanics, LSP-500). The finely dispersed magnetic f-MWCNTs solution was filtered to obtain a thin film, so-called BP, using vacuum filter with the help of PTFE membrane. The prepared magnetic f-MWCNTs-based BP was dried and infiltrated with PVA (2 wt.%) overnight at room temperature. The formed magnetic f-MWCNTs-based BP membrane was carefully peeled off from the underlying PTFE membrane and dried. The schematic synthesis of magnetic f-MWCNTs-based BP/ PVA is depicted in ***Fig. 3.3***:

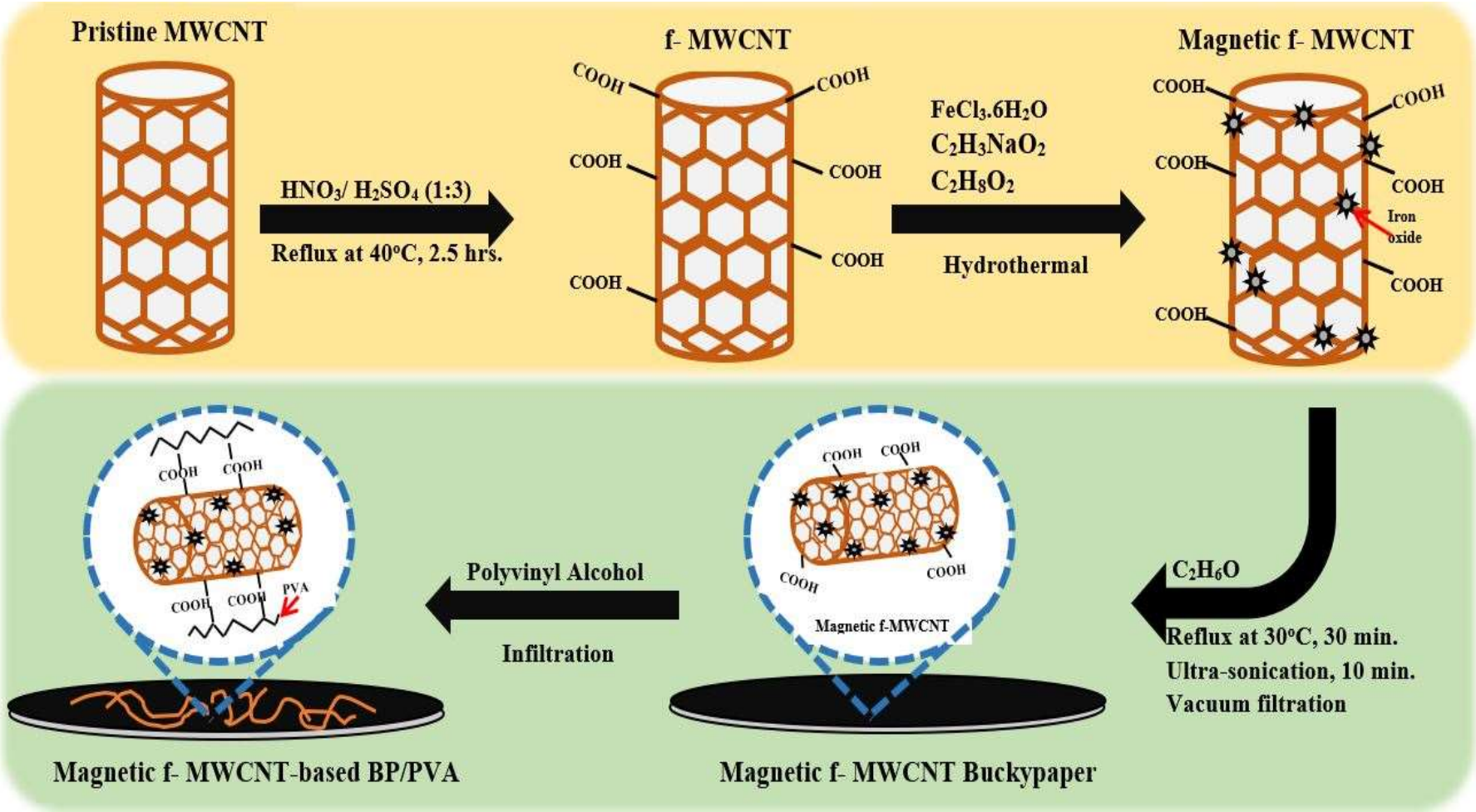

Fig. 3.3: Schematic representation of magnetic f-MWCNTs-based BP/PVA membrane

3.5 Batch treatment of FZD micropollutant using magnetic f-MWCNTs-based BP/PVA membrane

This part examined the treatment of FZD micropollutant solution from the aqueous phase using magnetic f-MWCNTs-based BP/PVA membrane. A 100 mL of FZD micropollutant solution with magnetic f-MWCNTs-based BP/PVA membrane of varying pH (4-8) was prepared at a 10 mg/L of FZD micropollutant concentration at room temperature. The Erlenmeyer flask was shaken by an orbital shaker at a given agitation speed (100-200 rpm), and aliquots were collected from the reaction mixtures at exact time intervals, i.e., 20-350 min. The concentration of the FZD micropollutant solution was analyzed via an ultraviolet spectrophotometer (Perkin Elmer Lambda 25 UV/Vis) at 365 nm (Cai et al. 2021).

The FZD micropollutant removal efficiency ($R_{\%}$) and adsorption capacity (q_e) were calculated using ***Equation 3.1***

$$R_{\%} = \left(\frac{C_i - C_o}{C_i}\right) \times 100 \qquad \text{Equation 3.1}$$

Where,

C_i = Initial concentration of FZD MP solution (mg/L)

C_o = Final concentration of FZD MP solution (mg/L)

3.5.1 Preparation of FZD micropollutant stock solution

Furazolidone shows carcinogenic and genotoxic effects, therefore it is indeed important to consider the safety measures and protocols employed during handling this pharmaceutical micropollutants, such as use of solvent restive gloves, and charcoal loaded respiratory mask. Moreover, it is also important to poured the waste solvent in the air-tight silica glass, wrapped in plastic to avoid its seepage, and hand over to the chemical disposal management authority.

Analytical grade FZD standard solution was utilized to make 100 mg/L stock solutions. The required concentration of FZD solution was achieved by diluting the stock solution with distilled water. Synthetic micropollutant solution offer

several advantages over real-world micropollutants, including reproducibility and consistency in laboratory testing conditions. Based on this being a preliminary investigation of FZD removal using magnetic buckypaper membrane, synthetic FZD micropollutant solution was utilized. The standard curve of FZD micropollutant and its properties were demonstrated in ***Appendix A***.

3.5.2 Optimization of FZD micropollutant removal efficiency in batch mode

Optimization technique entails understanding the effect of process parameters to achieve the best combination of settings from specific sets of relevant factors to offer a determined goal without exceeding the described limits. The main aim of optimization is to save time, costs, and resources and reduce errors while attaining the objective of the process.

This study employs a statistical design technique to optimize the process parameters for the FZD micropollutant removal using magnetic f-MWCNTs-based BP/PVA membrane. The central composite design was used for the optimization of process parameters. The primary aim of this section was to achieve the optimal conditions for eliminating FZD micropollutant using magnetic f-MWCNTs-based BP/PVA membrane.

3.5.3 Experimental design

To optimize the process parameters for FZD removal efficiency using magnetic f-MWCNTs-based BP/PVA membrane, the response surface methodology (RSM) was employed to determine the regression model with a few experiments. Also, RSM was used to study and examine the factor's mechanism and interaction, which can affect the process. The experimental design for FZD removal efficiency was conducted on Design-Expert software (CCD, Version 12.0). The design output comprised 24 experimental runs, with 2 center points. The pH of the FZD solution (A), agitation speed (B), and contact time (C) were selected as the process variables, while the FZD removal

efficiency was stated as the response of this study. Factors were examined at the high, center, and low levels, as mentioned in ***Tab. 3.4***. Based on the literature study on magnetic f-MWCNTs, the upper and lower values of the parameters were designated (Su et al. 2022, Gurav et al. 2020, Zhen-Yuan et al. 2015). The experimental matrix design for the optimization is presented in ***Tab. B.1, Appendix B***.

Tab. 3.4: Experimental range, codes, and levels of independent variables in center composite design

Variable	**Factor code**	**Unit**	**Level**		
			Low (-1)	**Centre (O)**	**High (+1)**
pH	A	-	4	6	8
Agitation speed	B	rpm	100	150	200
Contact time	C	min.	20	185	350

The quadratic polynomial equation was designated for predicting the optimal points and is expressed in ***Equation 3.2***

$$\boldsymbol{Y = \beta_o + \beta_1 A_1 + \beta_2 B_2 + \beta_3 C_3 + \beta_{11} A^2 + \beta_{22} B^2 + \beta_{33} C^2 + \beta_{12} AB + \beta_{13} AC + \beta_{23} BC} \quad \text{Equation 3.2}$$

Where,

Y	=	Predicted response
β_o	=	Off-set term
β_1, β_2	=	Linear co-efficient
$\beta_{11}, \beta_{22}, \beta_{33}$	=	Quadratic co-efficient
A,B,C	=	Coded value of independent variables

The quadratic polynomial equation was obtained via Design-Expert software. Moreover, the significance of these quadratic models was described using analysis of variance (ANOVA) based on the F (Fischer) and p (probability) values. The determination coefficients (R^2, Adj. R^2) were considered to compare the predicted vs. actual values. The 3-D plot of the process response regarding the removal efficiency of FZD micropollutant vs. independent variables was attained as a function of two variables at a time, while the others were kept constant at the middle level. Besides, the optimum conditions were

defined by fitting parameters for independent variables. At last, the RSM model was supported through model verification by performing the experiment on the optimum solution produced by RSM model to verify the removal efficiency of FZD micropollutant.

3.5.4 Reusability of magnetic f-MWCNTs-based BP/PVA membrane for FZD micropollutant removal under batch mode

The reusability tests for FZD micropollutant removal using magnetic f-MWCNTs-based BP/PVA membrane were performed at the optimum conditions. After every cycle, the supernatant was stored to determine the micropollutants concentration using UV-spectrophotometry. Experimental studies showed that absolute ethanol (purity 99.9%) is a suitable desorption solvent (Hossaini et al. 2022, Mohammed et al. 2022). Therefore, the magnetic f-MWCNTs-based BP/PVA membrane loaded with FZD micropollutant was sequentially washed with absolute ethanol and distilled water and then used in the next reaction cycle.

3.6 Characterization and Analytical Techniques

Several characterization and analytical techniques were applied to examine the specimen's surface morphology and chemical composition, i.e., f-MWCNTs, magnetic f-MWCNTs, and magnetic f-MWCNTs-based BP/PVA membrane. Field emission scanning electron microscope (FE-SEM) was utilized to characterize the surface structures of the samples at a 120,000x magnification (FEI Quanta 400 SEM). Furthermore, FE-SEM was coupled with energy-dispersive X-ray spectroscopy (EDX), which determined the elemental compositions of the samples. Also, Fourier transforms infrared spectrometer (FT-IR) (Perkin Elmer FTIR) was used to identify the functional groups present in the specimen by studying the vibrations of its chemical bond. Besides, FT-IR spectra of magnetic f-MWCNTs-based BP/PVA membrane before and after FZD micropollutant adsorption were also performed. Thermogravimetric analysis (TGA) (Perkin Elmer TG/DTA) was also

examined to determine the thermal stability of the membrane. The TGA study was conducted in the temperature range from 25°C to 900°C with a heating rate of 10°C/min under high purity oxygen gas flow of 100 mL/min. In addition, zeta potential and hydrodynamic size tests were also conducted by adding 20 mg of the pristine and f-MWCNTs in absolute ethanol (99.9%), followed by ultrasonication for 30 minutes with 15 seconds intervals. The vibrating sample magnetometer (VSM) (Squid VSM) was used to examine the magnetic property of the magnetic f-MWCNTs nanocomposites. The VSM study was performed in the -8000 to 8000 G magnetic field range to obtain a hysteresis loop. The XRD studies were conducted on magnetic f-MWCNTs nanocomposite with Cu source for x-rays generation. The nanocomposite sample was scanned at a speed of 2°/min. from 6° to 70° (2 Theta diffraction angle) at 45 kV tension with an incident beam path of 240 mm.

3.7 Adsorption studies of FZD micropollutant using magnetic f-MWCNTs-based BP/PVA membrane

The adsorption studies performed using magnetic f-MWCNTs-based BP/PVA membrane were examined in this section. To interpret the adsorption capacities of FZD micropollutant using magnetic f-MWCNTs-based BP/PVA membrane, adsorption isotherms model, kinetic model, and thermodynamic studies were analyzed.

3.7.1 Influence of initial micropollutant concentration and contact time on the adsorption capability

The adsorption experiments were conducted at the optimum conditions obtained from *Section 3.5.2*, using magnetic f-MWCNTs-based BP/PVA membrane under batch mode. The micropollutant samples were collected at different time interval up to 5 hrs. The micropollutant concentration samples that were collected at specific time were analyzed using ultraviolet spectrophotometer (Perkin Elmer Lambda 25 UV/Vis). The experiment was repeated by varying the FZD micropollutant concentration, ranges from 5 to 25

mg/L. The adsorption capacities (q_e) were calculated using ***Equations 3.3*** as mentioned below:

$$q_e = (C_i - C_o) \times \frac{V}{m} \qquad \text{Equation 3.3}$$

Where,

C_i = Initial concentration of FZD MP solution (mg/L)
C_o = Final concentration of FZD MP solution (mg/L)
V = Volume of FZD MP solution (L)
M = Dry weight of the magnetic f-MWCNTs-based BP/PVA membrane (g)

3.7.2 Adsorption isotherm models

Equilibrium adsorption isotherms were determined for the FZD micropollutant compound, and experimental results were studied through isotherm models such as Langmuir, Temkin, Freundlich, and Dubinin-Radushkevich. The equation and parameters of the selected isotherm models employed in this study are listed below in ***Tab. 3.5***:

Tab. 3.5: Adsorption isotherm equation and parameters

	Isotherm model	References
	Langmuir isotherm	
Assumption	Mono-layer adsorption on the homogeneous surface with similar sites	(Domagała et al. 2019)
Equation	$\frac{C_e}{q_e} = \frac{1}{q_m K_L} + \frac{C_e}{q_m}$	
Plot	$\frac{C_e}{q_e}$ vs C_e	
Parameters	q_m =maximum adsorption capacity (mg/g) K_L =adsorption capacity (L/mg)	
	Freundlich isotherm	
Assumption	Surface heterogeneity between the adsorbate and adsorbent	(Momenzadeh et al. 2011)
Equation	$L_n q_e = L_n K_F + \frac{1}{n} L_n C_e$	

Plot	$L_n q_e$ vs C_e	
Parameters	K_F = Adsorption coefficient n = Freundlich intensity	
	Temkin isotherm	
Assumption	Adsorption is described via even distribution of binding energies, which extend coverage because of the adsorbent-adsorbate interaction results in the reduction in heat of adsorption.	(Hua et al. 2017)
Equation	$q_e = BL_n k_T + BL_n C_e$	
Plot	$q_e vs L_n C_e$	
Parameters	$k_T =$ Temkin equilibrium constant (L/mg) B= Temkin constant	
	Dubinin-Radushkevich isotherm	
Assumption	Calculate the porosity features and free-energy of adsorption. In addition, define the nature of adsorption processes	(Said et al. 2018)
Equation	$L_n q_e = L_n q_s - \beta\varepsilon^2,\ \varepsilon = \frac{1}{\sqrt{2\beta}}$	
Plot	$L_n q_e$ vs ε^2	
Parameters	q_s =maximum adsorption capacity (mg/g) β= adsorption coefficient (mol.^{2}/J^2) ε= adsorption free-energy (kJ/mol.)	

3.7.3 Adsorption kinetic model

To examine further, adsorption kinetics were also conducted to explain the dynamics of the adsorption process in terms of the equilibrium adsorption capacity (q_e) and rate constant (k). The adsorption kinetics models employed in this study include Pseudo-first-order and Pseudo-second-order kinetic models. Both mentioned kinetic models help determine valuable information regarding the reaction rate, such as chemical reaction and diffusion mechanisms (Toudeshki et al. 2019). The equations and parameters of Pseudo-first-order and Pseudo-second-order kinetic models used in this research study are listed below in ***Tab. 3.6***

Tab. 3.6: Adsorption kinetic model equations and parameters

	Kinetic models	References
	Pseudo-first order kinetic model	
Assumption	Rate-limiting step is physisorption that engage in π-π interaction, Van der Waals force, and hydrogen bonded hydroxyl between adsorbent and adsorbate	(Moussout et al. 2018)
Equation	$\log(q_e - q_t) = \log q_t - k_1 t$	
Plot	$\log(q_e - q_t)$ vs. t	
Parameters	k_1 = Pseudo-first order rate constant (1/min.)	
	Pseudo-second order kinetic model	
Assumption	Rate-limiting step is a chemical adsorption that engage in exchanging / sharing of electrons between adsorbent and adsorbate	(Guo et al. 2019)
Equation	$\frac{t}{q_t} = \frac{1}{k_2 q_e^2} - \frac{1}{q_e} t$	
Plot	$\frac{t}{q_t}$ vs. t	
Parameters	k_2 = Pseudo-second order rate constant (g/mg.min.)	

3.7.4 Thermodynamic Analysis

To examine the influence of temperature on the adsorption process, a thermodynamic analysis was conducted. In the thermodynamic analysis, the pertinent thermodynamic variables, i.e., Gibbs free energy, entropy and enthalpy (Bai et al. 2020, Alasadi et al. 2019) were determined from the below-stated equations:

$$\Delta G^o = -RT\ln K \qquad \textit{Equation } 3.4$$

$$\Delta G^o = \Delta H^o - T\Delta S^o \qquad \textit{Equation } 3.5$$

$$\ln K = \frac{\Delta S^o}{R} - \frac{\Delta H^o}{RT} \qquad \textit{Equation } 3.6$$

Where,

ΔG^o = Gibbs free energy change (KJ/mol.)

R	=	Ideal gas constant (KJ/mol.K)
T	=	Absolute temperature (K)
K	=	Equilibrium constant
ΔH^o	=	Enthalpy change (KJ/mol.)
ΔS^o	=	Entropy change (KJ/mol.K)

$\Delta S^o$and ΔH^owere calculated from the intercept and slope of Van't Hoff plot between lnK and 1/T, respectively.

3.8 Optimization of FZD micropollutant removal efficiency using adaptive neuro-fuzzy interface system

Adaptive neuro-fuzzy inference system, abbreviated as ANFIS, is a powerful modeling tool mainly involving artificial neural networks supported with fuzzy logic, applied in high-speed modeling of complicated non-linear processes. Different models have been examined for adsorption data reliance on the variables. Among all, the fuzzy route is considered the most common route with respect to artificial intelligence (Mohan et al. 2021, Armaghani et al. 2021). Certainly, ANFIS is simple and flexible regarding the experimental numbers and forms, which allows it to be more appropriate for utilizing informal experimental patterns in contrast to statistical practices. According to the first-order Sugeno-fuzzy model, ANFIS is a multi-layer feed-forward network where every single layer incorporates neuro-fuzzy system elements, as reported in the literature (Walia et al. 2015).

The ANFIS model is depicted in ***Fig. 3.4***. The ANFIS architecture is stimulated as a five-layered neural network: fuzzy (*inputmf*), product (*rule*), normalized (*outputmf*), de-fuzzy and output layer, that utilizes the fuzzy inference system principle. Fixed nodes are included in second, third and fifth layers, whereas nodes in the first and fourth layers are adaptive (Naderpour et al. 2019, Sharifi et al. 2021). The literature review section (Chapter II) under ***Tab. 2.8***, describes each layer's detailed description and their respective equations.

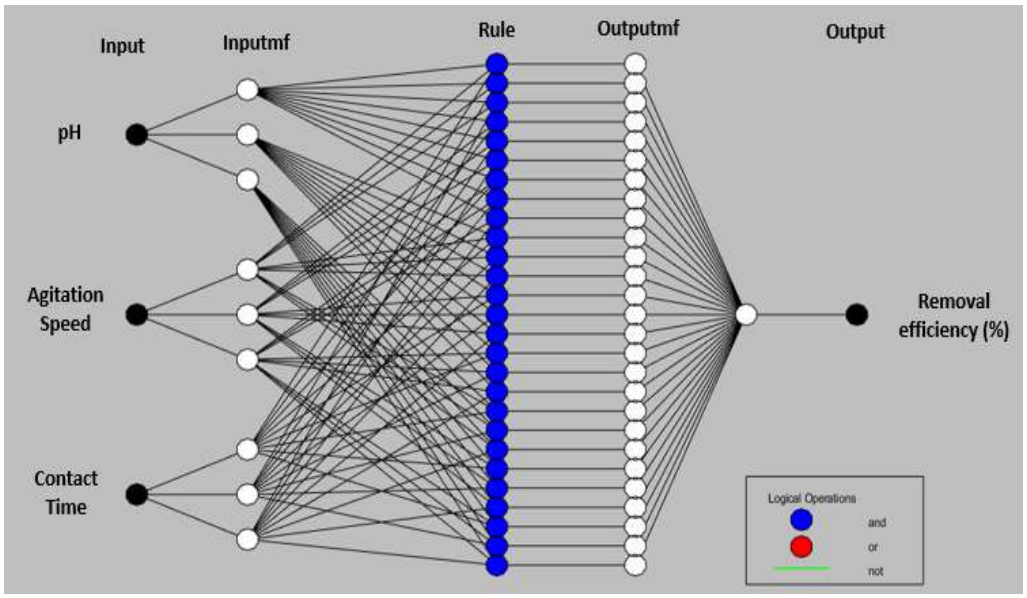

Fig. 3.4: ANFIS structure of the FZD micropollutant removal efficiency (Karaboga et al. 2019)

Based on the current research study, the first and last layers indicate the input variables (pH, agitation speed, and contact time) and output variable (removal efficiency (%)), respectively. Besides, the present model corresponds to first-order Sugeno inference system, which transforms input parameters into membership values via membership functions. The experimental data are used to train and validate the framework. Based on the literature, it has been stated that pH, agitation speed and contact time are the primary parameters in the adsorption process of FZD micropollutant from an aqueous solution (Tabelin et al. 2018, Ezzatahmadi et al. 2017, Malik et al. 2017).

3.8.1 Model development

The experimental data attained from RSM can be utilized to examine the ANFIS model, as reported in the previous studies (Onu et al. 2021, Islam et al. 2021). The ANFIS model performs better with higher experimental data sets, therefore, the RSM data sets were decoupled, giving 240 (two hundred forty) data sets that were used in the ANFIS study. MATLAB software (R2021a) was utilized in ANFIS modeling.

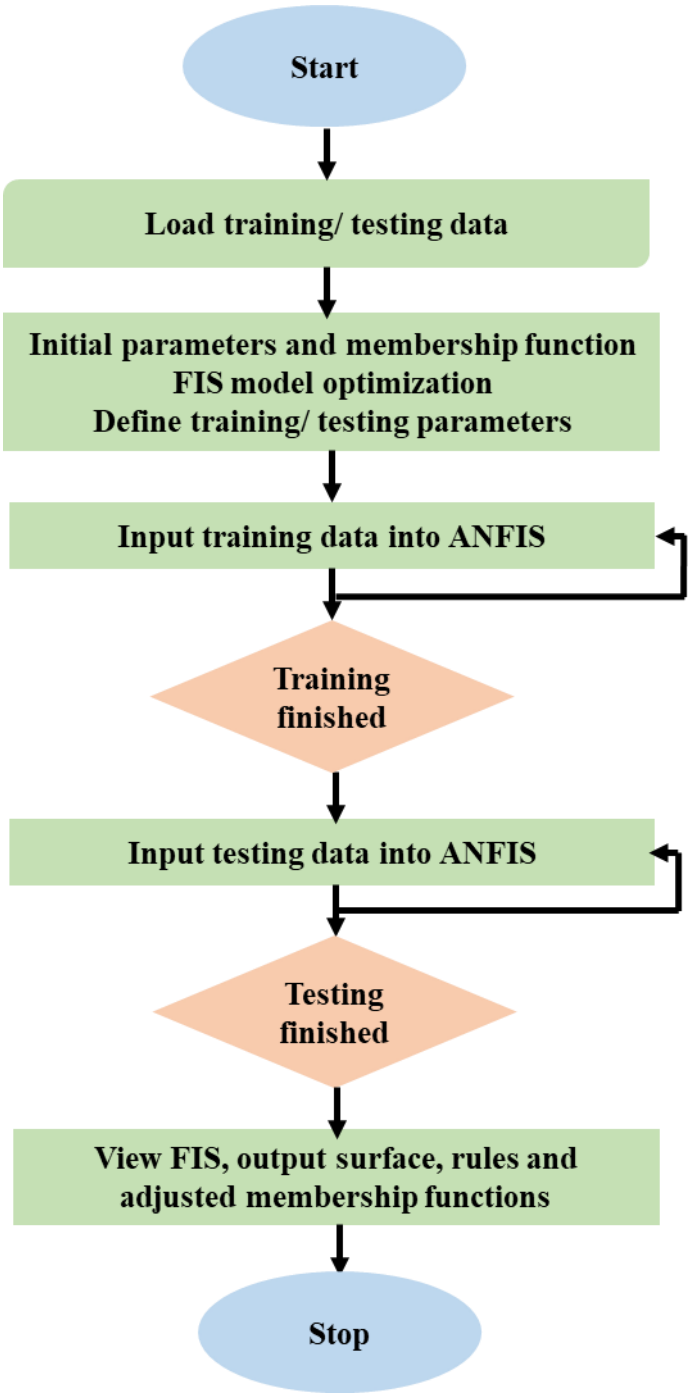

Fig. 3.5: Flowchart for ANFIS model (Samantaray et al. 2022)

Based on the literature, pH, agitation speed, and contact time are the primary parameters in the adsorption process of FZD micropollutant from an aqueous solution (Palansooriya et al. 2022, Gurav et al. 2020). Consequently, similar parameters were used in both RSM and ANFIS studies. The current ANFIS architecture's first and last layers indicate the input (pH, agitation speed, and contact time) and output (removal efficiency (%)) variables, respectively. Besides, the first-order Sugeno inference system, which transforms input parameters into membership values via membership functions was selected in the present ANFIS model (Chaudhari et al. 2014). The maximum amount of neurons in the hidden layer was concluded through a trial and error approach to have the highest correlation coefficient (R^2) (Bouhedda et al. 2019). This was to confirm the least deviation of predictions from experimental outcomes and lessen the overfitting possibility of the model.

It can be concluded that there is no accurate guidance on which ratio is recommended for the given data set. The most common practice ratios reported in literature are 80:20, 70: 30 and 60:40 (Gholamy et al. 2018). Thus, a 60:40 ratio was used in the present study, i.e. 60% for training and 40 for validating, as described in the prior studies (Mirbolouki et al. 2022). Holding more data set for training and less for validating helps enhance the model, and reduce the processing time. Besides, testing offered an independent rating of the network's performance; however, validation assisted in ensuring the network's generalization, which was stopped when no further improvement was observed to prevent over-fitting. ***Tab. 3.7*** displays the input parameters considered for the present ANFIS study along with their operating range.

Tab. 3.7: Input data and their corresponding operating ranges

Input parameter	Minimum	Maximum
pH	4	8
Agitation speed (rpm)	100	200
Contact time (min.)	20	350

3.9 Model statistical indicators

The model forecasts of the RSM and ANFIS were exposed to performance indices with the aim of laying out a ranking that underline the framework that had the finest prognostic ability with respect to the experimental data. Five high-ranking performance statistical-error functions were employed in the current study based on the previous study, and they are stated below:

- ***Mean relative error:***

$$\mathrm{RE} = \left(\frac{100}{\mathrm{N}}\right) \sum_{\mathrm{i}=1} \mathrm{N} \; \frac{\left|\mathrm{P}_{\mathrm{R,i,exp}} - \mathrm{P}_{\mathrm{R,i,cal}}\right|}{\mathrm{P}_{\mathrm{R,i,exp}}}$$ (Maryam et al. 2020)

- ***Absolute average relative error:***

$$\mathrm{AARE} = \left(\frac{1}{\mathrm{N}}\right) \sum_{\mathrm{i}=1} \mathrm{N} \left(\frac{\left|\mathrm{P}_{\mathrm{R,i,exp\,(i)}} - \mathrm{P}_{\mathrm{R,i,cal(i)}}\right|}{\mathrm{P}_{\mathrm{R,i,exp\,(i)}}}\right)$$ (González-Mariño et al. 2011)

- ***Root mean square:***

$$\mathrm{RMSE} = \sqrt{\left(\frac{1}{N}\right) \sum_{i=1} N \left(\frac{\left|\mathrm{P}_{\mathrm{R,i,exp\,(i)}} - \mathrm{P}_{\mathrm{R,i,cal(i)}}\right|}{\mathrm{P}_{\mathrm{R,i,exp\,(i)}}}\right)^2}$$ (Tarpø et al. 2019)

- ***Marquardt's standard error deviation:***

$$\mathrm{MSED} = \sqrt{\frac{\sum\left(\mathrm{P}_{\mathrm{R,exp}} - \mathrm{P}_{\mathrm{R,cal}}\right)^2}{\mathrm{N-P}}} \text{ x } 100$$ (Chowdhury et al. 2011)

- ***Hybrid fractional:***

$$\mathrm{HYBRID} = \frac{1}{\mathrm{N-P}} \sum \left[\frac{\mathrm{P}_{\mathrm{R,i,exp}} - \mathrm{P}_{\mathrm{R,i,cal}})^2}{\mathrm{P}_{\mathrm{R,i,exp}}}\right] \text{ x } 100$$ (Srenscek-Nazzal et al. 2015)

In the above-mentioned equation, N and P represents the experimental runs and factor number, respectively; $P_{R,cal(i)}$, $P_{R,cal}$, $P_{R,I,cal(i)}$ are model predictions, whereas, $P_{R,exp(i)}$, $P_{R,exp}$, $P_{R,I,exp(i)}$ are the experimental data of the ith experiment.

CHAPTER IV
RESULTS AND DISCUSSION

4.1 Introduction

This section investigated the elimination of FZD at different pH levels from water via magnetic f-MWCNT-based BP/PVA membrane through adsorption. First, several characterization analyses were conducted on pristine MWCNTs, f-MWCNTs, magnetic f-MWCNTs, and magnetic f-MWCNT-based BP/PVA membrane, such as FE-SEM, TGA, EDX, VSM, X-ray diffraction, zeta potential, and FT-IR to examine the surface structure, thermal stability, and chemical composition of raw MWCNTs and functionalized MWCNTs (f-MWCNTs). Next, statistical optimization of magnetic f-MWCNT-based BP/PVA membrane for FZD micropollutant removal under batch study was performed using response surface methodology (RSM). For the statistical optimization, the process variables include the initial pH of the FZD solution, agitation speed, and contact times. Besides, the application of adaptive neuro-fuzzy inference system was also employed in modeling to evaluate the removal efficiency of FZD micropollutant from the synthetic solution using magnetic f-MWCNTs-based BP/PVA membrane. In addition, the adsorption isotherms, kinetics, and thermodynamics on FZD micropollutant removal using magnetic f-MWCNT-based BP/PVA membrane under batch treatment were also analyzed in this section. Lastly, a reusability analysis was performed to determine the stability of the membrane.

4.2 Characterization Studies of Pristine and Surface Modified MWCNTs

Due to their remarkable aspects, such as chemical, physical, mechanical, and thermal properties, MWCNTs can be employed in several applications. Nevertheless, their hydrophobic nature, low dispersibility, and poor solubility have hindered further development of the material. Therefore, to fabricate an effective and efficient membrane for water applications, the functionalization of MWCNT is extremely important.

The research methodology has been comprehensively described in Chapter III and the characterization results of f-MWCNTs from dispersion test, XRD analysis, FE-SEM, TGA, EDX, Zeta potential, and FTIR were interpreted in this section. The section was discussed in the following sub-sections, with relevant tables, figures, and justifications.

4.2.1 Dispersion test

The dispersion test of raw MWCNT and f-MWCNTs was examined based on Glomstad et al.'s experimental study (Glomstad et al. 2018). Time-saving, rapid, and reliable outcomes are a few of the main advantages of this approach (Lau et al. 2020). ***Fig. 4.1*** shows the dispersion test of raw and purified MWCNTs after an 8 hrs. settling period. Raw MWCNTs were slowly untangled during the sonication stage, exfoliated from MWCNTs bundles, and aggregated (Yee et al. 2018). In contrast to raw MWCNTs, f-MWCNTs displayed better dispersibility based on the results, which might be due to the attachment of oxygenated functional groups on the surface of MWCNTs after acidic treatment. Moreover, surface modification of MWCNTs also decreases the Van der Waals interactions between themselves, and therefore, it depicted limited flocculation even after a long duration in the aqueous solution (Domagała et al. 2019). On the contrary, accumulation of raw MWCNTs was sometimes noted because of the hydrophobicity of raw MWCNTs sidewalls and π-π strong interaction among the individual tubes (Yu et al. 2015). The

poor dispersibility of raw MWCNTs in the aqueous phase could lead to the limited availability of surface sites (Ranjan et al. 2019).

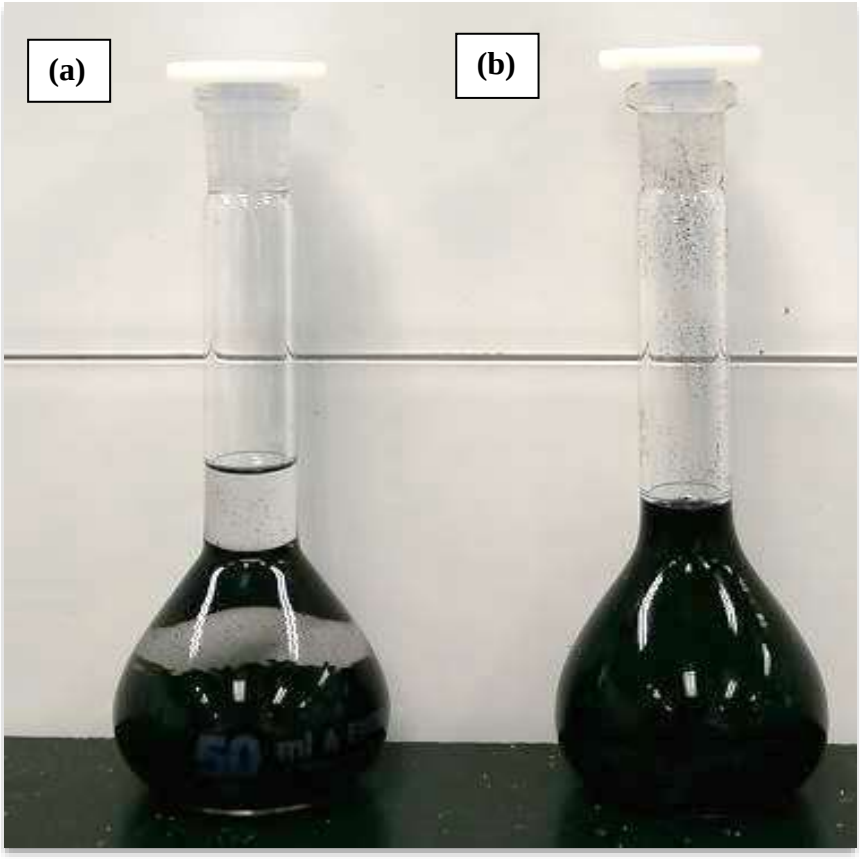

Fig. 4.1: Dispersion result after 8 hrs. (a) raw-MWCNTs, and (b) f-MWCNTs

4.2.2 Energy-dispersive x-ray spectroscopy (EDX) analysis

EDX analysis was employed to determine the quantitative contents of various elements present in raw and functionalized MWCNTs (f-MWCNTs), such as carbon (C), oxygen (O), aluminum (Al), and sulphur (S). The EDX result of raw and f-MWCNTs is presented in ***Tab. 4.1***. Before acid treatment, the EDX result of raw MWCNTs showed a low intensity of aluminum (Al), which uncovers the minor content of metal catalyst deposits stored in the carbon layers of raw MWCNTs. Whereas, after acid treatment, the f-MWCNTs displayed significant oxygen contents because of the attachment of oxygenated groups (Thou et al. 2021). The detection of the sulphur element in the EDX result of f-MWCNTs could be due to strong acid, i.e., H_2SO_4 (Rafiee et al.

2015). Moreover, Al mass fraction content increased mainly due to the aluminum stub installed in the EDX equipment (Roongraung et al. 2020). Besides, oxygen and carbon element detection by EDX spectrum in the f-MWCNTs was due to the hydrophilic treatment of MWCNTs by HNO_3/ H_2SO_4 (1:3 v/v), and carbon nanotubes, respectively. The EDX results of the present study are identical to the study performed earlier by Turgunov and co-associates (Turgunov et al. 2017). The EDX results for both raw and f-MWCNTs are depicted in ***Fig. 4.2 (a-b)***, respectively, with their corresponding quantitative weight values.

Tab. 4.1: Elemental composition of MWCNTs and f-MWCNTs sample

Sample	Elements composition (wt. %)			
	Carbon (C)	**Oxygen (O)**	**Aluminum (Al)**	**Sulphur (S)**
MWCNTs	91.49	5.78	2.73	-
f-MWCNTs	79.47	14.83	4.91	0.80

(a)

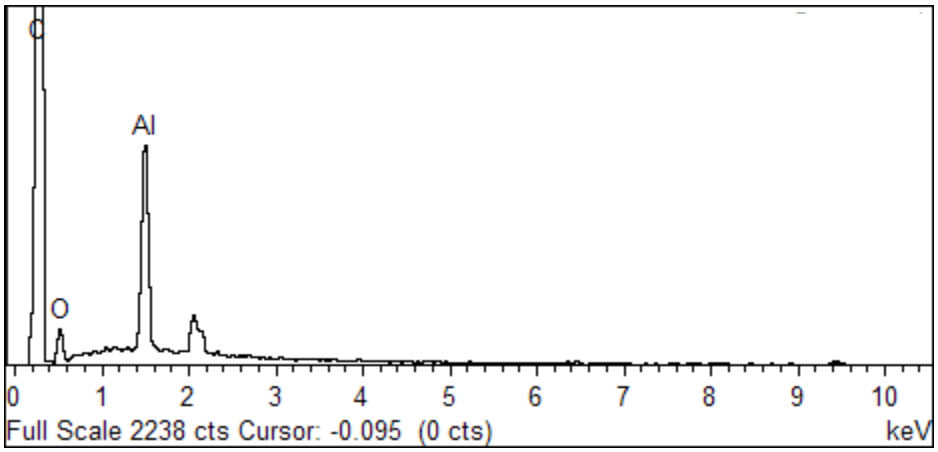

(b)

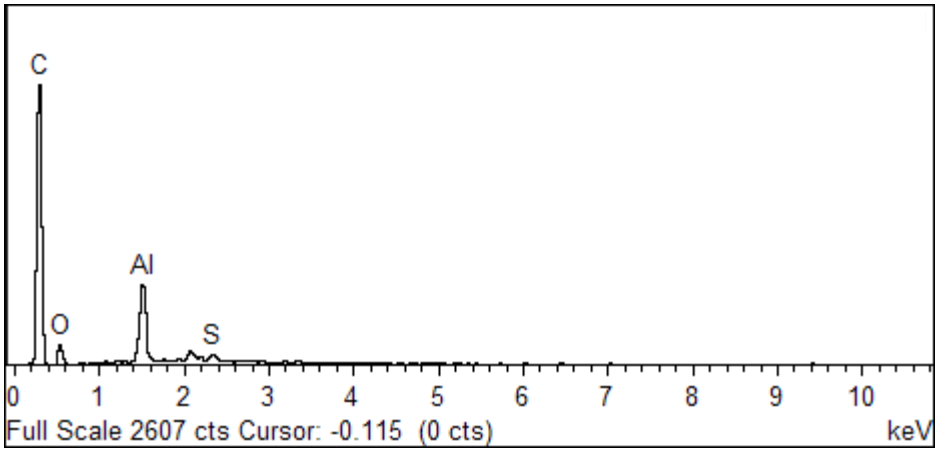

Fig. 4.2: EDX spectrum of (a) raw MWCNTs and (b) f-MWCNTs

4.2.3 Fourier Transform Infrared Spectrophotometry (FT-IR)

FT-IR study was conducted to identify the attachment of functional groups on MWCNTs' surface before and after acid treatment. In this research, the FT-IR study was performed based on the study conducted by Alghunaim and co-associates (Alghunaim 2016). The FT-IR spectrum for raw and purified MWCNTs, ranging from 500 to 4000 cm^{-1}, is illustrated in ***Fig. 4.3***.

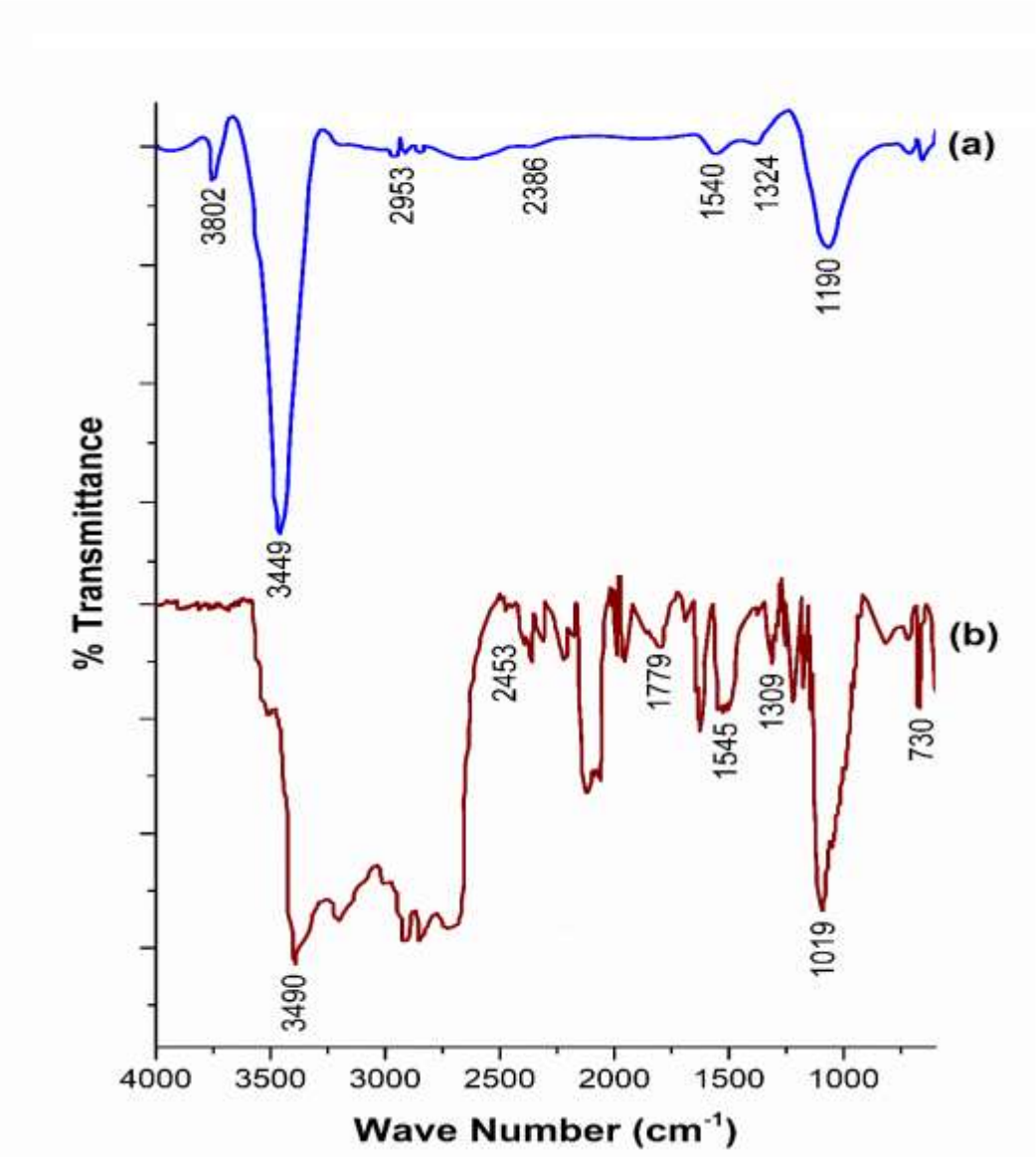

Fig. 4.3: FT-IR spectra of (a) raw MWCNTs and (b) f-MWCNTs

The FT-IR spectrum revealed some soft peaks for pristine MWCNTs, O-H groups at 2400- 3450 and 3800 cm^{-1}, C-H group at 2849- 2950 cm^{-1}, and C-O

stretch at 1190-1400 cm^{-1}. The presence of OH groups is due to the partial oxidation of the MWCNTs surface during the purification procedure (Mubarak et al. 2014). The OH stretch in the present study is similar to the analysis performed by Morsy and co-associates (Morsy et al. 2014). Besides, raw and f-MWCNTs specimens display the existence of C=C stretches at 1320 -1540cm^{-1}. This shows that the morphology of the MWCNTs backbone was preserved even after undergoing acid treatment (Carneiro et al. 2020).

Conversely, the FT-IR spectrum of f-MWCNTs in ***Fig. 4.3 (b)***, has displayed several intensive peaks after being treated with H_2SO_4/ HNO_3 acids at 702-730, 1019-1308, 1545, 1760, and 2500-3490 cm^{-1} that correspond respectively to C-C stretch, C-O stretch, C=C stretch, C=O stretch, and OH stretch. These peaks demonstrate that the MWCNT produces more polar groups after acid treatment, such as hydroxylic and carboxylic (Guadagno et al. 2018). The absorption peak at 702-730cm^{1} was associated with C-C. Besides, peak at 1019-1308 and 1760 cm^{-1} corresponds to carbonyl C-O and C=O groups, ascribed to the stretching vibrations of carboxyl moieties (-COOH) (Hof et al. 2013). The absorption peak at 1545 cm^{-1} was associated with C=C groups, which was ascribed to the oxygen-containing groups due to the inclination in the dipole moment corresponding with graphene vibrations (Estili et al. 2008). Distinct peaks observed at 1654, 2500, and 3490 cm^{-1} have confirmed that OH stretching of carboxyl moieties occupies a wide-ranging wavelength and reported similar outcomes in prior studies (Yee et al. 2018). The FT-IR result of f-MWCNTs proved the additions of carbonyl and hydroxyl bonded groups to MWCNTs, which related to the attributes of carboxyl functional moieties.

4.2.4 Field emission scanning electron microscope (FE-SEM)

Both specimens' surface and structural morphology, raw and f-MWCNTs, were examined using FE-SEM. The FE-SEM images of the samples are illustrated in ***Fig. 4.4 (a-d)*** with magnification of 10x and 30x. It can be stated that there are substantial variations in the structure of MWCNTs specimen after surface modification treatment. The MWCNTs, before acid treatment, have a

flatter surface with bungles of tangles tubes on its surface, whereas f-MWCNTs discovered a rougher surface structure. In addition, impurities were also observed evidently on the surface of pristine MWCNTs; however, f-MWCNTs showed no traces of impurities on their surface (Shanmugam et al. 2016). The surface roughness and impurity-free texture are due to the formation of defect sites and oxidation during acid treatment, respectively (Awasthi et al. 2019). These interpretations were based on the study's experimental outcomes obtained by Turgunov and co-associates (Turgunov et al. 2017).

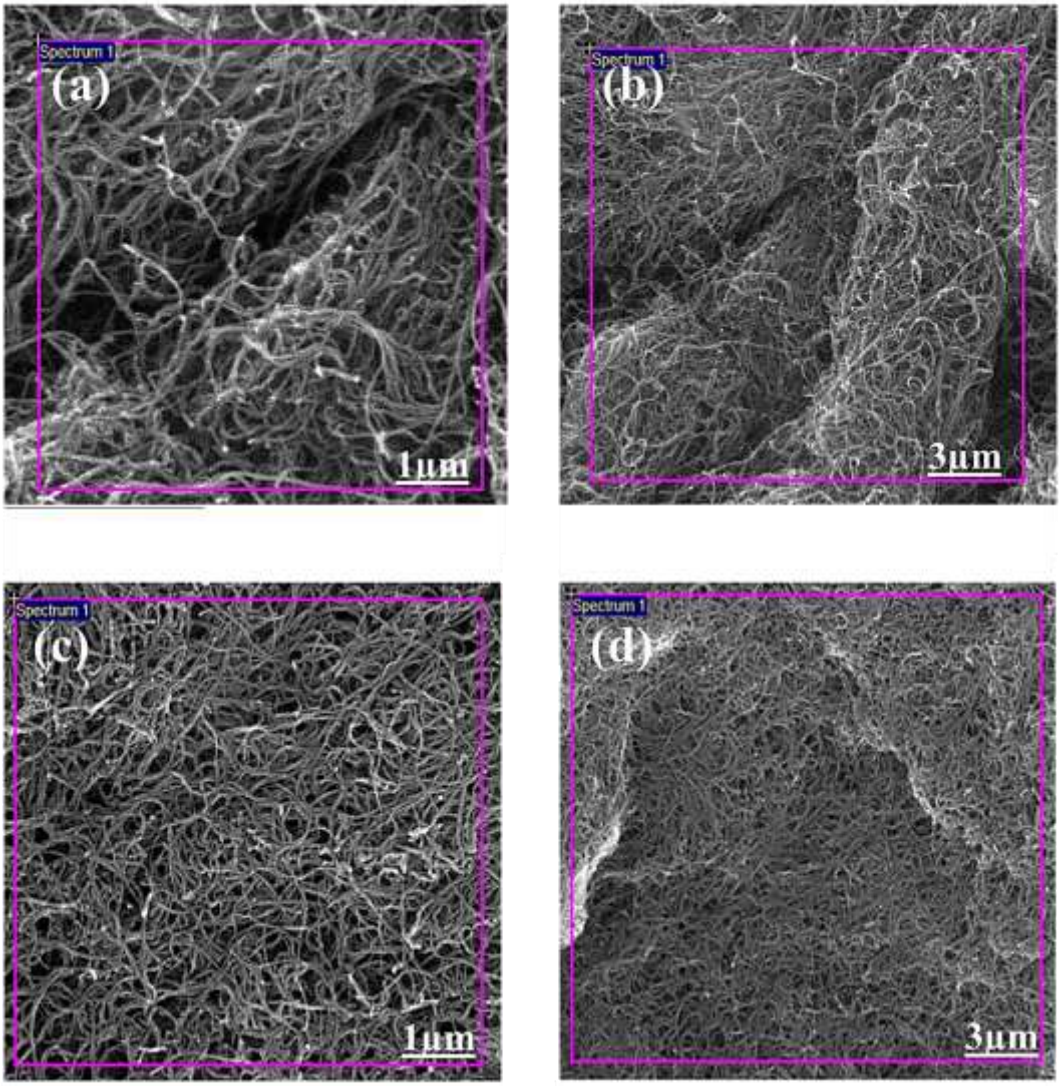

Fig. 4.4: FE-SEM micrographs of (a-b) MWCNTs, and (c-d) f-MWCNTs

4.2.5 Zeta potential and hydro-dynamic size

The dispersive effect of the MWCNTs specimen in the water phase can be better understood through zeta potential and hydro-dynamic size. Pristine MWCNTs display a greater tendency toward self-accumulation due to their hydrophobic aspects and Van der Waals force in most solvents (Punetha et al. 2017, Kharissova et al. 2013). Consequently, functionalization of MWCNTs is needed to resolve the drawback of raw MWCNT via modifying surface properties. The outstanding colloidal and dispersibility aspects of MWCNTs in solvents are essential for their practical handling in different industrial applications (Sadri et al. 2017).

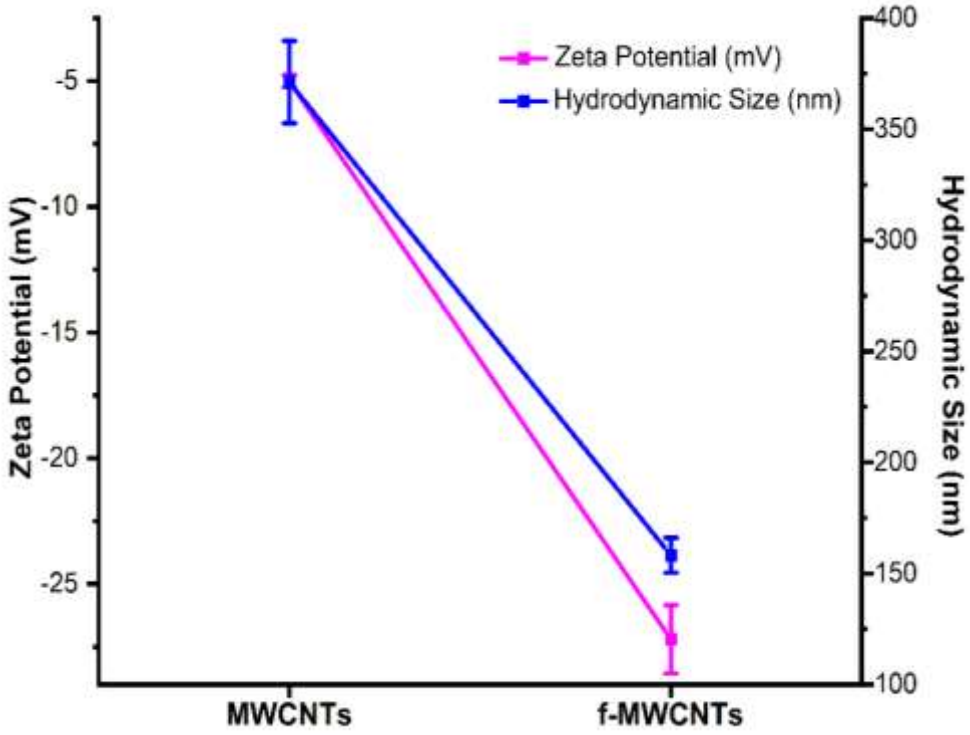

Fig. 4.5: Zeta potential and hydrodynamic size of MWCNTs and f-MWCNTs

The hydrodynamic size and zeta potential of raw and purified MWCNTs are demonstrated in ***Fig. 4.5***. The average hydrodynamic size of raw and f-MWCNTs was determined as 374 and 155 nm, respectively. The decline of the hydro-dynamic size indicates that the functionalization of MWCNTs would support size homogeneity and improve the MWCNTs' dispersibility in solvent (White et al. 2016, Cui et al. 2017). Besides, zeta potential measurements were

conducted by determining the surface capability of MWCNT for assessing their colloidal strength. The analysis outcomes depicted that the purified MWCNTs show greater zeta potential absolute values than pristine MWCNTs, i.e., -26.8 and -4.8 mV, respectively. It signifies that the surface of f-MWCNT exhibited more -ve charges than pristine MWCNT because of the attachment of carboxyl, hydroxyl and carbonyl groups as exposed in FT-IR results (Hamilton Jr et al. 2013). Hence, these purified MWCNTs display excellent stability and dispersibility in the water phase and a better functionality degree of f-MWCNT. The zeta potential results are within the standard limit as the suspensions with zeta values >15 or < -15 mV are counted to be stable because of the electrostatic repulsion mechanism. A zeta value of 40 mV is considered a sign of fine-quality MWCNTs dispersion stability in solvents (Parveen et al. 2017). In conclusion, electrostatic repulsion among the relatively charged surface of MWCNTs is essential for stabilizing the MWCNTs bundles in the aqueous phase.

4.2.6 Thermogravimetric (TGA)

TGA analysis was conducted to assess the purity of pristine and surface-modified MWCNTs. TGA for pristine and surface-modified MWCNTs concerning the temperature, ranging between 25 to 900°C at 10°C/min, is shown in ***Fig. 4.6***. The mass of the pristine MWCNTs slightly declined with rising temperature from 50 to 450°C. The initial mass loss was negligible due to the structural stability of pristine MWCNTs (Yañez-Macias et al. 2019). From 480 to 610°C, the mass of pristine MWCNTs declined sharply due to oxidation. Compared to the TGA curve of pristine MWCNTs, f-MWCNTs decomposed earlier because of the attachment of oxygenated groups on the surface of f-MWCNTs. The earlier combustion of f-MWCNTs specimen at a lower temperature is due to the fact that oxygenated groups were highly reactive to oxygen (Buang et al. 2012).

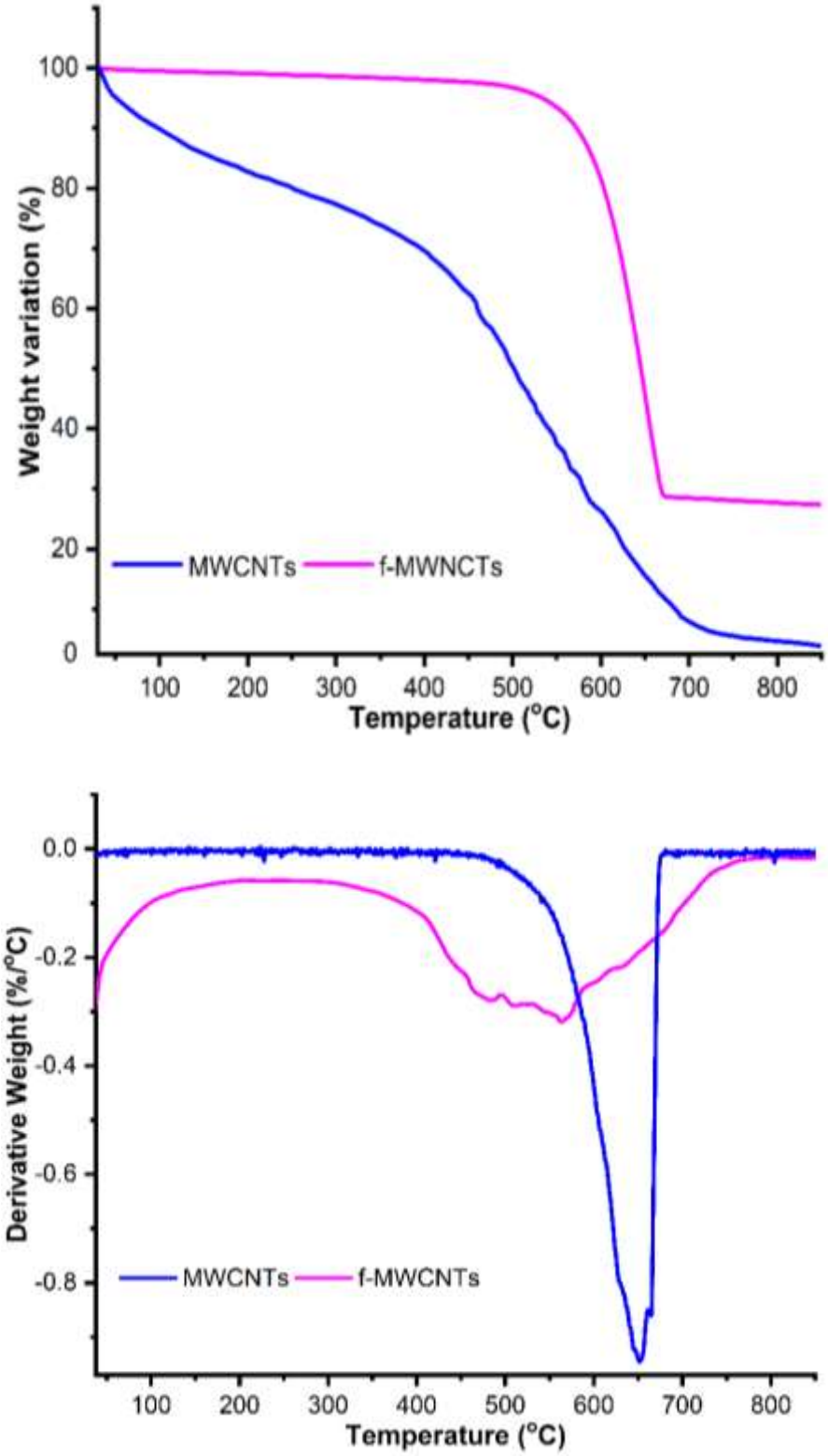

Fig. 4.6: Thermogravimetric analysis of MWCNTs, and f-MWCNTs

The thermal degradation of f-MWCNTs takes place in multi-stage processes. In the first stage, the initial mass reduction was observed from 40 to 150ºC due to water evaporation. Next, the second stage was noted from 150 to 330ºC,

which was caused due to the de-carboxylation of functional groups attached during the acid treatments (Qadir et al. 2016). The mass reduction from 330 to 450°C is marked as the third stage, ascribed to removal of impurities and oxidation of amorphous carbon (Shokry et al. 2014). Consequently, the weight loss of f-MWCNTs decreased steadily due to the combustion of the sample, ranging from 450 to 700°C. Lastly, pristine and f-MWCNT specimens show flat profiles after 690 and 660°C temperatures, respectively (Hoa 2018). It demonstrates that pristine and f-MWCNTs remain as residue after their respective on-set temperatures as they are not volatile (Rasana et al. 2019). Mujawar and co-associates have also obtained identical thermal behavior for pristine and f-MWCNTs as achieved in the current study (Mubarak et al. 2014).

In summary, the combined TGA analysis and DTG interpretation have not only provided insights into the thermal degradation behaviors of both pristine and f-MWCNTs, but have also highlighted the influence of surface modification on their thermal stability and reactivity. These results contribute to an enhanced comprehension of the thermal properties of both MWCNTs and f-MWCNTs, thereby holding significance for their broad-ranging applications in diverse fields.

4.2.7 Summary of functionalized MWCNTs sample

In this section, MWCNTs were functionalized with strong acids (HNO_3 and H_2SO_4) and compared to raw MWCNTs. The treatment of MWCNTs to transform its hydrophobic characteristic into hydrophilic primarily depends on various factors such as quantity of MWCNTs, concentration of acids, treatment approach and experimental temperature. In the present study, ultrasonication approach was considered to produce f-MWCNTs, and the characteristic analysis showed good outcomes compared to previous research reports (Avilés et al. 2009, Ngo et al. 2013). The dispersion test demonstrated that the MWCNTs, after acid treatment, changed its hydrophobic characteristic to hydrophilic, as it finely disperses in an aqueous medium. The EDX and FE-

SEM analysis showed higher content of oxygen groups attached to MWCNTs with no structural destruction. Thus, the study confirmed that the ultrasonication approach is relatively simple with high yield compared to reflux approach; therefore, the approach is highly recommended and has the potential to be employed for surface modification of MWCNTs with strong acids.

4.3 Characterization of magnetic functionalized MWCNTs nanocomposites

Based on the literature, suspended catalysts are more efficient and effective than immobilized to remove contaminants (Nguyen et al. 2020). Therefore, magnetic catalysts have been considered an effective alternative for removing micropollutants. In the present study, magnetite (Fe_3O_4) has been chosen to be incorporated onto f-MWCNTs surface to assist in the elimination of FZD micropollutant. The research aims to fabricate a magnetic buckypaper membrane that possesses magnetization features, incorporating magnetic nanoparticles in hydrophilic MWCNTs materials.

In this section, the characterization analysis such as VSM, EDX, XRD, FE-SEM, FT-IR and TGA, performed on prepared magnetic f-MWCNTs nanocomposites, were described. VSM was used to evaluate the magnetic property of all the prepared magnetic f-MWCNTs nanocomposites. Besides, EDX and FE-SEM analysis assisted to investigate the elemental compositions and surface morphologies of the magnetic f-MWCNTs nanocomposites with the highest magnetic strength, respectively. Moreover, FT-IR spectroscopy and XRD were also employed to examine the functional group and crystallite size of the magnetic f-MWCNTs nanocomposites, correspondingly. Finally, the TGA analysis was performed to evaluate the thermal stability and degradation of individual components of the magnetic f-MWCNTs nanocomposites.

4.3.1 Magnetic properties analysis

In the present study, the magnetic property of the nanocomposites was revealed using a vibrating sample magnetometer (VSM). Five samples under different operating conditions were synthesized using a reflux approach. The operating conditions of each sample are stated in *Section 3.4.3,* and ***Tab. 3.3***. The magnetization (M) vs. magnetic field (G) plots of samples A, B, C, D, and E are depicted in ***Fig. 4.7***. It can be seen from ***Fig. 4.7*** that all the samples exhibited immeasurable values of remanence and coercivity, concluding that each sample synthesized by the reflux approach induces super-paramagnetic features, and Fe_3O_4 was well reinforced in f-MWCNTs (Wurendaodi et al. 2017). Besides, ***Fig. 4.7*** also reveals that no hysteresis was observed in any of the composite samples. The hysteresis loop shape is mainly dependent on the size of the particle. When the particle size decreases, the magnetic domain/ particle is also reduced to the range where it is energetically critical for the domain wall to be present. Below a certain diameter, magnetic materials have a single domain; the material then exhibits super-paramagnetic characteristics (Aliahmad et al. 2013, Dutz et al. 2013). The nominal coercivity value is mainly due to the super-paramagnetic fluctuation, i.e., thermal energy; this fluctuation likely randomize the nanoparticles if no magnetic field is applied (Yi et al. 2014). It has been reported that the saturation magnetization (Ms) value of raw Fe_3O_4 nanoparticles is around 47emu/g for an average size of 7 nm (Guo et al. 2020).

In comparison, raw Fe_3O_4 exhibited ferromagnetic features with significant coercivity, Ms, and remanence due to their bulky size (ranging 20- 50 nm) and improved crystallinity (Wei et al. 2011). The Ms values of samples A, B, C, D, and E were 23.24, 30.33, 31.80, 32.03, and 44.76 emu/g, respectively. Based on ***Fig. 4.7***, it can also be observed that the Ms increased with the increase in the synthesizes temperature, which might be due to the size and amount of the core-nanoparticles, i.e., Fe, and the crystallized domains' size in the core-nanoparticles (Katsube et al. 2013). In a ferromagnetic system, spontaneous magnetization increases with the temperature within the critical temperature range; in particular, iron is a ferromagnetic type; therefore, a decline in

magnetic saturation can be expected once the critical temperature range is reached (Zhou et al. 2014). Furthermore, weakening the mean exchange interaction, primarily due to structural disorder, might also be the reason for reduction of Ms (Sousa et al. 2022). Among all samples, the Ms value of sample E demonstrated the highest value; however, it is lower than the raw Fe_3O_4, which might be ascribed to the influence of macromolecules and multi-walled carbon nanotube in the nanocomposite (Hasanzadeh et al. 2017). The results suggest that iron-oxide filled f-MWCNTs have the potential to be employed for extraction and magnetic separation processes. Besides, ***Tab. 4.2*** lists different studied magnetic CNT-based nanocomposites for various applications along with their Ms values:

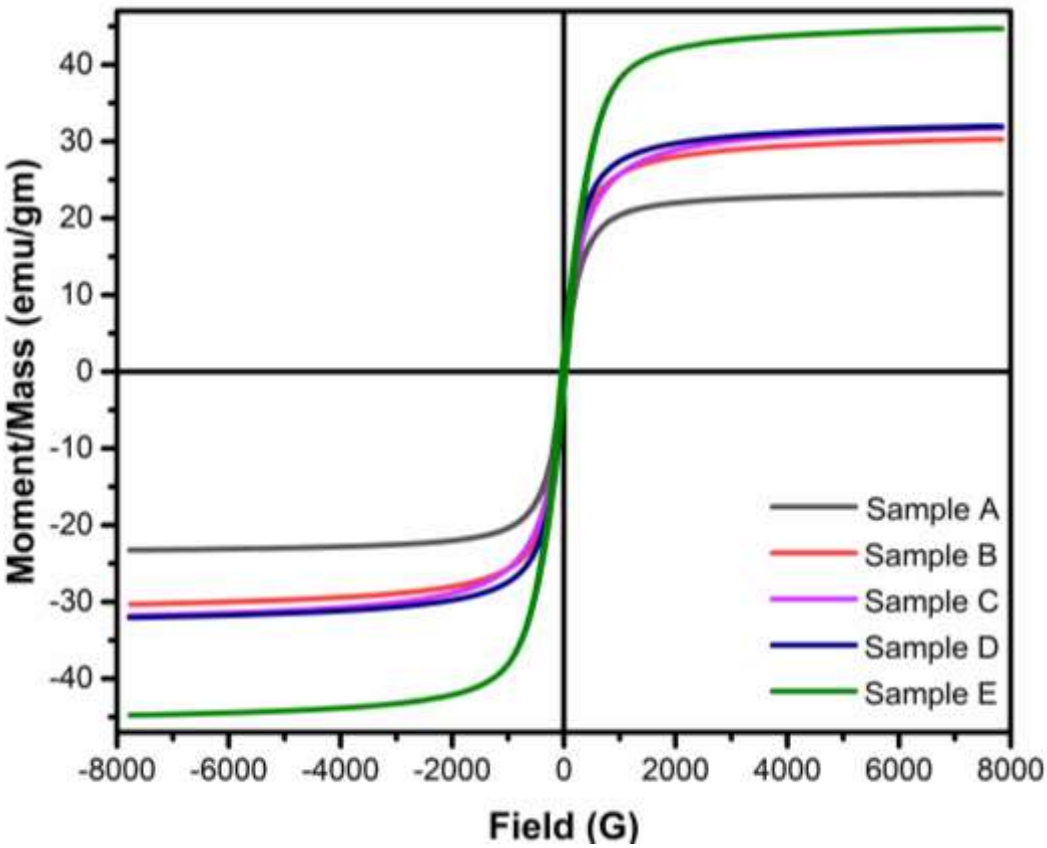

Fig. 4.7: Magnetic loop of magnetic f-MWCNTs nanocomposites

Tab. 4.2: Saturation magnetization of various magnetic- CNT based nanocomposites

Magnetic-based materials	Magnetization (emu/g)	Remarks	References
Fe_3O_4-biochar	41	• Magnetic biochar is prepared using sonication approach from banana pseudo-stem biomass. • At initial preparation stage, pyrolysis route is required, where the feedstock was dried up to 600 ^oC.	(Gurav et al. 2020)
Fe_3O_4-CNT	37 and 20	• Iron oxide (Fe_3O_4) was coated with CNTs to prepare magnetic nanocomposite • VSM, FT-IR, XRD, and SEM characterization were performed on the prepared results. • The prepared nanocomposites could be employed as fast regeneration, highly efficient, and cost-effective	(Nezhadheydari et al. 2019, Tang et al. 2021)
Fe_3O_4-MWCNTs	34.86	• Iron oxide was synthesized by decorating it with MWCNTs for nanofluids. • High yield nanocomposite was prepared using co-precipitation method	(Hussain et al. 2020)
Fe_3O_4 -f-MWCNTs	29.50	• The study claimed that they prepared the magnetic nanocomposite without using highly toxic chemicals; moreover, reported as economical and effective nanocomposite, in particular for iron removal from wastewater.	(Alimohammadi et al. 2017)
$NiFe_2O_4$-MWCNTs	30.78	• Hydrothermal method was used to synthesized the magnetic nanocomposite. • Potential to be employed in treatment of different dyestuff for medium scale application	(Zhu et al. 2015)
γ- Fe_3O_4 -MWCNTs	12.93	• The fabrication of γ- Fe_3O_4 -MWCNTs was performed with the support of dispersion method • γ- Fe_3O_4 dispersion was homogeneous; moreover, maintained selectivity on the	(Liu et al. 2019)

Magnetic-based materials	Magnetization (emu/g)	Remarks	References
		surface of the MWCNTs	
Fe_3O_4-f-MWCNTs	44.76	• Novel route to synthesize magnetic f-MWCNTs nanocomposite	Present study

4.3.2 Energy-dispersive X-ray spectroscopy (EDX)

The EDX results of magnetic f-MWCNTs nanocomposite are presented in ***Tab. 4.3***. In contrast to all the prepared magnetic f-MWCNTs nanocomposite samples, sample E i.e., 44.76 emu/g demonstrated the highest magnetic saturation value. Therefore, the present EDX study focused on the elemental composition identified from sample E. The EDX spectrum of the magnetic f-MWCNTs nanocomposite (sample E) is displayed in ***Fig. 4.8***.

Tab 4.3: Elemental composition (wt.%)

Sample	Elements composition (wt. %)					
	C	O	Al	S	Cl	Fe
f-MWCNTs	79.47	14.83	4.91	0.80	-	-
A	49.36	19.83	0.76	-	0.28	29.77
B	45.51	21.81	0.51	-	0.45	31.72
C	46.20	18.89	-	-	-	34.90
D	43.13	20.43	0.32	-	0.72	35.40
E	32.90	22.06	0.29	-	0.30	41.46

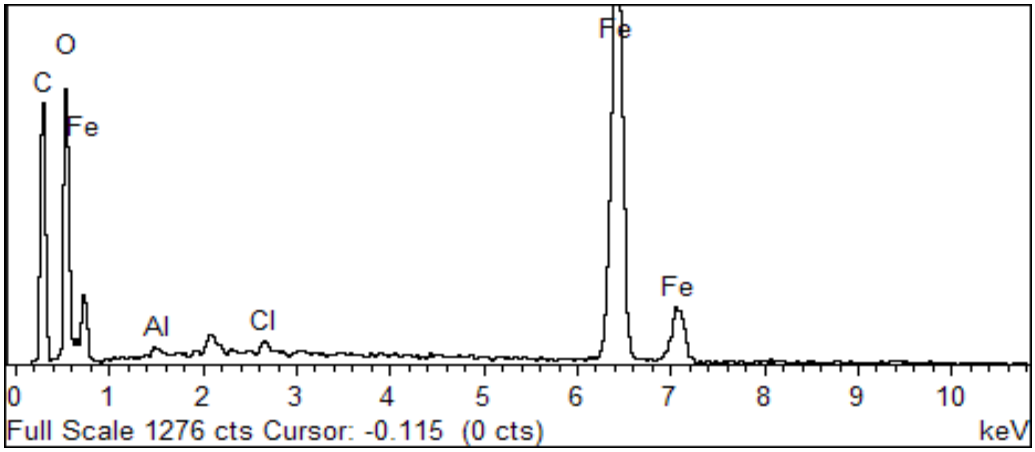

Fig 4.8: EDX spectrum of magnetic f- MWCNTs nanocomposite (Sample E)

The EDX spectrum of sample E displayed a higher weight percentage (%) for Fe than the remaining samples. When comparing hydrophilic MWCNTs to sample E, it can be observed that the EDX result for sample E showed a visible decline of carbon content (wt. %) and an increase in oxygen and iron weight content (%). The reduction in carbon and increase in oxygen content (wt. %) might be due to the presence of hydroxyl and carboxylic groups after strong

acid treatment and the integration of the new element of Fe appearing after Fe_3O_4 is loaded, respectively (Guo et al. 2021). The present study confirmed that using the reflux approach, the developed magnetic hydrophilic MWCNTs nanocomposite (sample E) generates a higher Fe content (wt.%).

4.3.3 X-ray diffraction

The X-ray powder diffraction (XRD) technique is one of the fundamental analyses through which the phase of crystalline material, as well as unit cell dimensions, can be identified. The XRD patterns of the synthesized magnetic f-MWCNTs nanocomposite (sample E) are depicted in ***Fig. 4.9***.

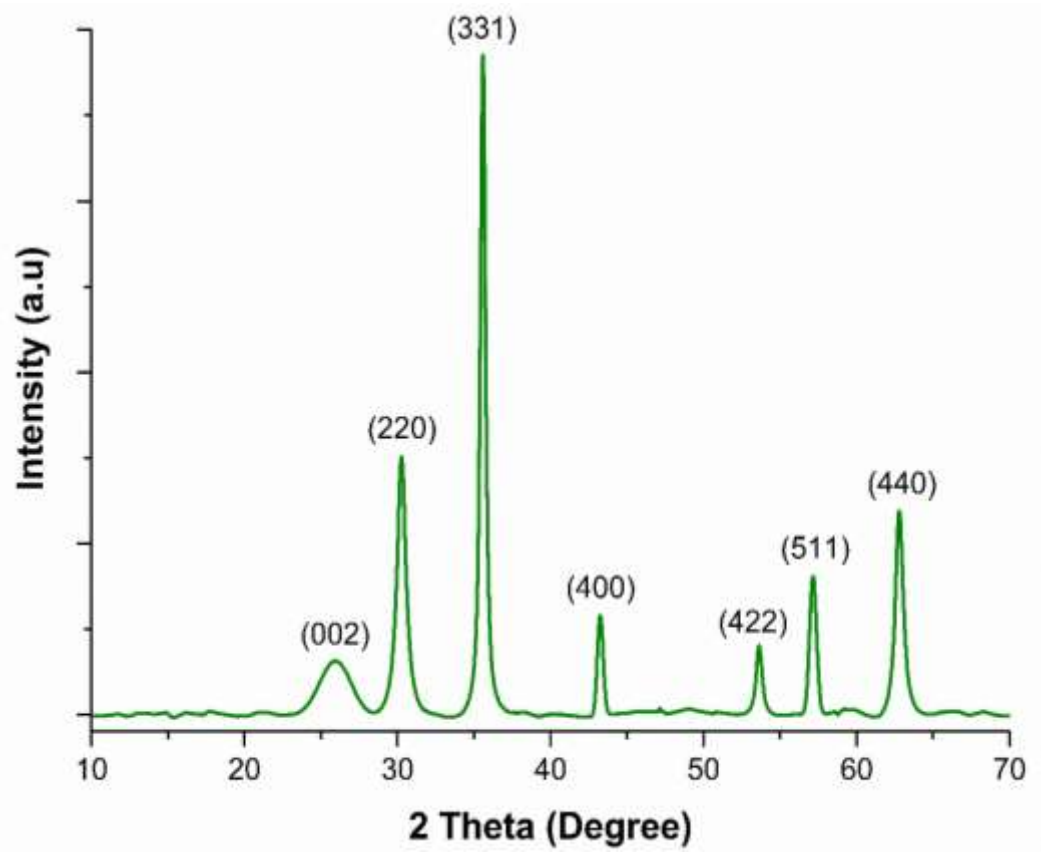

Fig. 4.9: X-ray diffraction pattern of magnetic f-MWCNTs (sample E)

Seven diffraction peaks are observed on the magnetic f-MWCNTs nanocomposite (sample E) XDR pattern, as illustrated in ***Fig. 4.9***. The crystalline diffraction peaks at 30.31°, 35.71°, 43.25°, 53.62 °, 57.21°, and

62.75° corresponded respectively to (2 2 0), (3 1 1), (4 0 0), (4 2 2), (5 1 1) and (4 4 0) planes of Fe_3O_4 spinal phase (Sadeghfar et al. 2018). Based on the literature, the CNTs diffraction peak was generally found at 25.80° (Alimohammadi et al. 2017), however, the magnetic f-MWCNTs nanocomposite (sample E) displayed a lower intensity peak, i.e., 26.21° for CNTs. This may be attributed to the finely decorated Fe_3O_4 on the f-MWCNTs' surface, as has been reported by a previous study (Hou et al. 2021).

In the present study, the crystalline size of Fe_3O_4 nanoparticles was calculated using Debye Scherer's equation (Safari et al. 2014), *Equation. 4.1*.

$$D_{hkl} = \frac{0.94\lambda}{\beta cos\Theta_{hkl}} \qquad Equation\ 4.1$$

Where,
D_{hkl} = Crystallite size (nm)
λ = wavelength (A°)
β = Average thickness of a crystal (radian)
Θ_{hkl} = Diffraction angle (radian)

The crystallite size of the Fe_3O_4 nanoparticles was determined from the diffraction peaks observed in the XRD pattern of magnetic f-MWCNTs nanocomposite (sample E). The average crystallite size of synthesized Fe_3O_4 nanoparticles was reported to be approximately 8.31 nm in the literature, whereas it decreased to 6.65 nm in the current study as calculated using Debye Scherer's equation. This reduction in crystallite size can be ascribed to the higher content of Fe_3O_4 nanoparticles in the nanocomposite, which subsequently leads to broadening of diffraction peaks and results in a smaller crystallite size according to Debye-Scherer's formula, respectively (Nadeem et al. 2022, Do et al. 2020). The diffraction peak of the magnetic f-MWCNTs nanocomposite (sample E), confirms the co-axial and cubic arrangement of f-MWCNTs and Fe_3O_4 nanoparticles, respectively. The relative intensity and position of all diffraction peaks observed in the XRD pattern correspond to the Fe_3O_4 standard diffraction data (JCPDS No. 41-1487) (Mumtaz et al. 2021). A similar trend has been reported for a novel Fe_3O_4-MWCNTs/Ag

nanocomposite employed for phthalic acid esters (PAEs) (Moazzen et al. 2019). The XRD analysis concludes that the Fe_3O_4 nanoparticles were successfully deposited on the surface of f-MWCNTs using the reflux technique.

4.3.4 Field emission scanning electron microscope

The surface and structural morphology of the magnetic f-MWCNTs nanocomposite (sample E) was further examined using a field emission scanning electron microscope (FE-SEM). ***Fig. 4.10*** shows the FE-SEM images captured at 10x, 30x and 60x for the magnetic hydrophilic MWCNTs nanocomposite. However, the FE-SEM images captioned in ***Fig. 4.10*** represent magnetic hydrophilic MWCNTs nanocomposite (sample E). According to ***Fig. 4.10***, the Fe_3O_4 nanoparticles are well dispersed on the surface of the f-MWCNTs nanocomposites. To ensure that the magnetic Fe_3O_4 nanoparticles are successfully captured on the hydrophilic MWCNTs, they are typically measured in the nanoscale, ranging from 18 to 100 nm (Huaccallo-Aguilar et al. 2021). Besides, it can also be observed that MWCNTs with varying lengths are surrounded by abundant Fe_3O_4 nanoparticles (Zhao et al. 2016). The Fe_3O_4 nanoparticles in spherical shape are uniformly distributed and form clusters with the rest of the Fe_3O_4 nanoparticles, owing to the interactions attributed to their magnetic features (Huaccallo-Aguilar et al. 2019). Furthermore, it can be stated that the hydrophilic MWCNTs were successfully synthesized and generated considerable defect sites after being treated with strong acids, allowing the Fe_3O_4 nanoparticles to be embedded on the outer-wall surface of hydrophilic MWCNTs. Consequently, the relationship between the functional groups of hydrophilic MWCNTs and Fe_3O_4 nanoparticles leads to orderly and stable nanocomposite materials (Safari et al. 2014).

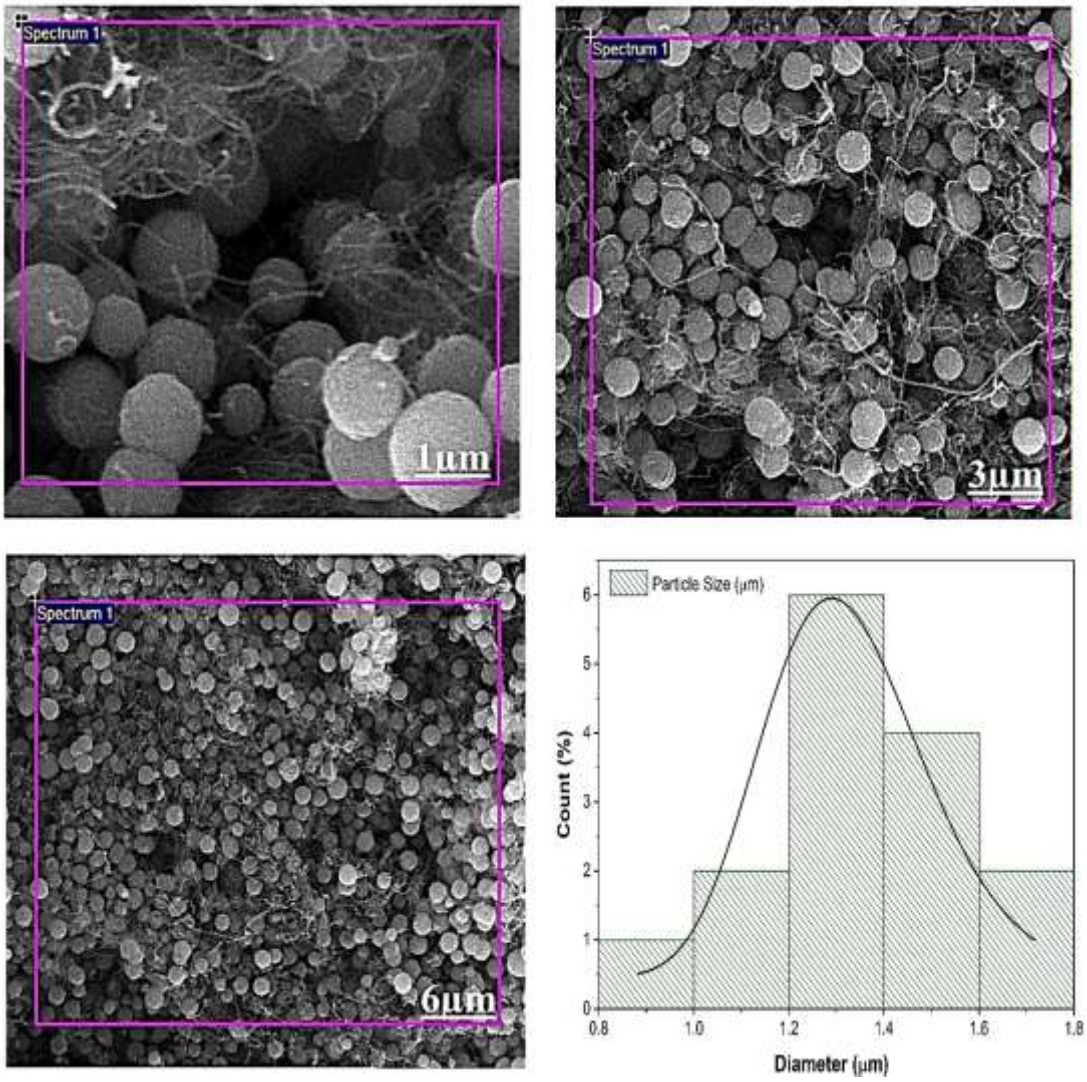

Fig 4.10: FE-SEM morphology of magnetic f-MWCNTs nanocomposite

4.3.5 Fourier Transform Infrared Spectrophotometry

To describe the functional groups present on the surface of magnetic f-MWCNTs nanocomposite (sample E), Fourier-Transform Infrared Spectrophotometry (FT-IR) study was employed in the present student. The FT-IR spectrum in the range of 500 to 4000 cm^{-1} for the magnetic f-MWCNTs nanocomposite is depicted in ***Fig. 4.11***.

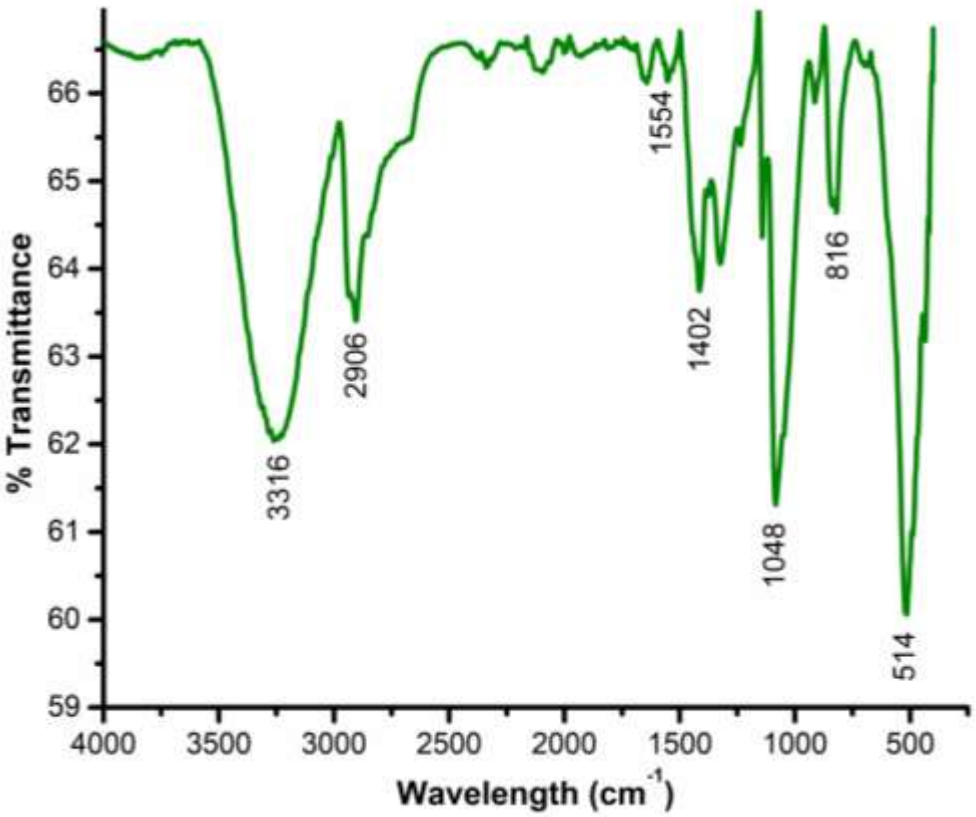

Fig. 4.11: FT-IR-spectra of magnetic f-MWCNTs nanocomposite

The FT-IR spectrum of magnetic f-MWCNTs nanocomposite (sample E) depicted new peaks after incorporating Fe_3O_4 nanoparticles. The FT-IR spectrum of magnetic f-MWCNTs nanocomposite formed distinct peaks at 514, 816, 1048, 1402, 1554, 2906, 3316 cm^{-1} associated respectively with Fe-O-Fe stretch, C-C stretch, C-O stretch, -COO stretch, C=O stretch, -CH stretch, and O-H stretch. The absorption peaks observed at 2348 and 3316 cm^{-1} are attributed to the O-H stretching vibration relating to the hydrogen moieties (Sadeghfar et al. 2018). The band at 2906 cm^{-1} corresponds to the -CH stretching peak, ascribed to the COOH moieties onto the outer-wall surface of the MWCNTs (Alimohammadi et al. 2017). Peak intensity at 1554 and 1402 cm^{-1} are related to C=O and -COO stretching, confirming that the synthesized magnetic f-MWCNTs nanocomposite possesses hydrophilic features (Zhao et al. 2016). The peak at 1048 cm^{-1} is assigned to the symmetric stretching of C-O in the carbonyl moieties. The low peak at 816 cm^{-1} is associated with C-C stretching. The maximum peak observed at 514 cm^{-1} corresponds to Fe-O-Fe, which proved that Fe_3O_4 nanoparticles were successfully incorporated in the prepared nanocomposite (sample E) (Baby et al. 2010) . A similar trend of FT-

IR spectrum for Fe_3O_4/f-MWCNTs nanocomposite has been observed in previous studies (Asfaram et al. 2016). Besides, the results confirmed a higher density of the Fe-O-Fe functional group on the f-MWCNTs' surface, which validates the FT-IR results attained from the present study.

4.3.6 Thermogravimetric analysis (TGA)

It is well-recognized that changes in the structural arrangement of carbon materials can impact their oxidation behavior, which is dependent on the availability of reactive sites. Amorphous carbons, for instance, tend to oxidize at nearly 500°C due to their lower activation energies for oxidation and/ or presence of many active sites (Terrones 2010).

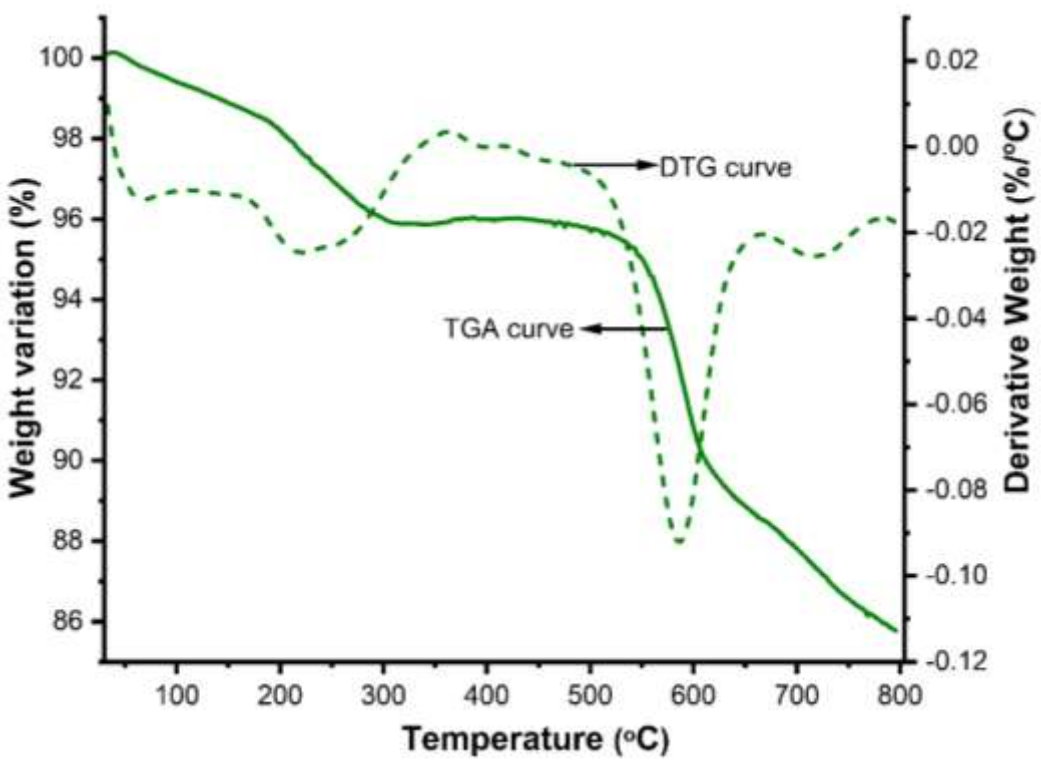

Fig 4.12: Thermogravimetric analysis of magnetic f-MWCNTs nanocomposite

The thermogravimetric study was performed on the magnetic f-MWCNTs nanocomposite (sample E). The thermogravimetric curves (TGA, DTG) of magnetic f-MWCNTs nanocomposite are illustrated in ***Fig. 4.12***, and as anticipated, thermal deprivation has taken place in several stages. Initially,

there is an up to 200°C temperature, weight variation of 2.69%, which can be attributed to the elimination of adsorbed moisture in the hydrophilic magnetic f-MWCNTs nanocomposite. Next, there is a weight variation of 10.65% observed from 200 to 480°C, which is related to the removal of volatile chemical moieties; for instance, de-carboxylation of the carboxyl moieties attached on the MWCNTs side-walls may occur (Schlachet et al. 2019). Following that there is an instant and significant weight variation of 27.47% observed at 480 to 690°C for the magnetic f-MWCNTs nanocomposite, corresponding to the oxidation of pre-oxidized MWCNTs present in the nanocomposite (Abdolkarimi-Mahabadi et al. 2015). The weight variation of 3.55% from 690 to 730°C attributed to the thermal oxidation of the residual amorphous carbon (Szabó et al. 2010). After 800°C, the magnetic f-MWCNTs nanocomposite residue can be ascribed to the oxidized magnetite in the Fe_2O_3 form. The temperature of maximum weight variation (T_{max}) for the magnetic f-MWCNTs nanocomposite was around 700 ^{o}C. The intensity peak displayed in the DTG curve for the magnetic f-MWCNTs nanocomposite (sample E) is consistent with the previous work (Huaccallo et al. 2019). The broad-band with the utmost peak of -0.0243%/^{o}C, is ascribed to the small amount of residue left after the thermal analysis. The outcome aligns with other described TGA studies of some nanocomposites synthesized (Huaccallo-Aguilar et al. 2021). In summary, the TGA and DTG analyses reveal the thermal degradation behavior of the magnetic f-MWCNTs nanocomposite (sample E), providing insights into the various stages of weight variation associated with different degradation processes and oxidation of the constituent materials.

4.3.7 Summary of magnetic f-MWCNTs nanocomposite

Based on the characterization analysis presented in *Section 4.3*, it can be concluded that the synthesis route employed for magnetic f-MWCNTs nanocomposite is simple, convenient, and one-step.. This makes the process feasible and suggests that it could be potentially used with other magnetic materials that are compatible with the properties of MWCNTs. The characterization results have confirmed the successful incorporation of Fe_3O_4

nanoparticles on the surface of f-MWCNTs, and all prepared samples exhibited superparamagnetic properties. Furthermore, thermogravimetric analysis (TGA) has validated the considerable improvement in the thermal stability of the magnetic f-MWCNTs nanocomposite, which can be attributed to its finely organized structure. Sample E has demonstrated the highest saturation magnetization compared to all prepared magnetic nanocomposites in this study. This highlights its potential as a promising material for various applications, including magnetic separation and extraction processes.

In summary, the prepared magnetic f-MWCNTs nanocomposite using reflux route shows favorable properties and can be utilized in different applications due to its super-paramagnetic behavior and improved thermal stability.

4.4 Characterization of magnetic functionalized MWCNTs-based buckypaper/ poly vinyl alcohol membrane

In contrast to various conventional membranes, carbon nanotubes (CNTs)-based membranes have emerged as significant players in water-related applications, such as dye and heavy metal ions removal. Mixed matrix CNTs-based membranes have also attained considerable attention recently, as they exhibit high flux rates and improve anti-fouling, wetting, and hydrophilic properties when used in water applications. In the present research, a magnetic f-MWCNTs nanocomposite is utilized to fabricate a thin-film membrane known as buckypaper (BP), which is then examined for its application in pharmaceutical micropollutant removal, specifically for FZD micropollutant (pharmaceutical micropollutant). However, before being employed for FZD removal, several investigations on the prepared magnetic f-MWCNT-based BP/PVA membrane are deemed essential.

This section provides a detailed interpretation and discussion of different characterization studies (EDX, FE-SEM, FT-IR and TGA) performed on the prepared magnetic f-MWCNT-based BP/PVA membrane. The results of these studies are presented and discussed in the following sub-sections, accompanied by linked figures and tables.

4.4.1 Energy-dispersive x-ray spectroscopy

The surface elemental composition of the magnetic f-MWCNT-based BP/PVA membrane was examined using energy dispersive X-ray spectroscopy (EDX), as illustrated in ***Fig. 4.13***. The EDX spectrum of the magnetic f-MWCNT-based BP/PVA membrane reveals the quantitative amount of elemental carbon (C), oxygen (O), chlorine (Cl), aluminum (Al), and iron (Fe). The mass fraction of C, O, Al, Cl and Fe are 33.82, 25.04, 0.20, 0.34 and 43.03% wt. %, respectively. The results confirm the presence of Fe_3O_4 nanoparticles on the f-MWCNTs' surface in the magnetic f-MWCNTs-based BP/PVA membrane, with the iron (Fe) being the most abundant element. The low intensity of aluminum (Al) observed in ***Fig. 4.13*** suggests that there is a minor content of metal catalyst deposits caught within the layers of buckypaper membrane. The decline in the carbon (C) content in the magnetic f-MWCNT-based BP/PVA membrane compared to f-MWCNTs can be attributed to the integration of new elements of Fe resulting from the loading of Fe_3O_4 nanoparticles. Additionally, the higher mass fraction of oxygen (O) observed in the fabricated membrane (25.04 wt. %) compared to f-MWCNTs (14.83 wt. %) and magnetic f-MWCNTs (22.06 wt. %) is due to the infiltration of PVA, which introduces OH and COOH groups on the magnetic f-MWCNT-based BP/PVA membrane. A similar trend has been reported for novel functionalized MWCNTs composite (MWCNTs/MnO_2/ Fe_3O_4) (Guo et al. 2020).

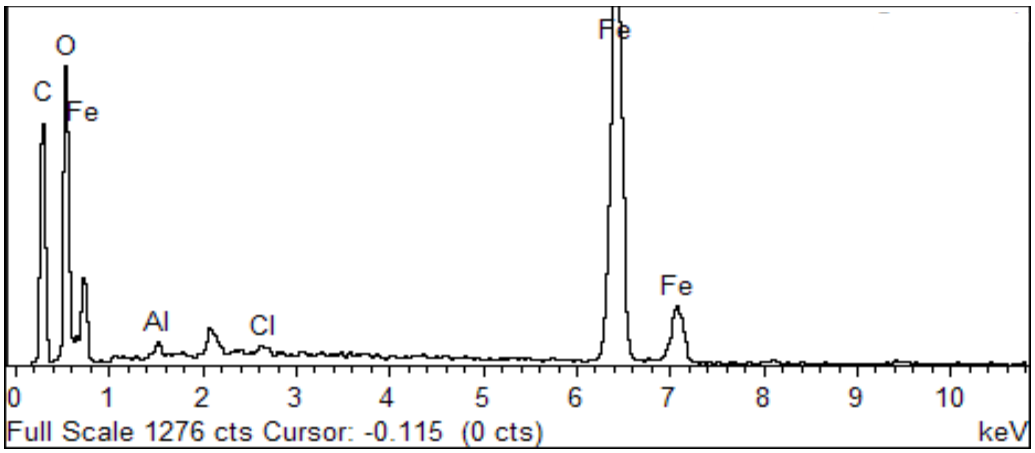

Fig 4.13: EDX patterns of magnetic f-MWCNT-based BP/PVA membrane

4.4.2 Field Emission Scanning Electron Microscope (FE-SEM)

The structural characteristics and surface morphology of the magnetic f-MWCNT-based BP/PVA membrane are presented in ***Fig. 4.14***, captured at 1, 3, and 6µm. The images in ***Fig. 4.14*** confirm the attachment of Fe_3O_4 nanoparticles to the surface of f-MWCNTs, validating the successful formation of the magnetic nanocomposite. Similar observations have been reported by Chauhan and the co-associates group during the fabrication of amperometric biosensors (Chauhan et al. 2011), further supporting the results. The fibrous morphology of the prepared membrane is evident in the images. The addition of polyvinyl alcohol (PVA) to the membrane surface has caused an increase in its diameter, resulting in a thicker membrane compared to the BP membrane without polymer infiltration. This is consistent with the findings from a prior study (Jun et al. 2020). The framework of Fe_3O_4/f-MWCNTs appears uniformly dispersed throughout the PVA matrix, indicating a homogeneous distribution of Fe_3O_4/f-MWCNTs within the membrane. This distribution is achieved through the control of homogeneity during chronological sequence of vacuum filtration and infiltration method (Xu et al. 2008). The images in ***Fig. 4.14*** also revealed that the prepared membrane has a smooth and porous surface without any visible delaminations, indicating its structural integrity. The coupled effect of the strong Fe_3O_4/f-MWCNTs-PVA interfacial interface and extended infiltration duration (i.e., 24 hrs.) contributes to the low porosity of magnetic f-MWCNT-based BP infiltrated with PVA (Yee et al. 2018).

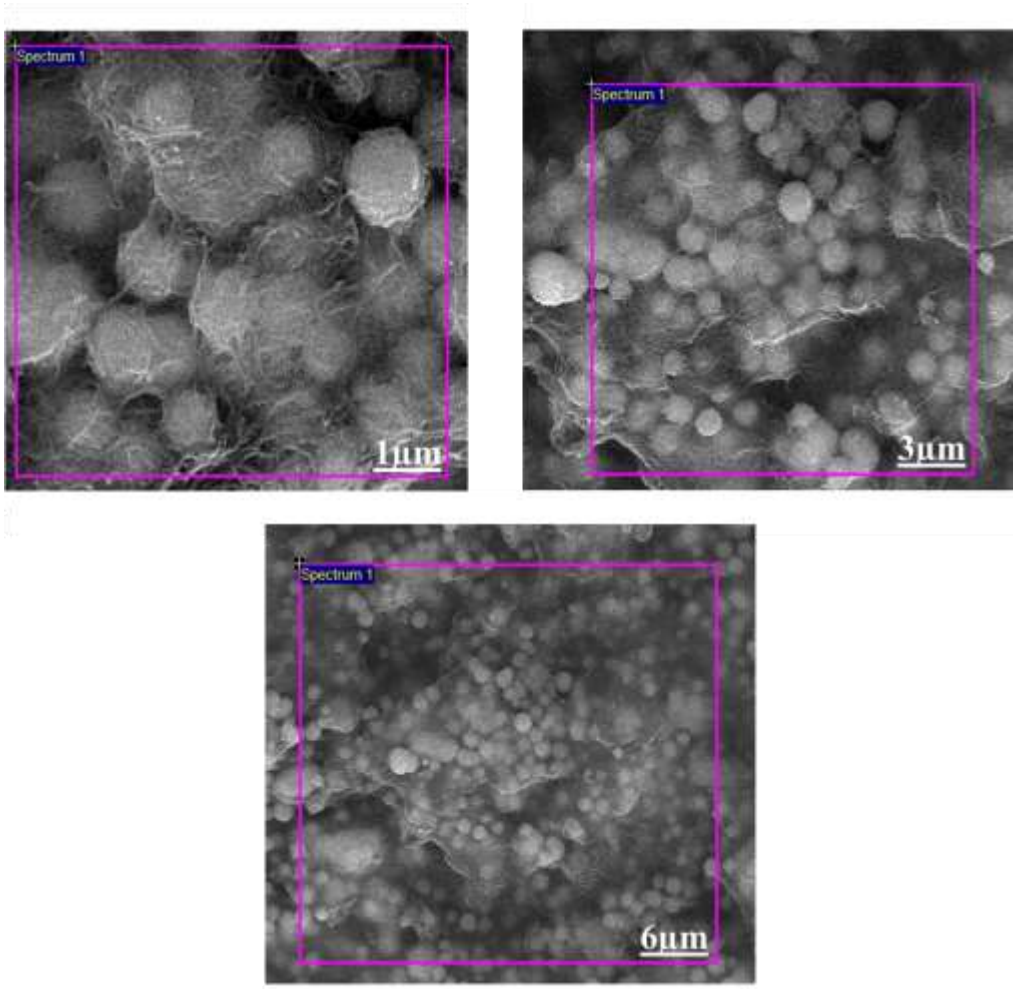

Fig. 4.14: FE-SEM morphology of magnetic f-MWCNTs-based BP/PVA

4.4.3 Fourier Transform Infrared Spectrophotometry (FT-IR)

The FT-IR spectral study is a valuable tool that allows us to comprehend the interaction behavior of various functional groups present on the membrane. In the current study, FT-IR analysis was employed to further investigate the magnetic f-MWCNTs-based BP/PVA membrane, and the results are displayed in ***Fig. 4.15***. To ensure reliable and accurate results, the prepared membrane was complexed with KBr powder before the spectral study, and the FT-IR spectral was conducted within the range of 4000-500 cm^{-1}. The FT-IR spectrum obtained in ***Fig. 4.15*** will provide valuable insights into the chemical composition and the interactions between different functional groups present in the magnetic f-MWCNTs-based BP/PVA membrane. This information is essential for understanding the membrane's properties and its potential applications in water treatment and micropollutant removal processes.

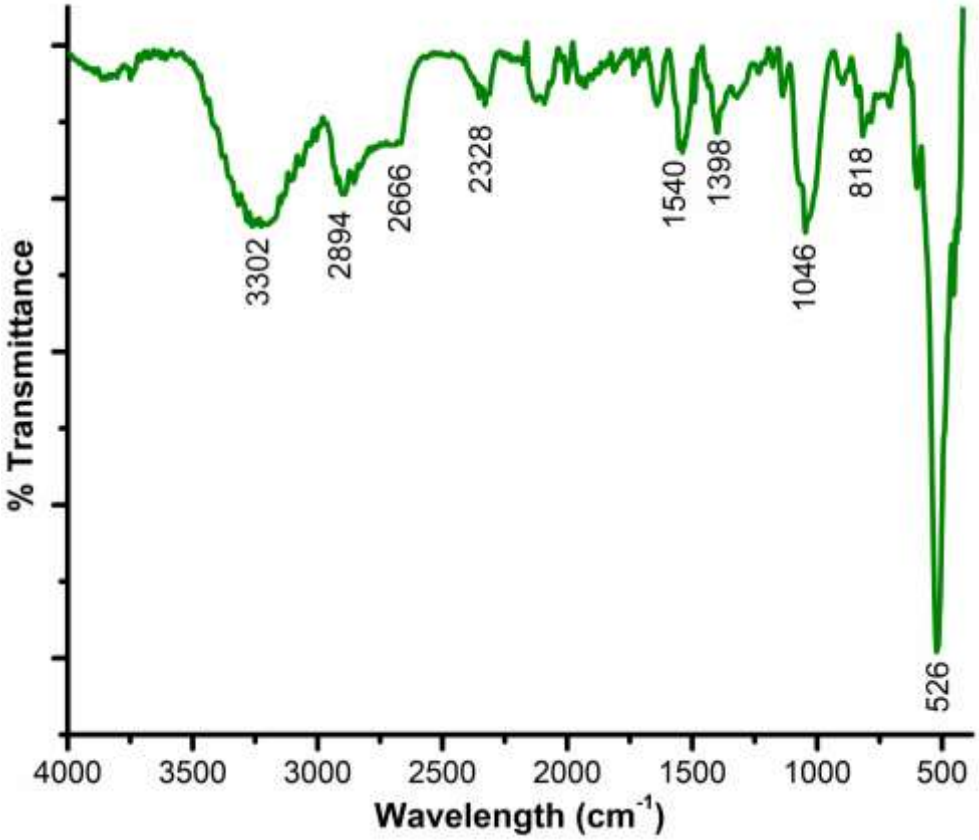

Fig. 4.15: FT-IR spectra of magnetic f-MWCNTs-based BP/PVA membrane

The FTIR spectra of the magnetic f-MWCNTs-based BP/PVA membrane exhibit a complex aspect of the prepared membrane. Several peaks in the spectrum can be associated with specific functional groups present in the membrane. The peak located at 3302 and 2328 cm^{-1} is associated with the hydroxyl group of PVA in the magnetic f-MWCNTs-based BP/PVA membrane (Malikov et al. 2014). Distinct peaks of hydrogen-bonded hydroxyl moieties verify that OH stretching depicts a broad wavelength range, consistent with the previous research findings (Liu et al. 2009, Baghayeri et al. 2018, Aliahmad et al. 2013). The peak observed at 2894 cm^{-1} is attributed to the C-O stretching bond, representing the CH_2 groups of PVA (Patil et al. 2021). This indicates that the morphology of the magnetic f-MWCNTs-based BP/PVA membrane was preserved. The peaks at 1398 and 1046 cm^{-1} correspond to the stretching vibration of -COO and CO groups, respectively. The peaks at 1540 and 818 cm^{-1} is denoted by the C=O bonds in the adsorbed carbon dioxide (Abo-Hamad et al. 2017). The presence of OH, C=O, and -COO functional

groups ensures that the prepared membrane retains hydrophilic characteristics. The broad stretch with a maximum peak at 526 cm^{-1} is associated with Fe-O-Fe stretching vibration in Fe_3O_4, confirming the presence of Fe_3O_4 nanoparticles in the membrane (Baby et al. 2010). The FT-IR findings from the present study are in good agreement with prior reported FT-IR studies (Sadeghfar et al. 2018, Huaccallo-Aguilar et al. 2019). A summary of the functional groups assigned in the magnetic f-MWCNTs-based BP/PVA membrane based on IR spectra is provided in ***Tab. 4.4***.

Tab 4.4: Functional groups assignment of magnetic f-MWCNTs-based BP/PVA based on IR spectra

Wavelength (cm^{-1})	**Functional group**
3316-2328	O-H stretching
2906	C-O stretching
1402	-COO stretching
1048	CO stretching
514	Fe-O-Fe stretching

4.4.4 Thermogravimetric (TGA) Analysis

The TGA and DTG curves of the magnetic f-MWCNTs-based BP/PVA membrane are presented in ***Fig. 4.16***. The TGA weight variation curve for the membrane exhibits several weight loss stages, each corresponding to different thermal degradation processes. In the initial stage, a slight weight loss is observed at 30 to 200°C, attributed to the elimination of water vapor and various volatile chemical moieties present in the membrane (Das et al. 2016, Américo-Pinheiro et al. 2022). The following decrease in weight loss is observed at 200 to 480°C, which can be attributed to the decomposition of grafted PVA side chains and carboxylic groups on the surface of the magnetic f-MWCNTs-based BP/PVA membrane (Wei et al. 2015, Song et al. 2017). Subsequently, a fast and essential weight decrease is observed in a temperature range from 480 to 620°C; which can be ascribed to the oxidation of the functionalized MWCNTs in the magnetic membrane material (Hua et al. 2017). The residue that remained after reaching 800°C is due to the magnetite

oxidized in the Fe_2O_3 form. The maximum weight loss of the magnetic f-MWCNTs-based BP/PVA membrane occurs close to 700ºC. Similar TGA observation have been reported for the synthesis of magnetic f-MWCNTs nanocomposites in the previous studies (Álvarez-Torrellas et al. 2018). Likewise, the DTG curve of the Fe_3O_4/ MWCNTs, and that of the present study both show an identical peak at -0.0259 %/ºC, indicating that a small quantity of residue remains after the thermal analysis (Huaccallo et al. 2019, Huaccallo-Aguilar et al. 2019).

The TGA studies showed an improvement in the thermal stability of the magnetic f-MWCNTs-based BP/PVA membrane compared to magnetic f-MWCNTs. This enhancement is evidenced by the observed shift in the onset temperature of thermal degradation to higher temperature, indicating that the magnetic f-MWCNTs-based BP/PVA membrane is more resistant to thermal decomposition (Terrones 2010). Besides, the weight loss observed from TGA indicate a reduced rate of mass loss at elevated temperatures, further affirming the enhanced thermal stability of the magnetic f-MWCNTs-based BP/PVA membrane.

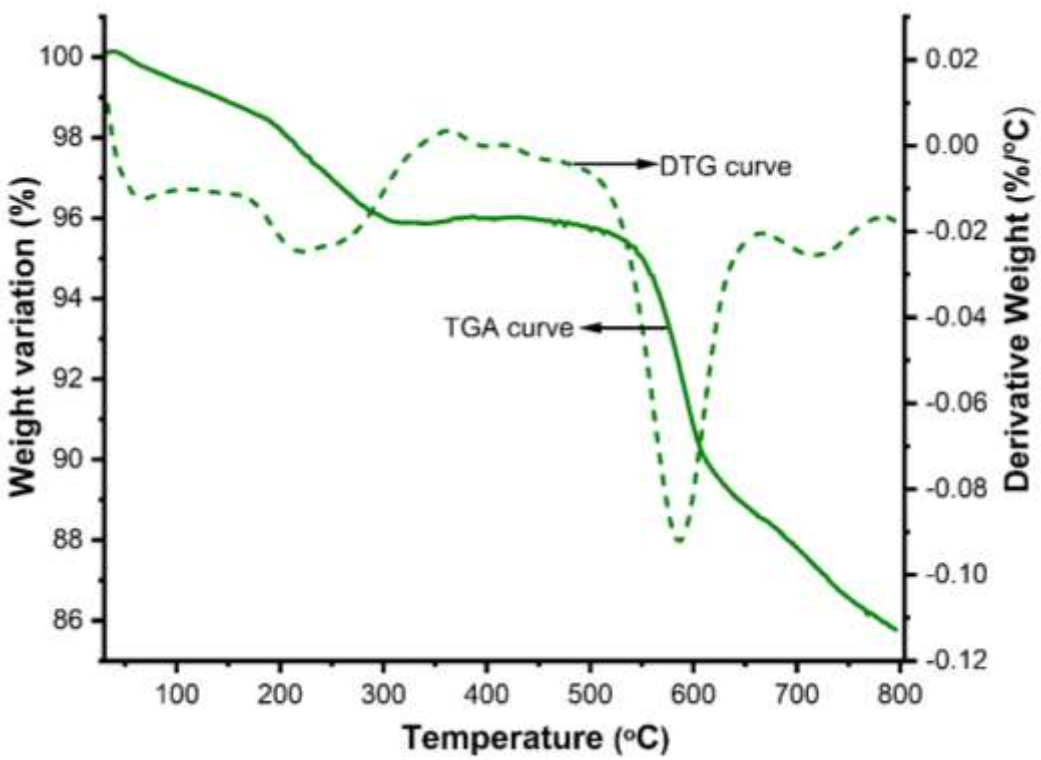

Fig 4.16: TGA analysis of magnetic f-MWCNTs-based BP/PVA membrane

4.4.5 Summary of magnetic f-MWCNTs-based BP/PVA membrane

In summary, the novel magnetic f-MWCNTs-based BP/PVA membrane was successfully fabricated using a vacuum filtration technique. The characterization results of the membrane revealed the following key findings: (i) magnetite (Fe_3O_4) nanoparticles were successfully deposited and formed a uniformly dispersed network of Fe_3O_4/f-MWCNTs on the membrane with PVA (ii) the surface of the membrane was found to be smooth and porous, with no deliminations observed (iii) the thermal stability of the membrane was substantially enhanced, making it suitable for applications involving elevated temperatures, and (iv) the infiltration of PVA into the membrane resulted in higher oxygen content (25.04 wt. %). Based on the characterisation analysis, the transformation observed between the magnetic f-MWCNTs nanocomposite and magnetic f-MWCNTs-based BP/PVA membrane was insignificant. This suggests that no significant chemical, thermal or morphological changes occurred during the membrane fabrication process, and the magnetic nanocomposite retained its distinctive identity. Overall, the fabricated membrane has the potential to be employed for various applications, particularly in water treatment due to its enhanced properties, magnetic features, and hydrophilic characteristics. The combination of magnetic properties and the capability to remove micropollutants makes the magnetic f-MWCNTs-based BP/PVA membrane a promising candidate for diverse water-related applications.

4.5 Response Surface methodology (RSM) modeling

The research objective of this section is to treat the Furazolidone (FZD) micropollutant using the magnetic f-MWCNTs-based BP/PVA membrane and evaluate its removal efficiency. FZD is an anti-bacterial and anti-protozoal agent commonly used in farms and aquaculture, but its improper disposal can lead to environmental instability when released into aquatic bodies (Zdarta et al. 2021).

To optimized the FZD removal process, the researchers used response surface methodology (RSM) modeling, a statistical tool that helps in optimizing processes by studying the influence of various input variables on the output response. RSM enables the researchers to systematically explore the effects of multiple independent factors (e.g., initial pH of FZD, agitation speed, contact time) on the dependent variable (FZD removal efficiency) with fewer experimental runs. It provided valuable insights into the optimum experimental conditions for achieving the highest removal efficiency of FZD.

Throughout this section, the performance of the magnetic f-MWCNTs-based BP/PVA membrane for FZD micropollutant removal is thoroughly evaluated using relevant graphs, figures, tables and explanations. The influence of the input reaction factors on the output response (FZD removal efficiency) is comprehensively discussed, allowing us to understand the key factors affecting the removal process.

4.5.1 Statistical optimization for FZD removal in batch treatment

In this study, central composite design (CCD) is employed in the RSM studies. When describing the correlation between input and output variables, the model statistics summary was compared, i.e., cubic, 2-factor interactions, cubic and quadratic models. The most appropriate model for the FZD micropollutant removal process was determined based on the correlation coefficient (R^2) and standard deviation (S.D). The determination coefficient (R^2) is the statistical parameter used to identify how closely the data and model are fitted. As the value gets closer to 1, the fitted model can offer outcomes closer to the actual values as a function of independent variables. A value of R^2 higher than 0.8 is recognized as a well-fitted (Najib et al. 2017). Among all, a quadratic model was recommended with the S.D of 6.53 and R^2 of 0.9344 in determining the removal efficiency of the FZD micropollutant.

Tab. 4.5: Statistical outline of the models

Source	Sequential p-value	Standard deviation	R^2	Adjusted R^2	Predicted R^2
Linear	<0.0001	11.18	0.7247	0.6834	0.6071
2-FI	0.0167	9.05	0.8468	0.7928	0.7501
Quadratic	0.0066	6.53	0.9344	0.8922	0.8046
Cubic	0.1299	5.39	0.9713	0.9266	0.8098

Additionally, the adjusted R-squared value is close to R^2 for the quadratic model, demonstrating a good adequate correlation between the input and output factors' values (Dhar et al. 2023). Adjusted R^2 quantifies the amount of variation explained by the model over the mean and takes into account the number of terms in the model. The predicted R-squared value was 0.8046, which was within 0.20 of the adjusted R-squared, implying no problem with the data or model (Jha et al. 2021).

4.5.2 Development of regression model equation

To investigate the significance of the quadratic model and the input factors, the summary of the analysis of variance (ANOVA) is shown in ***Tab. 4.6***. The primary factor that describes the significance of the quadratic model is the p-value with a confidence level of 95%. This means that terms with a p-value $\geq$ 0.05 are considered insignificant, while those with a p-value $\leq$ 0.05 are considered significant. Besides, the magnitude of the model's significance can be defined by Fisher's F-value. It was achieved by analyzing the model's mean square and residual error ratio. For every single significant term, a greater F-value implies a higher significance of the term on the response (Ghoreishi et al. 2016). The p-value and F-value in the present study were < 0.0001 and 22.14, respectively, further validating the adequacy of the quadratic model recommended in this research.

Tab. 4.6: ANOVA and model coefficient

Source	Sum of squares	Mean squares	F-value	p-value	Remarks
Model	8500	940	22	<0.0001	Significant
A-pH	940	940	22	0.0003	
B-Agitation speed	69	69	1.6	0.2	
C-Contact time	5130	5130	120	<0.0001	
AB	56	56	1.3	0.3	
AC	1000	1000	24	0.0003	
BC	17	17	0.4	0.5	
A^2	760	760	18	0.0009	
B^2	100	100	2.5	0.1	
C^2	2.5	2.5	0.1	0.8	
Residual	600	43			
Lack of fit	430	71	3.4	0.0577	Insignificant
Pure error	170	21			
Cor total	9100				

The ANOVA analysis for the removal of FZD micropollutant described the linear terms of pH (A), agitation speed (B) and contact time (C); inter-active terms of AB, AC, BC; and the quadratic terms of A^2, B^2 and C^2. Based on p-values, C (contact time) was observed to have the highest singular significant impact on the response, while A (pH) and B (agitation speed) demonstrated the slightest effect on the FZD micropollutant removal. In contrast, pH and the interaction of pH and contact time offered the most significant influence for the quadratic and inter-active terms, respectively.

Moreover, the lack of fit and pure error are also determined from the ANOVA analysis (***Tab. 4.6***). The critical term is the F-value of lack of fit, and its lower value represents that the lack of fit is insignificant compared to the pure error. Since the primary aim is to fit the model on the data, a negligible lack of fit is required (Dolatabadi et al. 2019). The present study's F-value of lack of fit was 3.4, confirming its insignificance. Furthermore, the p-value of lack of fit was estimated as 0.0577, which indicates that the lack of fit is negligible in contrast to pure error, and hence the model is satisfactory.

The signal-to-noise ratio and comparing the predicted design point values to the average prediction error is determined through adequate precision ratio (APR). The APR of RSM was *15*, which confirms sufficient signal. As reported in a previous study, the APR value > 4 validates that the model efficiency is satisfactory (Emmanuel Chinonye et al. 2018). A coefficient of variation (C.V.%) of 8.8 was attained, which indicates that the model was reasonably reproducible. The C.V.% was determined as the ratio of S.D: average of output factor. It has been reported that the C.V.% < 10% ensures that the model is reasonably reproducible (Qi et al. 2019). The quadratic regression model equation developed for the FZD micropollutant removal percentage in terms of input variables is stated in ***Equation 4.2***.

Furazolidone micropollutant removal (%)

$$= 79.19 + 7.24\,A - 1.92\,B + 16.58\,C - 1.87\,AB - 7.92\,AC + 1.01\,BC - 15.03\,A^2 + 6.15\,B^2 + 0.9571\,C^2 \qquad \text{Equation 4.2}$$

The above equation can be applied to predict the response for the particular variables. Besides, it is also essential to describe the variables' relative impact by evaluating the model coefficients. A +ve and -ve coefficients define the synergistic and antagonistic effects, respectively.

4.5.3 Diagnostic plots

Apart from the correlation coefficient, graphical illustrations were also used to define the characteristics of the residual, i.e., variations between experimental and predicted values. This section discusses the evaluation of the normality of the experimental data, displaying the residual for the predicted findings and the level of closeness between actual and predicted outcomes. ***Fig. 4.17 (a)*** illustrates the normal probability graph in which the marked points near the straight line confirm the normal distribution of errors with zero as an average value. Besides, the model adequacy can also be determined by investigating the residual vs. predicted graph as demonstrated in ***Fig. 4.17 (b)***; randomly

scattered points distributed evenly validate the model's adequacy. ***Fig. 4.17 (c)*** displays the values attained from the presented model compared to the actual obtained values. The points clustering close to the diagonal line signify a good relationship between the predicted and experimental values, ensuring the model's robustness (Karri et al. 2018). Besides, the plots of residuals displayed that the majority of the points were within the range of -1 to +1, which implies that most residuals were insignificant. Therefore, it can be concluded that the quadratic model accepted was adequate in modeling the elimination of FZD micropollutant onto the magnetic f-MWCNTs-based BP/PVA membrane.

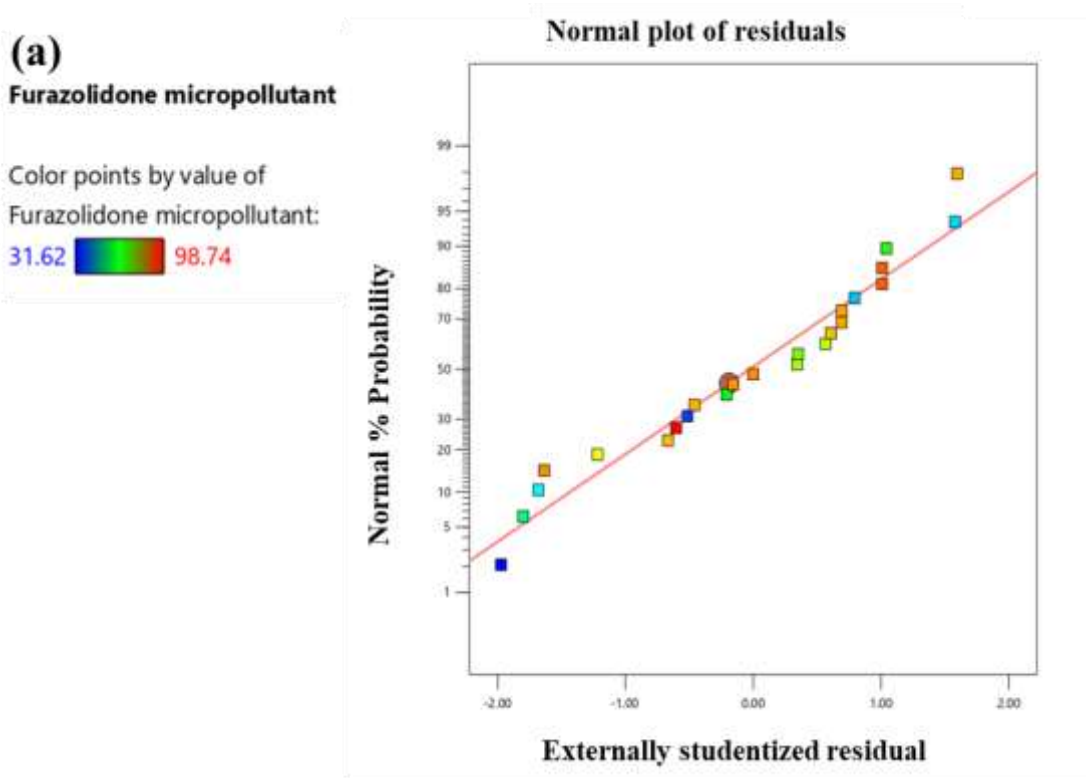

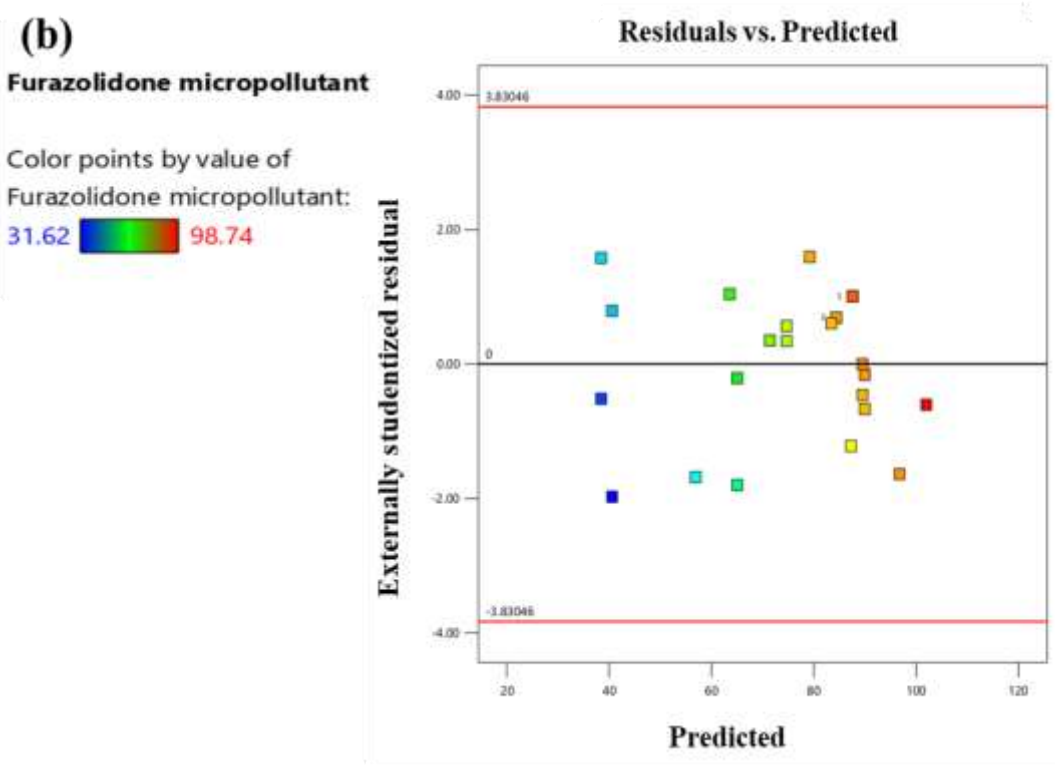

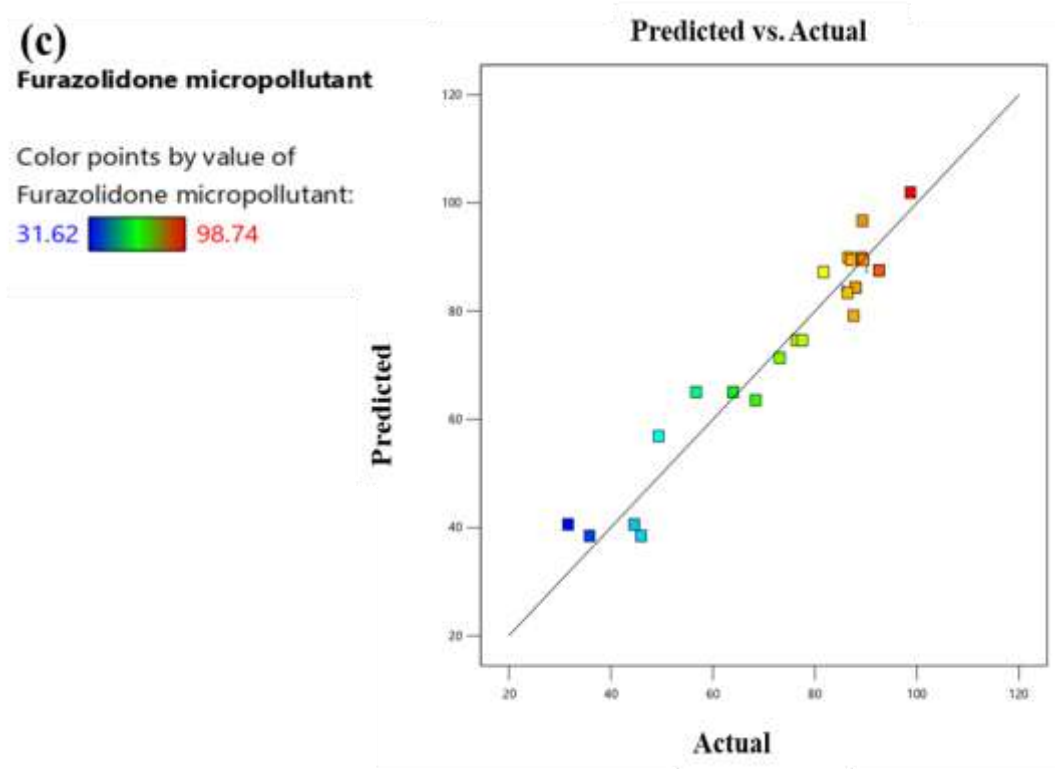

Fig 4.17: (a)Normal probability of residuals values by the model, (b) residual against predicted values by the model, (c) predicted against actual values by the model

4.5.4 Evaluation of the parameters' effect on FZD micropollutant removal

The interaction between the independent variables and their influence on FZD micropollutant elimination is depicted in ***Fig. 4.18 (a-c)***. The response for the FZD micropollutant was attained by varying two parameters while holding other variables constant. The 3-D response surface plots for various independent process parameters regarding FZD micropollutant removal using magnetic f-MWCNT-based BP/PVA membrane are demonstrated in ***Fig. 4.18***. The plots help to better understand the effect of two independent parameters and their interaction influences on the FZD micropollutant elimination.

As reported in the previous findings, the pH of the FZD micropollutant solution significantly impacts the FZD micropollutant removal efficiency using magnetic nanomaterials (Kashefi et al. 2019). The interaction influence of pH with agitation speed on FZD micropollutant removal efficiency is depicted in ***Fig. 4.18 (a)***. The maximum FZD micropollutant removal efficiency of 88% is observed at pH 6 and the agitation speed range of 150 to 200 rpm, based on a 3-D surface response plot. Moreover, ***Fig. 4.18 (b)*** displays the incorporated effect of pH and contact time for the FZD micropollutant removal percentage. Hence, the highest FZD micropollutant removal percentage could be achieved when both variables were set to a contact time of 185 min. and pH 6-6.5. Based on the results, it is observed clearly that the pH significantly impacts the FZD micropollutant removal efficiency. On the other hand, the low removal of FZD micropollutant is observed at low pH values due to the presence of a large amount of protons competing with the FZD micropollutant for adsorption sites (Mittal et al. 2010).

Besides, the elimination of organic or inorganic compounds mainly relies on the surface charge of the membrane, i.e. magnetic f-MWCNTs-based BP/PVA membrane, for electrostatic repulsion/ attraction, which depends on the point of zero charges (pH_{PZC}) (Inyang et al. 2014). The pH_{PZC} is the pH at which the overall internal and external surface charges on the membrane are zero (Kumar et al. 2021, Li et al. 2022). The iso-electric point of magnetic f-MWCNTs-based BP/PVA membrane (pH_{PZC}) was around 7 (Tran et al. 2016). If pH is

less than pH_{PZC}, the surface of the magnetic f-MWCNTs-based BP/PVA membrane contains +ve charge properties; and the FZD micropollutant has saturated nitrogen atom (Pashirova et al. 2019). Whereas pH is greater than pH_{PZC}, the +ve-charged groups on the membrane's surface merge with the unpaired electron of saturated nitrogen via electrostatic attraction (Zhen-Yuan et al. 2015). Besides, H^+ ion concentration decreases, resulting in a lower +ve charged density on the surface of magnetic f-MWCNTs-based BP/PVA membrane, leading to a reduction in electrostatic attraction when pH is greater than pH_{PZC} (Zhen-Yuan et al. 2015, Vyavahare et al. 2018) However, the FZD micropollutant is a non-ionic synthetic nitrofuran antibiotic with insignificant electrostatic interaction between the magnetic f-MWCNTs-based BP/PVA membrane and the FZD antibiotic. As a result, FZD removal mainly occurred due to hydrogen bonding because of non-charged antibiotics (Yang et al. 2015). Based on the current research study, the removal percentage of the FZD micropollutant started decreasing above pH 7, as it may affect the bond formation among the magnetic f-MWCNTs-based BP/PVA membrane and the FZD micropollutant. The aforementioned statement has also confirmed by the 3-D surface graph that above pH 7, the removal efficiency of the FZD micropollutant decreased to 75-76%. Due to this fact, the maximal FZD micropollutant removal efficiency of 98.54 was attained at pH 6 in the current study. Previous studies also reported a similar trend (Samal et al. 2021, Sadeghfar et al. 2018).

Fig. 4.18 (c) shows the 3-D surface graph for the integrated effect of contact time and agitation speed. The ANOVA results showed that the contact time is an essential variable influencing the removal percentage of the FZD micropollutant in this study. It is described that the FZD uptake capacity improves with extending contact time and agitation speed. It can be attributed to the increase in dispersion and surface area of the membrane in the FZD micropollutant solution (Khafri et al. 2017). The effect of contact time on the magnetic f-MWCNTs-based BP/PVA membrane's adsorption of FZD micropollutant is a crucial aspect to consider in the removal process. Based on the ***Fig. 4.18 (c)*** it shows the significance of understanding the relationship between contact time and FZD micropollutant adsorption efficiency. It could

be described that prolonged contact time allows more opportunities for the FZD micropollutant to interact with the magnetic f-MWCNTs-based BP/PVA membrane, potentially leading to increased adsorption capacity (Najib et al. 2017). However, there might be a point of saturation beyond which additional contact time may not significantly enhance adsorption. Optimal contact time is a critical parameter to determine for achieving efficient and effective FZD micropollutant removal using magnetic f-MWCNTs-based BP/PVA membrane-based adsorption approach. Likewise, agitation speed is also an essential and efficient tool that can improve the adsorption rate and minimize the contact time; therefore, it is more recommended than other conventional adsorption routes. The findings are identical to those described by the prior researchers (Ruthiraan et al. 2017).

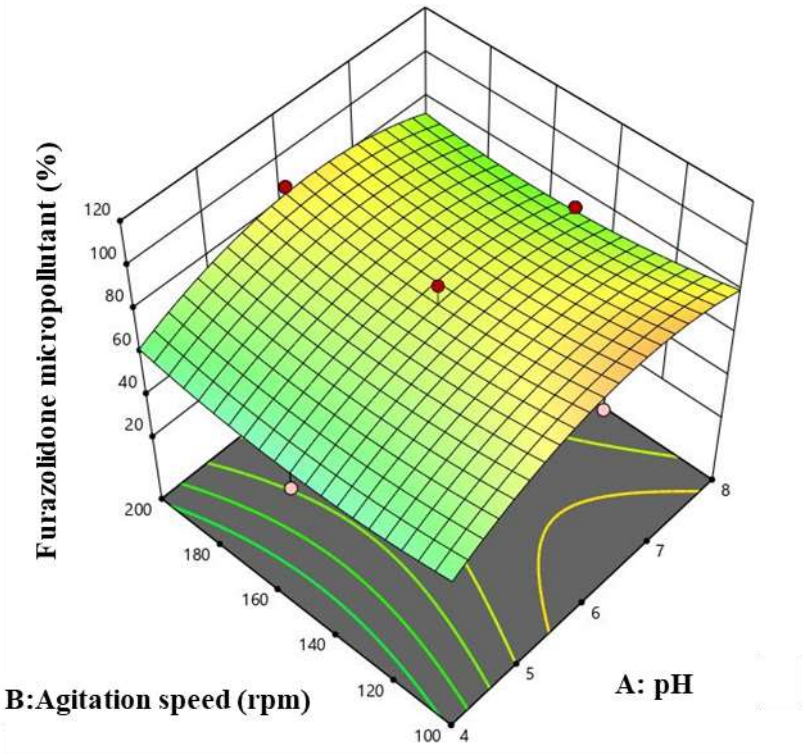
Furazolidone micropollutant (%)
120
100
80
60
40
20
200
180
160
140
120
100
B:Agitation speed (rpm)
4
5
6
7
8
A: pH

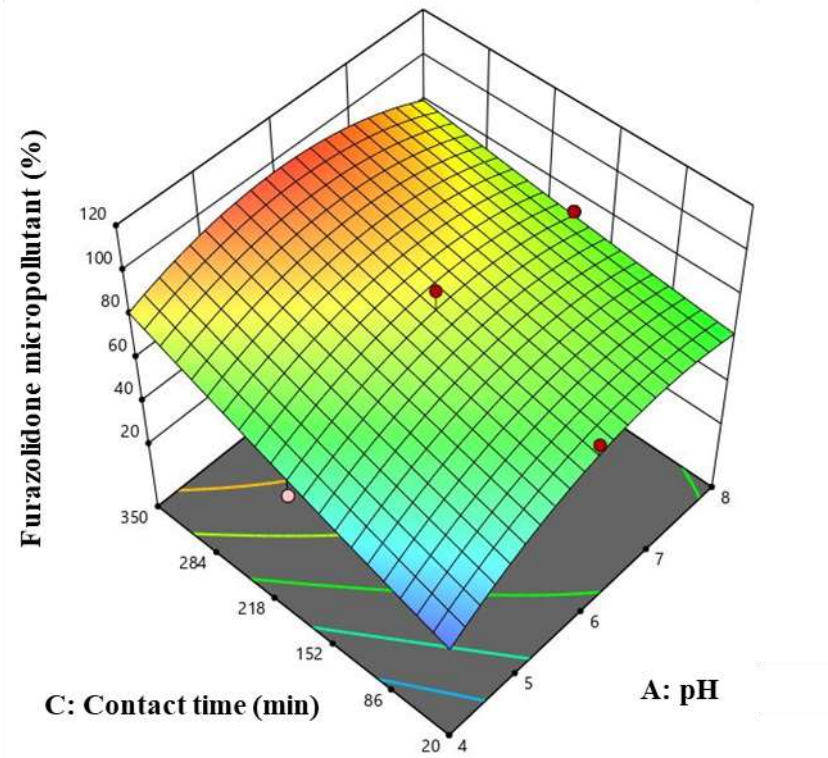
Furazolidone micropollutant (%)
120
100
80
60
40
20
350
284
218
152
86
20
C: Contact time (min)
4
5
6
7
8
A: pH

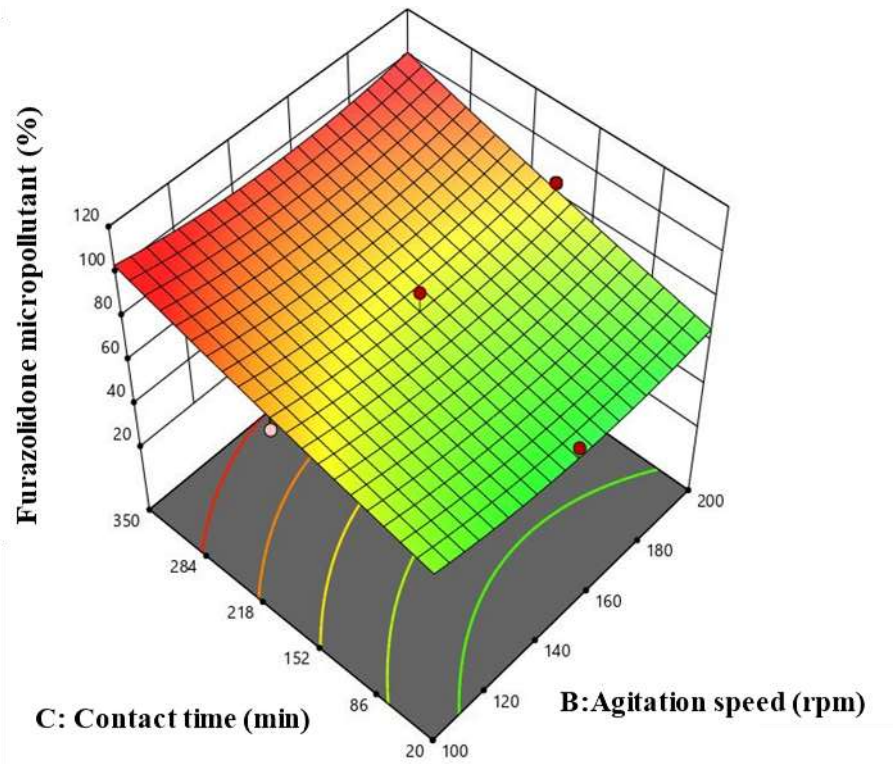

Fig 4.18: 3-D Plot for furazolidone micropollutant removal

4.5.5 Verification of the model

In terms of ANOVA outcomes, the optimum conditions to attain the maximum FZD micropollutant removal of 99.69% were at pH 6.404, 197 rpm, and 346 min. of the reaction time. To validate the optimized results achieved, three optimized conditions were taken for the model validation. In this research study, a conventional protocol was followed, entailing the repetition of each experimental procedure three times to verify the predicted efficiency %, and the outcomes were presented in ***Tab. 4.7***. It was noted that the experiment and predicted values agreed with each other, with a less than 2% standard error.

Tab 4.7: Model validation at optimum conditions

Solution	A	B	C	Furazolidone removal (%)	
	pH	**Agitation Speed (rpm)**	**Contact time (min.)**	**Predicted**	**Experimental**
1	6.4	197	346	99.69	98.74
2	5.9	106	328	99.79	98.45
3	6	122	345	98. 71	98.92

Based on the current study, the FZD micropollutant removal efficiency (%) obtained using magnetic f-MWCNT-based BP/PVA was higher and more efficient than many other researched magnetic adsorbents, particularly for FZD micropollutant (Su et al. 2022, Liu et al. 2015).

4.5.6 Summary of RSM modeling

RSM modeling was applied in the present study to predict FZD micropollutant elimination using a magnetic f-MWCNTs-based BP/PVA membrane. The model's predictive efficacy was evaluated using statistical correlation coefficient (R^2) measure. Based on the findings, the RSM model concludes the following: (i) 99.69% of FZD micropollutant removal was predicted at pH 6.4, agitation speed 197rpm, and contact time 346 with an R^2 value of 0.93, which defines the model's accuracy, and (ii) each independent process parameter is significant in FZD removal efficiency; however, the contact time is the most essential among all selected process parameters. The RSM results showed that the RSM model is an effective tool for the removal efficiency optimization of FZD micropollutant using magnetic f-MWCNTs-based BP/PVA membrane.

4.6 Adsorption Capacity for FZD micropollutant elimination using magnetic f-MWCNT-based BP/PVA membrane

This section evaluated the adsorption performance of the magnetic f-MWCNT-based BP/PVA membrane via adsorption isotherms, kinetics and thermodynamic studies.

4.6.1 Influence of initial micropollutant concentration and contact time on the adsorption capacity

The present study explored the adsorption performance of the magnetic f-MWCNTs-based BP/PVA membrane for the elimination of FZD micropollutant. ***Fig. 4.19*** depicts the effect of contact time on the adsorption of FZD micropollutant onto the magnetic f-MWCNTs-based BP/PVA membrane. The study of the initial concentration is a vital phase of the adsorption analysis process as it facilitates demonstrating the equilibrium position (Obayomi et al. 2019). This is the stage where the FZD micropollutant ion uptake on the membrane is in a dynamic equilibrium state (Khawar et al. 2019).

The initial concentration of the FZD micropollutant varied from 5 to 25 mg/L at optimum pH, temperature, and agitation speed. It was observed from the results that at the lower concentration of FZD micropollutant, the adsorption equilibrium was achieved more rapidly in comparison to the higher concentration of the FZD micropollutant. Initially, the uptake of FZD micropollutant at each concentration was fast, which slowed down as the time extended and reached a noticeable equilibrium at a lapse of 210 min. No appreciable adsorption uptake was reflected beyond this time. At early concentration, the maximal adsorption uptake can be attributed to the significantly greater number of active sites present on the magnetic f-MWCNTs-based BP/PVA membrane, and the gradual possession of those active sites with FZD micropollutant ions decreases the rate of adsorption at later concentrations (Madala et al. 2017). Besides, it can also be observed from ***Fig. 4.19*** that at 5 mg/L of the FZD micropollutant, the adsorption equilibrium was reached after 60 min. In contrast, it took 120, 150, 180, and 210 min. to attain adsorption equilibrium for 10, 15, 20, and 25 mg/L, respectively. This is

ascribed to the gradient concentration increase of the driving force to overcome the overall resistance of the FZD micropollutant ion mass transfer, consequently a greater adsorption rate (Banerjee et al. 2017). To ensure that the adsorption equilibrium was reached entirely, a further 60 min. contact time was kept. It was observed that there were slight changes in adsorption uptake after 300 min. Therefore, it can be concluded that the adsorption equilibrium positions were attained at 300 min, as the amount of the FZD micropollutant adsorbed and desorbed on the magnetic f-MWCNTs-based BP/PVA membrane was nearly even. Compared to the previous studies reported for FZD micropollutant removal, the magnetic f-MWCNTs-based BP/PVA membrane displayed higher adsorption uptake at different concentrations (Gurav et al. 2020, Zhen-Yuan et al. 2015).

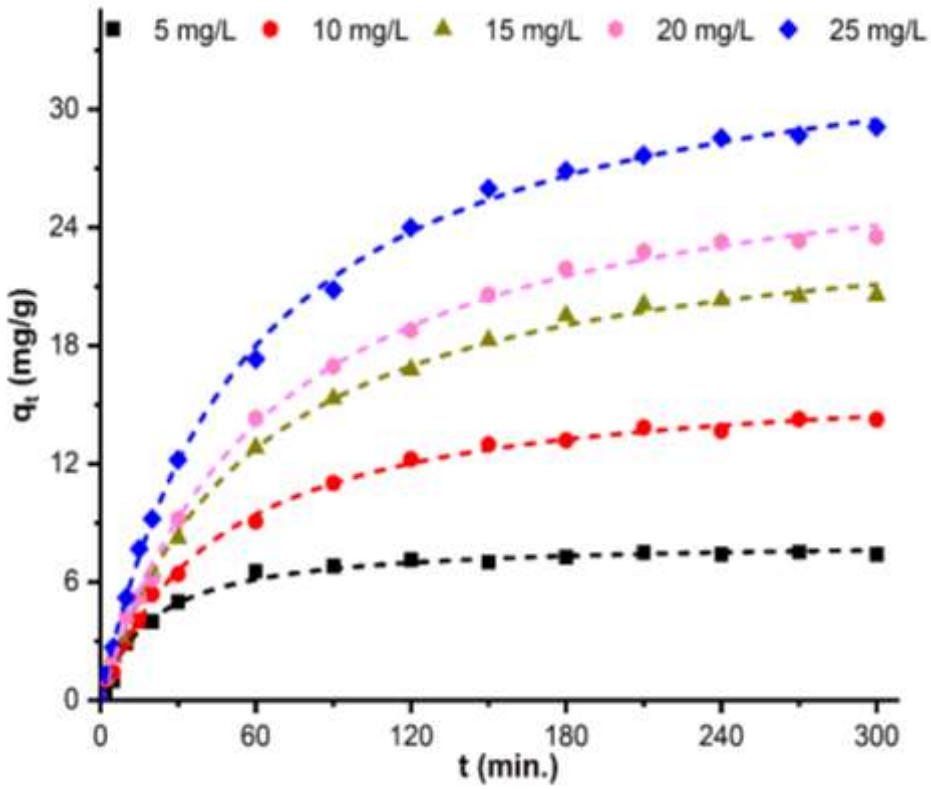

Fig 4.19: Effect of contact time on the adsorption capacity at different initial concentrations (pH 6, contact time 350 min, and agitation speed 200 rpm)

Tab. 4.8: Adsorption uptake of FZD micropollutant on different adsorbents

Material	Experimental conditions	Adsorption capacity (mg/g)	Remarks	References
Fe_3O_4- banana pseudo-stem biochar	Volume= 100 mL pH=3-12 Dosage=0.0025g Temperature=15-45 ºC Conc.=20 to 80 mg/L	31.45	• The fabrication of the material required extensive temperature, i.e., 600ºC. • The optimum concentration of the FZD micropollutant was kept at 20 mg/L. • HPLC chromatography was used to detect the pollutant at 365 nm. • The adsorption equilibrium time was reported at 540 min. (pH 7.5, temperature 45 ºC), whereas the removal efficiency of 96.81% was achieved in 9 hrs.	(Gurav et al. 2020)
Granular activated carbon (GAC)	Volume= 50 mL pH=2-13 Dosage=0.4 g Temperature=25 ºC Conc.=5 to 30 mg/L	3.23	• The adsorption equilibrium time of the FZD micropollutant on the GAC was 120 min. • The pollutant was detected using UV-spectrophotometer at 278 nm.	(Cheng et al. 2019)
Fe_3O_4- MWCNTs	Volume= 50 mL pH=3-9 Dosage=0.8 g	11.98	• In this study, the adsorption equilibrium state was accomplished at pH 6 and contact time 600 min.,	(Liu et al. 2015)

Material	Experimental conditions	Adsorption capacity (mg/g)	Remarks	References
	Temperature=25 ºC Conc.=1 to 15 mg/L		• At 365 nm, the pollutant was detected using UV- spectrophotometer • The removal percentage of the FZD micropollutant was noticed at 10 mg/L.	
magnetic f-MWCNTs-based BP/PVA membrane	Volume= 100 mL pH=4-8 Temperature=25 ºC Conc.=5 to 25 mg/L	29.67	• The membrane was fabricated under relatively normal conditions. • Adsorption equilibrium was observed at 180 min., pH 6, agitation speed 200 rpm. • The maximum degradation efficiency was found in 300 min. (98.54%, 10 mg/L).	Present study

4.6.2 Adsorption isotherms

Equating equilibrium data through empirical and theoretical models is essential for practical operation. In this study, the interaction mechanism between the adsorbate and adsorbent was examined by employing the adsorption isotherms described by Langmuir, Freundlich, Temkin, and Dubinin Radushkevich isotherms. Moreover, the adsorption isotherm models also reflect information on the adsorbate distribution on the surface of the membrane when the adsorption process has reached equilibrium.

The amount of FZD micropollutant adsorbed per unit mass of magnetic f-MWCNT-based BP/PVA membrane was determined using adsorption isotherm models as a function of solutes' equilibrium concentration at room temperature. ***Fig. 4.20 (a-d)*** illustrates the linearized plots for Langmuir, Freundlich, Temkin, and Dubinin Radushkevich adsorption isotherm models. All the important parameters and correlation coefficients (R^2) of each isotherm model studied are listed in ***Tab. 4.9***.

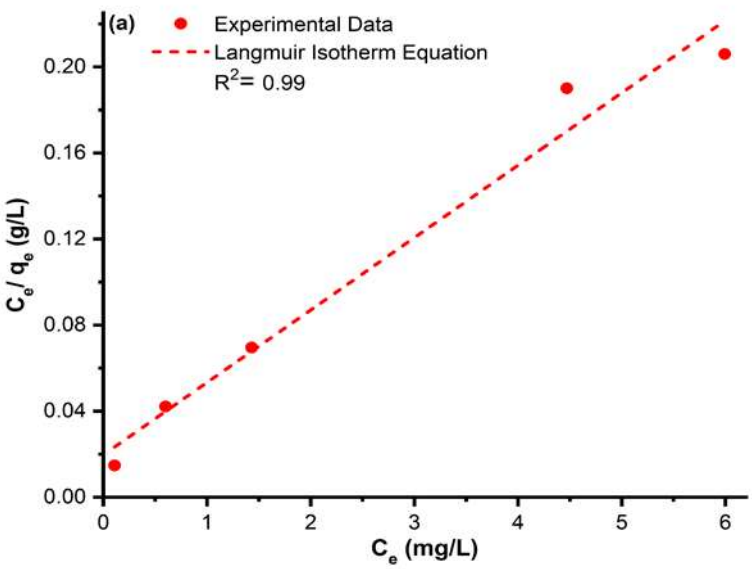

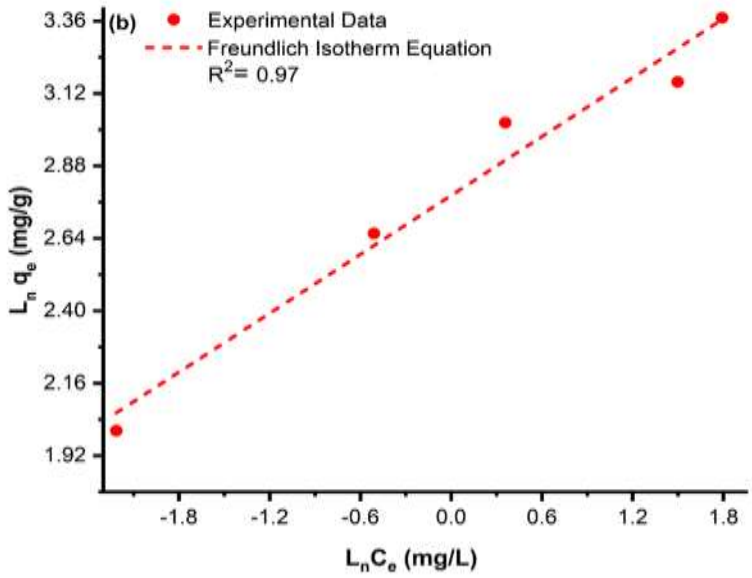
(b)
Experimental Data
Freundlich Isotherm Equation
R2= 0.97
3.36
3.12
2.88
2.64
2.40
2.16
1.92
Ln qe (mg/g)
-1.8
-1.2
-0.6
0.0
0.6
1.2
1.8
LnCe (mg/L)

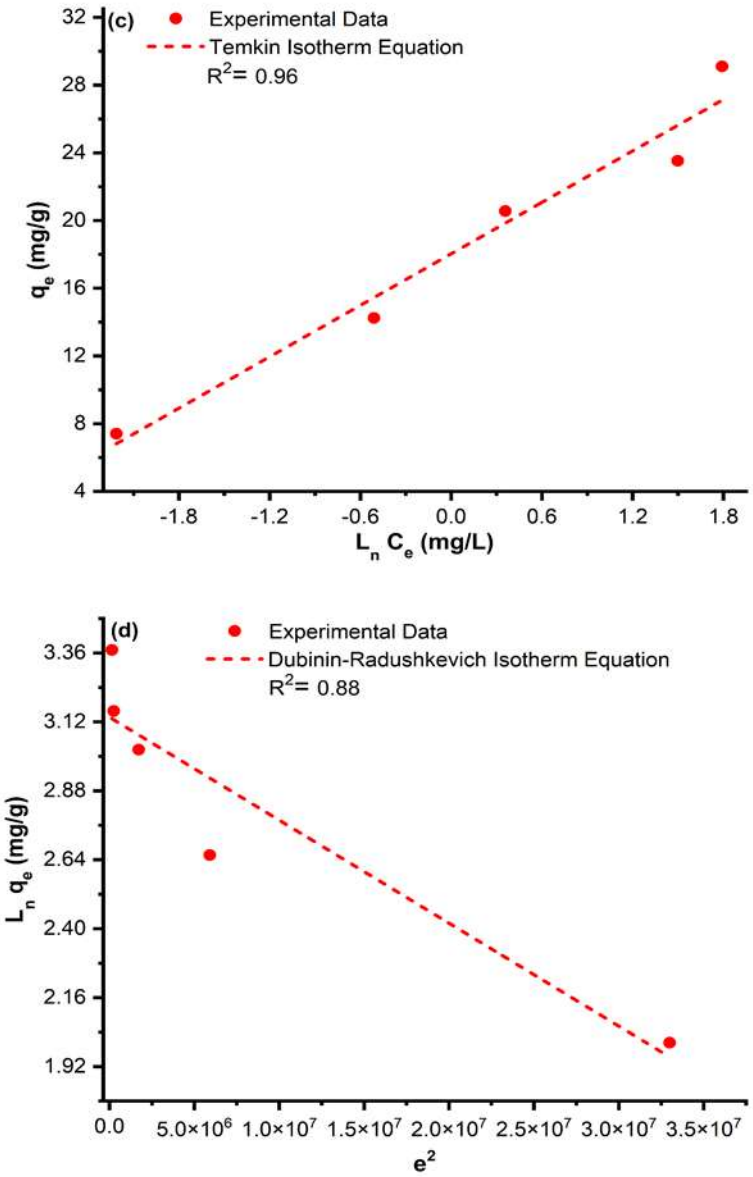

Fig. 4.20: Graphs of (a) Langmuir, (b) Freundlich, (c) Temkin and (d) Dubinin-Radushkevich adsorption isotherm for FZD micropollutant onto magnetic f-MWCNTs-based BP/PVA

In comparison to the R^2 value of Freundlich, Temkin, and Dubinin Radushkevich models, it was observed that the Langmuir isotherm model best-fit the FZD micropollutant adsorption onto the magnetic f-MWCNT-based BP/PVA membrane as it showed the highest R^2 value, i.e. 0.994. Based on the assumption defined by the Langmuir model, the adsorption process carried out a mono-layer and homogeneous mechanism, where the adsorbent and adsorbate are energetically similar at sorption sites (Jiang et al. 2020). The mono-layer adsorption capacity determined by the Langmuir isotherm model

was 29.67 mg/g. Freundlich isotherm model concluded that the adsorption surface of the fabricated membrane was heterogeneous and preferred FZD micropollutant adsorption as the 1/n value was within the range of 0 to 1 (Feng et al. 2021). Furthermore, the Dubinin Radushkevich isotherm model described that the adsorption approach is physical, as the mean adsorption energy (E) value was lower than 8 kJ/ mol (Ahmed et al. 2013). This confirms that there was a likelihood of physical interaction of FZD micropollutant on the membrane surface.

Tab. 4.9: Isotherm parameters for FZD micropollutant onto the magnetic f-MWCNTs-based BP/PVA membrane

Adsorption Isotherm Parameters				
	q_m (mg/g)	**K_L (L/mg)**		**R^2**
Langmuir	29.67	1.73		0.994
	K_F (mg/g)(L/mg^1)^n)	**1/n**		**R^2**
Freundlich	16.20	0.33		0.971
	k_T (L/mg)	**B**		**R^2**
Temkin	34.90	5.09		0.960
	q_s (mg/g)	**β (mol.^{2}/J^2)×10^{-8}**	**E (kJ.mol^1)**	**R^2**
Dubinin–Radushkevich	23.03	4	3.54	0.882

4.6.3 Adsorption Kinetics

The kinetics of FZD micropollutant adsorption onto the magnetic f-MWCNT-based BP/PVA membrane at various initial concentrations of FZD micropollutant were examined by plotting the adsorption data to two different kinetic models: pseudo-first and second-order kinetic models. Based on the pseudo-first and second order kinetic model, it is assumed that physisorption and chemisorption control the rate of adsorption, respectively, through transferring electrons among the adsorbate and adsorbent (Qin et al. 2020, Obayomi et al. 2020).

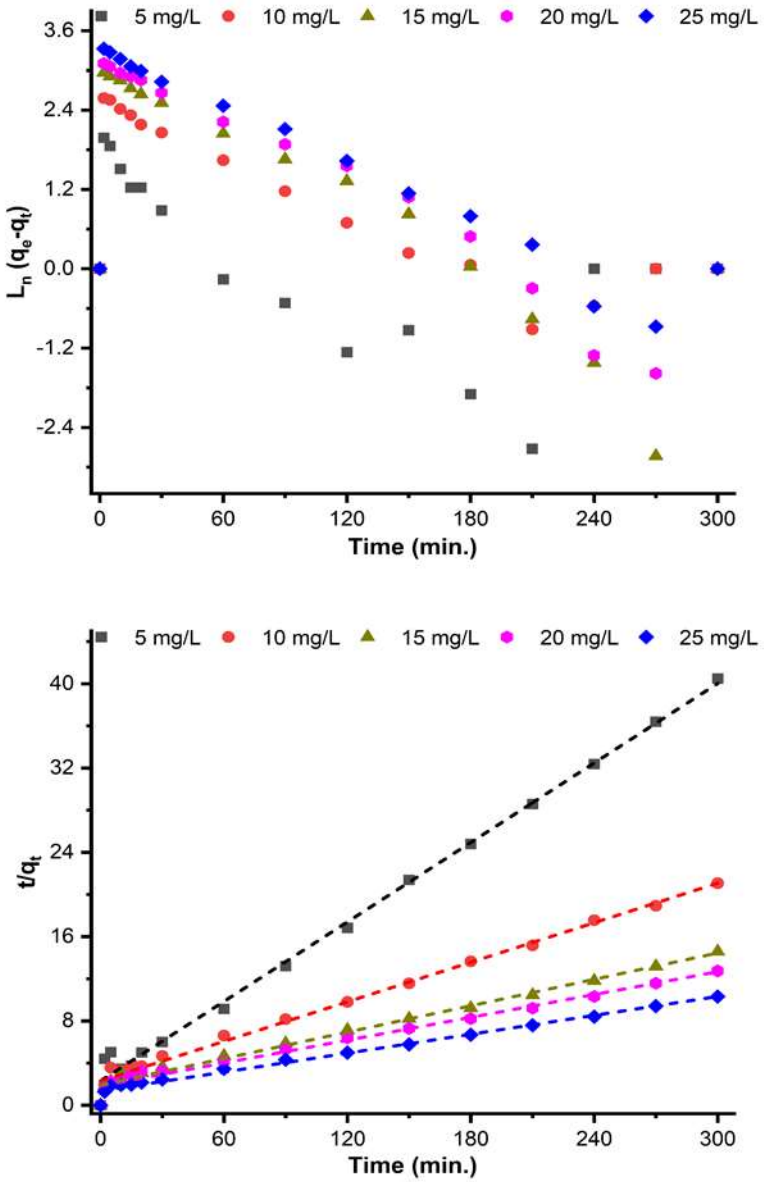

Fig. 4.21: (a) Pseudo first-order kinetic model, (b) Pseudo second-order Kinetic model for the adsorption of FZD micropollutant using magnetic f-MWCNTs-based BP/PVA membrane

Fig. 4.21 (a-b) illustrate the pseudo-first and second-order kinetic curves plotted from the data attained from experimental studies. The summary of the results assessed from the slopes and intercepts of the resultant regression curves, with the parameters k_1, k_2, and R^2, is described in ***Tab. 4.10***. In contrast to pseudo-first-order kinetic models, the pseudo-second-order kinetic model displayed a higher R^2 value. It can be observed that the R^2 value of the pseudo-second-order model for FZD micropollutant was close to 1, which was higher

than the pseudo-first-order model. Moreover, the $q_{e,EXP}$ (experimental value) was also close to $q_{e,CAL}$ (calculated value). This indicates that the adsorption kinetics of FZD micropollutant followed a pseudo-second-order kinetic model. This phenomenon is expected as the calculated values of the parameters on the pseudo-first-order kinetic model were associated with the experimental values of adsorption quantity (qe) at equilibrium. However, it was not easy to achieve in the actual process. In addition, the pseudo-second-order kinetic model involves different parameters such as particle diffusion and surface adsorption, which observes the entire adsorption mechanism of organic compounds on the solid surface (Kumar et al. 2012). Moreover, the pseudo-second-order kinetic model also confirmed that the calculated adsorption capacity ($q_{e,CAL}$) from the slopes and intercepts are close enough to the adsorption capacity ($q_{e,EXP}$) achieved from the experiment. It can be observed from ***Tab. 4.10*** that as the initial concentration of the FZD micropollutant increased, there was a decline in the pseudo-second-order rate constant (k_2). It is mainly because FZD micropollutant adsorption onto the magnetic f-MWCNT-based BP/PVA membrane attained equilibrium faster at lower concentrations than at higher concentrations (Amran et al. 2021). Moreover, the findings also determine that the chemisorption dominates and controls FZD micropollutant adsorption onto the magnetic f-MWCNT-based BP/PVA membrane. The interaction between the magnetic f-MWCNT-based BP/PVA membrane and FZD micropollutant implicates electron sharing/ exchanging (Wei et al. 2021). The present results are identical to the previous study, where they fabricated novel silver nanoparticles (AgNPs) for the Congo red dye removal (Obayomi et al. 2022). Based on the literature, it has been noticed that the pseudo-second-order kinetic model is widely employed for the sorption of aqueous contaminants, such as heavy metals, dyes, and micropollutants (Huang et al. 2015, Tang et al. 2021).

Tab. 4.10: Pseudo first-order kinetic model, and (b) Pseudo second-order Kinetic model for the adsorption of FZD micropollutant using magnetic f-MWCNTs-based BP/PVA membrane

Concentration (mg/L)	**q_e (exp.) (mg/g)**	**Magnetic f-MWCNTs-based BP/PVA membrane**					
		Pseudo First-order			**Pseudo Second-order**		
		q_e (cal.) (mg/g)	**k_1 (min^{-1})**	**R^2**	**q_e (cal.) (mg/g)**	**k_2 (g/mg·min)**	**R^2**
5	7.4	2.46	0.02	0.37	7.96	0.0068	0.997
10	14.2	7.58	0.02	0.66	16	0.0017	0.994
15	20.6	13.4	0.03	0.70	24	0.0009	0.983
20	23.5	15.1	0.03	0.70	27.7	0.0007	0.979
25	29.1	17.3	0.03	0.68	33.4	0.0006	0.984

4.6.4 Adsorption Thermodynamic

The change of free energy, including entropy (ΔS^0), enthalpy (ΔH^0), and Gibbs free energy (ΔG^0), for FZD micropollutant adsorption, was investigated at varying temperatures to describe the spontaneity and feasibility of the adsorption approach. The graph of L_nK_o vs. 1/T yielded a straight-line, which was plotted from the experimental results, and ΔH^0 and ΔS^0 were calculated from the slope and intercepts at different concentrations of the FZD micropollutant solution. The thermodynamic adsorption results at different FZD micropollutant concentrations are shown in ***Tab. 4.11***. The negative ΔG^0 value revealed that the adsorption of FZD micropollutant on the magnetic f-MWCNT-based BP/PVA membrane is spontaneous, feasible, and thermodynamically satisfactory (Zhen-Yuan et al. 2015). Moreover, the negative ΔS^0 and ΔH^0 values, as shown in ***Tab. 4.11*** imply exothermic and random decline at the adsorbate-membrane interface during the adsorption of FZD micropollutant onto the magnetic f-MWCNT-based BP/PVA membrane (Khawar et al. 2019). Based on the thermodynamic results, it can be concluded that the adsorption efficiency of the magnetic f-MWCNT-based BP/PVA membrane towards FZD micropollutant molecules was favorable at lower

temperatures. Similar findings have been reported by several researchers (Liu et al. 2009, Obayomi et al. 2020, Chen et al. 2009).

Tab. 4.11: Thermodynamic parameters for FZD micropollutant onto the magnetic f-MWCNTs-based BP/PVA membrane

Micropollutant conc. (mg/L)	**ΔH^O (kJ/mol.)**	**ΔS^O (J/mol.)**	**ΔG^O (kJ/mol.)**		
			298 K	**308 K**	**318 K**
5	-49	-129	-11	-9.4	-8.1
10	-40	-110	-7.9	-6.8	-5.8
15	-24	-58	-6.6	-6.1	-5.5
20	-12	-31	-3.2	-2.9	-2.5
25	-11	-31	-2.2	-1.9	-1.6

4.7 Reusability of magnetic f-MWCNT-based BP/PVA membrane

Reusability is one of the vital aspects of sustainable industrial application. In the current study, the reusability of the magnetic f-MWCNT-based BP/PVA membrane was evaluated under batch treatment using ethanol as a solvent for five cycles. The outcome of the reusability performance is demonstrated in ***Fig. 4.22***. In contrast to magnetic MWCNTs as adsorbents, the magnetic f-MWCNTs-based BP/PVA membrane have a similar FZD micropollutant removal efficiency for the first cycle (Zhen-Yuan et al. 2015). However, after the first cycle, the results exhibited that magnetic f-MWCNTs-based BP/PVA membrane displayed higher FZD micropollutant elimination efficiency than magnetic MWCNTs. The decline of removal capacity for magnetic MWCNTs adsorbents can be linked to its internal conditions, for instance, decomposition of the adsorbent or quantity loss of the adsorbent (Hussain et al. 2021).

On the other hand, the magnetic f-MWCNTs-based BP/PVA membrane still displays higher removal efficiency after the first cycle than in previous studies due to higher adsorption site availability on the prepared membrane (Stango et al. 2019). The higher adsorption sites availability on the membrane surface is mainly due to the acid treatment of MWCNTs. Over the time removal

efficiency declined, resulting in the loss of adsorption sites on the fabricated membrane.

In the study, as mentioned earlier, Zhen and co-associates maintained the reusability efficiency of magnetic MWCNTs after the five cycle as 70% (Zhen-Yuan et al. 2015). Whereas the magnetic f-MWCNTs-based BP/PVA membrane still sustained a high removal rate of FZD micropollutant, which was 88% compared to the first round. Based on the current result, it can be expected that even after the fifth round, the removal rate of FZD micropollutant would be higher than many other magnetic materials studied. Therefore, it can be stated that the magnetic f-MWCNT-based BP/PVA membrane can be efficiently reused by using ethanol as solvent.

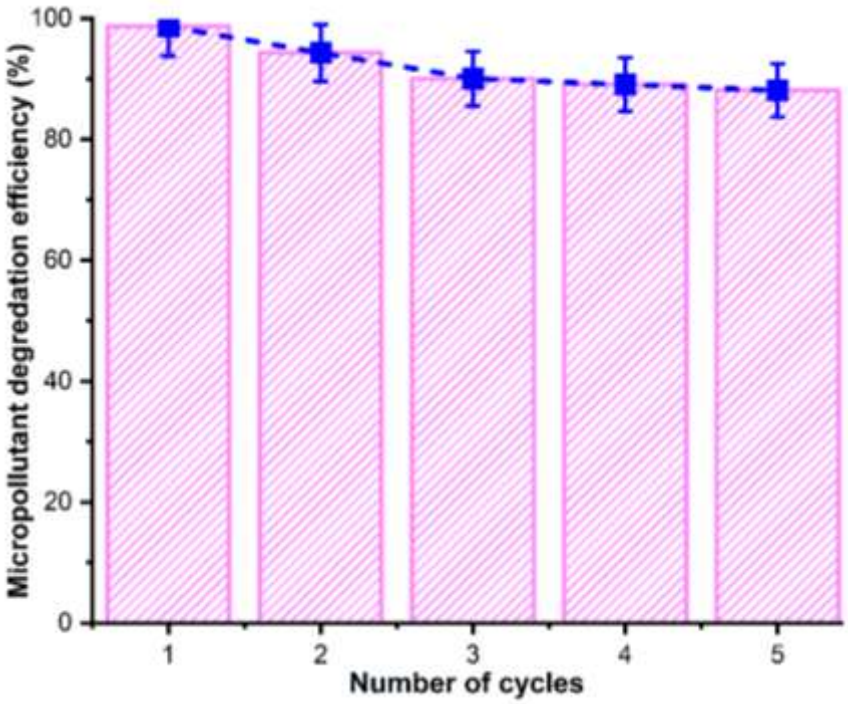

Fig 4.22: Reusability of magnetic f-MWCNTs-based BP/PVA membrane for FZD micropollutant removal efficiency (%)

4.8 Characterisation of FZD micropollutant molecules- magnetic f-MWCNTs-based BP/PVA membrane interaction

The characterisation analyses were conducted in this section to investigate the interaction of FZD micropollutant molecules with the magnetic f-MWCNTs-

based BP/PVA membrane. Fourier transform infrared spectrophotometry (FT-IR) and Field emission scanning electron microscope (FE-SEM) were employed to describe the available surface functional moieties and surface morphology of the magnetic f-MWCNTs-based BP/PVA membrane.

4.8.1 Fourier transform infrared spectrophotometry (FT-IR) analysis

Fig. 4.23 illustrates the comparison of the FT-IR spectrum of the magnetic f-MWCNTs-based BP/PVA membrane before and after the elimination of the FZD micropollutant. The study aimed to describe the availability of functional moieties before and after the elimination of FZD micropollutant. ***Fig. 4.23*** verified the formation of magnetite (Fe_3O_4) nanoparticles. The spectrum demonstrated a sharp and distinct peak at 514 cm^{-1}, which came from the stretching vibration of the metal-oxygen bond and verified the development of the Fe_3O_4 spinel oxide. Besides, the 526 cm^{-1} band is also related to Fe^{3+} vibration in the octahedral hole in the spinel network (Mahdavi et al. 2013). The peaks at 3302 and 2328 cm^{-1} corresponded to hydroxyl stretching vibration due to the hydrogen bonds (Aliahmad et al. 2013). The absorbance band at 2894 cm^{-1} is associated with C-O, and two adsorption bands at 1398 and 1046 cm^{-1} are ascribed to -COO and CO moieties, respectively. In addition, two absorbance peaks at 1540 and 818 cm^{-1} are related to C=O bonds in the carbon dioxide adsorbed (Mittan et al. 2008). The findings from the FT-IR analysis of the magnetic f-MWCNTs-based BP/PVA membrane were similar to the previous study reported for ultra-sound assisted removal of methylene blue on the surface of PVA/ Fe_3O_4-CNTs nanocomposite (Sadeghfar et al. 2018).

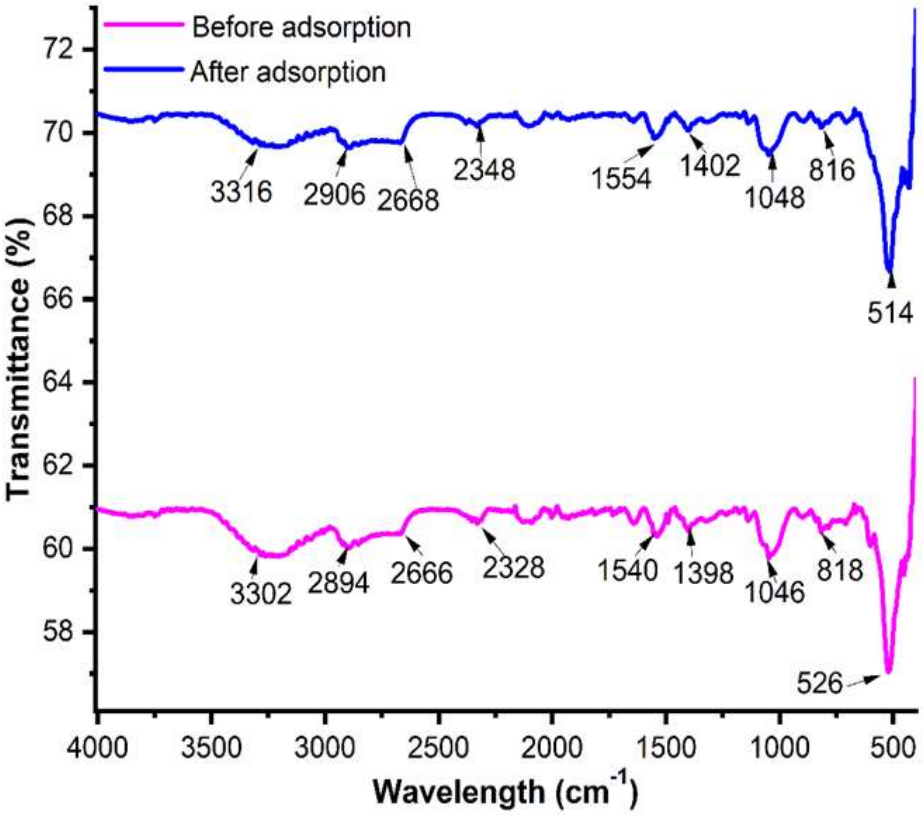

Fig. 4.23: FT-IR spectra of magnetic f-MWCNTs-based BP/PVA membrane before and after FZD adsorption

It was visible from ***Fig. 4.23*** that there were some variations in intensities and positions of infrared bands noted before and after the elimination of FZD micropollutant on the magnetic f-MWCNTs-based BP/PVA membrane. ***Fig. 4.23*** displayed the FT-IR spectrum after loading the FZD micropollutant on the magnetic f-MWCNTs-based BP/PVA membrane, and it showed that some peaks had formed, shifted, and disappeared due to the FZD micropollutant adsorption on the magnetic f-MWCNTs-based BP/PVA membrane. These variations in intensities and position might be due to the decrease and loss of surface hydrogen-bonded hydroxyl (OH) moieties and the interaction of the cyanide group from the FZD micropollutant during the FZD micropollutant extraction (Moazzen et al. 2019). For example, as shown in ***Fig. 4.23***, it can be observed that the adsorption peaks at 3302, 2894, 2328, 1540, 1398, 1046, 818 and 526 cm^{-1} are shifted respectively to 3316, 2906, 2348, 1554, 1402, 1048, 816, and 514 cm^{-1}, suggesting the contribution of these functional bonds in the binding of the FZD micropollutant ion on the magnetic f-MWCNTs-based BP/PVA membrane (Kumar et al. 2020). These outcomes revealed that

hydrogen bonding plays a vital role in the adsorption of the FZD micropollutant using magnetic f-MWCNTs-based BP/PVA membrane.

4.8.2 Field emission scanning electron microscope (FE-SEM) analysis

FE-SEM was employed to compare the surface morphology of the magnetic f-MWCNTs-based BP/PVA membrane before and after the elimination of the FZD micropollutant. ***Fig. 4.24*** depicts the FE-SEM images of the magnetic f-MWCNTs-based BP/PVA membrane before and after the adsorption of the FZD micropollutant. ***Fig. 4.24 (a-b)*** displayed that the surface of the magnetic f-MWCNTs-based BP/PVA membrane is uniformly dispersed with the network of Fe_3O_4/ f-MWCNTs, indicating the homogeneous distribution of Fe_3O_4/ f-MWCNTs in the polyvinyl alcohol matrix. Besides, it is noted that the prepared membrane has a smooth and porous surface, which is important in the adsorption of FZD micropollutant molecules. High porosity is an important aspect of an excellent adsorbent. After loading the FZD micropollutant, the membrane's surface transformed into a rougher and thicker surface with saturated pores, as illustrated in ***Fig. 4.24 (c-d)***. Due to the precipitate formation from the adsorbed micropollutant molecules, the thicker membrane surface was observed, subsequently resulted decline in the FZD micropollutant uptake after several cycles.

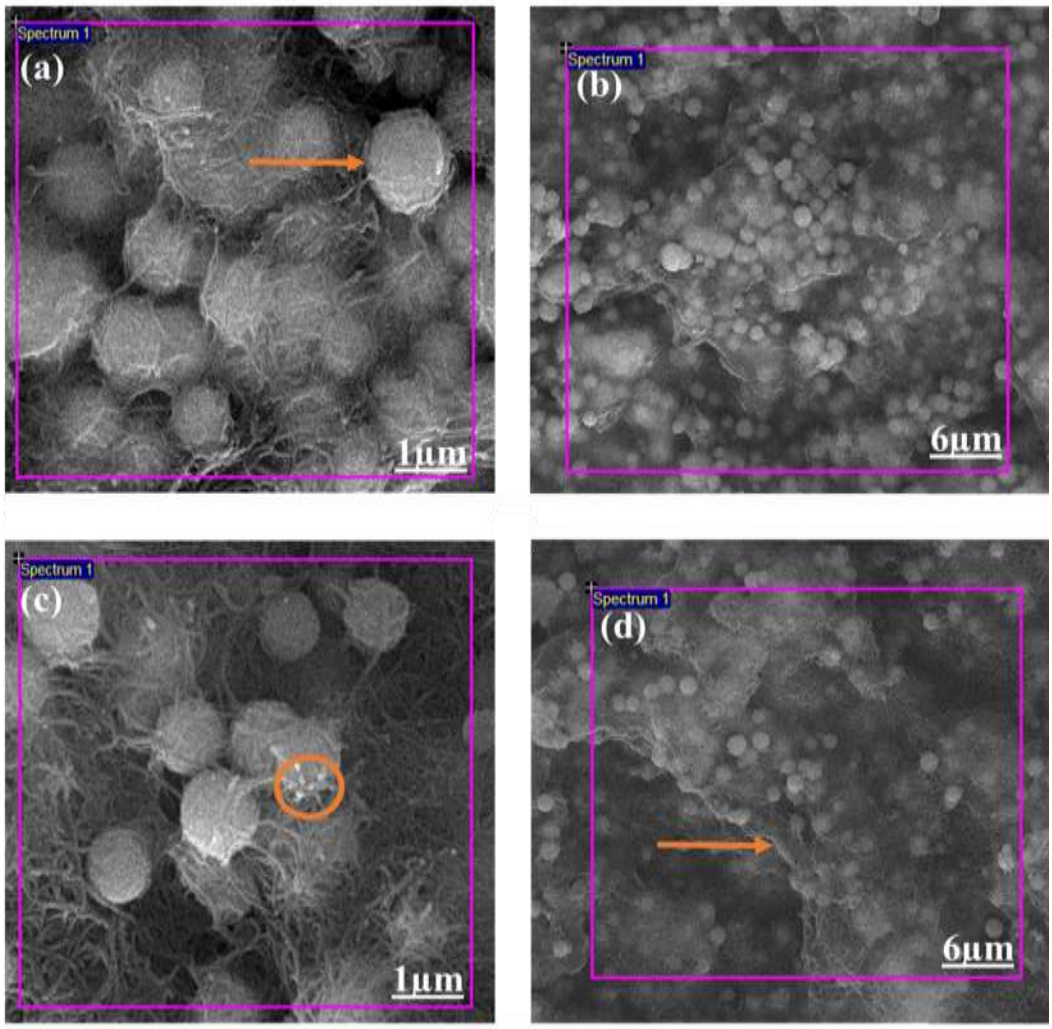

Fig. 4.24: FE-SEM morphology of magnetic f-MWCNTs-based BP/PVA membrane before (a-b) and after (c-d) FZD adsorption

4.9 Adaptive neuro-fuzzy inference system (ANFIS) modeling

Adaptive neuro-fuzzy inference system (ANFIS) is based on mathematical computation, which is apt to explain complex and non-linear problems as its process is coupled to the Takagi- Sugeno fuzzy inference framework (Adday et al. 2022). Therefore, there has recently been tremendous attention given to the application of ANFIS to various processes. Besides, ANFIS has also gained extensive attention in modeling chemical engineering applications, such as predicting specific energy consumption, reduction in moisture content, adsorption uptake, etc. (Afriyie Mensah et al. 2020). Researchers who have utilized ANFIS modeling conclude that they have found ANFIS to be an adequate computing technique; moreover, the model's ability to predict

experimental results and mathematical clarifications is also suitable for their particular research studies.

This section aims to use the ANFIS soft computational technique to predict the removal percentage model for FZD micropollutant. Subsequently, the experimental and predicted results were compared, and the ANFIS modeling outcomes were depicted to deliver strong theoretical evidence for FZD micropollutant batch removal treatment. In addition, a critical comparison of the predictive capabilities of the RSM and ANFIS models was also described. Statistical error functions were also employed to evaluate the performance of the two models under study.

4.9.1 Optimization of fuzzy inference system

As mentioned earlier, the ANFIS modeling framework combines neural and fuzzy logic networks, which derive the optimum rules and provide the concluding model through training data (Olatunji et al. 2022). In the present study, Takagi-Sugeno fuzzy inference systems were applied to model the percentage of FZD removal by the magnetic f-MWCNTs-based BP/PVA membrane because it can accurately follow the non-linear data. Furthermore, data were normalized in the fuzzy model study to enhance the system's efficiency.

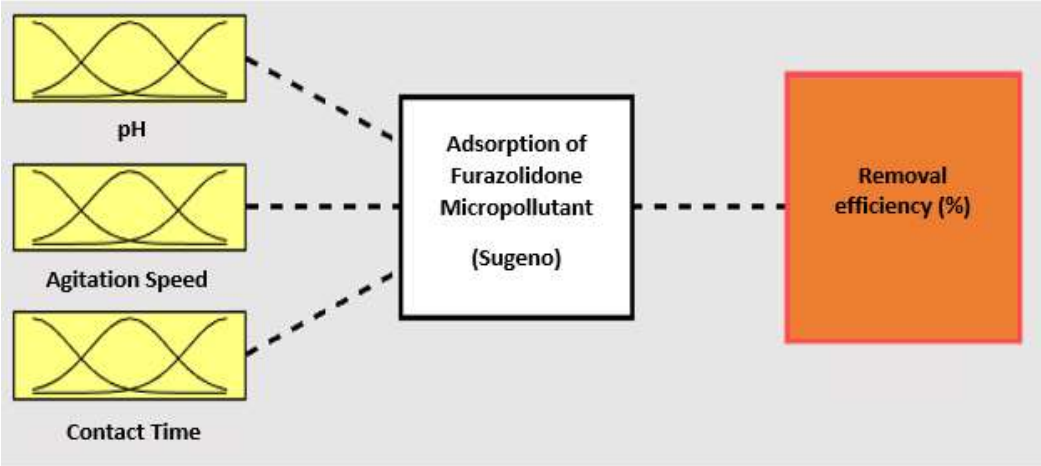

Fig. 4.25: ANFIS Sugeno type structure

The ANFIS data used in the MATLAB (R2021a) m-file consisted of a 240 x 5 matrix, representing 240 runs of 3 input factors (pH, agitation speed (rpm), contact time (min)), and 240 runs of a single output factor (removal efficiency (%)). The data was divided into a ratio of 60:40 for training and testing modes. The data comprising pH, agitation speed and contact time was given through the fuzzy model (trimf membership function) during the training mode. The main strength of ANFIS is in attaining limited error through improving fuzzy controllers with self-learning ability (Shariati et al. 2020). The data was trained at 0 to 100 epoch iterations error tolerance. An error magnitude of 2.651 after 100 epoch iteration was produced during training mode, which ensured the satisfaction of the fuzzy system in modeling the elimination of FZD micropollutant in the removal process. During the training and testing phase in the ANFIS modeling, the coefficient of determination (R^2) was found to be 0.985, confirming that the model is highly precise. The ANFIS framework and training data are shown in ***Tab. 4.12***, which lends credence to the suitability of the fuzzy inference (FIS) system framework in predicting the removal of FZD micropollutant using magnetic f-MWCNTs-based BP/PVA membrane. It has been reported that if the R^2 value is close to 1, the predicted data of the model will best fit the experimental point better, which means that the predicted and experimental data are more comparable and the model error is nearly insignificant (Igwilo et al. 2022, Onyejiuwa et al. 2022).

Fig. 4.26 illustrates the graphical correlation between the experimental and predicted ANFIS model results. Prior studies have reported that the ANFIS model displays better predictive capability than other neural models, such as artificial neural network (Olabi et al. 2023, Kaveh et al. 2018). Based on ***Fig. 4.26***, the experimental and model-predicted plots displayed a good closeness among them, consequently, exact predictability with the ANFIS tool. Besides, a high ANFIS R^2 value of 0.985 was achieved for the response of FZD micropollutant removal efficiency (%), which revealed that the model offered positive prediction, thus confirming an adequate adjustment of the ANFIS model by using simulated data and displayed higher model performance. The results of the ANFIS model proved the accuracy and robustness of the ANFIS model.

Tab. 4.12: ANFIS framework and training parameters

ANFIS parameters	FZD micropollutant
Number of nodes	78
Number of linear parameters	27
Number of non-linear parameters	27
Total number of parameters	54
Number of training data pairs	144
Average training error	2.7
Average testing error	2.7
Membership function	trimf
Output membership function	Constant
Number of epochs	100
Number of checking data pairs	0
Method of optimization	Hybrid
Number of fuzzy rules	27

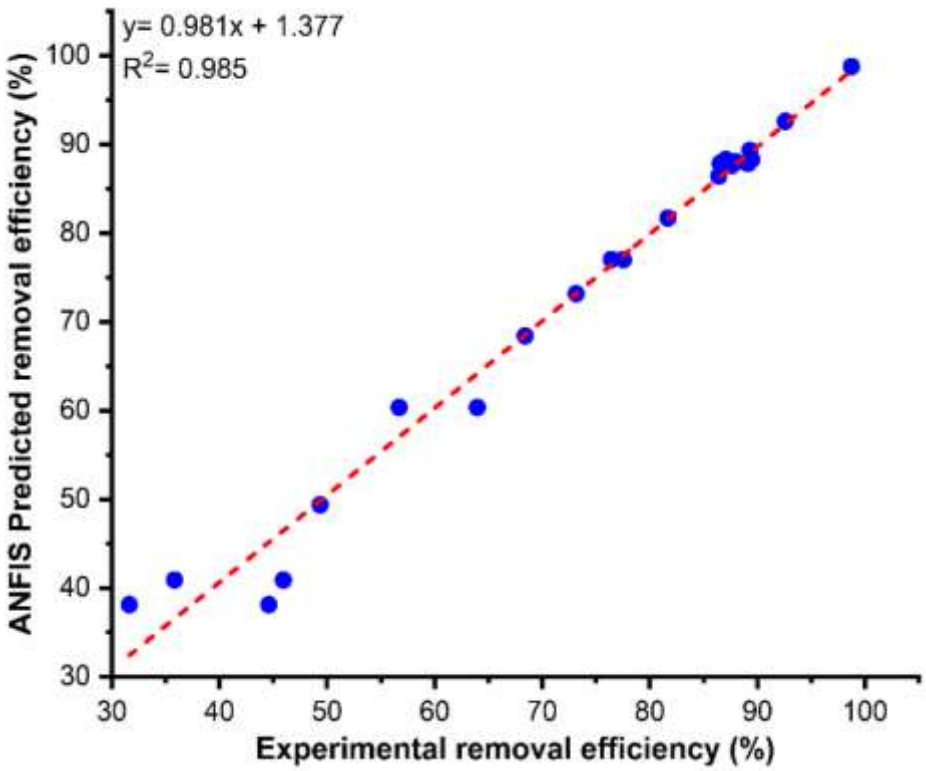

Fig. 4.26: Correlation plot of ANFIS predicted and experimental removal efficiency

4.9.2 Sensitivity using ANFIS

The outcomes from the 3-D surface for the elimination of the FZD micropollutant as a function of two varied input parameters are illustrated in ***Fig. 4.27 (a-c)***. These graphs support a better comprehension of the influence of two independent parameters and their interaction impacts on the FZD micropollutant removal.

It is clear, based on ***Fig. 4.27***, that the elimination rate of the FZD micropollutant increased with the increasing contact time and pH, as predicted by the ANFIS model. ***Fig. 4.27 (a)*** displayed that the removal efficiency of the FZD micropollutant reached up to 88% when the pH and contact time were within the range of 5.5 to 6.5 and 140 to 170 rpm, respectively. It revealed that an increase in agitation speed initially increases the elimination rate of the FZD micropollutant, which is mainly due to the extend contact of FZD ions with the active sites and inner pores of the magnetic f-MWCNTs-based BP/PVA membrane. Conversely, after exceeding the agitation speed of 170 rpm, the removal of the FZD micropollutant declined. This could be due to the fact that a higher speed of stirring has led to more movement of particles and, in turn, has weakened the contact between the particles and the surface of the membrane (Sadeghizadeh et al. 2019). Thus, the removal efficiency is decreased, and this high speed could even result in the segregation of previous adsorbed particles.

Fig. 4.27 (b) displays the 3-D surface graph for the integrated effect of contact time and pH. The highest FZD micropollutant removal percentage could be achieved when both variables were at a contact time of 200 min. and pH 6-6.5. Based on the results, it was observed clearly that the pH significantly impacts the FZD micropollutant removal efficiency. On the other hand, the low removal of the FZD micropollutant was noticed at a low pH value due to the large amount of protons that compete with the FZD micropollutant for adsorption sites.

Fig. 4.27 (c) shows the 3-D surface graph for the integrated effect of contact time and agitation speed. The results showed that the agitation speed is an essential variable influencing the removal percentage of FZD micropollutant in this study (Elboughdiri 2020). It was described that the FZD uptake capacity improves with extending contact time and agitation speed. It can be attributed to the increase in dispersion and surface area of the membrane in the FZD micropollutant solution. The agitation speed is an essential and efficient tool that can improve the adsorption rate and minimize the contact time (Shahid et al. 2021); therefore, it is more recommended than other conventional adsorption routes.

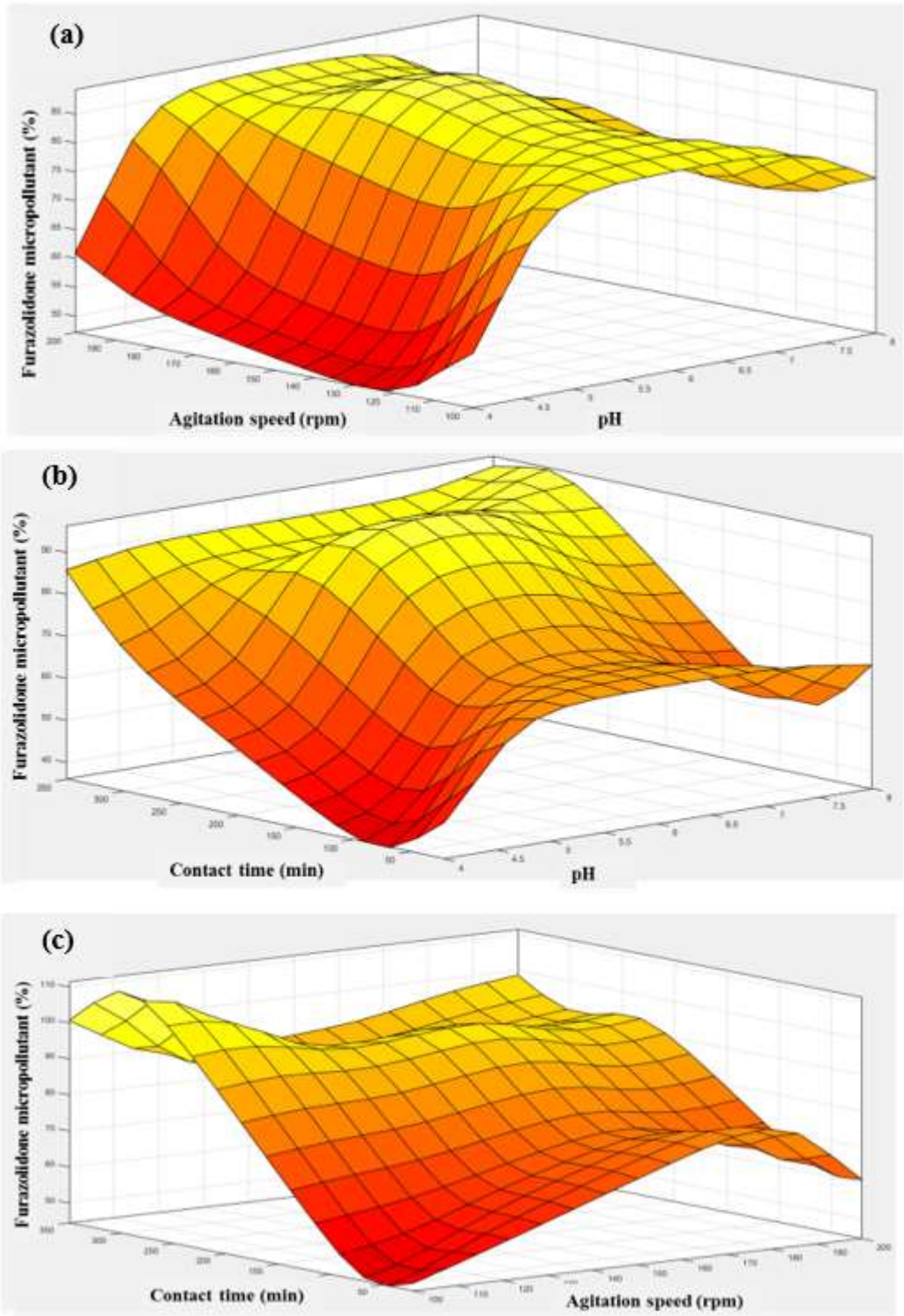

Fig. 4.27: ANFIS prediction 3D surfaces of the FZD removal

4.9.3 Model efficiency

Statistical analysis was employed to demonstrate the data fitting and evaluate the accuracy of the model predictions (Mossavi et al. 2019). To further assess

the precision capability of the models, five statistical error functions were used, as shown in ***Tab. 4.13***. The results indicated minor error values for both the RSM and ANFIS models, signifying good model predictions. Additionally, R^2 and adjusted R^2 were calculated for both models. It is well-known that higher the R^2 and adjusted R^2 values indicate better the model predictions, and these values should ideally be at least 0.8 (Hamzah et al. 2021).

Tab. 4.13: Comparison of statistical parameters from RSM and ANFIS models

Statistical parameters	**Model**	
	RSM	**ANFIS**
RMSE	0.019	0.008
AARE	0.015	0.003
HYBRID (%)	3.547	0.561
R^2	0.934	0.985
Adj-R^2	0.892	0.997

In general, the ANFIS process showed clear superiority, and the values calculated from statistical parameters indicate that the RSM model was inadequate (Azqhandi et al. 2017). However, data values from residuals vs. predicted can provide further insights into the model's fitting for the dataset. For example, if the residuals behave randomly, it shows that the model accurately captures the data (Foroughi et al. 2020, Mousazadeh et al. 2021). But, if the residuals do not exhibit randomness, it indicates that the model does not fit well.

The diagnostic plots between the experimental and predicted values by the RSM and ANFIS processes are shown in ***Fig. 4.28***. The residuals plotted for both models indicate that the allocation of residuals has random behavior. Besides, the fluctuations of residuals are relatively insignificant for ANFIS compared to RSM. The RSM model depicts higher deviations than the ANFIS model. The present study's outcomes were in good agreement with the previous work reported, and all concluded that ANFIS is comparatively more accurate in predicting the FZD micropollutant elimination efficiency from the

aqueous solution using magnetic f-MWCNTs-based BP/PVA membrane than the RSM model (Kaveh et al. 2018, Azari et al. 2019).

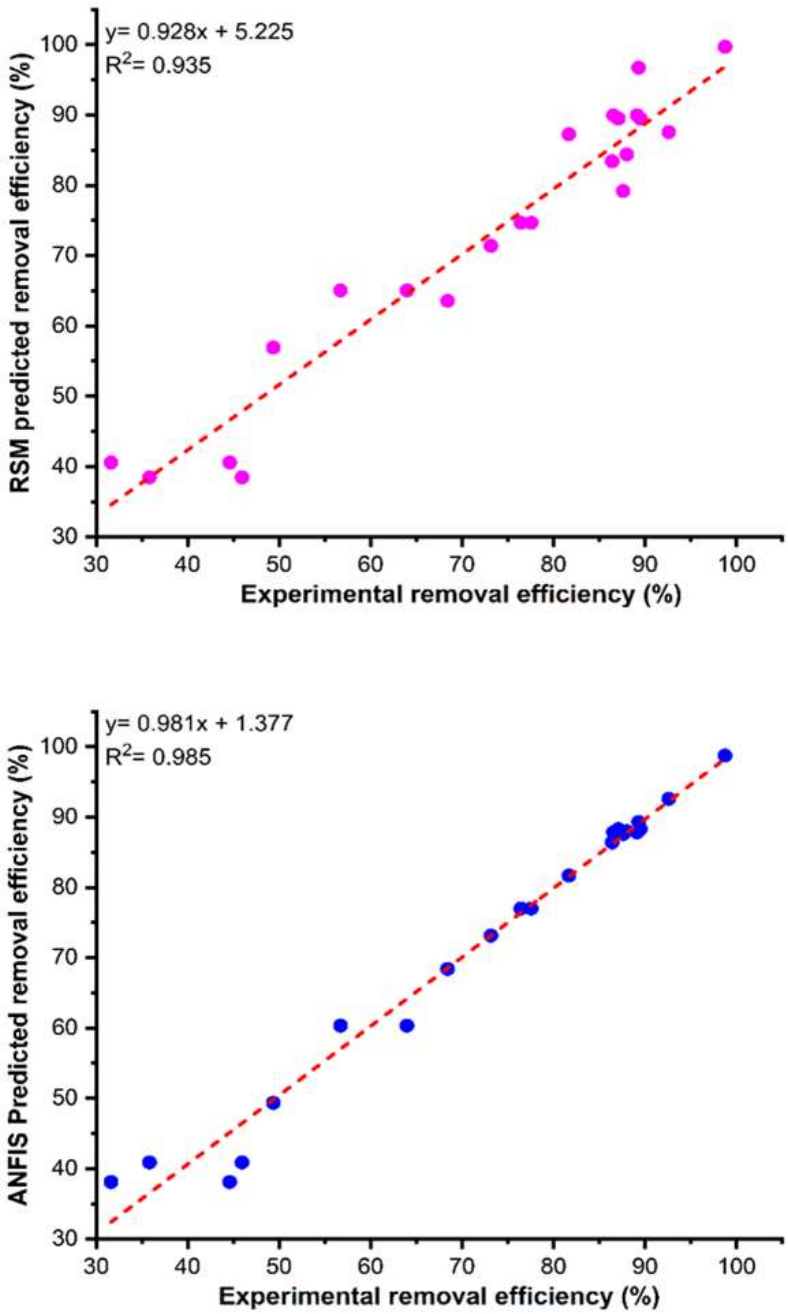

Fig. 4.28: Diagnostic plots of RSM and ANFIS models against experimental removal efficiency

4.9.4 Summary of ANFIS modeling

The primary objective of the current study was to construct and develop a new model that could provide a reliable prediction of FZD micropollutant removal

using magnetic f-MWCNTs-based BP/PVA membrane. Apart from RSM, ANFIS was also employed for predicting the elimination of FZD micropollutant. The summary and predictive performance of both RSM and ANFIS were evaluated through statistical measures of the HYBRID%, ARE%, AARE%, RMSE, adj. R^2, and R^2, as well as the analysis of residuals. All five models adequately predicted the FZD micropollutant elimination by the magnetic f-MWCNTs-based BP/PVA membrane. Based on the results, it can be seen that the ANFIS model is more accurate in modeling the elimination of FZD micropollutant than RSM.

Moreover, while RSM is most widely employed for elimination optimization, the ANFIS model can present a better substitute even with a limited dataset. The outcome from this section confirmed that the ANFIS modeling capability is potentially substantial.

4.10 Performance comparison

This section compares the results achieved in the current study with different published scientific articles on the FZD micropollutant uptake using various adsorbents. The comparison is mainly based on various aspects, such as removal efficiency, adsorption analysis (isotherms, kinetics and thermodynamics), reusability and predictive models. Besides, this section is described with the relevant tables, figures and explanation.

4.10.1 Removal efficiency

In the current study, the magnetic f-MWCNTs-based BP/PVA membrane demonstrated an impressive maximum removal efficiency of 98.74% for FZD micropollutant. This efficiency was achieved under the optimized conditions of pH 6, agitation speed 200 rpm, and contact time of 350 min. When compared to other published studies on FZD micropollutant removal, the magnetic f-MWCNTs-based BP/PVA membrane outperformed various other adsorbents.

(Gurav et al. 2020) achieved a removal efficiency of 96.81% using Fe_3O_4-biochar at initial pH of 7.5 , operating temperature of 30ºC, and initial FZD concentration of 80 mg/L (Cheng et al. 2019) reported approximately 97.25% FZD micropollutant removal using granular activated carbon at an initial pH of 7, an adsorbent dosage of 6 g/L, and operating temperature of 28 ºC. (Zhen-Yuan et al. 2015) achieved up to 97.76% removal of FZD micropollutant using magnetic MWCNTs at an initial pH of 7, an initial concentration of 10 mg/L, contact time of 360 min., agitation speed of 150 rpm, adsorbent dosage of 2.4 g/L and operating temperature of 25ºC.

It is evident that the magnetic f-MWCNTs-based BP/PVA membrane demonstrated a higher removal efficiency compared to other reported adsorbent for FZD micropollutant. This indicates the potential and effectiveness of the magnetic f-MWCNTs-based Bp/PVA membrane as a promising material for the removal of noxious pharmaceutical micropollutants from different water sources.

However, it is important to note that the efficiency of the magnetic f-MWCNTs-based BP/PVA membrane may vary based on specific water sources, micropollutant concentrations, and other operating conditions. Further research and investigation are warranted to explore the applicability and performance of this adsorbent in various real-world scenarios. The study's findings open new avenues for the development of advanced materials and technologies to address the growing concern of pharmaceutical micropollutants in water bodies.

4.10.2 Adsorption analysis

The comparison in ***Tab. 4.14***. demonstrates the adsorption capacities of different adsorbents for FZD micropollutant uptake. The magnetic f-MWCNTs-based BP/PVA membrane exhibited an adsorption capacity of 29.67 mg/g within 300 min. of contact time. This adsorption capacity is comparable to the other reported adsorbents, and it indicates the efficient performance of

the magnetic f-MWCNTs-based BP/PVA membrane for FZD micropollutant removal from aqueous solutions.

Notably, the magnetic f-MWCNTs-based BP/PVA membrane showed a relatively shorter contact time for achieving the maximum adsorption capacity compared to some of the other reported adsorbents. This indicates the potential of the current study's adsorbent for rapid and efficient removal of FZD micropollutant from water sources.

It is evident from the comparison that various adsorbents have been investigated for FZD micropollutant uptake, and each shows promising results. However, the magnetic f-MWCNTs-based BP/PVA membrane stands out as an efficient adsorbent, offering comparable adsorption capacity to other materials. The findings from the present study support the use of this magnetic composite membrane as a viable option for the removal of FZD micropollutant and highlight its potential in environmental remediation applications. Further research and application-oriented studies can explore its practical implementation for water treatment purposes.

Tab. 4.14: Comparison of FZD micropollutant uptake on different adsorbents

Material	Adsorption capacity (mg/g)	Equilibrium time (min.)	Isotherm model	Kinetic model	Adsorption thermodynamic	References
Fe_3O_4- biochar	31.45	600	-	-	-	(Gurav et al. 2020)
Fe_3O_4- MWCNTs	7.45	360	Langmuir (R^2 ~0.998)	Pseudo-second order kinetic (R^2 ~1)	Exothermic and physical process	(Zhen-Yuan et al. 2015)
Granular activated carbon (GAC)	3.23	120	Langmuir (R^2 ~0.992)	Pseudo-second order kinetic (R^2 ~1)	-	(Cheng et al. 2019)
Fe_3O_4- MWCNTs	11.98	300	Langmuir (R^2 ~0.995)	Pseudo-second order kinetic (R^2 ~0.99)	Exothermic and physical process	(Liu et al. 2015)
Magnetic f-MWCNTs-based BP/PVA membrane	29.67	300	Langmuir (R^2 ~0.994)	Pseudo-second order kinetic (R^2 ~0.997)	Exothermic and physical process	Present study

4.10.3 Reusability analysis

The reusability analysis of the magnetic f-MWCNTs-based BP/PVA membrane presented in the current study demonstrates its outstanding performance and mechanical durability over multiple cycles. The membrane maintained a high removal efficiency of FZD micropollutant even five sequential cycles, with no signs of mechanical failure. The removal efficiency achieved by the membrane after five cycles was reported to be 98.74%, which is remarkably high compared to the reported results of other materials.

The reusability of the magnetic f-MWCNTs-based BP/PVA membrane not only contributes to economic benefits but also reflects its mechanical durability and stability during extended operation in the adsorption process. (Khawar et al. 2019). In the current study, the membrane was fabricated by incorporating magnetic nanoparticles into f-MWCNTs, which were later formed into a buckypaper membrane. This approach of filling material into CNTs has been shown to improve the storage modulus, maximum strength, and fracture toughness (Zhou et al. 2008, Mishra 2022, Raza et al. 2020). A decline in the storage modulus might indicate poor dispersion of CNTs in the nanocomposite.

However, in the present study, the FE-SEM images of the magnetic f-MWCNTs-based BP/PVA membrane (*Section 4.4.2*) confirmed a uniformly dispersed network of Fe_3O_4/ f-MWCNTs, indicating good structural integrity. Additionally, the use of the polymer PVA also a crucial role in enhancing the mechanical strength of the prepared buckypaper membrane (Nakano et al. 2001, Yashima et al. 2016). Polymer intercalation of the buckypaper membrane promotes effective load transfer from the polymer matrix to the incorporated f-MWCNTs, leading to improved mechanical properties (Han et al. 2014, Qamar et al. 2022). The mechanical strength and stability of the magnetic f-MWCNTs-based BP/PVA membrane are evident from its successful reusability over five sequential cycles, as depicted in ***Fig. 4.***29. Even after repeated use, the membrane did not undergo any mechanical failure, demonstrating its robustness and potential for long-term practical applications.

The combination of magnetic nanoparticles, f-MWCNTs and PVA in the membrane's composition contributes to its enhanced mechanical properties, making it a promising and reliable sorbent for repeated use in the adsorption process. This reusability aspect not only contributes to cost-effectiveness but also indicates the membrane's stability to withstand various environmental conditions, including mechanical stress, chemical exposure and temperature fluctuations, over an extended period of operation. As such, the magnetic f-MWCNTs-based BP/PVA membrane holds great potential for practical applications in the removal of FZD micropollutant and other similar contaminants from water sources.

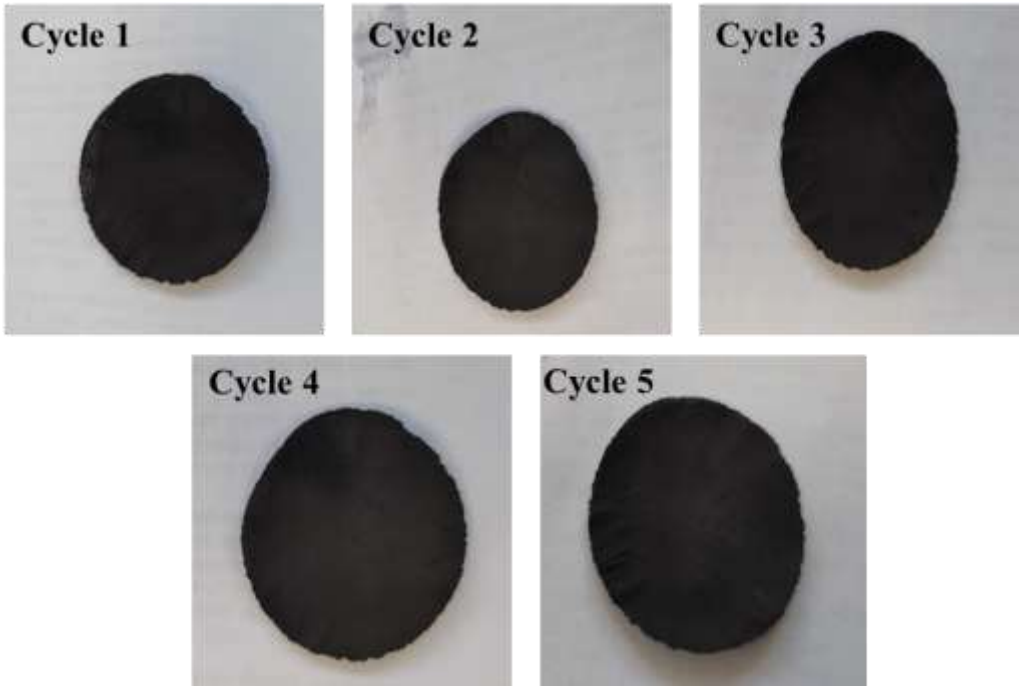

Fig. 4.29: Image of magnetic f-MWCNTs-based BP/PVA membrane after each cycle

(Queirós et al. 2022) fabricated composite membranes (UiO-66-NH_2/PVDF-HEP) for the elimination of chromium (Cr (VI)), and their reusability study showed a significant decline in removal efficiency after three cycles, with the membrane removing only 58% of Cr (VI) at that point. The decrease in the membrane elimination efficiency for both anionic and cationic pollutants in their study could be attributed to the weakening of the interaction strength between the adsorbate and adsorbent, particularly due to ion exchange mechanism (Nguyen et al. 2021). Similarly, (Sadeghfar et al. 2018) synthesized

PVA/ 3%Fe_3O_4-CNT for methylene blue removal, and their reusability study revealed that the nanocomposite was efficient for up to three cycles, after which there was a slight decline in removal efficiency. In contrast, the magnetic f-MWCNTs-based BP/PVA membrane showed higher removal efficiency even after five cycles, indicating its potential as an efficient and reusable adsorbent. The mechanical strength and stable structure of the membrane, coupled with the effective adsorption capability, contribute to its superior performance in repeated use.

Therefore, the results from the present study suggest that the magnetic f-MWCNTs-based BP/PVA membrane can be efficiently employed as a regeneration membrane for FZD micropollutant removal. Its reusability and sustained high removal efficiency make it a promising and practical solution for water treatment applications, contributing to the sustainable removal of micropollutants from water sources.

4.10.4 Predictive model's

The current study utilized two different models, response surface methodology (RSM) and adaptive neuro-fuzzy inference system (ANFIS), to predict the removal efficiency of FZD micropollutant using magnetic f-MWCNTs-based BP/PVA membrane. RSM is a statistical approach commonly used for process optimizing, while ANFIS is a mathematical computation model that incorporates both neural and fuzzy logic networks for precise predictions (Sharma et al. 2022). The comparison of the predictive accuracy of RSM and ANFIS was done through graphical and statistical analyses. Both models were found to be effective in forecasting the removal efficiency of FZD micropollutant, and the residual analysis showed a close approximation between the experimental and predicted values. However, the ANFIS model demonstrated superiority over RSM in capturing the non-linear nature of FZD micropollutant removal, as evidenced by the smaller and more insignificant residual values. The comparative plots shown in ***Fig. 4.28*** (*Section 4.9.3*),

described a satisfactory relationship between the experimental and forecasting values.

Due to their popularity in terms of simplicity and time-saving, scientific researchers have been extensively employing these models for their respective output. (Onu et al. 2021) compared the application of ANFIS, artificial neural network (ANN), and RSM in the adsorption of eriochrome black-T dye using Nteje clay. The results showed that the ANFIS model provided the highest accuracy and precision compared to ANN and RSM. Another study by (Taheri et al. 2013) utilized the ANFIS and RSM model to predict the removal efficiency of Reactive Blue 19 dye using the electro-coagulation/ coagulation method. They also found that the ANFIS model outperformed RSM in terms of accuracy and prediction.

In ***Tab. 4.15***, the optimized conditions for the micropollutant elimination reported in the scientific articles by RSM and ANFIS are compared with the current study. This comparison further supports the efficacy of the ANFIS model in providing more accurate and reliable predictions for the removal efficiency of FZD micropollutant using magnetic f-MWCNTs-based BP/PVA membrane.

***Tab. 4.15**:* Published scientific literature for the prediction/ optimization of removal efficiency of micropollutant

Adsorbent	Micropollutant name	Operating parameters	Model prediction	Remarks	References
f-MWNCTs/Fe_3O_4	Ciprofloxacin	pH= 5.4 dosage= 0.78 g/L time= 24 min. conc.= 59 mg/L	RSM	• R^2 value of 0.9103 with optimization of operating parameters. • Model predicted 88% removal of ciprofloxacin	(Yousefi et al. 2021)
g-CN/Ag_3VO_4/PAN	Tetracycline	conc.= 15 mg/L dosage= 0.02 g time= 120 min	ANFIS	• R^2 value of 0.999 • Model predicted the removal of tetracycline percentage of 97.32	(Deylami et al. 2023)
Chitosan-mussel	Tetracycline	dosage= 0.4 g conc.= 90.5 mg/L time= 35.9 min. temperature= 30ºC	RSM	• Coefficient of determination R^2, value of 0.9320 • Model predicted adsorption capacity of 34.40 mg/g	(Topal et al. 2020)
LDH-GO-CNTs	Para nitrophenol	pH= 5.35 dosage= 10 mg temperature= 50 ºC conc.= 16.22 mg/L time= 13.36 min.	RSM ANFIS	• R^2 value of 0.958 and 0.9998 for RSM and ANFIS, respectively • 94% removal efficiency	(Khomeyrani et al. 2021)
Magnetic nanoparticles-rGO-chitosan	Cefixime	pH= 8 conc.= 42.81 mg/L dosage= 5 mg	RSM	• R^2 gave the highest value of 0.994 • Adsorption capacity of 30.80 mg/g predicted	(Ciğeroğlu et al. 2021)

Adsorbent	Micropollutant name	Operating parameters	Model prediction	Remarks	References
Magnetic f-MWCNTs-based BP/PVA	Furazolidone	pH= 6 time= 300 min speed= 200 rpm	RSM ANFIS	• R^2 value of 0.934 and 0.985 for RSM and ANFIS, respectively • Removal efficiency predicted for FZD micropollutant was 98.74%	Present study

CHAPTER V
CONCLUSIONS AND RECOMMENDATIONS

5.1 Conclusions

A significant number of emerging micropollutants have been detected in different water sources. While several volatile, hydrophobic and biodegradable substance can be removed in the wastewater treatment plants, they are not equipped to effectively treat these emerging pollutants. As a result, the presence of various micropollutants poses a threat to clean and safe water availability. To address this issue, the current study focused on using membrane technology for treating these micropollutants, with a particular emphasis on furazolidone, a pharmaceutical micropollutant.

In this context, a nanocomposite was synthesized by incorporating magnetite nanoparticles into functionalized multi-walled carbon nanotubes. This nanocomposite was then used to fabricate a magnetic buckypaper membrane, which was further enhanced by infiltrating it with polyvinyl alcohol. The objective was to investigate the effectiveness of this membrane in removing furazolidone micropollutant from aqueous solutions.

By exploring this approach, the study aimed to contribute to the development of an efficient method for eliminating micropollutants from water sources, thereby safeguarding the availability of clean and safe water. Membrane technology, combined with nanocomposite materials, holds promise for addressing the challenges posed by emerging micropollutants in wastewater and improving water treatment processes

Based on *Objective 1*, the magnetic f-MWCNTs-based BP/ PVA membrane was fabricated as follows (a) surface modification of MWCNTs using H_2SO_4 and HNO_3, (b) synthesis of magnetic f-MWCNTs nanocomposite with the support of reflux approach, and (c) vacuum and infiltration approach. The magnetic f-MWCNTs-based BP/ PVA membrane was characterized, and the analysis revealed a highly porous surface, remarkable adsorption ability, and mechanical and thermal stability. The maximum removal efficiency of FZD micropollutant on the magnetic f-MWCNTs-based BP/ PVA membrane (98.74%) was attained at a pH of 6, agitation speed of 200 rpm, and contact time of 350 min.

For *Objective 2*, the characterization analysis confirmed the attachment of magnetite nanoparticles on the buckypaper membrane. Based on the FESEM findings, uniformly dispersed frameworks of Fe_3O_4/ f-MWCNTs were observed, indicating the homogenous distribution of Fe_3O_4/ f-MWCNTs in the PVA matrix. Moreover, the VSM result showed a high saturation magnetization (44.76 emu/g) of the magnetic f-MWCNTs nanocomposite, allowing the FZD micropollutant to be instantly attracted to the prepared magnetic f-MWCNTs-based BP/ PVA membrane instantly. Furthermore, the EDX results also confirmed a higher mass fraction of iron (Fe) and oxygen (O) due to the Fe_3O_4 and PVA infiltration. Finally, TGA analysis revealed the significant improvement in the thermal stability of the magnetic f-MWCNTs-based BP/ PVA membrane due to its well-organized structure.

As for *Objective 3*, the maximum FZD micropollutant uptake was 29.67 mg/g. Furthermore, the kinetic model best-fit the pseudo-second-order kinetic model. Additionally, the adsorption thermodynamics suggested the spontaneous, feasible and exothermic nature of FZD micropollutant adsorption over the magnetic f-MWCNTs-based BP/ PVA membrane. Moreover, the reusability study revealed that the magnetic f-MWCNTs-based BP/ PVA membrane could remove up to 88% of FZD micropollutant after five successive cycles without any mechanical failure.

To address the final objective, i.e., *Objective 4*, the efficacy of the predictive capability of RSM and ANFIS in modeling the FZD micropollutant elimination using magnetic f-MWCNTs-based BP/ PVA membrane was compared. The ANFIS model was found to be more satisfactory and comparable in forecasting the FZD micropollutant elimination compared to the RSM model. Additionally, five statistical parameters also confirmed that ANFIS provides the highest precision and accuracy compared to the RSM model.

5.2 Recommendations

Based on the work conducted in this study, the following recommendations for future research can be made:

i. Conduct fouling studies: To gain better understanding of the long-term performance and durability of the magnetic f-MWCNTs-based BP/PVA membrane after pollutant treatment, fouling studies should be conducted. This will help assess how the membrane's performance is affected over time due to the accumulation of pollutants and other substance on its surface.

ii. Explore anti-bacterial efficiency: Since bacterial colonization can lead to membrane fouling and decrease adsorption efficiency, it is essential to investigate the anti-bacterial properties of the developed membrane. Understanding its resistance to bacterial growth will contribute to improving its long-term performance.

iii. Assess individual wastewater treatment application: To determine the viability of the magnetic f-MWCNTs-based BP/PVA membrane for industrial wastewater treatment, a detailed economic analysis should be carried out. This will help evaluate the cost-effectiveness and practicality of using membrane in the real-world industrial settings.

iv. Investigate selective adsorption: Further research can be done to understand the selective adsorption capabilities of the magnetic f-MWCNTs-based BP/PVA membrane for different types of micropollutants commonly found in the industrial wastewater. This knowledge can aid in tailoring the membrane's application to specific wastewater treatment needs.

v. Perform acute toxicity tests: After pollutant removal treatment, conducting acute toxicity test on the treated water can help assess the safety and environmental impact of using the magnetic f-MWCNTs-

based BP/PVA membrane. This information is crucial for ensuring that the treated water meets regulatory standards.

vi. Evaluate large-scale water treatment applications: A thorough economic analysis should be performed to assess the feasibility of using magnetic f-MWCNTs-based BP/PVA membrane for large-scale water treatment applications. This will provide insights into the scalability and cost-effectiveness of implementing the technology on a larger scale.

vii. Explore continuous FZD micropollutant elimination: Conducting experiments using a column process with the magnetic f-MWCNTs-based BP/ PVA membrane will provide valuable insights into its performance under continuous flow conditions. This will help understand the membrane's removal capacity and efficiency over an extended period, which is crucial for practical applications in continuous water treatment systems.

viii. Perform mass transfer simulation: Utilizing mass transfer simulation techniques can provide a deeper understanding of the mechanism and kinetics involved in the micropollutant elimination process using magnetic f-MWCNTs-based BP/PVA membrane. This simulation can help optimize the design and operation of the membrane-based water treatment systems and shed light on the transport phenomena governing the adsorption process.

REFERENCES

Abascal, E, L Gómez-Coma, I Ortiz, and A Ortiz. 2022. "Global diagnosis of nitrate pollution in groundwater and review of removal technologies." *Science of the Total Environment* no. 810:152233.

Abdelhalim, Ahmed, Alaa Abdellah, Giuseppe Scarpa, and Paolo Lugli. 2013. "Fabrication of carbon nanotube thin films on flexible substrates by spray deposition and transfer printing." *Carbon* no. 61:72-79.

Abdelkareem, Mohammad Ali, Maryam Abdullah Lootah, Enas Taha Sayed, Tabbi Wilberforce, Hussain Alawadhi, Bashria AA Yousef, and AG Olabi. 2021. "Fuel cells for carbon capture applications." *Science of The Total Environment* no. 769:144243.

Abdolkarimi-Mahabadi, M, and M Manteghian. 2015. "Chemical oxidation of multi-walled carbon nanotube by sodium hypochlorite for production of graphene oxide nanosheets." *Fullerenes, Nanotubes and Carbon Nanostructures* no. 23:860-864.

Abdullah, N, N Yusof, WJ Lau, J Jaafar, and AF Ismail. 2019. "Recent trends of heavy metal removal from water/wastewater by membrane technologies." *Journal of Industrial and Engineering Chemistry* no. 76:17-38.

Abo-Hamad, Ali, Maan Hayyan, Mohammed AbdulHakim AlSaadi, Mohamed ES Mirghani, and Mohd Ali Hashim. 2017. "Functionalization of carbon nanotubes using eutectic mixtures: a promising route for enhanced aqueous dispersibility and electrochemical activity." *Chemical Engineering Journal* no. 311:326-339.

Adamczak, Michał, Gabriela Kaminska, and Jolanta Bohdziewicz. 2021. "Relationship between the addition of carbon nanotubes and cut-off of ultrafiltration membranes and their effect on retention of microcontaminants." *Desalination Water Treat* no. 214:263-272.

Adday, Ghaihab Hassan, Shamala K Subramaniam, Zuriati Ahmad Zukarnain, and Normalia Samian. 2022. "Fault Tolerance Structures in Wireless Sensor Networks (WSNs): Survey, Classification, and Future Directions." *Sensors* no. 22:6041.

Adeleye, Adeyemi S, Jon R Conway, Kendra Garner, Yuxiong Huang, Yiming Su, and Arturo A Keller. 2016. "Engineered nanomaterials for water treatment and remediation: Costs, benefits, and applicability." *Chemical Engineering Journal* no. 286:640-662.

Afriyie Mensah, Rhoda, Jie Xiao, Oisik Das, Lin Jiang, Qiang Xu, and Mohammed Okoe Alhassan. 2020. "Application of adaptive neuro-fuzzy inference system in flammability parameter prediction." *Polymers* no. 12:122.

Ahmad, Tausif, Chandan Guria, and Ajay Mandal. 2020. "A review of oily wastewater treatment using ultrafiltration membrane: A parametric study to enhance the membrane performance." *Journal of Water Process Engineering* no. 36:101289.

Ahmadi, Hossein, Marsa Gholamzadeh, Leila Shahmoradi, Mehrbakhsh Nilashi, and Pooria Rashvand. 2018. "Diseases diagnosis using fuzzy logic methods: A systematic and meta-analysis review." *Computer Methods and Programs in Biomedicine* no. 161:145-172.

Ahmed, Muthanna J, and Samar K Theydan. 2013. "Microporous activated carbon from Siris seed pods by microwave-induced KOH activation for metronidazole adsorption." *Journal of Analytical and Applied Pyrolysis* no. 99:101-109.

Ahn, Chang Hoon, Youngbin Baek, Changha Lee, Sang Ouk Kim, Suhan Kim, Sangho Lee, Seung-Hyun Kim, Sang Seek Bae, Jaebeom Park, and Jeyong Yoon. 2012. "Carbon nanotube-based membranes: Fabrication and application to desalination." *Journal of Industrial and Engineering Chemistry* no. 18:1551-1559.

Aidonojie, Paul Atagamen. 2023. "Environmental Hazard: The Legal Issues Concerning Environmental Justice in Nigeria." *Journal of Human Rights, Culture and Legal System* no. 3:17-32.

Akhtar, Naseem, Muhammad Izzuddin Syakir Ishak, Showkat Ahmad Bhawani, and Khalid Umar. 2021. "Various natural and anthropogenic factors responsible for water quality degradation: A review." *Water* no. 13:2660.

Al-Khateeb, Lateefa A, Abdualah Y Obaid, Najwa A Asiri, and Mohamad Abdel Salam. 2014. "Adsorption behavior of estrogenic compounds on carbon nanotubes from aqueous solutions: Kinetic and thermodynamic studies." *Journal of Industrial and Engineering Chemistry* no. 20:916-924.

Al-Shaalan, Nora Hamad, Imran Ali, Zeid A ALOthman, Lamya Hamad Al-Wahaibi, and Hadeel Alabdulmonem. 2019. "High performance removal and simulation studies of diuron pesticide in water on MWCNTs." *Journal of Molecular Liquids* no. 289:111039.

Al-Tohamy, Rania, Sameh S Ali, Fanghua Li, Kamal M Okasha, Yehia A-G Mahmoud, Tamer Elsamahy, Haixin Jiao, Yinyi Fu, and Jianzhong Sun. 2022. "A critical review on the treatment of dye-containing wastewater: Ecotoxicological and health concerns of textile dyes and possible remediation approaches for environmental safety." *Ecotoxicology and Environmental Safety* no. 231:113160.

Alahmadi, Nadiyah. 2022. "Recent Progress in Photocatalytic Removal of Environmental Pollution Hazards in Water Using Nanostructured Materials." *Separations* no. 9:264.

Alasadi, Aisha, Fawwaz Khaili, and Akl Awwad. 2019. "Adsorption of Cu (II), Ni (II) and Zn (II) ions by nano kaolinite: Thermodynamics and kinetics studies." *Chemistry International* no. 5:258-26.

Alghunaim, Naziha Suliman. 2016. "Optimization and spectroscopic studies on carbon nanotubes/PVA nanocomposites." *Results in Physics* no. 6:456-460.

Ali, Sharafat, Syed Aziz Ur Rehman, Hong-Yan Luan, Muhammad Usman Farid, and Haiou Huang. 2019. "Challenges and opportunities in functional carbon nanotubes for membrane-based water treatment and desalination." *Science of the Total Environment* no. 646:1126-1139.

Aliahmad, M, and N Nasiri Moghaddam. 2013. "Synthesis of maghemite (γ-Fe 2 O 3) nanoparticles by thermal-decomposition of magnetite (Fe 3 O 4) nanoparticles." *Materials Science-Poland* no. 31:264-268.

Alimohammadi, Vahid, Mehdi Sedighi, and Ehsan Jabbari. 2017. "Experimental study on efficient removal of total iron from wastewater using magnetic-modified multi-walled carbon nanotubes." *Ecological Engineering* no. 102:90-97.

Alizadeh Fard, Mohammad, Behnoush Aminzadeh, and Hossein Vahidi. 2013. "Degradation of petroleum aromatic hydrocarbons using TiO2 nanopowder film." *Environmental Technology* no. 34:1183-1190.

Alrashed, Abdullah AAA, Arash Karimipour, Seyed Amin Bagherzadeh, Mohammad Reza Safaei, and Masoud Afrand. 2018. "Electro-and

thermophysical properties of water-based nanofluids containing copper ferrite nanoparticles coated with silica: experimental data, modeling through enhanced ANN and curve fitting." *International Journal of Heat and Mass Transfer* no. 127:925-935.

Althanoon, Zeina, Ibrahim M Faisal, Abdulla A Ahmad, Marwan M Merkhan, and Marwan M Merkhan. 2020. "Pharmacological aspects of statins are relevant to their structural and physicochemical properties." *Systematic Reviews in Pharmacy* no. 11:167-71.

Álvarez-Torrellas, S, A Rodríguez, G Ovejero, and J García. 2016. "Comparative adsorption performance of ibuprofen and tetracycline from aqueous solution by carbonaceous materials." *Chemical Engineering Journal* no. 283:936-947.

Álvarez-Torrellas, Silvia, Macarena Munoz, Jan Gläsel, Zahara M de Pedro, Carmen M Domínguez, Juan García, Bastian JM Etzold, and Jose A Casas. 2018. "Highly efficient removal of pharmaceuticals from water by well-defined carbide-derived carbons." *Chemical Engineering Journal* no. 347:595-606.

Amalraj, Antolin Jesila Jesu, Umesh Narasimha Murthy, and Sea-Fue Wang. 2021. "The simultaneous electrochemical determination of furazolidone and dimetridazole using transition metal titanates with an ilmenite type structure." *Journal of Materials Chemistry C* no. 9:15263-15275.

Amara, Daniel, and Shlomo Margel. 2013. "Synthesis and characterization of ferromagnetic Fe 3 C/C composite nanoparticles as a catalyst for carbon nanotube growth." *Colloid and Polymer Science* no. 291:2121-2129.

Américo-Pinheiro, Juliana Heloisa Pinê, Claudomiro Vinicius Moreno Paschoa, Gledson Renan Salomão, Ianny Andrade Cruz, William Deodato Isique, Luiz Fernando Romanholo Ferreira, Farooq Sher, Nádia Hortense Torres, Vineet Kumar, and Rafael Silvio Bonilha Pinheiro. 2022. "Adsorptive remediation of naproxen from water using in-house developed hybrid material functionalized with iron oxide." *Chemosphere* no. 289:133222.

Amin, Muhammad Tahir, Abdulrehman Ali Alazba, and Umair Manzoor. 2014. "A review of removal of pollutants from water/wastewater using different types of nanomaterials." *Advances in Materials Science and Engineering* no. 2014:1-24.

Amjadi, Morteza, Ki-Uk Kyung, Inkyu Park, and Metin Sitti. 2016. "Stretchable, skin-mountable, and wearable strain sensors and their potential applications: a review." *Advanced Functional Materials* no. 26:1678-1698.

Amprako, Jessica Lucinda. 2016. "The United Nations World Water Development Report 2015." *Future of Food: Journal on Food, Agriculture and Society* no. 4:64-65.

Amran, Fadina, and Muhammad Abbas Ahmad Zaini. 2021. "Sodium hydroxide-activated Casuarina empty fruit: Isotherm, kinetics and thermodynamics of methylene blue and congo red adsorption." *Environmental Technology & Innovation* no. 23:101727.

Anh, Nguyen Tuan, Nguyen Ngoc Huyen, Ngo Xuan Dinh, Nguyen Thanh Vinh, Nguyen Van Quy, Vu Dinh Lam, and Anh-Tuan Le. 2022. "ZnO/ZnFe 2 O 4 nanocomposite-based electrochemical nanosensors for the detection of furazolidone in pork and shrimp samples: exploring the role of crystallinity, phase ratio, and heterojunction formation." *New Journal of Chemistry* no. 46:7090-7102.

Ankley, Gerald T, David L Defoe, Michael D Kahl, Kathleen M Jensen, Elizabeth A Makynen, Ann Miracle, Phillip Hartig, L Earl Gray, Mary Cardon, and Vickie Wilson. 2004. "Evaluation of the model anti-androgen flutamide for assessing the mechanistic basis of responses to an androgen in the fathead minnow (Pimephales promelas)." *Environmental Science & Technology* no. 38:6322-6327.

Arab, Saeedreza, Kianaz Rezaee, and Ghazaleh Moghaddam. 2021. "A novel fuzzy expert system design to assist with peptic ulcer disease diagnosis." *Cogent Engineering* no. 8:1861730.

Armaghani, Danial Jahed, and Panagiotis G Asteris. 2021. "A comparative study of ANN and ANFIS models for the prediction of cement-based mortar materials compressive strength." *Neural Computing and Applications* no. 33:4501-4532.

Arrieta, Alejandro Barredo, Natalia Díaz-Rodríguez, Javier Del Ser, Adrien Bennetot, Siham Tabik, Alberto Barbado, Salvador García, Sergio Gil-López, Daniel Molina, and Richard Benjamins. 2020. "Explainable Artificial Intelligence (XAI): Concepts, taxonomies, opportunities and challenges toward responsible AI." *Information Fusion* no. 58:82-115.

Asfaram, Arash, Mehrorang Ghaedi, Shaaker Hajati, and Alireza Goudarzi. 2016. "Synthesis of magnetic γ-Fe2O3-based nanomaterial for ultrasonic assisted dyes adsorption: modeling and optimization." *Ultrasonics Sonochemistry* no. 32:418-431.

Ashraf, Muhammad, Muhammad Ehsan Safdar, Sher Muhammad Shahzad, Ahsan Aziz, Muhammad Awais Piracaha, Muhammad Suleman, and Muhammad Bilal Ahmad. 2018. "Challenges and opportunities for using wastewater in agriculture: a review." *Journal of Applied Agriculture and Biotechnology* no. 2:1-20.

Aslam, Mian Muhammad-Ahson, Hsion-Wen Kuo, Walter Den, Muhammad Usman, Muhammad Sultan, and Hadeed Ashraf. 2021. "Functionalized carbon nanotubes (Cnts) for water and wastewater treatment: Preparation to application." *Sustainability* no. 13:5717.

Avcı, Ayça, İsmail İnci, and Nilay Baylan. 2020. "Adsorption of ciprofloxacin hydrochloride on multiwall carbon nanotube." *Journal of Molecular Structure* no. 1206:127711.

Avilés, F, JV Cauich-Rodríguez, L Moo-Tah, A May-Pat, and R Vargas-Coronado. 2009. "Evaluation of mild acid oxidation treatments for MWCNT functionalization." *Carbon* no. 47:2970-2975.

Awad, Abdelrahman M, Rem Jalab, Abdelbaki Benamor, Mustafa S Nasser, Muneer M Ba-Abbad, Muftah El-Naas, and Abdul Wahab Mohammad. 2020. "Adsorption of organic pollutants by nanomaterial-based adsorbents: An overview." *Journal of Molecular Liquids* no. 301:112335.

Awad, Eman Sh, Tamara M Sabirova, Natalia A Tretyakova, Qusay F Alsalhy, Alberto Figoli, and Issam K Salih. 2021. "A mini-review of enhancing ultrafiltration membranes (UF) for wastewater treatment: Performance and stability." *Chemical Engineering* no. 5:34.

Awasthi, Anuradha, Pradip Jadhao, and Kanchan Kumari. 2019. "Clay nano-adsorbent: structures, applications and mechanism for water treatment." *SN Applied Sciences* no. 1:1-21.

Azam, Mohd Asyadi, Elyas Talib, and Raja Noor Amalina Raja Seman. 2018. "Direct deposition of multi-walled carbon nanotubes onto stainless steel and YEF foils using a simple electrophoretic deposition for electrochemical capacitor electrode." *Materials Research Express* no. 6:015501.

Azari, Ali, Mohammad Hassan Mahmoudian, Maryam Hazrati Niari, Ismail Eş, Emad Dehganifard, Amin Kiani, Allahbakhsh Javid, Hossein Azari, Yadolah Fakhri, and Amin Mousavi Khaneghah. 2019. "Rapid and efficient ultrasonic assisted adsorption of diethyl phthalate onto FeIIFe2IIIO4@ GO: ANN-GA and RSM-DF modeling, isotherm, kinetic and mechanism study." *Microchemical Journal* no. 150:104144.

Azevedo, Renato M, João B Costa, Philippe Serp, José M Loureiro, Joaquim L Faria, Cláudia G Silva, and Ana PM Tavares. 2015. "A strategy for improving peroxidase stability via immobilization on surface modified multi-walled carbon nanotubes." *Journal of Chemical Technology & Biotechnology* no. 90:1570-1578.

Azqhandi, Mohammad Hossein Ahmadi, Bahman Vasheghani Farahani, and Nasibe Dehghani. 2017. "Encapsulation of methotrexate and cyclophosphamide in interpolymer complexes formed between poly acrylic acid and poly ethylene glycol on multi-walled carbon nanotubes as drug delivery systems." *Materials Science and Engineering: C* no. 79:841-847.

Baby, Tessy Theres, and S Ramaprabhu. 2010. "SiO2 coated Fe3O4 magnetic nanoparticle dispersed multiwalled carbon nanotubes based amperometric glucose biosensor." *Talanta* no. 80:2016-2022.

Bachmann, Till M, and Jonathan van der Kamp. 2014. "Environmental cost-benefit analysis and the EU (European Union) Industrial Emissions Directive: Exploring the societal efficiency of a DeNOx retrofit at a coal-fired power plant." *Energy* no. 68:125-139.

Backhaus, Thomas, Rolf Altenburger, Michael Faust, Daniel Frein, Tobias Frische, Per Johansson, Anja Kehrer, and Tobias Porsbring. 2013. "Proposal for environmental mixture risk assessment in the context of the biocidal product authorization in the EU." *Environmental Sciences Europe* no. 25:1-9.

Badnjevic, Almir, Lejla Gurbeta, and Eddie Custovic. 2018. "An expert diagnostic system to automatically identify asthma and chronic obstructive pulmonary disease in clinical settings." *Scientific Reports* no. 8:1-9.

Baek, Youngbin, Cholin Kim, Dong Kyun Seo, Taewoo Kim, Jeong Seok Lee, Yong Hyup Kim, Kyung Hyun Ahn, Sang Seek Bae, Sang Cheol Lee, and Jaelim Lim. 2014. "High performance and antifouling vertically aligned carbon

nanotube membrane for water purification." *Journal of Membrane Science* no. 460:171-177.

Baghayeri, Mehdi, Reza Ansari, Marzieh Nodehi, Iman Razavipanah, and Hojat Veisi. 2018. "Voltammetric aptasensor for bisphenol A based on the use of a MWCNT/Fe 3 O 4@ gold nanocomposite." *Microchimica Acta* no. 185:1-9.

Baghbani, Abolfazl, Tanveer Choudhury, Susanga Costa, and Johannes Reiner. 2022. "Application of artificial intelligence in geotechnical engineering: A state-of-the-art review." *Earth-Science Reviews* no. 228:103991.

Bahrami, Mehrdad, Mohammad Akbari, Seyed Amin Bagherzadeh, Arash Karimipour, Masoud Afrand, and Marjan Goodarzi. 2019. "Develop 24 dissimilar ANNs by suitable architectures & training algorithms via sensitivity analysis to better statistical presentation: Measure MSEs between targets & ANN for Fe–CuO/Eg–Water nanofluid." *Physica A: Statistical Mechanics and its Applications* no. 519:159-168.

Bai, Chengling, Lei Wang, and Zhenya Zhu. 2020. "Adsorption of Cr (III) and Pb (II) by graphene oxide/alginate hydrogel membrane: Characterization, adsorption kinetics, isotherm and thermodynamics studies." *International Journal of Biological Macromolecules* no. 147:898-910.

Bainbridge, Z, S Lewis, R Bartley, K Fabricius, C Collier, J Waterhouse, A Garzon-Garcia, B Robson, J Burton, and A Wenger. 2018. "Fine sediment and particulate organic matter: A review and case study on ridge-to-reef transport, transformations, fates, and impacts on marine ecosystems." *Marine Pollution Bulletin* no. 135:1205-1220.

Bakr, Ahmed Refaat, and Md Saifur Rahaman. 2019. "Crossflow electrochemical filtration for elimination of ibuprofen and bisphenol a from pure and competing electrolytic solution conditions." *Journal of Hazardous Materials* no. 365:615-621.

Balasubramanian, Paramasivam, Muthaiah Annalakshmi, Shen-Ming Chen, and Tse-Wei Chen. 2019. "Sonochemical synthesis of molybdenum oxide (MoO3) microspheres anchored graphitic carbon nitride (g-C3N4) ultrathin sheets for enhanced electrochemical sensing of Furazolidone." *Ultrasonics Sonochemistry* no. 50:96-104.

Banerjee, Sushmita, and MC Chattopadhyaya. 2017. "Adsorption characteristics for the removal of a toxic dye, tartrazine from aqueous solutions by a low cost agricultural by-product." *Arabian Journal of Chemistry* no. 10:S1629-S1638.

Barrejón, Myriam, and Maurizio Prato. 2022. "Carbon nanotube membranes in water treatment applications." *Advanced Materials Interfaces* no. 9:2101260.

Beliatskaya, AV, II Krasnyuk, AO Elagina, II Krasnyuk, IM Kashlikova, OI Stepanova, AN Vorob'yov, AN Kuzmenko, SG Iskenderova, and DR Kannieva. 2020. "Study of the solubility of furazolidone from solid dispersions with polyvinylpyrrolidone." *Moscow University Chemistry Bulletin* no. 75:43-46.

Benner, Jessica, Damian E Helbling, Hans-Peter E Kohler, Janneke Wittebol, Elena Kaiser, Carsten Prasse, Thomas A Ternes, Christian N Albers, Jens Aamand, and Benjamin Horemans. 2013. "Is biological treatment a viable alternative for micropollutant removal in drinking water treatment processes?" *Water Research* no. 47:5955-5976.

Bennion, Helen, and Rick Battarbee. 2007. "The European Union water framework directive: opportunities for palaeolimnology." *Journal of Paleolimnology* no. 38:285-295.

Bernal, Valentina, Liliana Giraldo, and Juan C Moreno-Piraján. 2021. "Physicochemical parameters of the methylparaben adsorption from aqueous solution onto activated carbon and their relationship with the surface chemistry." *ACS Omega* no. 6:8797-8807.

Bernardo, Gabriel, Tiago Araújo, Telmo da Silva Lopes, José Sousa, and Adélio Mendes. 2020. "Recent advances in membrane technologies for hydrogen purification." *International Journal of Hydrogen Energy* no. 45:7313-7338.

Besra, Laxmidhar, and Meilin Liu. 2007. "A review on fundamentals and applications of electrophoretic deposition (EPD)." *Progress in Materials Science* no. 52:1-61.

Bhadra, Madhuleena, Sagar Roy, and Somenath Mitra. 2016a. "A bilayered structure comprised of functionalized carbon nanotubes for desalination by membrane distillation." *ACS Applied Materials & Interfaces* no. 8:19507-19513.

Bhadra, Madhuleena, Sagar Roy, and Somenath Mitra. 2016b. "Flux enhancement in direct contact membrane distillation by implementing carbon nanotube immobilized PTFE membrane." *Separation and Purification Technology* no. 161:136-143.

Bhatia, Drishti, Dipaloy Datta, Abhishek Joshi, Sagar Gupta, and Yogesh Gote. 2019. "Adsorption of isonicotinic acid from aqueous solution using multi-walled carbon nanotubes/Fe3O4." *Journal of Molecular Liquids* no. 276:163-169.

Bhol, Prangya, Sudesh Yadav, Ali Altaee, Manav Saxena, Pramila Kumari Misra, and Akshaya K Samal. 2021. "Graphene-based membranes for water and wastewater treatment: a review." *ACS Applied Nano Materials* no. 4:3274-3293.

Birošová, Lucia, Tomáš Mackuľak, Igor Bodík, Jozef Ryba, Jaroslav Škubák, and Roman Grabic. 2014. "Pilot study of seasonal occurrence and distribution of antibiotics and drug resistant bacteria in wastewater treatment plants in Slovakia." *Science of the Total Environment* no. 490:440-444.

Bock, Claudia, Petra Gowik, and Carolin Stachel. 2007. "Matrix-comprehensive in-house validation and robustness check of a confirmatory method for the determination of four nitrofuran metabolites in poultry muscle and shrimp by LC–MS/MS." *Journal of Chromatography B* no. 856:178-189.

Bohdziewicz, Jolanta, and Gabriela Kamińska. 2013. "Kinetics and equilibrium of the sorption of bisphenol A by carbon nanotubes from wastewater." *Water Science and Technology* no. 68:1306-1314.

Bolong, Nurmin, AF Ismail, Mohd Razman Salim, and T Matsuura. 2009. "A review of the effects of emerging contaminants in wastewater and options for their removal." *Desalination* no. 239:229-246.

Bouhedda, Mounir, Sonia Lefnaoui, Samia Rebouh, and Madiha M Yahoum. 2019. "Predictive model based on Adaptive Neuro-Fuzzy Inference System for estimation of Cephalexin adsorption on the Octenyl Succinic Anhydride starch." *Chemometrics and Intelligent Laboratory Systems* no. 193:103843.

Bounos, G, KS Andrikopoulos, H Moschopoulou, G Ch Lainioti, David Roilo, Riccardo Checchetto, T Ioannides, JK Kallitsis, and GA Voyiatzis. 2017. "Enhancing water vapor permeability in mixed matrix polypropylene

membranes through carbon nanotubes dispersion." *Journal of Membrane Science* no. 524:576-584.

Brixius-Anderko, Simone, and Emily E Scott. 2019. "Structure of human cortisol-producing cytochrome P450 11B1 bound to the breast cancer drug fadrozole provides insights for drug design." *Journal of Biological Chemistry* no. 294:453-460.

Buang, Nor Aziah, Fatirah Fadil, Zaiton Abdul Majid, and Shafinaz Shahir. 2012. "Characteristic of mild acid functionalized multiwalled carbon nanotubes towards high dispersion with low structural defects." *Digest Journal of Nanomaterials and Biostructures* no. 7:33-39.

Bui, Ngoc, Eric R Meshot, Sangil Kim, José Peña, Phillip W Gibson, Kuang Jen Wu, and Francesco Fornasiero. 2016. "Ultrabreathable and protective membranes with sub-5 nm carbon nanotube pores." *Advanced Materials* no. 28:5871-5877.

Bulmer, John S, Adarsh Kaniyoor, and James A Elliott. 2021. "A Meta-Analysis of Conductive and Strong Carbon Nanotube Materials." *Advanced Materials* no. 33:2008432.

Bundschuh, Mirco, Mark O Gessner, Guido Fink, Thomas A Ternes, Christine Sögding, and Ralf Schulz. 2011. "Ecotoxicologial evaluation of wastewater ozonation based on detritus–detritivore interactions." *Chemosphere* no. 82:355-361.

Buxton, Herbert T, and Dana W Kolpin. 2005. "Pharmaceuticals, hormones, and other organic wastewater contaminants in US streams." *Water Encyclopedia* no. 5:605-608.

Cabezas, Francisco. 2012. "The European water framework directive: a framework?" *International Journal of Water Resources Development* no. 28:19-26.

Cai, Nan, and Philip Larese-Casanova. 2014. "Sorption of carbamazepine by commercial graphene oxides: a comparative study with granular activated carbon and multiwalled carbon nanotubes." *Journal of Colloid and Interface Science* no. 426:152-161.

Cai, Zhifeng, Liangliang Wu, Kaifei Qi, Chenhua Deng, and Caifeng Zhang. 2021. "Blue-emitting glutathione-capped copper nanoclusters as fluorescent

probes for the highly specific biosensing of furazolidone." *Spectrochimica Acta Part A: Molecular and Biomolecular Spectroscopy* no. 247:119145.

Caliskan Salihi, Elif, and Emine Ceren Tulay. 2022. "Adsorptive removal of antipsychotic drug by carbon nanofibers in a batch and fixed bed column system." *Particulate Science and Technology* no. 40:899-910.

Campo, Julian, Ana Masiá, Cristina Blasco, and Yolanda Picó. 2013. "Occurrence and removal efficiency of pesticides in sewage treatment plants of four Mediterranean River Basins." *Journal of Hazardous Materials* no. 263:146-157.

Carmona, Eric, Vicente Andreu, and Yolanda Picó. 2014. "Occurrence of acidic pharmaceuticals and personal care products in Turia River Basin: from waste to drinking water." *Science of the Total Environment* no. 484:53-63.

Carneiro, Íris, and Sónia Simões. 2020. "Effect of morphology and structure of MWCNTs on metal matrix nanocomposites." *Materials* no. 13:5557.

Cha, Chaenyung, Su Ryon Shin, Nasim Annabi, Mehmet R Dokmeci, and Ali Khademhosseini. 2013. "Carbon-based nanomaterials: multifunctional materials for biomedical engineering." *ACS Nanomaterials* no. 7:2891-2897.

Chapartegui, M, J Barcena, X Irastorza, C Elizetxea, E Fiamegkou, V Kostopoulos, and A Santamaria. 2013. "Manufacturing, characterization and thermal conductivity of epoxy and benzoxazine multi-walled carbon nanotube buckypaper composites." *Journal of Composite Materials* no. 47:1705-1715.

Chatzikomis, Christoforos, Sebastian W Pattinson, Krzysztof KK Koziol, and Ian M Hutchings. 2012. "Patterning of carbon nanotube structures by inkjet printing of catalyst." *Journal of Materials Science* no. 47:5760-5765.

Chaudhari, Swati R, and Manoj E Patil. 2014. "Comparative analysis of fuzzy inference systems for air conditioner." *International Journal of Advanced computer research* no. 4:922.

Chauhan, Nidhi, and Chandra Shekhar Pundir. 2011. "An amperometric biosensor based on acetylcholinesterase immobilized onto iron oxide nanoparticles/multi-walled carbon nanotubes modified gold electrode for measurement of organophosphorus insecticides." *Analytica Chimica Acta* no. 701:66-74.

Chen, Changlun, Jun Hu, Dadong Shao, Jiaxing Li, and Xiangke Wang. 2009. "Adsorption behavior of multiwall carbon nanotube/iron oxide magnetic

composites for Ni (II) and Sr (II)." *Journal of Hazardous Materials* no. 164:923-928.

Chen, Guang-Cai, Xiao-Quan Shan, Zhi-Guo Pei, Huanhua Wang, Li-Rong Zheng, Jing Zhang, and Ya-Ning Xie. 2011. "Adsorption of diuron and dichlobenil on multiwalled carbon nanotubes as affected by lead." *Journal of Hazardous Materials* no. 188:156-163.

Chen, Guang-Cai, Xiao-Quan Shan, Yu-Sheng Wang, Zhi-Guo Pei, Xiu-E Shen, Bei Wen, and Gary Owens. 2008. "Effects of copper, lead, and cadmium on the sorption and desorption of atrazine onto and from carbon nanotubes." *Environmental Science & Technology* no. 42:8297-8302.

Chen, Heng, Liuyang Zhang, Jinbao Chen, Matthew Becton, Xianqiao Wang, and Hong Nie. 2016. "Energy dissipation capability and impact response of carbon nanotube buckypaper: A coarse-grained molecular dynamics study." *Carbon* no. 103:242-254.

Chen, Mei, Klas Ohman, Chris Metcalfe, Michael G Ikonomou, Prasanna L Amatya, and Jeffrey Wilson. 2006. "Pharmaceuticals and endocrine disruptors in wastewater treatment effluents and in the water supply system of Calgary, Alberta, Canada." *Water Quality Research Journal* no. 41:351-364.

Cheng, Dongle, Huu Hao Ngo, Wenshan Guo, Soon Woong Chang, Dinh Duc Nguyen, Yiwen Liu, Qin Wei, and Dong Wei. 2020. "A critical review on antibiotics and hormones in swine wastewater: Water pollution problems and control approaches." *Journal of Hazardous Materials* no. 387:121682.

Cheng, Xiaoshi, Suna Wang, Wenxuan Huang, Feng Wang, Shiyu Fang, Ran Ge, Qin Zhang, Le Zhang, Wei Du, and Fang Fang. 2022. "Current status of hypochlorite technology on the wastewater treatment and sludge disposal: Performance, principals and prospects." *Science of the Total Environment* no. 803:150085.

Cheng, Xingxing, Chunli Zheng, Qiang Lu, Jianhui Liu, Qiaorui Wang, YuRui Fan, and JianYu Zhang. 2019. "Adsorption of furazolidone, D-cycloserine, and chloramphenicol on granular activated carbon made from corn stover." *Journal of Environmental Engineering* no. 145:04019038.

Cheriyamundath, Sanith, and Sirisha L Vavilala. 2021. "Nanotechnology-based wastewater treatment." *Water and Environment Journal* no. 35:123-132.

Chitranshi, Megha, Anuptha Pujari, Vianessa Ng, Daniel Chen, Devika Chauhan, Ronald Hudepohl, Motahareh Saleminik, Sung Yong Kim, Ashley Kubley, and Vesselin Shanov. 2020. "Carbon nanotube sheet-synthesis and applications." *Nanomaterials* no. 10:2023.

Cho, Hyun-Hee, Haiou Huang, and Kellogg Schwab. 2011. "Effects of solution chemistry on the adsorption of ibuprofen and triclosan onto carbon nanotubes." *Langmuir* no. 27:12960-12967.

Choi, In-Hwan, Sung-Hyun Yoo, Jun-Ho Jung, Myo-Taeg Lim, Jung-Jun Oh, Moon-Kyou Song, and Choon-Ki Ahn. 2015. "Design of Neuro-Fuzzy based intelligent inference algorithm for energy management system with legacy device." *The Transactions of the Korean Institute of Electrical Engineers* no. 64:779-785.

Choi, Yong-Keun, and Eunsung Kan. 2019. "Effects of pyrolysis temperature on the physicochemical properties of alfalfa-derived biochar for the adsorption of bisphenol A and sulfamethoxazole in water." *Chemosphere* no. 218:741-748.

Chowdhury, Shamik, and Papita Saha. 2011. "Adsorption kinetic modeling of safranin onto rice husk biomatrix using pseudo-first-and pseudo-second-order kinetic models: Comparison of linear and non-linear methods." *Clean–Soil, Air, Water* no. 39:274-282.

Chu, Yiwen, Peng Zhang, Jianghua Hu, Wuli Yang, and Changchun Wang. 2009. "Synthesis of monodispersed Co (Fe)/carbon nanocomposite microspheres with very high saturation magnetization." *The Journal of Physical Chemistry C* no. 113:4047-4052.

Ciğeroğlu, Zeynep, Gürkan Küçükyıldız, Berna Erim, and Erdem Alp. 2021. "Easy preparation of magnetic nanoparticles-rGO-chitosan composite beads: Optimization study on cefixime removal based on RSM and ANN by using Genetic Algorithm Approach." *Journal of Molecular Structure* no. 1224:129182.

Čížková, Hana, Jan Květ, Francisco A Comin, Raija Laiho, Jan Pokorný, and David Pithart. 2013. "Actual state of European wetlands and their possible future in the context of global climate change." *Aquatic Sciences* no. 75:3-26.

Clara, Manfred, Birgit Strenn, and Norbert Kreuzinger. 2004. "Carbamazepine as a possible anthropogenic marker in the aquatic environment: investigations

on the behaviour of carbamazepine in wastewater treatment and during groundwater infiltration." *Water Research* no. 38:947-954.

Cohen, Lorenzo, and Alison Jefferies. 2019. "Environmental exposures and cancer: using the precautionary principle." *ecancermedicalscience* no. 13.

Collins, Christopher, Denis Dennehy, Kieran Conboy, and Patrick Mikalef. 2021. "Artificial intelligence in information systems research: A systematic literature review and research agenda." *International Journal of Information Management* no. 60:102383.

Commission, European. 2013. "Directive 2013/39/EU of the European Parliament and of the Council of 12 August 2013 amending Directives 2000/60/EC and 2008/105/EC as regards priority substances in the field of water policy." *Official Journal of European Union* no. 226:1-17.

Cong, Hailin, Jianmin Zhang, Maciej Radosz, and Youqing Shen. 2007. "Carbon nanotube composite membranes of brominated poly (2, 6-diphenyl-1, 4-phenylene oxide) for gas separation." *Journal of Membrane Science* no. 294:178-185.

Cooper, Kevin Mark, Robert J Mccracken, Marijn Buurman, and David Glenn Kennedy. 2008. "Residues of nitrofuran antibiotic parent compounds and metabolites in eyes of broiler chickens." *Food Additives and Contaminants* no. 25:548-556.

Cui, Hongzhi, Xiantong Yan, Manuel Monasterio, and Feng Xing. 2017. "Effects of various surfactants on the dispersion of MWCNTs–OH in aqueous solution." *Nanomaterials* no. 7:262.

Das, Rasel, Md Eaqub Ali, Sharifah Bee Abd Hamid, Seeram Ramakrishna, and Zaira Zaman Chowdhury. 2014. "Carbon nanotube membranes for water purification: A bright future in water desalination." *Desalination* no. 336:97-109.

Das, Rasel, Sharifah Bee Abd Hamid, and Mohamad Suffian Mohamad Annuar. 2016. "Highly efficient and stable novel nanobiohybrid catalyst to avert 3, 4-dihydroxybenzoic acid pollutant in water." *Scientific Reports* no. 6:1-11.

Das, Sumistha, Biswarup Sen, and Nitai Debnath. 2015. "Recent trends in nanomaterials applications in environmental monitoring and remediation." *Environmental Science and Pollution Research* no. 22:18333-18344.

Dastjerd, Niousha K, Onur Can Sert, Tansel Ozyer, and Reda Alhajj. 2019. "Fuzzy classification methods based diagnosis of Parkinson's disease from speech test cases." *Current Aging Science* no. 12:100-120.

Davenport, Douglas M, Cody L Ritt, Rhea Verbeke, Marcel Dickmann, Werner Egger, Ivo FJ Vankelecom, and Menachem Elimelech. 2020. "Thin film composite membrane compaction in high-pressure reverse osmosis." *Journal of Membrane Science* no. 610:118268.

De Volder, Michael FL, Sameh H Tawfick, Ray H Baughman, and A John Hart. 2013. "Carbon nanotubes: present and future commercial applications." *Science* no. 339:535-539.

Dehkordi, Shima Kouhi, Hamed Paknejad, Ludek Blaha, Helena Svecova, Roman Grabic, Zdenek Simek, Alena Otoupalikova, and Michal Bittner. 2021. "Instrumental and bioanalytical assessment of pharmaceuticals and hormone-like compounds in a major drinking water source—Wastewater receiving Zayandeh Rood river, Iran." *Environmental Science and Pollution Research*:1-15.

Deng, Yanchun, Yong Sik Ok, Dinesh Mohan, Charles U Pittman Jr, and Xiaomin Dou. 2019. "Carbamazepine removal from water by carbon dot-modified magnetic carbon nanotubes." *Environmental Research* no. 169:434-444.

Desai, M, JK Jellyman, and MG Ross. 2015. "Epigenomics, gestational programming and risk of metabolic syndrome." *International Journal of Obesity* no. 39:633-641.

Deylami, Sh, M Hosseini Sabzevari, M Ghaedi, MH Ahmadi Azqhandi, and F Marahel. 2023. "Efficient photodegradation of disulfine blue dye and Tetracycline over Robust and Green g-CN/Ag3VO4/PAN nanofibers: Experimental design, RSM, RBF-NN and ANFIS modeling." *Process Safety and Environmental Protection* no. 169:71-81.

Dhar, Avik Kumar, Humayra Akhter Himu, Maitry Bhattacharjee, Md Golam Mostufa, and Fahmida Parvin. 2023. "Insights on applications of bentonite clays for the removal of dyes and heavy metals from wastewater: a review." *Environmental Science and Pollution Research* no. 30:5440-5474.

Diamanti-Kandarakis, Evanthia, Jean-Pierre Bourguignon, Linda C Giudice, Russ Hauser, Gail S Prins, Ana M Soto, R Thomas Zoeller, and Andrea C

Gore. 2009. "Endocrine-disrupting chemicals: an Endocrine Society scientific statement." *Endocrine Reviews* no. 30:293-342.

Directive, EC. 2008. "105/EC of the European Parliament and of the Council of 16 December 2008 on environmental quality standards in the field of water policy, amending and subsequently repealing Council Directives 82/176." *Eec* no. 83:84-97.

Djamila, Bouneb, Bahi Tahar, and Merabet Hichem. 2018. "Vibration for detection and diagnosis bearing faults using adaptive neuro-fuzzy inference system." *Journal of Electrical Systems* no. 14:95-104.

Do, Hung Manh, Thi Hong Le, Xuan Phuc Nguyen, Hong Nam Pham, Thi Hong Ngo, Trung Hieu Nguyen, Thanh Phong Pham, Manh Huong Phan, Jozef Kováč, and Ivan Skorvanek. 2020. "Oxidation-controlled magnetism and Verwey transition in Fe/Fe3O4 lamellae." *Journal of Science: Advanced Materials and Devices* no. 5:263-269.

Dolatabadi, Maryam, and Saeid Ahmadzadeh. 2019. "A rapid and efficient removal approach for degradation of metformin in pharmaceutical wastewater using electro-Fenton process; optimization by response surface methodology." *Water Science and Technology* no. 80:685-694.

Domagała, Kamila, Mario Borlaf, Jacqueline Traber, Dariusz Kata, and Thomas Graule. 2019. "Purification and functionalisation of multi-walled carbon nanotubes." *Materials Letters* no. 253:272-275.

Dong, Xiuli, Mohamad Al Awak, Ping Wang, Ya-Ping Sun, and Liju Yang. 2018. "Carbon dot incorporated multi-walled carbon nanotube coated filters for bacterial removal and inactivation." *RSC Advances* no. 8:8292-8301.

Drioli, Enrico, Aamer Ali, and Francesca Macedonio. 2015. "Membrane distillation: Recent developments and perspectives." *Desalination* no. 356:56-84.

Dubey, Rama, Dhiraj Dutta, Arpan Sarkar, and Pronobesh Chattopadhyay. 2021. "Functionalized carbon nanotubes: Synthesis, properties and applications in water purification, drug delivery, and material and biomedical sciences." *Nanoscale Advances* no. 3:5722-5744.

Duman, Osman, Ceren Özcan, Tülin Gürkan Polat, and Sibel Tunc. 2019. "Carbon nanotube-based magnetic and non-magnetic adsorbents for the high-efficiency removal of diquat dibromide herbicide from water: OMWCNT,

OMWCNT-Fe3O4 and OMWCNT-κ-carrageenan-Fe3O4 nanocomposites." *Environmental Pollution* no. 244:723-732.

Dumée, Ludovic, Vincent Germain, Kallista Sears, Jürg Schütz, Niall Finn, Mikel Duke, Sophie Cerneaux, David Cornu, and Stephen Gray. 2011. "Enhanced durability and hydrophobicity of carbon nanotube bucky paper membranes in membrane distillation." *Journal of Membrane Science* no. 376:241-246.

Dutz, Silvio, and Rudolf Hergt. 2013. "Magnetic nanoparticle heating and heat transfer on a microscale: Basic principles, realities and physical limitations of hyperthermia for tumour therapy." *International Journal of Hyperthermia* no. 29:790-800.

Ebele, Anekwe Jennifer, Mohamed Abou-Elwafa Abdallah, and Stuart Harrad. 2017. "Pharmaceuticals and personal care products (PPCPs) in the freshwater aquatic environment." *Emerging Contaminants* no. 3:1-16.

Ehiguese, Friday Ojie, Maria L Rodgers, Cristiano VM Araújo, Robert J Griffitt, and M Laura Martin-Diaz. 2021. "Galaxolide and tonalide modulate neuroendocrine activity in marine species from two taxonomic groups." *Environmental Research* no. 196:110960.

El-Aswar, Eslam Ibrahim, Hassan Ramadan, Hussin Elkik, and Ahmed G Taha. 2022. "A comprehensive review on preparation, functionalization and recent applications of nanofiber membranes in wastewater treatment." *Journal of Environmental Management* no. 301:113908.

Elboughdiri, Noureddine. 2020. "The use of natural zeolite to remove heavy metals Cu (II), Pb (II) and Cd (II), from industrial wastewater." *Cogent Engineering* no. 7:1782623.

Emembolu, Loveth Nwanneka, Paschal Enyinnaya Ohale, Chijioke Elijah Onu, and Nonye Jennifer Ohale. 2022. "Comparison of RSM and ANFIS modeling techniques in corrosion inhibition studies of Aspilia Africana leaf extract on mild steel and aluminium metal in acidic medium." *Applied Surface Science Advances* no. 11:100316.

Emmanuel Chinonye, Okpe, Asadu Christian Oluchukwu, and Onu Chijioke Elijah. 2018. "Statistical analysis for orange G adsorption using kola nut shell activated carbon." *Journal of the Chinese Advanced Materials Society* no. 6:605-619.

Erdirencelebi, Dilek, and Sukran Yalpir. 2011. "Adaptive network fuzzy inference system modeling for the input selection and prediction of anaerobic digestion effluent quality." *Applied Mathematical Modelling* no. 35:3821-3832.

Estili, Mehdi, Akira Kawasaki, Hiroki Sakamoto, Yutaka Mekuchi, Masaki Kuno, and Takayuki Tsukada. 2008. "The homogeneous dispersion of surfactantless, slightly disordered, crystalline, multiwalled carbon nanotubes in α-alumina ceramics for structural reinforcement." *Acta Materialia* no. 56:4070-4079.

Ezzatahmadi, Naeim, Godwin A Ayoko, Graeme J Millar, Robert Speight, Cheng Yan, Jihong Li, Shizhong Li, Jianxi Zhu, and Yunfei Xi. 2017. "Clay-supported nanoscale zero-valent iron composite materials for the remediation of contaminated aqueous solutions: a review." *Chemical Engineering Journal* no. 312:336-350.

Fallah, Zari, Ehsan Nazarzadeh Zare, Matineh Ghomi, Farhad Ahmadijokani, Majed Amini, Mahmood Tajbakhsh, Mohammad Arjmand, Gaurav Sharma, Hamna Ali, and Awais Ahmad. 2021. "Toxicity and remediation of pharmaceuticals and pesticides using metal oxides and carbon nanomaterials." *Chemosphere* no. 275:130055.

Fan, Xinfei, Yanming Liu, Xie Quan, Huimin Zhao, Shuo Chen, Gang Yi, and Lei Du. 2016. "High desalination permeability, wetting and fouling resistance on superhydrophobic carbon nanotube hollow fiber membrane under self-powered electrochemical assistance." *Journal of Membrane Science* no. 514:501-509.

Fang, Binbin, Jing Guo, Fuxing Li, John P Giesy, Lianjun Wang, and Wei Shi. 2017. "Bioassay directed identification of toxicants in sludge and related reused materials from industrial wastewater treatment plants in the Yangtze River Delta." *Chemosphere* no. 168:191-198.

Fantke, Peter, Nicolò Aurisano, Jeroen Provoost, Panagiotis G Karamertzanis, and Michael Hauschild. 2020. "Toward effective use of REACH data for science and policy." *Environment International* no. 135:10.1016.

Fard, Mohammad Alizadeh, and Brian Barkdoll. 2018. "Using recyclable magnetic carbon nanotube to remove micropollutants from aqueous solutions." *Journal of Molecular Liquids* no. 249:193-202.

Farghali, AA, Mohamed Bahgat, A Enaiet Allah, and MH Khedr. 2013. "Adsorption of Pb (II) ions from aqueous solutions using copper oxide nanostructures." *Beni-Suef University Journal of Basic and Applied Sciences* no. 2:61-71.

Fawell, John, and Choon Nam Ong. 2012. "Emerging contaminants and the implications for drinking water." *International Journal of Water Resources Development* no. 28:247-263.

Feitosa, Ivan Brito, Bruno Mori, Ana Paula de Azevedo dos Santos, Janaína Cecília Oliveira Villanova, Carolina Bioni Garcia Teles, and Allyson Guimarães Costa. 2021. "What are the immunopharmacological effects of furazolidone? A systematic review." *Immunopharmacology and Immunotoxicology* no. 43:674-679.

Feng, Yilin, Hui Wang, Junhuai Xu, Xiaosheng Du, Xu Cheng, Zongliang Du, and Haibo Wang. 2021. "Fabrication of MXene/PEI functionalized sodium alginate aerogel and its excellent adsorption behavior for Cr (VI) and Congo Red from aqueous solution." *Journal of Hazardous Materials* no. 416:125777.

Ferreira, Rita, John S Schneekloth Jr, Konstantin I Panov, Katherine M Hannan, and Ross D Hannan. 2020. "Targeting the RNA polymerase I transcription for cancer therapy comes of age." *Cells* no. 9:266.

Fontananova, E, MA Bahattab, SA Aljlil, M Alowairdy, G Rinaldi, D Vuono, JB Nagy, E Drioli, and G Di Profio. 2015. "From hydrophobic to hydrophilic polyvinylidenefluoride (PVDF) membranes by gaining new insight into material's properties." *RSC Advances* no. 5:56219-56231.

Forgacs, Esther, Tibor Cserháti, and Gyula Oros. 2004. "Removal of synthetic dyes from wastewaters: a review." *Environment International* no. 30:953-971.

Foroughi, Maryam, Mohammad Hossein Ahmadi Azqhandi, and Somayeh Kakhki. 2020. "Bio-inspired, high, and fast adsorption of tetracycline from aqueous media using Fe3O4-g-CN@ PEI-β-CD nanocomposite: Modeling by response surface methodology (RSM), boosted regression tree (BRT), and general regression neural network (GRNN)." *Journal of Hazardous Materials* no. 388:121769.

Fram, Miranda S, and Kenneth Belitz. 2011. "Occurrence and concentrations of pharmaceutical compounds in groundwater used for public drinking-water supply in California." *Science of the Total Environment* no. 409:3409-3417.

Fung, Tak, Keith D Farnsworth, David G Reid, and Axel G Rossberg. 2012. "Recent data suggest no further recovery in North Sea Large Fish Indicator."

Gagné, F, C André, P Cejka, Robert Hausler, and M Fournier. 2011. "Evidence of neuroendocrine disruption in freshwater mussels exposed to municipal wastewaters." *Science of the Total Environment* no. 409:3711-3718.

Gao, Yifan, Kshitjia Shah, Ivy Kwok, Meng Wang, Leonard H Rome, and Shaily Mahendra. 2022. "Immobilized fungal enzymes: Innovations and potential applications in biodegradation and biosynthesis." *Biotechnology Advances*:107936.

Gasim, Mohamed Faisal, Jun-Wei Lim, Siew-Chun Low, Kun-Yi Andrew Lin, and Wen-Da Oh. 2022. "Can biochar and hydrochar be used as sustainable catalyst for persulfate activation?" *Chemosphere* no. 287:132458.

Gaya, Muhammad Sani, N Abdul Wahab, YM Sam, and Sahratul Izah Samsudin. 2014. "ANFIS modelling of carbon and nitrogen removal in domestic wastewater treatment plant." *Journal Teknologi* no. 67.

Gerbersdorf, Sabine U, Carla Cimatoribus, Holger Class, Karl-H Engesser, Steffen Helbich, Henner Hollert, Claudia Lange, Martin Kranert, Jörg Metzger, and Wolfgang Nowak. 2015. "Anthropogenic Trace Compounds (ATCs) in aquatic habitats—Research needs on sources, fate, detection and toxicity to ensure timely elimination strategies and risk management." *Environment International* no. 79:85-105.

Ghirardini, A, V Grillini, and P Verlicchi. 2020. "A review of the occurrence of selected micropollutants and microorganisms in different raw and treated manure–environmental risk due to antibiotics after application to soil." *Science of the Total Environment* no. 707:136118.

Gholamy, Afshin, Vladik Kreinovich, and Olga Kosheleva. 2018. "Why 70/30 or 80/20 relation between training and testing sets: A pedagogical explanation."

Ghoreishi, SM, Ali Hedayati, and SO Mousavi. 2016. "Quercetin extraction from Rosa damascena Mill via supercritical CO2: Neural network and adaptive neuro fuzzy interface system modeling and response surface optimization." *The Journal of Supercritical Fluids* no. 112:57-66.

Gibs, Jacob, Heather A Heckathorn, Michael T Meyer, Frank R Klapinski, Marzooq Alebus, and Robert L Lippincott. 2013. "Occurrence and partitioning of antibiotic compounds found in the water column and bottom sediments from

a stream receiving two wastewater treatment plant effluents in Northern New Jersey, 2008." *Science of the Total Environment* no. 458:107-116.

Gillis, Patricia L, François Gagné, Rodney McInnis, Tina M Hooey, Emily S Choy, Chantale André, Md Ehsanul Hoque, and Chris D Metcalfe. 2014. "The impact of municipal wastewater effluent on field-deployed freshwater mussels in the Grand River (Ontario, Canada)." *Environmental Toxicology and Chemistry* no. 33:134-143.

Giulivo, Monica, Miren Lopez de Alda, Ettore Capri, and Damià Barceló. 2016. "Human exposure to endocrine disrupting compounds: Their role in reproductive systems, metabolic syndrome and breast cancer. A review." *Environmental Research* no. 151:251-264.

Glomstad, Berit, Florian Zindler, Bjørn M Jenssen, and Andy M Booth. 2018. "Dispersibility and dispersion stability of carbon nanotubes in synthetic aquatic growth media and natural freshwater." *Chemosphere* no. 201:269-277.

Goh, Guo Liang, Shweta Agarwala, and Wai Yee Yeong. 2019. "Directed and on-demand alignment of carbon nanotube: a review toward 3D printing of electronics." *Advanced Materials Interfaces* no. 6:1801318.

Goh, Shalene Xue Lin, Esther Xue Yi Goh, and Hian Kee Lee. 2021. "Sodium dodecyl sulfate-multi-walled carbon nanotubes-coated-membrane solid phase extraction of glucocorticoids in aqueous matrices." *Talanta* no. 221:121624.

González-Mariño, Iria, José Benito Quintana, Isaac Rodríguez, and Rafael Cela. 2011. "Evaluation of the occurrence and biodegradation of parabens and halogenated by-products in wastewater by accurate-mass liquid chromatography-quadrupole-time-of-flight-mass spectrometry (LC-QTOF-MS)." *Water Research* no. 45:6770-6780.

Gross, AJ, M Holzinger, and S Cosnier. 2018. "Buckypaper bioelectrodes: Emerging materials for implantable and wearable biofuel cells." *Energy & Environmental Science* no. 11:1670-1687.

Guadagno, L, M Raimondo, L Vertuccio, C Naddeo, G Barra, P Longo, P Lamberti, G Spinelli, and MR Nobile. 2018. "Morphological, rheological and electrical properties of composites filled with carbon nanotubes functionalized with 1-pyrenebutyric acid." *Composites Part B: Engineering* no. 147:12-21.

Guardado, Ana Luisa Parra, Stéphanie Druon-Bocquet, Marie-Pierre Belleville, and Jose Sanchez-Marcano. 2021. "A novel process for the covalent

immobilization of laccases on silica gel and its application for the elimination of pharmaceutical micropollutants." *Environmental Science and Pollution Research* no. 28:25579-25593.

Guner, Sibel. 2011. "United Nations World Water Assessment Programme."

Guo, Jiabei, Hui Jiang, Yan Teng, Yue Xiong, Zhuhui Chen, Linjun You, and Deli Xiao. 2021. "Recent advances in magnetic carbon nanotubes: synthesis, challenges and highlighted applications." *Journal of Materials Chemistry B* no. 9:9076-9099.

Guo, Xiaojing, Yejing Huang, Wanxiang Yu, Xiao Yu, Xiufen Han, and Haiyun Zhai. 2020. "Multi-walled carbon nanotubes modified with iron oxide and manganese dioxide (MWCNTs-Fe3O4− MnO2) as a novel adsorbent for the determination of BPA." *Microchemical Journal* no. 157:104867.

Guo, Xuan, and Jianlong Wang. 2019. "A general kinetic model for adsorption: theoretical analysis and modeling." *Journal of Molecular Liquids* no. 288:111100.

Gupta, Vinod Kumar, Rajeev Kumar, Arunima Nayak, Tawfik A Saleh, and MA Barakat. 2013. "Adsorptive removal of dyes from aqueous solution onto carbon nanotubes: a review." *Advances in Colloid and Interface Science* no. 193:24-34.

Gupta, VK, O Moradi, I Tyagi, S Agarwal, H Sadegh, R Shahryari-Ghoshekandi, ASH Makhlouf, M Goodarzi, and A Garshasbi. 2016. "Study on the removal of heavy metal ions from industry waste by carbon nanotubes: effect of the surface modification: a review." *Critical Reviews in Environmental Science and Technology* no. 46:93-118.

Gurav, Ranjit, Shashi Kant Bhatia, Tae-Rim Choi, Ye-Lim Park, Jun Young Park, Yeong-Hoon Han, Govind Vyavahare, Jyoti Jadhav, Hun-Suk Song, and Peizhou Yang. 2020. "Treatment of furazolidone contaminated water using banana pseudostem biochar engineered with facile synthesized magnetic nanocomposites." *Bioresource Technology* no. 297:122472.

Gutiérrez, Marina, Andrea Ghirardini, Michela Borghesi, Stefano Bonnini, Dragana Mutavdžić Pavlović, and Paola Verlicchi. 2022. "Removal of micropollutants using a membrane bioreactor coupled with powdered activated carbon—A statistical analysis approach." *Science of The Total Environment* no. 840:156557.

Hamilton Jr, Raymond F, Chengcheng Xiang, Ming Li, Ibrahima Ka, Feng Yang, Dongling Ma, Dale W Porter, Nianqiang Wu, and Andrij Holian. 2013. "Purification and sidewall functionalization of multiwalled carbon nanotubes and resulting bioactivity in two macrophage models." *Inhalation Toxicology* no. 25:199-210.

Hamzah, Fatimah Bibi, F Mohd Hamzah, SF Mohd Razali, and Hafiza Samad. 2021. "A comparison of multiple imputation methods for recovering missing data in hydrological studies." *Civil Engineering Journal* no. 7:1608-1619.

Han, Jin-Hua, Hui Zhang, Ming-Ji Chen, Guo-Rui Wang, and Zhong Zhang. 2014. "CNT buckypaper/thermoplastic polyurethane composites with enhanced stiffness, strength and toughness." *Composites Science and Technology* no. 103:63-71.

Hanumanthu, Joga Rao, Gokulan Ravindiran, Ragunath Subramanian, and Praveen Saravanan. 2021. "Optimization of process conditions using RSM and ANFIS for the removal of Remazol Brilliant Orange 3R in a packed bed column." *Journal of the Indian Chemical Society* no. 98:100086.

Hasanzadeh, Reza, Peyman Najafi Moghadam, Naeimeh Bahri-Laleh, and Mika Sillanpää. 2017. "Effective removal of toxic metal ions from aqueous solutions: 2-Bifunctional magnetic nanocomposite base on novel reactive PGMA-MAn copolymer@ Fe3O4 nanoparticles." *Journal of Colloid and Interface Science* no. 490:727-746.

Haznedar, Bülent, and Adem Kalinli. 2018. "Training ANFIS structure using simulated annealing algorithm for dynamic systems identification." *Neurocomputing* no. 302:66-74.

Heravi, Majid M, and Vahideh Zadsirjan. 2020. "Prescribed drugs containing nitrogen heterocycles: an overview." *RSC Advances* no. 10:44247-44311.

Ho, Shinn-Ying, Kuang-Chyi Lee, Shih-Shin Chen, and Shinn-Jang Ho. 2002. "Accurate modeling and prediction of surface roughness by computer vision in turning operations using an adaptive neuro-fuzzy inference system." *International Journal of Machine Tools and Manufacture* no. 42:1441-1446.

Hoa, L Thi Mai. 2018. "Characterization of multi-walled carbon nanotubes functionalized by a mixture of HNO3/H2SO4." *Diamond Related Materials* no. 89:43-51.

Hof, Ferdinand, Sebastian Bosch, Siegfried Eigler, Frank Hauke, and Andreas Hirsch. 2013. "New basic insight into reductive functionalization sequences of single walled carbon nanotubes (SWCNTs)." *Journal of the American Chemical Society* no. 135:18385-18395.

Hong, Yang, Jingchao Zhang, Chongqin Zhu, Xiao Cheng Zeng, and Joseph S Francisco. 2019. "Water desalination through rim functionalized carbon nanotubes." *Journal of Materials Chemistry A* no. 7:3583-3591.

Hopkins, Zachary R, Sebastian Snowberger, and Lee Blaney. 2017. "Ozonation of the oxybenzone, octinoxate, and octocrylene UV-filters: Reaction kinetics, absorbance characteristics, and transformation products." *Journal of Hazardous Materials* no. 338:23-32.

Hossaini, Zinatossadat, Annataj Noushin, Peiman Valipour, Maryam Ghazvini, and Mohammad Hosseinnasab Rostam. 2022. "Reusable Fe3O4/ZnO/MWCNTs Magnetic Nanocomposites Promoted Synthesis of New Naphthyridines." *Polycyclic Aromatic Compounds* no. 42:2927-2946.

Hou, Peng-Xiang, Feng Zhang, Lili Zhang, Chang Liu, and Hui-Ming Cheng. 2022. "Synthesis of carbon nanotubes by floating catalyst chemical vapor deposition and their applications." *Advanced Functional Materials* no. 32:2108541.

Hou, Xianbo, Rubing Zhang, and Daining Fang. 2021. "Flexible and robust polyimide membranes with adjustable surface structure and hierarchical pore distribution for oil/water emulsion and heavy oil separation." *Journal of Membrane Science* no. 640:119769.

House, Mallard, and Peasholme Green. 2008. "Assessment of the impact on crop protection in the UK of the ‘cut-off criteria’and substitution provisions in the proposed Regulation of the European Parliament and of the Council concerning the placing of plant protection products in the market." *Pesticide Safe Direct* no. 4:35-46.

Houtman, Corine J, Jan Kroesbergen, Karin Lekkerkerker-Teunissen, and Jan Peter van der Hoek. 2014. "Human health risk assessment of the mixture of pharmaceuticals in Dutch drinking water and its sources based on frequent monitoring data." *Science of the Total Environment* no. 496:54-62.

Hua, Yani, Sha Wang, Juan Xiao, Chang Cui, and Chuan Wang. 2017. "Preparation and characterization of Fe 3 O 4/gallic acid/graphene oxide

magnetic nanocomposites as highly efficient Fenton catalysts." *RSC Advances* no. 7:28979-28986.

Huaccallo-Aguilar, Y, S Álvarez-Torrellas, M Larriba, VI Águeda, JA Delgado, G Ovejero, JA Peres, and J García. 2021. "Naproxen removal by CWPO with Fe3O4/multi-walled carbon nanotubes in a fixed-bed reactor." *Journal of Environmental Chemical Engineering* no. 9:105110.

Huaccallo-Aguilar, Ysabel, Silvia Álvarez-Torrellas, Marcos Larriba, V Ismael Águeda, José Antonio Delgado, Gabriel Ovejero, and Juan García. 2019. "Optimization parameters, kinetics, and mechanism of naproxen removal by catalytic wet peroxide oxidation with a hybrid iron-based magnetic catalyst." *Catalysts* no. 9:287.

Huaccallo, Ysabel, Silvia Álvarez-Torrellas, María Pilar Marín, María Victoria Gil, Marcos Larriba, Vicente Ismael Águeda, Gabriel Ovejero, and Juan García. 2019. "Magnetic Fe 3 O 4/multi-walled carbon nanotubes materials for a highly efficient depletion of diclofenac by catalytic wet peroxideoxidation." *Environmental Science and Pollution Research* no. 26:22372-22388.

Huang, Zhuo-nan, Xiao-ling Wang, and De-suo Yang. 2015. "Adsorption of Cr (VI) in wastewater using magnetic multi-wall carbon nanotubes." *Water Science and Engineering* no. 8:226-232.

Hussain, Athar, Sangeeta Madan, and Richa Madan. 2021. "Removal of heavy metals from wastewater by adsorption." *Heavy Metals—Their Environmental Impacts and Mitigation*.

Hussain, Shahir, Md Mottahir Alam, Mohd Imran, Nasser Zouli, Abdul Aziz, Kashif Irshad, Mohammad Haider, and Afzal Khan. 2020. "Fe3O4 nanoparticles decorated multi-walled carbon nanotubes based magnetic nanofluid for heat transfer application." *Materials Letters* no. 274:128043.

Igwegbe, Chinenye Adaobi, Stephen N Oba, Chukwunonso O Aniagor, Adewale George Adeniyi, and Joshua O Ighalo. 2021. "Adsorption of ciprofloxacin from water: a comprehensive review." *Journal of Industrial and Engineering Chemistry* no. 93:57-77.

Igwilo, Christopher Nnaemeka, Callistus Nonso Ude, and Maxwell Ikechukwu Onoh. 2022. "RSM, ANN and ANFIS applications in modelling fermentable sugar production from enzymatic hydrolysis of Colocynthis vulgaris Shrad seeds shell." *Egyptian Journal of Petroleum* no. 31:31-36.

İlyasoglu, Gülmire, Borte Kose-Mutlu, Oyku Mutlu-Salmanli, and Ismail Koyuncu. 2022. "Removal of organic micropollutans by adsorptive membrane." *Chemosphere*:134775.

Inyang, Mandu, Bin Gao, Andrew Zimmerman, Ming Zhang, and Hao Chen. 2014. "Synthesis, characterization, and dye sorption ability of carbon nanotube–biochar nanocomposites." *Chemical Engineering Journal* no. 236:39-46.

Ioniță, Mariana, Livia Elena Crică, Stefan Ioan Voicu, Sorina Dinescu, Florin Miculescu, Marieta Costache, and Horia Iovu. 2018. "Synergistic effect of carbon nanotubes and graphene for high performance cellulose acetate membranes in biomedical applications." *Carbohydrate Polymers* no. 183:50-61.

Islam, Aminul, Siow Hwa Teo, Yun Hin Taufiq-Yap, Chi Huey Ng, Dai-Viet N Vo, Mohd Lokman Ibrahim, Md Munjur Hasan, M Azizur R Khan, Alam SM Nur, and Md Rabiul Awual. 2021. "Step towards the sustainable toxic dyes removal and recycling from aqueous solution-A comprehensive review." *Resources, Conservation and Recycling* no. 175:105849.

Jafari, Ali, Amir Hossein Mahvi, Simin Nasseri, Alimorad Rashidi, Ramin Nabizadeh, and Reza Rezaee. 2015. "Ultrafiltration of natural organic matter from water by vertically aligned carbon nanotube membrane." *Journal of Environmental Health Science and Engineering* no. 13:1-9.

Jha, Avinash Kumar, and Nandan Sit. 2021. "Comparison of response surface methodology (RSM) and artificial neural network (ANN) modelling for supercritical fluid extraction of phytochemicals from Terminalia chebula pulp and optimization using RSM coupled with desirability function (DF) and genetic algorithm (GA) and ANN with GA." *Industrial Crops and Products* no. 170:113769.

Ji, Chao, Jingwei Hou, and Vicki Chen. 2016. "Cross-linked carbon nanotubes-based biocatalytic membranes for micro-pollutants degradation: performance, stability, and regeneration." *Journal of Membrane Science* no. 520:869-880.

Ji, Liangliang, Wei Chen, Shourong Zheng, Zhaoyi Xu, and Dongqiang Zhu. 2009. "Adsorption of sulfonamide antibiotics to multiwalled carbon nanotubes." *Langmuir* no. 25:11608-11613.

Ji, Liangliang, Fengling Liu, Zhaoyi Xu, Shourong Zheng, and Dongqiang Zhu. 2010. "Adsorption of pharmaceutical antibiotics on template-synthesized ordered micro-and mesoporous carbons." *Environmental Science & Technology* no. 44:3116-3122.

Jiang, Chenhui, Aiying Wang, Xufan Bao, Tongyuan Ni, and Jin Ling. 2020. "A review on geopolymer in potential coating application: Materials, preparation and basic properties." *Journal of Building Engineering* no. 32:101734.

Jiang, Chenxiao, Hanlin Chen, Yilue Zhang, Hongyan Feng, Muhammad Aamir Shehzad, Yaoming Wang, and Tongwen Xu. 2018. "Complexation Electrodialysis as a general method to simultaneously treat wastewaters with metal and organic matter." *Chemical Engineering Journal* no. 348:952-959.

Jiang, Qinting, Xuanhong Zhou, Ruili Wang, Weiping Ding, Yi Chu, Sizhe Tang, Xiaoyun Jia, and Xiaolong Xu. 2022. "Intelligent monitoring for infectious diseases with fuzzy systems and edge computing: A survey." *Applied Soft Computing*:108835.

Jiang, Wen-Li, Muhammad Rizwan Haider, Jing-Long Han, Yang-Cheng Ding, Xi-Qi Li, Hong-Cheng Wang, Hafiz Muhammad Adeel Sharif, Ai-Jie Wang, and Nan-Qi Ren. 2021. "Carbon nanotubes intercalated RGO electro-Fenton membrane for coenhanced permeability, rejection and catalytic oxidation of organic micropollutants." *Journal of Membrane Science* no. 623:119069.

Joseph, Lesley, Linkel K Boateng, Joseph RV Flora, Yong-Gyun Park, Ahjeong Son, Mohammed Badawy, and Yeomin Yoon. 2013. "Removal of bisphenol A and 17α-ethinyl estradiol by combined coagulation and adsorption using carbon nanomaterials and powdered activated carbon." *Separation and Purification Technology* no. 107:37-47.

Jovanovic, Oriana, Carlos F Amábile-Cuevas, Chii Shang, Chao Wang, and King Wah Ngai. 2021. "What water professionals should know about antibiotics and antibiotic resistance: an overview." *ACS Enivornmental Science & Technology Water* no. 1:1334-1351.

Julian, Helen, Novesa Nurgirisia, Guanglei Qiu, Yen-Peng Ting, and I Gede Wenten. 2022. "Membrane distillation for wastewater treatment: Current

trends, challenges and prospects of dense membrane distillation." *Journal of Water Process Engineering* no. 46:102615.

Jun, Lau Yien, Rama Rao Karri, Lau Sie Yon, NM Mubarak, Chua Han Bing, Khalid Mohammad, Priyanka Jagadish, and EC Abdullah. 2020. "Modeling and optimization by particle swarm embedded neural network for adsorption of methylene blue by jicama peroxidase immobilized on buckypaper/polyvinyl alcohol membrane." *Environmental Research* no. 183:109158.

Jun, Lau Yien, Lau Sie Yon, NM Mubarak, Chua Han Bing, Sharadwata Pan, Michael K Danquah, EC Abdullah, and Mohammad Khalid. 2019. "An overview of immobilized enzyme technologies for dye and phenolic removal from wastewater." *Journal of Environmental Chemical Engineering* no. 7:102961.

Kaiser, Jean-Pierre, Peter Wick, Pius Manser, Philipp Spohn, and Arie Bruinink. 2008. "Single walled carbon nanotubes (SWCNT) affect cell physiology and cell architecture." *Journal of Materials Science: Materials in Medicine* no. 19:1523-1527.

Kamali, Mohammadreza, DP Suhas, Maria Elisabete Costa, Isabel Capela, and Tejraj M Aminabhavi. 2019. "Sustainability considerations in membrane-based technologies for industrial effluents treatment." *Chemical Engineering Journal* no. 368:474-494.

Kaminska, G, J Bohdziewicz, JI Calvo, P Prádanos, L Palacio, and A Hernández. 2015. "Fabrication and characterization of polyethersulfone nanocomposite membranes for the removal of endocrine disrupting micropollutants from wastewater. Mechanisms and performance." *Journal of Membrane Science* no. 493:66-79.

Kampouropoulos, Konstantinos, Fabio Andrade Rengifo, Antonio García Espinosa, and José Luis Romeral Martínez. 2014. "A combined methodology of adaptive neuro-fuzzy inference system and genetic algorithm for short-term energy forecasting." *Advances in Electrical and Computer Engineering* no. 14:9-14.

Kang, Jian, Huayang Zhang, Xiaoguang Duan, Hongqi Sun, Xiaoyao Tan, Shaomin Liu, and Shaobin Wang. 2019. "Magnetic Ni-Co alloy encapsulated N-doped carbon nanotubes for catalytic membrane degradation of emerging contaminants." *Chemical Engineering Journal* no. 362:251-261.

Karaboga, Dervis, and Ebubekir Kaya. 2019. "Adaptive network based fuzzy inference system (ANFIS) training approaches: a comprehensive survey." *Artificial Intelligence Review* no. 52:2263-2293.

Karimi, Hayde, Ahmad Rahimpour, and Mohammad Reza Shirzad Kebria. 2016. "Pesticides removal from water using modified piperazine-based nanofiltration (NF) membranes." *Desalination and Water Treatment* no. 57:24844-24854.

Karkeh-Abadi, Fatemeh, Samaneh Saber-Samandari, and Saeed Saber-Samandari. 2016. "The impact of functionalized CNT in the network of sodium alginate-based nanocomposite beads on the removal of Co (II) ions from aqueous solutions." *Journal of Hazardous Materials* no. 312:224-233.

Karn, Barbara, Todd Kuiken, and Martha Otto. 2009. "Nanotechnology and in situ remediation: a review of the benefits and potential risks." *Environmental Health Perspectives* no. 117:1813-1831.

Karri, Rama Rao, Marjan Tanzifi, Mohammad Tavakkoli Yaraki, and JN Sahu. 2018. "Optimization and modeling of methyl orange adsorption onto polyaniline nano-adsorbent through response surface methodology and differential evolution embedded neural network." *Journal of Environmental Management* no. 223:517-529.

Kashefi, Saeed, Seyed Mehdi Borghei, and Niyaz Mohammad Mahmoodi. 2019. "Superparamagnetic enzyme-graphene oxide magnetic nanocomposite as an environmentally friendly biocatalyst: Synthesis and biodegradation of dye using response surface methodology." *Microchemical Journal* no. 145:547-558.

Katsube, Yoshihiro, Takahiro Fukuda, and Toru Maekawa. 2013. "Synthesis of magnetic carbon nanotubes: Functionalisation of carbon nanotubes with nickel/sulphur nanoparticles via self-assembly in near-critical acetone." *The Journal of Supercritical Fluids* no. 83:1-5.

Kaveh, Mohammad, Vali Rasooli Sharabiani, Reza Amiri Chayjan, Ebrahim Taghinezhad, Yousef Abbaspour-Gilandeh, and Iman Golpour. 2018. "ANFIS and ANNs model for prediction of moisture diffusivity and specific energy consumption potato, garlic and cantaloupe drying under convective hot air dryer." *Information Processing in Agriculture* no. 5:372-387.

Kean, Walter F, and W Watson Buchanan. 2005. "The use of NSAIDs in rheumatic disorders 2005: a global perspective." *Inflammopharmacology* no. 13:343-370.

Khafri, Hossein Zare, Mehrorang Ghaedi, Arash Asfaram, and Mohammad Safarpoor. 2017. "Synthesis and characterization of ZnS: Ni-NPs loaded on AC derived from apple tree wood and their applicability for the ultrasound assisted comparative adsorption of cationic dyes based on the experimental design." *Ultrasonics Sonochemistry* no. 38:371-380.

Khalid, Arsalan, Abdulhadi A Al-Juhani, Othman Charles Al-Hamouz, Tahar Laoui, Zafarullah Khan, and Mautaz Ali Atieh. 2015. "Preparation and properties of nanocomposite polysulfone/multi-walled carbon nanotubes membranes for desalination." *Desalination* no. 367:134-144.

Khan, Fahad Saleem Ahmed, Nabisab Mujawar Mubarak, Mohammad Khalid, Yie Hua Tan, Ezzat Chan Abdullah, Muhammad Ekhlasur Rahman, and Rama Rao Karri. 2021. "A comprehensive review on micropollutants removal using carbon nanotubes-based adsorbents and membranes." *Journal of Environmental Chemical Engineering* no. 9:106647.

Khan, Fahad Saleem Ahmed, Nabisab Mujawar Mubarak, Yie Hua Tan, Rama Rao Karri, Mohammad Khalid, Rashmi Walvekar, Ezzat Chan Abdullah, Shaukat Ali Mazari, and Sabzoi Nizamuddin. 2020. "Magnetic nanoparticles incorporation into different substrates for dyes and heavy metals removal—a review." *Environmental Science and Pollution Research* no. 27:43526-43541.

Kharissova, Oxana V, Boris I Kharisov, and Edgar Gerardo de Casas Ortiz. 2013. "Dispersion of carbon nanotubes in water and non-aqueous solvents." *RSC Advances* no. 3:24812-24852.

Khashei, Mehdi, Ali Zeinal Hamadani, and Mehdi Bijari. 2012. "A fuzzy intelligent approach to the classification problem in gene expression data analysis." *Knowledge-Based Systems* no. 27:465-474.

Khawar, Ayyub, Zaheer Aslam, Abdul Zahir, Imran Akbar, and Aamir Abbas. 2019. "Synthesis of Femur extracted hydroxyapatite reinforced nanocomposite and its application for Pb (II) ions abatement from aqueous phase." *International journal of biological macromolecules* no. 122:667-676.

Khomeyrani, Seyedeh Fatemeh Noorani, Mohammad Hossein Ahmadi Azqhandi, and Bahram Ghalami-Choobar. 2021. "Rapid and efficient

ultrasonic assisted adsorption of PNP onto LDH-GO-CNTs: ANFIS, GRNN and RSM modeling, optimization, isotherm, kinetic, and thermodynamic study." *Journal of Molecular Liquids* no. 333:115917.

Kim, Hyunook, Yu Sik Hwang, and Virender K Sharma. 2014. "Adsorption of antibiotics and iopromide onto single-walled and multi-walled carbon nanotubes." *Chemical Engineering Journal* no. 255:23-27.

Kim, Jinsoo, Benjamin K Sovacool, Morgan Bazilian, Steve Griffiths, Junghwan Lee, Minyoung Yang, and Jordy Lee. 2022. "Decarbonizing the iron and steel industry: A systematic review of sociotechnical systems, technological innovations, and policy options." *Energy Research & Social Science* no. 89:102565.

Kim, Joon-Woo, Hyo-Sang Jang, Jong-Gu Kim, Hiroshi Ishibashi, Masashi Hirano, Kazuaki Nasu, Nobuhiro Ichikawa, Yuji Takao, Ryota Shinohara, and Koji Arizono. 2009. "Occurrence of pharmaceutical and personal care products (PPCPs) in surface water from Mankyung River, South Korea." *Journal of Health Science* no. 55:249-258.

Kim, Ju-Sang, Ramasamy Harikrishnan, Man-Chul Kim, Chellam Balasundaram, and Moon-Soo Heo. 2012. "Broussonetia kazinoki as a feed additive enhances disease resistance against Streptococcus parauberis in Paralichthys olivaceus." *Fish Pathology* no. 47:20-22.

Kim, Moon-Kyung, and Kyung-Duk Zoh. 2016. "Occurrence and removals of micropollutants in water environment." *Environmental Engineering Research* no. 21:319-332.

King, Dawn N, Maura J Donohue, Stephen J Vesper, Eric N Villegas, Michael W Ware, Megan E Vogel, Edward F Furlong, Dana W Kolpin, Susan T Glassmeyer, and Stacy Pfaller. 2016. "Microbial pathogens in source and treated waters from drinking water treatment plants in the United States and implications for human health." *Science of the Total Environment* no. 562:987-995.

Kleywegt, Sonya, Vince Pileggi, Paul Yang, Chunyan Hao, Xiaoming Zhao, Carline Rocks, Serei Thach, Patrick Cheung, and Brian Whitehead. 2011. "Pharmaceuticals, hormones and bisphenol A in untreated source and finished drinking water in Ontario, Canada—occurrence and treatment efficiency." *Science of the Total Environment* no. 409:1481-1488.

Kobyliukh, Anastasiia, Karolina Olszowska, Urszula Szeluga, and Sławomira Pusz. 2020. "Iron oxides/graphene hybrid structures–Preparation, modification, and application as fillers of polymer composites." *Advances in Colloid and Interface Science* no. 285:102285.

Komatsu, Kazuhiro, Takashi Onodera, Ayato Kohzu, Kazuaki Syutsubo, and Akio Imai. 2020. "Characterization of dissolved organic matter in wastewater during aerobic, anaerobic, and anoxic treatment processes by molecular size and fluorescence analyses." *Water Research* no. 171:115459.

Kong, Lingxiao, Kiwao Kadokami, Shaopo Wang, Hanh Thi Duong, and Hong Thi Cam Chau. 2015. "Monitoring of 1300 organic micro-pollutants in surface waters from Tianjin, North China." *Chemosphere* no. 122:125-130.

Kosek, Klaudia, Aneta Luczkiewicz, Sylwia Fudala-Książek, Katarzyna Jankowska, Małgorzata Szopińska, Ola Svahn, Jens Tränckner, Alena Kaiser, Valdas Langas, and Erland Björklund. 2020. "Implementation of advanced micropollutants removal technologies in wastewater treatment plants (WWTPs)-Examples and challenges based on selected EU countries." *Environmental Science & Policy* no. 112:213-226.

Krishna, Venkatramana D, Kai Wu, Diqing Su, Maxim CJ Cheeran, Jian-Ping Wang, and Andres Perez. 2018. "Nanotechnology: Review of concepts and potential application of sensing platforms in food safety." *Food Microbiology* no. 75:47-54.

Kumar, A Kiran, and S Venkata Mohan. 2012. "Removal of natural and synthetic endocrine disrupting estrogens by multi-walled carbon nanotubes (MWCNT) as adsorbent: kinetic and mechanistic evaluation." *Separation and Purification Technology* no. 87:22-30.

Kumar, Amit, Anu Kumari, Gaurav Sharma, Mu Naushad, Tansir Ahamad, and Florian J Stadler. 2018. "Utilizing recycled LiFePO4 from batteries in combination with B@ C3N4 and CuFe2O4 as sustainable nano-junctions for high performance degradation of atenolol." *Chemosphere* no. 209:457-469.

Kumar, GJ Pavan, and R Lalitha Narayana. 2015. "Prediction of surface roughness in turning process using soft computing techniques." *International Journal of Mechanical Engineering and Robotics Research* no. 4:561.

Kumar, Goutam, Nusrat Tazeen Tonu, Palash Kumar Dhar, and Md Mahiuddin. 2021. "Removal of Fe3+ Ions from Wastewater by Activated Borassus flabellifer Male Flower Charcoal." *Pollution* no. 7:693-707.

Kumar, Shravan, Chandi Patra, Selvaraju Narayanasamy, and Prasanna Venkatesh Rajaraman. 2020. "Performance of acid-activated water caltrop (Trapa natans) shell in fixed bed column for hexavalent chromium removal from simulated wastewater." *Environmental Science and Pollution Research* no. 27:28042-28052.

Kwon, Yeon Ju, Youn Kim, Hyerin Jeon, Sehyeon Cho, Wonoh Lee, and Jea Uk Lee. 2017. "Graphene/carbon nanotube hybrid as a multi-functional interfacial reinforcement for carbon fiber-reinforced composites." *Composites Part B: Engineering* no. 122:23-30.

Lalwani, Jitesh, Ashutosh Gupta, Shashidhar Thatikonda, and Challapalli Subrahmanyam. 2020. "An industrial insight on treatment strategies of the pharmaceutical industry effluent with varying qualitative characteristics." *Journal of Environmental Chemical Engineering* no. 8:104190.

Lapworth, DJ, Nicole Baran, ME Stuart, and RS Ward. 2012. "Emerging organic contaminants in groundwater: a review of sources, fate and occurrence." *Environmental Pollution* no. 163:287-303.

Lara-Martín, Pablo A, Eduardo González-Mazo, Mira Petrovic, Damià Barceló, and Bruce J Brownawell. 2014. "Occurrence, distribution and partitioning of nonionic surfactants and pharmaceuticals in the urbanized Long Island Sound Estuary (NY)." *Marine Pollution Bulletin* no. 85:710-719.

Lau, Yien Jun, Rama Rao Karri, Nabisab Mujawar Mubarak, Sie Yon Lau, Han Bing Chua, Mohammad Khalid, Priyanka Jagadish, and Ezzat Chan Abdullah. 2020. "Removal of dye using peroxidase-immobilized Buckypaper/polyvinyl alcohol membrane in a multi-stage filtration column via RSM and ANFIS." *Environmental Science and Pollution Research* no. 27:40121-40134.

Le, Ngoc Lieu, and Suzana P Nunes. 2016. "Materials and membrane technologies for water and energy sustainability." *Sustainable Materials and Technologies* no. 7:1-28.

Lee, Bo-Yeon, Jiyoon Kim, Hyungjin Kim, Chiwoo Kim, and Sin-Doo Lee. 2016. "Low-cost flexible pressure sensor based on dielectric elastomer film with micro-pores." *Sensors and Actuators A: Physical* no. 240:103-109.

Lee, Chee Huei, Bishnu Tiwari, Dongyan Zhang, and Yoke Khin Yap. 2017. "Water purification: oil–water separation by nanotechnology and environmental concerns." *Environmental Science: Nano* no. 4:514-525.

Lee, Kian Mun, Christelle Pau Ping Wong, Tong Ling Tan, and Chin Wei Lai. 2018. "Functionalized carbon nanotubes for adsorptive removal of water pollutants." *Materials Science and Engineering: B* no. 236:61-69.

Leston, Sara, Margarida Nunes, Ivan Viegas, Fernando Ramos, and Miguel Ângelo Pardal. 2013. "The effects of chloramphenicol on Ulva lactuca." *Chemosphere* no. 91:552-557.

Li, Richard, Noa Lachman, Peter Florin, H Daniel Wagner, and Brian L Wardle. 2015. "Hierarchical carbon nanotube carbon fiber unidirectional composites with preserved tensile and interfacial properties." *Composites Science and Technology* no. 117:139-145.

Li, Sai, Tong Yue, Wei Sun, Chenyang Zhang, Jianyong He, Mingjun Han, Hongliang Zhang, Heng Yu, and Wenyuan Li. 2022. "Intense removal of Ni (II) chelated by EDTA from wastewater via Fe3+ replacement–chelating precipitation." *Process Safety and Environmental Protection* no. 159:1082-1091.

Liang, Jie, Junfeng Liu, Xingzhong Yuan, Haoran Dong, Guangming Zeng, Haipeng Wu, Hou Wang, Jiayu Liu, Shanshan Hua, and Shuqu Zhang. 2015. "Facile synthesis of alumina-decorated multi-walled carbon nanotubes for simultaneous adsorption of cadmium ion and trichloroethylene." *Chemical Engineering Journal* no. 273:101-110.

Liew, KM, MF Kai, and LW Zhang. 2016. "Carbon nanotube reinforced cementitious composites: An overview." *Composites Part A: Applied Science and Manufacturing* no. 91:301-323.

Lim, Fang Yee, Say Leong Ong, and Jiangyong Hu. 2017. "Recent advances in the use of chemical markers for tracing wastewater contamination in aquatic environment: a review." *Water* no. 9:143.

Lin, Angela Yu-Chen, Yu-Ting Tsai, Tsung-Hsien Yu, Xiao-Huan Wang, and Cheng-Fang Lin. 2011. "Occurrence and fate of pharmaceuticals and personal care products in Taiwan's aquatic environment." *Desalination and Water Treatment* no. 32:57-64.

Liu, Bo, Xiaoyi Li, Baolei Li, Bingqian Xu, and Yuliang Zhao. 2009. "Carbon nanotube based artificial water channel protein: membrane perturbation and water transportation." *Nano Letters* no. 9:1386-1394.

Liu, Fuyao, Qianqian Wang, Gongxun Zhai, Hengxue Xiang, Jialiang Zhou, Chao Jia, Liping Zhu, Qilin Wu, and Meifang Zhu. 2022. "Continuously processing waste lignin into high-value carbon nanotube fibers." *Nature Communications* no. 13:5755.

Liu, Jianming, Chao Wang, and Zhenhu Xiong. 2015. "Adsorption behavior of magnetic multiwalled carbon nanotubes for the simultaneous adsorption of furazolidone and Cu (II) from aqueous solutions." *Environmental Engineering Science* no. 32:960-969.

Liu, Xiao, Joshua Caleb Steele, and Xiang-Zhou Meng. 2017. "Usage, residue, and human health risk of antibiotics in Chinese aquaculture: a review." *Environmental Pollution* no. 223:161-169.

Liu, Yanzhu, Linru Guo, Hongye Huang, Jibo Dou, Qiang Huang, Defu Gan, Junyu Chen, Yongxiu Li, Xiaoyong Zhang, and Yen Wei. 2019. "Facile preparation of magnetic composites based on carbon nanotubes: Utilization for removal of environmental pollutants." *Journal of Colloid and Interface Science* no. 545:8-15.

Loos, Robert, Raquel Carvalho, Diana C António, Sara Comero, Giovanni Locoro, Simona Tavazzi, Bruno Paracchini, Michela Ghiani, Teresa Lettieri, and Ludek Blaha. 2013. "EU-wide monitoring survey on emerging polar organic contaminants in wastewater treatment plant effluents." *Water Research* no. 47:6475-6487.

Loos, Robert, Bernd Manfred Gawlik, Giovanni Locoro, Erika Rimaviciute, Serafino Contini, and Giovanni Bidoglio. 2009. "EU-wide survey of polar organic persistent pollutants in European river waters." *Environmental Pollution* no. 157:561-568.

López-Serna, Rebeca, Anna Jurado, Enric Vázquez-Suñé, Jesus Carrera, Mira Petrović, and Damià Barceló. 2013. "Occurrence of 95 pharmaceuticals and transformation products in urban groundwaters underlying the metropolis of Barcelona, Spain." *Environmental Pollution* no. 174:305-315.

Lozovik, PA, AK Morozov, MB Zobkov, TA Dukhovicheva, and LA Osipova. 2007. "Allochthonous and autochthonous organic matter in surface waters in Karelia." *Water Resources* no. 34:204-216.

Lu, Feng, and Didier Astruc. 2020. "Nanocatalysts and other nanomaterials for water remediation from organic pollutants." *Coordination Chemistry Reviews* no. 408:213180.

Lu, Qingchen, Nana Li, and Xiaoming Zhang. 2022. "Supramolecular recognition PVDF/PVA ultrafiltration membrane for rapid removing aromatic compounds from water." *Chemical Engineering Journal* no. 436:132889.

Luo, Shu, Yufeng Luo, Hengcai Wu, Mengya Li, Lingjia Yan, Kaili Jiang, Liang Liu, Qunqing Li, Shoushan Fan, and Jiaping Wang. 2017. "Self-assembly of 3D Carbon Nanotube Sponges: A Simple and Controllable Way to Build Macroscopic and Ultralight Porous Architectures." *Advanced Materials* no. 29:1603549.

Luo, Yunlong, Wenshan Guo, Huu Hao Ngo, Long Duc Nghiem, Faisal Ibney Hai, Jian Zhang, Shuang Liang, and Xiaochang C Wang. 2014. "A review on the occurrence of micropollutants in the aquatic environment and their fate and removal during wastewater treatment." *Science of the Total Environment* no. 473:619-641.

Ma, Hongyang, Christian Burger, Benjamin S Hsiao, and Benjamin Chu. 2012. "Nanofibrous microfiltration membrane based on cellulose nanowhiskers." *Biomacromolecules* no. 13:180-186.

Ma, Jiping, Lianhua Jiang, Gege Wu, Yan Xia, Wenhui Lu, Jinhua Li, and Lingxin Chen. 2016. "Determination of six sulfonylurea herbicides in environmental water samples by magnetic solid-phase extraction using multi-walled carbon nanotubes as adsorbents coupled with high-performance liquid chromatography." *Journal of Chromatography A* no. 1466:12-20.

Machado, Fernando M, Sophia A Carmalin, Eder C Lima, Silvio LP Dias, Lizie DT Prola, Caroline Saucier, Iuri M Jauris, Ivana Zanella, and Solange B Fagan. 2016. "Adsorption of alizarin red S dye by carbon nanotubes: an experimental and theoretical investigation." *The Journal of Physical Chemistry C* no. 120:18296-18306.

Madala, Suguna, Siva Kumar Nadavala, Sreenivasulu Vudagandla, Veera M Boddu, and Krishnaiah Abburi. 2017. "Equilibrium, kinetics and

thermodynamics of Cadmium (II) biosorption on to composite chitosan biosorbent." *Arabian Journal of Chemistry* no. 10:S1883-S1893.

Madhura, Lavanya, Shalini Singh, Suvardhan Kanchi, Myalowenkosi Sabela, and Krishna Bisetty. 2019. "Nanotechnology-based water quality management for wastewater treatment." *Environmental Chemistry Letters* no. 17:65-121.

Magalhães, Francisco Ernani Alves, Caio Átila Prata Bezerra de Sousa, Sacha Aubrey Alves Rodrigues Santos, Renata Barbosa Menezes, Francisco Lucas Alves Batista, Angela Oliveira Abreu, Messias Vital de Oliveira, Luiz Francisco Wemmenson Gonçalves Moura, Ramon da Silva Raposo, and Adriana Rolim Campos. 2017. "Adult zebrafish (Danio rerio): an alternative behavioral model of formalin-induced nociception." *Zebrafish* no. 14:422-429.

Mahdavi, Mahnaz, Mansor Bin Ahmad, Md Jelas Haron, Farideh Namvar, Behzad Nadi, Mohamad Zaki Ab Rahman, and Jamileh Amin. 2013. "Synthesis, surface modification and characterisation of biocompatible magnetic iron oxide nanoparticles for biomedical applications." *Molecules* no. 18:7533-7548.

Mahdiani, Maryam, Azam Sobhani, and Masoud Salavati-Niasari. 2017. "Enhancement of magnetic, electrochemical and photocatalytic properties of lead hexaferrites with coating graphene and CNT: Sol-gel auto-combustion synthesis by valine." *Separation and Purification Technology* no. 185:140-148.

Mailler, R, J Gasperi, Y Coquet, C Derome, A Buleté, E Vulliet, Adèle Bressy, G Varrault, G Chebbo, and V Rocher. 2016. "Removal of emerging micropollutants from wastewater by activated carbon adsorption: Experimental study of different activated carbons and factors influencing the adsorption of micropollutants in wastewater." *Journal of Environmental Chemical Engineering* no. 4:1102-1109.

Maksymowicz, Marcela, Piotr Artur Machowiec, Gabriela Ręka, Anna Korzeniowska, Patryk Leszczyk, and Halina Piecewicz Szczęsna. 2021. "Mechanism of action of triclosan as an endocrine-disrupting chemical with its impact on human health–literature review." *Journal of Pre-Clinical and Clinical Research* no. 15:169-175.

Malik, DS, CK Jain, and Anuj K Yadav. 2017. "Removal of heavy metals from emerging cellulosic low-cost adsorbents: a review." *Applied Water Science* no. 7:2113-2136.

Malikov, Elvin Y, Mustafa B Muradov, Oktay H Akperov, Goncha M Eyvazova, Róbert Puskás, Dániel Madarász, L Nagy, Ákos Kukovecz, and Zoltán Kónya. 2014. "Synthesis and characterization of polyvinyl alcohol based multiwalled carbon nanotube nanocomposites." *Physica E: Low-dimensional Systems and Nanostructures* no. 61:129-134.

Mallakpour, Shadpour, and Elham Khadem. 2016. "Carbon nanotube–metal oxide nanocomposites: Fabrication, properties and applications." *Chemical Engineering Journal* no. 302:344-367.

Mamani, JB, Antônio José da Costa-Filho, Daniel Reinaldo Cornejo, ED Vieira, and Lionel Fernel Gamarra. 2013. "Synthesis and characterization of magnetite nanoparticles coated with lauric acid." *Materials Characterization* no. 81:28-36.

Manickum, T, and W John. 2014. "Occurrence, fate and environmental risk assessment of endocrine disrupting compounds at the wastewater treatment works in Pietermaritzburg (South Africa)." *Science of the Total Environment* no. 468:584-597.

Marani, Mohsen, Mohammadjavad Zeinali, Jules Kouam, Victor Songmene, and Chris K Mechefske. 2020. "Prediction of cutting tool wear during a turning process using artificial intelligence techniques." *The International Journal of Advanced Manufacturing Technology* no. 111:505-515.

Margot, Jonas, Luca Rossi, David A Barry, and Christof Holliger. 2015. "A review of the fate of micropollutants in wastewater treatment plants." *Wiley Interdisciplinary Reviews: Water* no. 2:457-487.

Maryam, Bareera, Valentina Buscio, Sevde Ustun Odabasi, and Hanife Buyukgungor. 2020. "A study on behavior, interaction and rejection of Paracetamol, Diclofenac and Ibuprofen (PhACs) from wastewater by nanofiltration membranes." *Environmental Technology & Innovation* no. 18:100641.

Marzi, Hosein, Ahmed Haj Darwish, and Humam Helfawi. 2017. "Training ANFIS using the enhanced Bees Algorithm and least squares estimation." *Intelligent Automation & Soft Computing* no. 23:227-234.

Masjoudi, Mahsa, Mitra Golgoli, Zahra Ghobadi Nejad, Sadegh Sadeghzadeh, and Seyed Mehdi Borghei. 2021. "Pharmaceuticals removal by immobilized

laccase on polyvinylidene fluoride nanocomposite with multi-walled carbon nanotubes." *Chemosphere* no. 263:128043.

Masri, Selma, Zheng Liu, Sheryl Phung, Emily Wang, Yate-Ching Yuan, and Shiuan Chen. 2010. "The role of microRNA-128a in regulating TGFbeta signaling in letrozole-resistant breast cancer cells." *Breast Cancer Research and Treatment* no. 124:89-99.

Matyjaszczyk, Ewa. 2018. "Plant protection means used in organic farming throughout the European Union." *Pest Management Science* no. 74:505-510.

Mehinto, Alvine C, Elizabeth M Hill, and Charles R Tyler. 2010. "Uptake and biological effects of environmentally relevant concentrations of the nonsteroidal anti-inflammatory pharmaceutical diclofenac in rainbow trout (Oncorhynchus mykiss)." *Environmental Science & Technology* no. 44:2176-2182.

Meng, Cheng, Wang Zhikun, Lv Qiang, Li Chunling, Sun Shuangqing, and Hu Songqing. 2018. "Preparation of amino-functionalized Fe3O4@ mSiO2 core-shell magnetic nanoparticles and their application for aqueous Fe3+ removal." *Journal of Hazardous Materials* no. 341:198-206.

Meng, Lingjie, Chuanlong Fu, and Qinghua Lu. 2009. "Advanced technology for functionalization of carbon nanotubes." *Progress in Natural Science* no. 19:801-810.

Merabet, Hichem, Tahar Bahi, D Drici, N Halam, and Khouloud Bedoud. 2017. "Diagnosis of rotor fault using neuro-fuzzy inference system." *Journal Of Fundamental And Applied Sciences* no. 9:170-182.

Metz, Florence, and Karin Ingold. 2014. "Sustainable wastewater management: is it possible to regulate micropollution in the future by learning from the past? A policy analysis." *Sustainability* no. 6:1992-2012.

Mirbolouki, Amin, Salim Heddam, Kulwinder Singh Parmar, Slavisa Trajkovic, Mojtaba Mehraein, and Ozgur Kisi. 2022. "Comparison of the advanced machine learning methods for better prediction accuracy of solar radiation using only temperature data: A case study." *International Journal of Energy Research* no. 46:2709-2736.

Mishra, Geetika. 2022. "Co-effect of carbon nanotube and nano-sized silica on dispersion and mechanical performance in cementitious system." *Diamond and Related Materials* no. 127:109162.

Mitchelmore, Carys L, Emily E Burns, Annaleise Conway, Andrew Heyes, and Iain A Davies. 2021. "A critical review of organic ultraviolet filter exposure, hazard, and risk to corals." *Environmental Toxicology and Chemistry* no. 40:967-988.

Mittal, Alok, Jyoti Mittal, Arti Malviya, Dipika Kaur, and VK Gupta. 2010. "Decoloration treatment of a hazardous triarylmethane dye, Light Green SF (Yellowish) by waste material adsorbents." *Journal of Colloid and Interface Science* no. 342:518-527.

Mittan, Dhirender Singh, Pradeep Kumar, SP Venkatesh Prasad, Lalit Kumar, and Sudhir Kumar. 2008. "Development and validation of new spectroscopic method for the estimation of furazolidone in bulk and solid dosage form." *Oriental Journal of Chemistry* no. 24:1009.

Moazzen, Mojtaba, Amin Mousavi Khaneghah, Nabi Shariatifar, Mahsa Ahmadloo, Ismail Eş, Abbas Norouzian Baghani, Saeed Yousefinejad, Mahmood Alimohammadi, Ali Azari, and Sina Dobaradaran. 2019. "Multi-walled carbon nanotubes modified with iron oxide and silver nanoparticles (MWCNT-Fe3O4/Ag) as a novel adsorbent for determining PAEs in carbonated soft drinks using magnetic SPE-GC/MS method." *Arabian Journal of Chemistry* no. 12:476-488.

Mohammad, Abdul Wahab, YH Teow, WL Ang, YT Chung, DL Oatley-Radcliffe, and Nidal Hilal. 2015. "Nanofiltration membranes review: Recent advances and future prospects." *Desalination* no. 356:226-254.

Mohammadi, Asadollah, and Payam Veisi. 2018. "High adsorption performance of β-cyclodextrin-functionalized multi-walled carbon nanotubes for the removal of organic dyes from water and industrial wastewater." *Journal of Environmental Chemical Engineering* no. 6:4634-4643.

Mohammed, Faris H, Aseel M Aljeboree, Nour Abd Alrazzak, Ayad F Alkaim, Yasir Salam Karim, Sarah A Hamood, Ahmed B Mahdi, Mohammed Abed Jawad, and Salam Ahjel. 2022. "An update on half-decade recent advances in functionalized Fe3O4 nanoparticles as heterogeneous nanocatalysts for the synthesis of six-membered compounds containing nitrogen: A mini-review." *Iranian Journal of Catalysis* no. 12:237-259.

Mohan, Amrita, Amit Kumar Singh, Basant Kumar, and Ramji Dwivedi. 2021. "Review on remote sensing methods for landslide detection using machine and

deep learning." *Transactions on Emerging Telecommunications Technologies* no. 32:e3998.

Mohmood, Iram, Cláudia Batista Lopes, Isabel Lopes, Iqbal Ahmad, Armando C Duarte, and Eduarda Pereira. 2013. "Nanoscale materials and their use in water contaminants removal—a review." *Environmental Science and Pollution Research* no. 20:1239-1260.

Momenzadeh, H, Ali Reza Tehrani-Bagha, A Khosravi, K Gharanjig, and Krister Holmberg. 2011. "Reactive dye removal from wastewater using a chitosan nanodispersion." *Desalination* no. 271:225-230.

Monteiro, Pedro Ribeiro Rocha, Maria Armanda Reis-Henriques, and Joao Coimbra. 2000. "Polycyclic aromatic hydrocarbons inhibit in vitro ovarian steroidogenesis in the flounder (Platichthys flesus L.)." *Aquatic Toxicology* no. 48:549-559.

Moradi, O, M Yari, P Moaveni, and M Norouzi. 2012. "Removal of p-nitrophenol and naphthalene from petrochemical wastewater using SWCNTs and SWCNT-COOH surfaces." *Fullerenes, Nanotubes and Carbon Nanostructures* no. 20:85-98.

Morel, Mauricio, Francisco Martínez, and Edgar Mosquera. 2013. "Synthesis and characterization of magnetite nanoparticles from mineral magnetite." *Journal of Magnetism and Magnetic Materials* no. 343:76-81.

Morsy, Mohamed, Magdy Helal, Mohamed El-Okr, and Medhat Ibrahim. 2014. "Preparation, purification and characterization of high purity multi-wall carbon nanotube." *Spectrochimica Acta Part A: Molecular and Biomolecular Spectroscopy* no. 132:594-598.

Mossavi, E, M Hosseini Sabzevari, M Ghaedi, MH Ahmadi Azqhandi, and SJ Hosseini. 2019. "A rapid and efficient sono-chemistry process for removal of pollutant: Statistical modeling study." *Polyhedron* no. 171:65-76.

Mousazadeh, Milad, Zohreh Naghdali, Zakaria Al-Qodah, SM Alizadeh, Elnaz Karamati Niaragh, Sima Malekmohammadi, PV Nidheesh, Edward PL Roberts, Mika Sillanpää, and Mohammad Mahdi Emamjomeh. 2021. "A systematic diagnosis of state of the art in the use of electrocoagulation as a sustainable technology for pollutant treatment: An updated review." *Sustainable Energy Technologies and Assessments* no. 47:101353.

Moussout, Hamou, Hammou Ahlafi, Mustapha Aazza, and Hamid Maghat. 2018. "Critical of linear and nonlinear equations of pseudo-first order and pseudo-second order kinetic models." *Karbala International Journal of Modern Science* no. 4:244-254.

Mpatani, Farid Mzee, Runping Han, Aaron Albert Aryee, Alexander Nti Kani, Zhaohui Li, and Lingbo Qu. 2021. "Adsorption performance of modified agricultural waste materials for removal of emerging micro-contaminant bisphenol A: a comprehensive review." *Science of the Total Environment* no. 780:146629.

Mubarak, NM, JN Sahu, EC Abdullah, NS Jayakumar, and P Ganesan. 2014. "Single stage production of carbon nanotubes using microwave technology." *Diamond and Related Materials* no. 48:52-59.

Muhamad, Sarah Umeera, Nurul Hayati Idris, Hanis Mohd Yusoff, MF Md Din, and SR Majid. 2017. "In-situ encapsulation of nickel nanoparticles in polypyrrole nanofibres with enhanced performance for supercapacitor." *Electrochimica Acta* no. 249:9-15.

Mumtaz, M, Mehwish Hassan, Shafiq Ullah, and Zubair Ahmad. 2021. "Nanohybrids of multi-walled carbon nanotubes and cobalt ferrite nanoparticles: High performance anode material for lithium-ion batteries." *Carbon* no. 171:179-187.

Mund, Muhammad Danish, Umair Hassan Khan, Uruj Tahir, Bahar-E-Mustafa, and Asad Fayyaz. 2017. "Antimicrobial drug residues in poultry products and implications on public health: A review." *International Journal of Food Properties* no. 20:1433-1446.

Nadeem, Muhammad, Sumbul Purree, MGB Ashiq, and Hafiz Muhammad Ali. 2022. "Stability Analysis of Fe3O4-OA-MWCNT Nanocomposite-Based Nanofluid." *Journal of Nanomaterials* no. 2022.

Naderpour, Hosein, and Masoomeh Mirrashid. 2019. "Shear failure capacity prediction of concrete beam–column joints in terms of ANFIS and GMDH." *Practice Periodical on Structural Design and Construction* no. 24:04019006.

Nagy, Zsuzsanna Magdolna, Mónika Molnár, Ildikó Fekete-Kertész, Ibolya Molnár-Perl, Éva Fenyvesi, and Katalin Gruiz. 2014. "Removal of emerging micropollutants from water using cyclodextrin." *Science of the Total Environment* no. 485:711-719.

Najib, Tahereh, Mostafa Solgi, Abbas Farazmand, Seyed Mohammad Heydarian, and Bahram Nasernejad. 2017. "Optimization of sulfate removal by sulfate reducing bacteria using response surface methodology and heavy metal removal in a sulfidogenic UASB reactor." *Journal of Environmental Chemical Engineering* no. 5:3256-3265.

Nakano, Tamaki, and Yoshio Okamoto. 2001. "Synthetic helical polymers: conformation and function." *Chemical Reviews* no. 101:4013-4038.

Nardecchia, Stefania, Daniel Carriazo, M Luisa Ferrer, María C Gutiérrez, and Francisco del Monte. 2013. "Three dimensional macroporous architectures and aerogels built of carbon nanotubes and/or graphene: synthesis and applications." *Chemical Society Reviews* no. 42:794-830.

Nasrollahzadeh, Mahmoud, Mohaddeseh Sajjadi, Siavash Iravani, and Rajender S Varma. 2021. "Carbon-based sustainable nanomaterials for water treatment: state-of-art and future perspectives." *Chemosphere* no. 263:128005.

Ncibi, Mohamed Chaker, and Mika Sillanpää. 2015. "Optimized removal of antibiotic drugs from aqueous solutions using single, double and multi-walled carbon nanotubes." *Journal of Hazardous Materials* no. 298:102-110.

Neto, José de Oliveira Marques, Carlos Roberto Bellato, and Danilo de Castro Silva. 2019. "Iron oxide/carbon nanotubes/chitosan magnetic composite film for chromium species removal." *Chemosphere* no. 218:391-401.

Nezhadheydari, Hasan, Kamran Rezaei Tavabe, Alireza Mirvaghefi, Akbar Heydari, and Michael Frinsko. 2019. "Effects of different concentrations of Fe3O4@ ZnO and Fe3O4@ CNT magnetic nanoparticles separately and in combination on aquaculture wastewater treatment." *Environmental Technology & Innovation* no. 15:100414.

Ngo, Cao Long, Quoc Trung Le, Trinh Tung Ngo, Duc Nghia Nguyen, and Minh Thanh Vu. 2013. "Surface modification and functionalization of carbon nanotube with some organic compounds." *Advances in Natural Sciences: Nanoscience and Nanotechnology* no. 4:035017.

Nguyen, Van-Huy, Quoc Ba Tran, Xuan Cuong Nguyen, Thi Thanh Tam Ho, Mohammadreza Shokouhimehr, Dai-Viet N Vo, Su Shiung Lam, Hai Phong Nguyen, Cong Tin Hoang, and Quang Viet Ly. 2020. "Submerged photocatalytic membrane reactor with suspended and immobilized N-doped

TiO2 under visible irradiation for diclofenac removal from wastewater." *Process Safety and Environmental Protection* no. 142:229-237.

Nguyen, Vy T, Lam Q Ha, Tu DL Nguyen, Phuong H Ly, Dang Mao Nguyen, and DongQuy Hoang. 2021. "Nanocellulose and graphene oxide aerogels for adsorption and removal methylene blue from an aqueous environment." *ACS Omega* no. 7:1003-1013.

Nie, Yafeng, Zhimin Qiang, Heqing Zhang, and Weiwei Ben. 2012. "Fate and seasonal variation of endocrine-disrupting chemicals in a sewage treatment plant with A/A/O process." *Separation and Purification Technology* no. 84:9-15.

Nieto, Pedro, Emilio Custodio, and Marisol Manzano. 2005. "Baseline groundwater quality: a European approach." *Environmental Science & Policy* no. 8:399-409.

Niranjan, Mukesh Kumar, and Rashmi Srivastava. 2019. "Expression of estrogen receptor alpha in developing brain, ovary and shell gland of Gallus gallus domesticus: Impact of stress and estrogen." *Steroids* no. 146:21-33.

Nishant, Rohit, Mike Kennedy, and Jacqueline Corbett. 2020. "Artificial intelligence for sustainability: Challenges, opportunities, and a research agenda." *International Journal of Information Management* no. 53:102104.

Noyes, Pamela D, Matthew K McElwee, Hilary D Miller, Bryan W Clark, Lindsey A Van Tiem, Kia C Walcott, Kyle N Erwin, and Edward D Levin. 2009. "The toxicology of climate change: environmental contaminants in a warming world." *Environment International* no. 35:971-986.

Oaks, J Lindsay, Martin Gilbert, Munir Z Virani, Richard T Watson, Carol U Meteyer, Bruce A Rideout, HL Shivaprasad, Shakeel Ahmed, Muhammad Jamshed Iqbal Chaudhry, and Muhammad Arshad. 2004. "Diclofenac residues as the cause of vulture population decline in Pakistan." *Nature* no. 427:630-633.

Oatley-Radcliffe, Darren L, Matthew Walters, Thomas J Ainscough, Paul M Williams, Abdul Wahab Mohammad, and Nidal Hilal. 2017. "Nanofiltration membranes and processes: A review of research trends over the past decade." *Journal of Water Process Engineering* no. 19:164-171.

Oba, Stephen N, Joshua O Ighalo, Chukwunonso O Aniagor, and Chinenye Adaobi Igwegbe. 2021. "Removal of ibuprofen from aqueous media by

adsorption: A comprehensive review." *Science of The Total Environment* no. 780:146608.

Obayomi, Kehinde Shola, Sie Yon Lau, Divine Akubuo-Casmir, Muibat Diekola Yahya, Manase Auta, ASM Fazle Bari, Ayomide Elizabeth Oluwadiya, Oluwatobi Victoria Obayomi, and Mohammad Mahmudur Rahman. 2022. "Adsorption of endocrine disruptive Congo red onto biosynthesized silver nanoparticles loaded on hildegardia barteri activated carbon." *Journal of Molecular Liquids* no. 352:118735.

Obayomi, KS, JO Bello, JS Nnoruka, AA Adediran, and PO Olajide. 2019. "Development of low-cost bio-adsorbent from agricultural waste composite for Pb (II) and As (III) sorption from aqueous solution." *Cogent Engineering* no. 6:1687274.

Obayomi, KS, JO Bello, Muibat Diekola Yahya, E Chukwunedum, and JB Adeoye. 2020. "Statistical analyses on effective removal of cadmium and hexavalent chromium ions by multiwall carbon nanotubes (MWCNTs)." *Heliyon* no. 6:e04174.

Oh, Jun Young, Seung Jae Yang, Jun Young Park, Taehoon Kim, Kunsil Lee, Yern Seung Kim, Heung Nam Han, and Chong Rae Park. 2015. "Easy preparation of self-assembled high-density buckypaper with enhanced mechanical properties." *Nano Letters* no. 15:190-197.

Olabi, AG, Hegazy Rezk, Enas Taha Sayed, Rania M Ghoniem, and Mohammad Ali Abdelkareem. 2023. "Boosting carbon dioxide adsorption capacity applying Jellyfish optimization and ANFIS-based modelling." *Ain Shams Engineering Journal* no. 14:101931.

Olatunji, Kehinde O, Noor A Ahmed, Daniel M Madyira, Ademola O Adebayo, Oyetola Ogunkunle, and Oluwatobi Adeleke. 2022. "Performance evaluation of ANFIS and RSM modeling in predicting biogas and methane yields from Arachis hypogea shells pretreated with size reduction." *Renewable Energy* no. 189:288-303.

Olvera, Rafael Castañeda, Sein León Silva, Eduardo Robles-Belmont, and Edgar Záyago Lau. 2017. "Review of nanotechnology value chain for water treatment applications in Mexico." *Resource-Efficient Technologies* no. 3:1-11.

Omer, Ahmed M, Rana Dey, Abdelazeem S Eltaweil, Eman M Abd El-Monaem, and Zyta M Ziora. 2022. "Insights into recent advances of chitosan-

based adsorbents for sustainable removal of heavy metals and anions." *Arabian Journal of Chemistry* no. 15:103543.

Onu, Chijioke Elijah, Joseph T Nwabanne, Paschal E Ohale, and Christian O Asadu. 2021. "Comparative analysis of RSM, ANN and ANFIS and the mechanistic modeling in eriochrome black-T dye adsorption using modified clay." *South African Journal of Chemical Engineering* no. 36:24-42.

Onyejiuwa, Chime Thompson, Eme Njoku Chijioke, and Onoh Ikechukwu Maxwell. 2022. "Optimization Study on the Filtration Loss of Water Based Drilling Fluid using Groundnut (Arachis hypogaea) Shells Cellulose." *Journal of Engineering Research and Reports* no. 23:64-72.

Ornostay, Anna, Joshua Marr, Jennifer R Loughery, and Christopher J Martyniuk. 2016. "Transcriptional networks associated with 5-alpha-dihydrotestosterone in the fathead minnow (Pimephales promelas) ovary." *General and Comparative Endocrinology* no. 225:23-32.

Overturf, Matthew D, Jordan C Anderson, Zacharias Pandelides, Lindsay Beyger, and Douglas A Holdway. 2015. "Pharmaceuticals and personal care products: A critical review of the impacts on fish reproduction." *Critical Reviews in Toxicology* no. 45:469-491.

Owumi, Solomon E, Ruth A Anaikor, Uche O Arunsi, Oluwatosin A Adaramoye, and Adegboyega K Oyelere. 2021. "Chlorogenic acid co-administration abates tamoxifen-mediated reproductive toxicities in male rats: An experimental approach." *Journal of Food Biochemistry* no. 45:e13615.

Pae, Dong Sung, In Hwan Choi, Tae Koo Kang, and Myo Taeg Lim. 2018. "Vehicle detection framework for challenging lighting driving environment based on feature fusion method using adaptive neuro-fuzzy inference system." *International Journal of Advanced Robotic Systems* no. 15:1729881418770545.

Palani, Geetha, A Arputhalatha, Karthik Kannan, Sivarama Krishna Lakkaboyana, Marlia M Hanafiah, Vinay Kumar, and Ravi Kumar Marella. 2021. "Current trends in the application of nanomaterials for the removal of pollutants from industrial wastewater treatment—a review." *Molecules* no. 26:2799.

Palansooriya, Kumuduni N, Jie Li, Pavani D Dissanayake, Manu Suvarna, Lanyu Li, Xiangzhou Yuan, Binoy Sarkar, Daniel CW Tsang, Jörg Rinklebe,

and Xiaonan Wang. 2022. "Prediction of soil heavy metal immobilization by biochar using machine learning." *Environmental Science & Technology* no. 56:4187-4198.

Papadakis, Emmanouil-Nikolaos, Aggeliki Tsaboula, Athina Kotopoulou, Katerina Kintzikoglou, Zisis Vryzas, and Euphemia Papadopoulou-Mourkidou. 2015. "Pesticides in the surface waters of Lake Vistonis Basin, Greece: Occurrence and environmental risk assessment." *Science of the Total Environment* no. 536:793-802.

Parida, Vishal Kumar, Duduku Saidulu, Abhradeep Majumder, Ashish Srivastava, Bramha Gupta, and Ashok Kumar Gupta. 2021. "Emerging contaminants in wastewater: A critical review on occurrence, existing legislations, risk assessment, and sustainable treatment alternatives." *Journal of Environmental Chemical Engineering* no. 9:105966.

Park, Ho Bum, Jovan Kamcev, Lloyd M Robeson, Menachem Elimelech, and Benny D Freeman. 2017. "Maximizing the right stuff: The trade-off between membrane permeability and selectivity." *Science* no. 356:eaab0530.

Parliament, European, and the Council of the European Union. 2000. "Directive 2000/60/EC of the European Parliament and of the Council of 23 October 2000 establishing a framework for Community action in the field of water policy." *Official Journal of the European Communities* no. 327:1-72.

Parveen, Shama, Sohel Rana, Raul Fangueiro, and MC Paiva. 2017. "Characterizing dispersion and long term stability of concentrated carbon nanotube aqueous suspensions for fabricating ductile cementitious composites." *Powder Technology* no. 307:1-9.

Pashirova, Tatiana N, Evgeniya A Burilova, Svetlana S Lukashenko, Nail K Gaysin, Oleg I Gnezdilov, Anastasia S Sapunova, Ana R Fernandes, Aleksandra D Voloshina, Eliana B Souto, and Elena P Zhiltsova. 2019. "Nontoxic antimicrobial micellar systems based on mono-and dicationic Dabco-surfactants and furazolidone: Structure-solubilization properties relationships." *Journal of Molecular Liquids* no. 296:112062.

Patil, Mangesh R, Saurabh B Ganorkar, Amod S Patil, Atul A Shirkhedkar, and Sanjay J Surana. 2021. "Hydrotropic solubilization in pharmaceutical analysis: Origin, evolution, cumulative trend and precise applications." *Critical Reviews in Analytical Chemistry* no. 51:278-288.

Patiño, Yolanda, Eva Díaz, Salvador Ordóñez, Esteban Gallegos-Suarez, Antonio Guerrero-Ruiz, and Inmaculada Rodríguez-Ramos. 2015. "Adsorption of emerging pollutants on functionalized multiwall carbon nanotubes." *Chemosphere* no. 136:174-180.

Pedrazzani, Roberta, Elisabetta Ceretti, Ilaria Zerbini, Rosario Casale, Eleonora Gozio, Giorgio Bertanza, Umberto Gelatti, Francesco Donato, and Donatella Feretti. 2012. "Biodegradability, toxicity and mutagenicity of detergents: Integrated experimental evaluations." *Ecotoxicology and Environmental Safety* no. 84:274-281.

Pendergast, MaryTheresa M, and Eric MV Hoek. 2011. "A review of water treatment membrane nanotechnologies." *Energy & Environmental Science* no. 4:1946-1971.

Peng, Jiali, Yongli He, Chenying Zhou, Shijun Su, and Bo Lai. 2021. "The carbon nanotubes-based materials and their applications for organic pollutant removal: A critical review." *Chinese Chemical Letters* no. 32:1626-1636.

Peschke, Katharina, Jonas Geburzi, Heinz-R Ko, Karl Wurm, and Rita Triebskorn. 2014. "Invertebrates as indicators for chemical stress in sewage-influenced stream systems: toxic and endocrine effects in gammarids and reactions at the community level in two tributaries of Lake Constance, Schussen and Argen." *Ecotoxicology and Environmental Safety* no. 106:115-125.

Peydayesh, Mohammad, and Raffaele Mezzenga. 2021. "Protein nanofibrils for next generation sustainable water purification." *Nature Communications* no. 12:3248.

Poudel, Yuba Raj, and Wenzhi Li. 2018. "Synthesis, properties, and applications of carbon nanotubes filled with foreign materials: A review." *Materials Today Physics* no. 7:7-34.

Prabhakaran, K, R Nagarajan, F Merlin Franco, and A Anand Kumar. 2017. "Biomonitoring of Malaysian aquatic environments: A review of status and prospects." *Ecohydrology & Hydrobiology* no. 17:134-147.

Precup, Radu-Emil, Stefan Preitl, Emil M Petriu, Raul-Cristian Roman, Claudia-Adina Bojan-Dragos, Elena-Lorena Hedrea, and Alexandra-Iulia Szedlak-Stinean. 2020. "A center manifold theory-based approach to the

stability analysis of state feedback Takagi-Sugeno-Kang fuzzy control systems." *Facta Universitatis, Series: Mechanical Engineering* no. 18:189-204.

Punetha, Vinay Deep, Sravendra Rana, Hye Jin Yoo, Alok Chaurasia, James T McLeskey Jr, Madeshwaran Sekkarapatti Ramasamy, Nanda Gopal Sahoo, and Jae Whan Cho. 2017. "Functionalization of carbon nanomaterials for advanced polymer nanocomposites: A comparison study between CNT and graphene." *Progress in Polymer Science* no. 67:1-47.

Qadir, Najam U, Syed AM Said, Rached B Mansour, Khalid Mezghani, and Anwar Ul-Hamid. 2016. "Synthesis, characterization, and water adsorption properties of a novel multi-walled carbon nanotube/MIL-100 (Fe) composite." *Dalton Transactions* no. 45:15621-15633.

Qamar, Sarmad Ahmad, Mahpara Qamar, Aneela Basharat, Muhammad Bilal, Hairong Cheng, and Hafiz MN Iqbal. 2022. "Alginate-based nano-adsorbent materials–Bioinspired solution to mitigate hazardous environmental pollutants." *Chemosphere* no. 288:132618.

Qi, Jiangtao, Wenwen Zhao, Za Kan, Hewei Meng, and Yaping Li. 2019. "Parameter optimization of double-blade normal milk processing and mixing performance based on RSM and BP-GA." *Food Science & Nutrition* no. 7:3501-3512.

Qin, Huaqing, Tianjue Hu, Yunbo Zhai, Ningqin Lu, and Jamila Aliyeva. 2020. "The improved methods of heavy metals removal by biosorbents: A review." *Environmental Pollution* no. 258:113777.

Qu, Xiaolei, Pedro JJ Alvarez, and Qilin Li. 2013. "Applications of nanotechnology in water and wastewater treatment." *Water Research* no. 47:3931-3946.

Queirós, Joana M, H Salazar, A Valverde, Gabriela Botelho, R Fernández de Luis, J Teixeira, PM Martins, and S Lanceros-Mendez. 2022. "Reusable composite membranes for highly efficient chromium removal from real water matrixes." *Chemosphere* no. 307:135922.

Rad, Samira Mosalaei, Ajay K Ray, and Shahzad Barghi. 2022. "Water Pollution and Agriculture Pesticide." *Clean Technologies* no. 4:1088-1102.

Rafiee, Roham, and Reza Pourazizi. 2015. "Influence of CNT functionalization on the interphase region between CNT and polymer." *Computational Materials Science* no. 96:573-578.

Ramezani, Mahyar, Ayoub Dehghani, and Muhammad M Sherif. 2022. "Carbon nanotube reinforced cementitious composites: A comprehensive review." *Construction and Building Materials* no. 315:125100.

Ranjan, Bibhuti, Santhosh Pillai, Kugenthiren Permaul, and Suren Singh. 2019. "Simultaneous removal of heavy metals and cyanate in a wastewater sample using immobilized cyanate hydratase on magnetic-multiwall carbon nanotubes." *Journal of Hazardous Materials* no. 363:73-80.

Rao, Rahul, Cary L Pint, Ahmad E Islam, Robert S Weatherup, Stephan Hofmann, Eric R Meshot, Fanqi Wu, Chongwu Zhou, Nicholas Dee, and Placidus B Amama. 2018. "Carbon nanotubes and related nanomaterials: critical advances and challenges for synthesis toward mainstream commercial applications." *ACS Nanomaterials* no. 12:11756-11784.

Raoof, Jahan Bakhsh, Mehdi Baghayeri, and Reza Ojani. 2012. "A high sensitive voltammetric sensor for qualitative and quantitative determination of phenobarbital as an antiepileptic drug in presence of acetaminophen." *Colloids and Surfaces B: Biointerfaces* no. 95:121-128.

Rasana, N, K Jayanarayanan, BDS Deeraj, and K Joseph. 2019. "The thermal degradation and dynamic mechanical properties modeling of MWCNT/glass fiber multiscale filler reinforced polypropylene composites." *Composites Science and Technology* no. 169:249-259.

Rashed, Ahmed O, Andrea Merenda, Takeshi Kondo, Marcio Lima, Joselito Razal, Lingxue Kong, Chi Huynh, and Ludovic F Dumée. 2021. "Carbon nanotube membranes–Strategies and challenges towards scalable manufacturing and practical separation applications." *Separation and Purification Technology* no. 257:117929.

Rasheed, Sajida, Luiza C Campos, Jong K Kim, Qizhi Zhou, and Imran Hashmi. 2016. "Optimization of total trihalomethanes'(TTHMs) and their precursors' removal by granulated activated carbon (GAC) and sand dual media by response surface methodology (RSM)." *Water Science and Technology: Water Supply* no. 16:783-793.

Rathanasamy, Rajasekar, Sumanta Sahoo, Joong Hee Lee, Ashok Kumar Das, Mahalakshmi Somasundaram, Sathish Kumar Palaniappan, and Santhosh Sivaraj. 2021. "Carbon-based multi-layered films for electronic application: a review." *Journal of Electronic Materials* no. 50:1845-1892.

Rathi, B Senthil, P Senthil Kumar, and Pau-Loke Show. 2021. "A review on effective removal of emerging contaminants from aquatic systems: Current trends and scope for further research." *Journal of Hazardous Materials* no. 409:124413.

Ratnasari, Anisa, Achmad Syafiuddin, Nur Syamimi Zaidi, Ahmad Beng Hong Kueh, Tony Hadibarata, Dedy Dwi Prastyo, Rajagounder Ravikumar, and Palanivel Sathishkumar. 2022. "Bioremediation of micropollutants using living and non-living algae-Current perspectives and challenges." *Environmental Pollution* no. 292:118474.

Raza, Ali, Manan Bhandari, Hyeong-Ki Kim, Hyeong-Min Son, Baofeng Huang, and Il-Woo Nam. 2020. "A study on mechanical characteristics of cement composites fabricated with nano-silica and carbon nanotube." *Applied Sciences* no. 11:152.

Razmkhah, Kasra, Hassan Sereshti, Sara Soltani, and Hamid Rashidi Nodeh. 2018. "Extraction and determination of three steroid molecules in milk using functionalized magnetic carbon nanotube-based solid phase extraction coupled with HPLC." *Food Analytical Methods* no. 11:3179-3189.

Ribeiro, Penha Patrícia Cabral, Karla Suzanne Florentino da Silva Chaves, Bruno Oliveira de Veras, João Ricardhis Saturnino de Oliveira, Vera Lúcia de Menezes Lima, Caio Rodrigo Dias de Assis, Marcia Vanusa da Silva, Francisco Canindé de Sousa Júnior, Cristiane Fernandes de Assis, and Carlos Eduardo de Araújo Padilha. 2021. "Chemical and biological activities of faveleira (Cnidoscolus quercifolius Pohl) seed oil for potential health applications." *Food Chemistry* no. 337:127771.

Richardson, Susan D, and Susana Y Kimura. 2019. "Water analysis: emerging contaminants and current issues." *Analytical Chemistry* no. 92:473-505.

Rivera-Utrilla, José, Manuel Sánchez-Polo, María Ángeles Ferro-García, Gonzalo Prados-Joya, and Raúl Ocampo-Pérez. 2013. "Pharmaceuticals as emerging contaminants and their removal from water. A review." *Chemosphere* no. 93:1268-1287.

Rodrigues, Raphael, José Carlos Mierzwa, and Chad D Vecitis. 2019. "Mixed matrix polysulfone/clay nanoparticles ultrafiltration membranes for water treatment." *Journal of Water Process Engineering* no. 31:100788.

Rogowska, Justyna, Monika Cieszynska-Semenowicz, Wojciech Ratajczyk, and Lidia Wolska. 2020. "Micropollutants in treated wastewater." *Ambio* no. 49:487-503.

Roongraung, Kamonchanok, Surawut Chuangchote, Navadol Laosiripojana, and Takashi Sagawa. 2020. "Electrospun Ag-TiO2 nanofibers for photocatalytic glucose conversion to high-value chemicals." *ACS Omega* no. 5:5862-5872.

Roy, Sagar, Madhuleena Bhadra, and Somenath Mitra. 2014. "Enhanced desalination via functionalized carbon nanotube immobilized membrane in direct contact membrane distillation." *Separation and Purification Technology* no. 136:58-65.

Ruan, Xiao-Lin, Jing-Jing Qiu, Chuan Wu, Tao Huang, Rui-Bo Meng, and Yong-Qiang Lai. 2014. "Magnetic single-walled carbon nanotubes–dispersive solid-phase extraction method combined with liquid chromatography–tandem mass spectrometry for the determination of paraquat in urine." *Journal of Chromatography B* no. 965:85-90.

Ruthiraan, M, EC Abdullah, NM Mubarak, and MN Noraini. 2017. "A promising route of magnetic based materials for removal of cadmium and methylene blue from waste water." *Journal of Environmental Chemical Engineering* no. 5:1447-1455.

Sadegh, Hamidreza, Ramin Shahryari-ghoshekandi, and Maryam Kazemi. 2014. "Study in synthesis and characterization of carbon nanotubes decorated by magnetic iron oxide nanoparticles." *International Nano Letters* no. 4:129-135.

Sadeghfar, Fardin, Mehrorang Ghaedi, Arash Asfaram, Ramin Jannesar, Hamedreza Javadian, and Vahid Pezeshkpour. 2018. "Polyvinyl alcohol/Fe3O4@ carbon nanotubes nanocomposite: Electrochemical-assisted synthesis, physicochemical characterization, optical properties, cytotoxicity effects and ultrasound-assisted treatment of aqueous based organic compound." *Journal of Industrial and Engineering Chemistry* no. 65:349-362.

Sadeghizadeh, Amin, Farbod Ebrahimi, Maryam Heydari, Milad Tahmasebikohyani, Farshad Ebrahimi, and Afsoon Sadeghizadeh. 2019. "Adsorptive removal of Pb (II) by means of hydroxyapatite/chitosan

nanocomposite hybrid nanoadsorbent: ANFIS modeling and experimental study." *Journal of Environmental Management* no. 232:342-353.

Sadri, Rad, Maryam Hosseini, SN Kazi, Samira Bagheri, Nashrul Zubir, KH Solangi, Tuan Zaharinie, and A Badarudin. 2017. "A bio-based, facile approach for the preparation of covalently functionalized carbon nanotubes aqueous suspensions and their potential as heat transfer fluids." *Journal of Colloid and Interface Science* no. 504:115-123.

Safari, Javad, and Soheila Gandomi-Ravandi. 2014. "Fe 3 O 4–CNTs nanocomposites: a novel and excellent catalyst in the synthesis of diarylpyrimidinones using grindstone chemistry." *RSC Advances* no. 4:11486-11492.

Said, Khairul Anwar Mohamad, Nor Zakirah Ismail, Ramizah Liyana Jama'in, Nurul Ain Mohamed Alipah, Norsuzailina Mohamed Sutan, Genevieve George Gadung, Rubiyah Baini, and Nur Syuhada Ahmad Zauzi. 2018. "Application of Freundlich and Temkin isotherm to study the removal of Pb (II) via adsorption on activated carbon equipped polysulfone membrane." *International Journal of Engineering Technology* no. 7:91-93.

Sakurai, Shunsuke, Fuminori Kamada, Don N Futaba, Motoo Yumura, and Kenji Hata. 2013. "Influence of lengths of millimeter-scale single-walled carbon nanotube on electrical and mechanical properties of buckypaper." *Nanoscale Research Letters* no. 8:546.

Samadishadlou, Mehrdad, Masoud Farshbaf, Nasim Annabi, Taras Kavetskyy, Rovshan Khalilov, Siamak Saghfi, Abolfazl Akbarzadeh, and Sepideh Mousavi. 2018. "Magnetic carbon nanotubes: preparation, physical properties, and applications in biomedicine." *Artificial Cells, Nanomedicine, and Biotechnology* no. 46:1314-1330.

Samal, Kundan, and Rajesh Roshan Dash. 2021. "Modelling of pollutants removal in Integrated Vermifilter (IVmF) using response surface methodology." *Cleaner Engineering and Technology* no. 2:100060.

Samantaray, Sandeep, Chinmayee Biswakalyani, Deepak Kumar Singh, Abinash Sahoo, and Deba Prakash Satapathy. 2022. "Prediction of groundwater fluctuation based on hybrid ANFIS-GWO approach in arid Watershed, India." *Soft Computing* no. 26:5251-5273.

Samsami, Shakiba, Maryam Mohamadizaniani, Mohammad-Hossein Sarrafzadeh, Eldon R Rene, and Meysam Firoozbahr. 2020. "Recent advances in the treatment of dye-containing wastewater from textile industries: Overview and perspectives." *Process Safety and Environmental Protection* no. 143:138-163.

Sanderson, Hans. 2011. "Presence and risk assessment of pharmaceuticals in surface water and drinking water." *Water Science and Technology* no. 63:2143-2148.

Santen, RJ. 2015. "Vaginal administration of estradiol: effects of dose, preparation and timing on plasma estradiol levels." *Climacteric* no. 18:121-134.

Santhosh, Chella, Venugopal Velmurugan, George Jacob, Soon Kwan Jeong, Andrews Nirmala Grace, and Amit Bhatnagar. 2016. "Role of nanomaterials in water treatment applications: a review." *Chemical Engineering Journal* no. 306:1116-1137.

Saraswathi, Meenakshi Sundaram Sri Abirami, Alagumalai Nagendran, and Dipak Rana. 2019. "Tailored polymer nanocomposite membranes based on carbon, metal oxide and silicon nanomaterials: a review." *Journal of Materials Chemistry A* no. 7:8723-8745.

Sarıkaya, Murat, Munish Kumar Gupta, Italo Tomaz, Danil Yu Pimenov, Mustafa Kuntoğlu, Navneet Khanna, Çağrı Vakkas Yıldırım, and Grzegorz M Krolczyk. 2021. "A state-of-the-art review on tool wear and surface integrity characteristics in machining of superalloys." *CIRP Journal of Manufacturing Science and Technology* no. 35:624-658.

Sayadi, MH, RK Trivedy, and RK Pathak. 2010. "Pollution of pharmaceuticals in environment." *I Control Pollution* no. 26:89-94.

Schlachet, Inbar, Jiří Trousil, Dmytro Rak, Kenneth D Knudsen, Ewa Pavlova, Bo Nyström, and Alejandro Sosnik. 2019. "Chitosan-graft-poly (methyl methacrylate) amphiphilic nanoparticles: Self-association and physicochemical characterization." *Carbohydrate Polymers* no. 212:412-420.

Schneider, M, M Weiser, S Ferl, C Krasmann, A Potthoff, K Voigt, and P Malcher. 2021. "Facile deposition of multiwalled carbon nanotubes via electrophoretic deposition in an environmentally friendly suspension." *Surface and Coatings Technology* no. 406:126741.

Schneider, M, M Weiser, C Schrötke, F Meißner, I Endler, and A Michaelis. 2015. "Pulse plating of manganese oxide nanoparticles on aligned MWCNT." *Surface Engineering* no. 31:214-220.

Schwarzenbach, René P, Beate I Escher, Kathrin Fenner, Thomas B Hofstetter, C Annette Johnson, Urs Von Gunten, and Bernhard Wehrli. 2006. "The challenge of micropollutants in aquatic systems." *Science* no. 313:1072-1077.

Sehgal, Vinit, Rajeev Ranjan Sahay, and Chandranath Chatterjee. 2014. "Effect of utilization of discrete wavelet components on flood forecasting performance of wavelet based ANFIS models." *Water Resources Management* no. 28:1733-1749.

Selimefendigil, Fatih, and Hakan F Öztop. 2018. "Numerical analysis and ANFIS modeling for mixed convection of CNT-water nanofluid filled branching channel with an annulus and a rotating inner surface at the junction." *International Journal of Heat and Mass Transfer* no. 127:583-599.

Selvaraj, Munirasu, Abdul Hai, Fawzi Banat, and Mohammad Abu Haija. 2020. "Application and prospects of carbon nanostructured materials in water treatment: A review." *Journal of Water Process Engineering* no. 33:100996.

Seyedmajidi, Mohammad Reza, Seyed Ashkan Hosseini, and Jamshid Vafaeimanesh. 2021. "Comparing the Effect of Two Low-dose and High-dose Four-drug Regimens of Furazolidone in Eradicating Helicobacter Pylori." *Middle East Journal of Digestive Diseases* no. 13:131.

Shahid, Usman Bin, and Ahmed Abdala. 2021. "A critical review of phase change material composite performance through Figure-of-Merit analysis: Graphene vs Boron Nitride." *Energy Storage Materials* no. 34:365-387.

Shanmugam, Ranganathan, Palani Barathi, Jyh-Myng Zen, and Annamalai Senthil Kumar. 2016. "An unusual electrochemical oxidation of phenothiazine dye to phenothiazine-bi-1, 4-quinone derivative (a donor-acceptor type molecular hybrid) on MWCNT surface and its cysteine electrocatalytic oxidation function." *Electrochimica Acta* no. 187:34-45.

Shanmuganathan, Sukanyah, Paripurnanda Loganathan, Christian Kazner, MAH Johir, and Saravanamuthu Vigneswaran. 2017. "Submerged membrane filtration adsorption hybrid system for the removal of organic micropollutants from a water reclamation plant reverse osmosis concentrate." *Desalination* no. 401:134-141.

Shariati, Mahdi, Mohammad Saeed Mafipour, James H Haido, Salim T Yousif, Ali Toghroli, Nguyen Thoi Trung, and Ali Shariati. 2020. "Identification of the most influencing parameters on the properties of corroded concrete beams using an Adaptive Neuro-Fuzzy Inference System (ANFIS)." *Steel Composite Structure* no. 34:155.

Sharifi, Habibeh, Abbas Roozbahani, and Seied Mehdy Hashemy Shahdany. 2021. "Evaluating the performance of agricultural water distribution systems using FIS, ANN and ANFIS intelligent models." *Water Resources Management* no. 35:1797-1816.

Sharma, Prabhakar, and Bibhuti B Sahoo. 2022. "An ANFIS-RSM based modeling and multi-objective optimization of syngas powered dual-fuel engine." *International Journal of Hydrogen Energy* no. 47:19298-19318.

Sharma, Priyanka R, Sunil K Sharma, Tom Lindström, and Benjamin S Hsiao. 2020. "Nanocellulose-enabled membranes for water purification: perspectives." *Advanced Sustainable Systems* no. 4:1900114.

Sharpe, Rainie L, Deborah L MacLatchy, Simon C Courtenay, and Glen J Van Der Kraak. 2004. "Effects of a model androgen (methyl testosterone) and a model anti-androgen (cyproterone acetate) on reproductive endocrine endpoints in a short-term adult mummichog (Fundulus heteroclitus) bioassay." *Aquatic Toxicology* no. 67:203-215.

Shen, Jiang-nan, Hui-min Ruan, Li-guang Wu, and Cong-jie Gao. 2011. "Preparation and characterization of PES–SiO2 organic–inorganic composite ultrafiltration membrane for raw water pretreatment." *Chemical Engineering Journal* no. 168:1272-1278.

Sher, Farooq, Kashif Hanif, Abdul Rafey, Ushna Khalid, Ayesha Zafar, Mariam Ameen, and Eder C Lima. 2021. "Removal of micropollutants from municipal wastewater using different types of activated carbons." *Journal of Environmental Management* no. 278:111302.

Shokry, SA, AK El Morsi, MS Sabaa, RR Mohamed, and HE El Sorogy. 2014. "Study of the productivity of MWCNT over Fe and Fe–Co catalysts supported on SiO2, Al2O3 and MgO." *Egyptian Journal of Petroleum* no. 23:183-189.

Shukla, Parul, Balendu Shekhar Giri, Rakesh K Mishra, Ashok Pandey, and Preeti Chaturvedi. 2021. "Lignocellulosic biomass-based engineered biochar composites: A facile strategy for abatement of emerging pollutants and

utilization in industrial applications." *Renewable and Sustainable Energy Reviews* no. 152:111643.

Shukla, Saurabh, Ramsha Khan, and Achlesh Daverey. 2021. "Synthesis and characterization of magnetic nanoparticles, and their applications in wastewater treatment: A review." *Environmental Technology & Innovation* no. 24:101924.

Siddiqui, Muhammad Tahir Hussain, Sabzoi Nizamuddin, Humair Ahmed Baloch, NM Mubarak, Maha Al-Ali, Shaukat A Mazari, AW Bhutto, Rashid Abro, Madapusi Srinivasan, and Gregory Griffin. 2019. "Fabrication of advance magnetic carbon nano-materials and their potential applications: a review." *Journal of Environmental Chemical Engineering* no. 7:102812.

Sithamparanathan, Elackiya, Katarzyna Kujawa-Roeleveld, Jill AR Soedarso, Nora B Sutton, Katja Grolle, Harry Bruning, and Huub HM Rijnaarts. 2021. "Sorption of micropollutants to hydroponic substrata: Effects of physico-chemical properties." *Environmental Advances* no. 4:100049.

Song, Yanhua, Zhaoyang Sun, Lan Xu, and Zhongbiao Shao. 2017. "Preparation and characterization of highly aligned carbon nanotubes/polyacrylonitrile composite nanofibers." *Polymers* no. 9:1.

Sotelo, José L, Araceli R Rodríguez, María M Mateos, Sergio D Hernández, Silvia A Torrellas, and Juan G Rodríguez. 2012. "Adsorption of pharmaceutical compounds and an endocrine disruptor from aqueous solutions by carbon materials." *Journal of Environmental Science and Health, Part B* no. 47:640-652.

Sousa, Ana Paula, and Bruno Nunes. 2020. "Standard and biochemical toxicological effects of zinc pyrithione in Daphnia magna and Daphnia longispina." *Environmental Toxicology and Pharmacology* no. 80:103402.

Sousa, WJ, Y Guerra, R Peña-Garcia, and E Padrón-Hernández. 2022. "Saturation magnetization as a function of temperature in Zn doped YIG nanoparticles." *Physica E: Low-dimensional Systems and Nanostructures* no. 138:115054.

Spongberg, Alison L, Jason D Witter, Jenaro Acuña, José Vargas, Manuel Murillo, Gerardo Umaña, Eddy Gómez, and Greivin Perez. 2011. "Reconnaissance of selected PPCP compounds in Costa Rican surface waters." *Water Research* no. 45:6709-6717.

Srenscek-Nazzal, Joanna, Urszula Narkiewicz, Antoni W Morawski, Rafał J Wróbel, and Beata Michalkiewicz. 2015. "Comparison of optimized isotherm models and error functions for carbon dioxide adsorption on activated carbon." *Journal of Chemical & Engineering Data* no. 60:3148-3158.

Stango, S Arul Xavier, and U Vijayalakshmi. 2019. "Synthesis and characterization of hydroxyapatite/carboxylic acid functionalized MWCNTS composites and its triple layer coatings for biomedical applications." *Ceramics International* no. 45:69-81.

Stasinakis, Athanasios S, Smaragdi Mermigka, Vasilios G Samaras, Eleni Farmaki, and Nikolaos S Thomaidis. 2012. "Occurrence of endocrine disrupters and selected pharmaceuticals in Aisonas River (Greece) and environmental risk assessment using hazard indexes." *Environmental Science and Pollution Research* no. 19:1574-1583.

Stepien, DK, J Regnery, Christoph Merz, and W Püttmann. 2013. "Behavior of organophosphates and hydrophilic ethers during bank filtration and their potential application as organic tracers. A field study from the Oderbruch, Germany." *Science of the Total Environment* no. 458:150-159.

Su, Pengchen, Anrui Zhang, Long Yu, Hongwei Ge, Ning Wang, Shuyi Huang, Yuejie Ai, Xiangke Wang, and Suhua Wang. 2022. "Dual-functional UiO-type metal-organic frameworks for the sensitive sensing and effective removal of nitrofurans from water." *Sensors and Actuators B: Chemical* no. 350:130865.

Subedi, Bikram, Keshava Balakrishna, Derrick Ian Joshua, and Kurunthachalam Kannan. 2017. "Mass loading and removal of pharmaceuticals and personal care products including psychoactives, antihypertensives, and antibiotics in two sewage treatment plants in southern India." *Chemosphere* no. 167:429-437.

Subedi, Bikram, Neculai Codru, David M Dziewulski, Lloyd R Wilson, Jingchuan Xue, Sehun Yun, Ellen Braun-Howland, Christine Minihane, and Kurunthachalam Kannan. 2015. "A pilot study on the assessment of trace organic contaminants including pharmaceuticals and personal care products from on-site wastewater treatment systems along Skaneateles Lake in New York State, USA." *Water Research* no. 72:28-39.

Sumida, Kenji, David L Rogow, Jarad A Mason, Thomas M McDonald, Eric D Bloch, Zoey R Herm, Tae-Hyun Bae, and Jeffrey R Long. 2012. "Carbon

dioxide capture in metal–organic frameworks." *Chemical Reviews* no. 112:724-781.

Surapathi, Anil, Jose Herrera-Alonso, Feras Rabie, Steve Martin, and Eva Marand. 2011. "Fabrication and gas transport properties of SWNT/polyacrylic nanocomposite membranes." *Journal of Membrane Science* no. 375:150-156.

Susantyoko, Rahmat Agung, Zainab Karam, Sara Alkhoori, Ibrahim Mustafa, Chieh-Han Wu, and Saif Almheiri. 2017. "A surface-engineered tape-casting fabrication technique toward the commercialisation of freestanding carbon nanotube sheets." *Journal of Materials Chemistry A* no. 5:19255-19266.

Svalina, Ilija, Goran Simunovic, and Katica Simunovic. 2013. "Machined surface roughness prediction using adaptive neurofuzzy inference system." *Applied Artificial Intelligence* no. 27:803-817.

Sweetman, Martin J, Steve May, Nick Mebberson, Phillip Pendleton, Krasimir Vasilev, Sally E Plush, and John D Hayball. 2017. "Activated carbon, carbon nanotubes and graphene: materials and composites for advanced water purification." *Carbon* no. 3:18.

Szabó, Andrea, Caterina Perri, Anita Csató, Girolamo Giordano, Danilo Vuono, and János B Nagy. 2010. "Synthesis methods of carbon nanotubes and related materials." *Materials* no. 3:3092-3140.

Tabelin, Carlito Baltazar, Toshifumi Igarashi, Mylah Villacorte-Tabelin, Ilhwan Park, Einstine M Opiso, Mayumi Ito, and Naoki Hiroyoshi. 2018. "Arsenic, selenium, boron, lead, cadmium, copper, and zinc in naturally contaminated rocks: A review of their sources, modes of enrichment, mechanisms of release, and mitigation strategies." *Science of the Total Environment* no. 645:1522-1553.

Taheri, M, MR Alavi Moghaddam, and M Arami. 2013. "Techno-economical optimization of Reactive Blue 19 removal by combined electrocoagulation/coagulation process through MOPSO using RSM and ANFIS models." *Journal of Environmental Management* no. 128:798-806.

Tang, Ye, Suhua Zhang, Yinglong Su, Dong Wu, Yaping Zhao, and Bing Xie. 2021. "Removal of microplastics from aqueous solutions by magnetic carbon nanotubes." *Chemical Engineering Journal* no. 406:126804.

Tarpø, Marius, Tobias Friis, Peter Olsen, Martin Juul, Christos Georgakis, and Rune Brincker. 2019. "Automated reduction of statistical errors in the

estimated correlation function matrix for operational modal analysis." *Mechanical Systems and Signal Processing* no. 132:790-805.

Terrones, Mauricio. 2010. "Sharpening the chemical scissors to unzip carbon nanotubes: crystalline graphene nanoribbons." *ACS Nano* no. 4:1775-1781.

Tetreault, Gerald R, C James Bennett, Carl Cheng, Mark R Servos, and Mark E McMaster. 2012. "Reproductive and histopathological effects in wild fish inhabiting an effluent-dominated stream, Wascana Creek, SK, Canada." *Aquatic Toxicology* no. 110:149-161.

Thamaraiselvan, Chidambaram, Sofia Lerman, Kamira Weinfeld-Cohen, and Carlos G Dosoretz. 2018. "Characterization of a support-free carbon nanotube-microporous membrane for water and wastewater filtration." *Separation and Purification Technology* no. 202:1-8.

Thamaraiselvan, Chidambaram, Jingbo Wang, Dustin K James, Pradnya Narkhede, Swatantra P Singh, David Jassby, James M Tour, and Christopher J Arnusch. 2020. "Laser-induced graphene and carbon nanotubes as conductive carbon-based materials in environmental technology." *Materials Today* no. 34:115-131.

Theerthagiri, Jayaraman, K Karuppasamy, Seung Jun Lee, R Shwetharani, Hyun-Seok Kim, SK Khadheer Pasha, Muthupandian Ashokkumar, and Myong Yong Choi. 2022. "Fundamentals and comprehensive insights on pulsed laser synthesis of advanced materials for diverse photo-and electrocatalytic applications." *Light: Science & Applications* no. 11:250.

Thines, RK, NM Mubarak, Sabzoi Nizamuddin, JN Sahu, EC Abdullah, and P Ganesan. 2017. "Application potential of carbon nanomaterials in water and wastewater treatment: a review." *Journal of the Taiwan Institute of Chemical Engineers* no. 72:116-133.

Thou, Chin Zhen, Fahad Saleem Ahmed Khan, NM Mubarak, Awais Ahmad, Mohammad Khalid, Priyanka Jagadish, Rashmi Walvekar, EC Abdullah, Safia Khan, and Mariam Khan. 2021. "Surface charge on chitosan/cellulose nanowhiskers composite via functionalized and untreated carbon nanotube." *Arabian Journal of Chemistry* no. 14:103022.

Topal, Murat, and E Işıl Arslan Topal. 2020. "Optimization of tetracycline removal with chitosan obtained from mussel shells using RSM." *Journal of Industrial and Engineering Chemistry* no. 84:315-321.

Tosun, Jale, Simon Schaub, and Andreas Fleig. 2020. "What determines regulatory preferences? Insights from micropollutants in surface waters." *Environmental Science & Policy* no. 106:136-144.

Toudeshki, Reza Mohammadi, Shayessteh Dadfarnia, and Ali Mohammad Haji Shabani. 2019. "Surface molecularly imprinted polymer on magnetic multi-walled carbon nanotubes for selective recognition and preconcentration of metformin in biological fluids prior to its sensitive chemiluminescence determination: Central composite design optimization." *Analytica Chimica Acta* no. 1089:78-89.

Tran, Hai Nguyen, Sheng-Jie You, and Huan-Ping Chao. 2016. "Effect of pyrolysis temperatures and times on the adsorption of cadmium onto orange peel derived biochar." *Waste Management & Research* no. 34:129-138.

Triebskorn, R, H Casper, A Heyd, R Eikemper, H-R Köhler, and J Schwaiger. 2004. "Toxic effects of the non-steroidal anti-inflammatory drug diclofenac: Part II. Cytological effects in liver, kidney, gills and intestine of rainbow trout (Oncorhynchus mykiss)." *Aquatic Toxicology* no. 68:151-166.

Truong, Lisa, Skylar Marvel, David M Reif, Dennis G Thomas, Paritosh Pande, Subham Dasgupta, Michael T Simonich, Katrina M Waters, and Robyn L Tanguay. 2020. "The multi-dimensional embryonic zebrafish platform predicts flame retardant bioactivity." *Reproductive Toxicology* no. 96:359-369.

Tsui, Mirabelle MP, HW Leung, Paul KS Lam, and Margaret B Murphy. 2014. "Seasonal occurrence, removal efficiencies and preliminary risk assessment of multiple classes of organic UV filters in wastewater treatment plants." *Water Research* no. 53:58-67.

Tung, Tran Minh, and Zaher Mundher Yaseen. 2020. "A survey on river water quality modelling using artificial intelligence models: 2000–2020." *Journal of Hydrology* no. 585:124670.

Turgunov, Muhammad Ali, and H Hyo Noh. 2017. "C-CVD Grown MWCNTs disclosure of defects by influence of drying condition on carboxyl functionalized structure." *Journal of Nanotechnology Material Science* no. 4:1-9.

Uçar, Tamer, Adem Karahoca, and Dilek Karahoca. 2013. "Tuberculosis disease diagnosis by using adaptive neuro fuzzy inference system and rough sets." *Neural Computing and Applications* no. 23:471-483.

Uheida, Abdusalam, Alaa Mohamed, Majdouline Belaqziz, and Walaa S Nasser. 2019. "Photocatalytic degradation of Ibuprofen, Naproxen, and Cetirizine using PAN-MWCNT nanofibers crosslinked TiO2-NH2 nanoparticles under visible light irradiation." *Separation and Purification Technology* no. 212:110-118.

Union, Ejojeul. 2012. "Regulation (EU) No 528/2012 of the European Parliament and of the Council of 22 May 2012 concerning the making available on the market and use of biocidal products." *Official Journal of European Union Lex* no. 167:1-116.

Van der Bruggen, Bart, and Carlo Vandecasteele. 2003. "Removal of pollutants from surface water and groundwater by nanofiltration: overview of possible applications in the drinking water industry." *Environmental Pollution* no. 122:435-445.

Van der Meer, Thomas P, Francisco Artacho-Cordón, Dick F Swaab, Dicky Struik, Konstantinos C Makris, Bruce HR Wolffenbuttel, Hanne Frederiksen, and Jana V van Vliet-Ostaptchouk. 2017. "Distribution of non-persistent endocrine disruptors in two different regions of the human brain." *International Journal of Environmental Research and Public Health* no. 14:1059.

Vasilachi, Ionela Cătălina, Dana Mihaela Asiminicesei, Daniela Ionela Fertu, and Maria Gavrilescu. 2021. "Occurrence and fate of emerging pollutants in water environment and options for their removal." *Water* no. 13:181.

Vatanpour, Vahid, and Naser Zoqi. 2017. "Surface modification of commercial seawater reverse osmosis membranes by grafting of hydrophilic monomer blended with carboxylated multiwalled carbon nanotubes." *Applied Surface Science* no. 396:1478-1489.

Vedamanikam, VJ, and NAM Shazilli. 2008. "Comparative toxicity of nine metals to two Malaysian aquatic dipterian larvae with reference to temperature variation." *Bulletin of Environmental Contamination and Toxicology* no. 80:516-520.

Venegas, María, Ana María Leiva, Carolina Reyes-Contreras, Patricio Neumann, Benjamín Piña, and Gladys Vidal. 2021. "Presence and fate of micropollutants during anaerobic digestion of sewage and their implications for the circular economy: A short review." *Journal of Environmental Chemical Engineering* no. 9:104931.

Vilardi, Giorgio, Thanasis Mpouras, Dimitris Dermatas, Nicola Verdone, Angeliki Polydera, and Luca Di Palma. 2018. "Nanomaterials application for heavy metals recovery from polluted water: The combination of nano zero-valent iron and carbon nanotubes. Competitive adsorption non-linear modeling." *Chemosphere* no. 201:716-729.

Vilk Ayalon, Naama, Lior Segev, Abraham O Samson, Simcha Yagel, Sarah M Cohen, Tamar Green, and Hila Hochler. 2022. "Norethisterone Reduces Vaginal Bleeding Caused by Progesterone-Only Birth Control Pills." *Journal of Clinical Medicine* no. 11:3389.

Vinas, P, N Campillo, L Carrasco, and M Hernández-Córdoba. 2007. "Analysis of nitrofuran residues in animal feed using liquid chromatography and photodiode-array detection." *Chromatographia* no. 65:85-89.

Vulliet, Emmanuelle, and Cécile Cren-Olivé. 2011. "Screening of pharmaceuticals and hormones at the regional scale, in surface and groundwaters intended to human consumption." *Environmental Pollution* no. 159:2929-2934.

Vyavahare, Govind D, Ranjit G Gurav, Pooja P Jadhav, Ravishankar R Patil, Chetan B Aware, and Jyoti P Jadhav. 2018. "Response surface methodology optimization for sorption of malachite green dye on sugarcane bagasse biochar and evaluating the residual dye for phyto and cytogenotoxicity." *Chemosphere* no. 194:306-315.

Walia, Navneet, Harsukhpreet Singh, and Anurag Sharma. 2015. "ANFIS: Adaptive neuro-fuzzy inference system-a survey." *International Journal of Computer Applications* no. 123.

Wang, Chuan, Honglan Shi, Craig D Adams, Sanjeewa Gamagedara, Isaac Stayton, Terry Timmons, and Yinfa Ma. 2011. "Investigation of pharmaceuticals in Missouri natural and drinking water using high performance liquid chromatography-tandem mass spectrometry." *Water Research* no. 45:1818-1828.

Wang, Fei, Weiling Sun, Weiyi Pan, and Nan Xu. 2015. "Adsorption of sulfamethoxazole and 17β-estradiol by carbon nanotubes/CoFe2O4 composites." *Chemical Engineering Journal* no. 274:17-29.

Wang, Jianlong, and Xuan Guo. 2020. "Adsorption isotherm models: Classification, physical meaning, application and solving method." *Chemosphere* no. 258:127279.

Wang, Jingjing, Sen Lin, Na Tian, Tianyi Ma, Yihe Zhang, and Hongwei Huang. 2021. "Nanostructured metal sulfides: classification, modification strategy, and solar-driven CO2 reduction application." *Advanced Functional Materials* no. 31:2008008.

Wang, Qian, and Barry C Kelly. 2017. "Occurrence and distribution of synthetic musks, triclosan and methyl triclosan in a tropical urban catchment: Influence of land-use proximity, rainfall and physicochemical properties." *Science of the Total Environment* no. 574:1439-1447.

Wang, Zhenyu, Xiaodong Yu, Bo Pan, and Baoshan Xing. 2010. "Norfloxacin sorption and its thermodynamics on surface-modified carbon nanotubes." *Environmental Science & Technology* no. 44:978-984.

Wang, Zhifang, Sainan Zhang, Yao Chen, Zhenjie Zhang, and Shengqian Ma. 2020. "Covalent organic frameworks for separation applications." *Chemical Society Reviews* no. 49:708-735.

Warner, Wiebke, Tobias Licha, and Karsten Nödler. 2019. "Qualitative and quantitative use of micropollutants as source and process indicators. A review." *Science of the Total Environment* no. 686:75-89.

Warsinger, David M, Sudip Chakraborty, Emily W Tow, Megan H Plumlee, Christopher Bellona, Savvina Loutatidou, Leila Karimi, Anne M Mikelonis, Andrea Achilli, and Abbas Ghassemi. 2018. "A review of polymeric membranes and processes for potable water reuse." *Progress in Polymer Science* no. 81:209-237.

Wei, Shuhui, and Ali Reza Kamali. 2021. "Waste plastic derived Co3Fe7/CoFe2O4@ carbon magnetic nanostructures for efficient dye adsorption." *Journal of Alloys and Compounds* no. 886:161201.

Wei, Xiucheng, Zhiwei Wei, Liping Zhang, Yingqi Liu, and Deyan He. 2011. "Highly water-soluble nanocrystal powders of magnetite and maghemite coated with gluconic acid: Preparation, structure characterization, and surface coordination." *Journal of Colloid and Interface Science* no. 354:76-81.

Wei, Zhimei, Minle Peng, Fang Qiu, Xiaojun Wang, and Jie Yang. 2015. "Development of a novel preparation method for conductive PES ultrafine

fibers with self-formed thin PES/CNTs composite layer by vapor treatment." *RSC Advances* no. 5:42305-42310.

Weinberger II, Joel, and Rebecca Klaper. 2014. "Environmental concentrations of the selective serotonin reuptake inhibitor fluoxetine impact specific behaviors involved in reproduction, feeding and predator avoidance in the fish Pimephales promelas (fathead minnow)." *Aquatic Toxicology* no. 151:77-83.

Werber, Jay R, Chinedum O Osuji, and Menachem Elimelech. 2016. "Materials for next-generation desalination and water purification membranes." *Nature Reviews Materials* no. 1:1-15.

Westerhoff, Paul, Pedro Alvarez, Qilin Li, Jorge Gardea-Torresdey, and Julie Zimmerman. 2016. "Overcoming implementation barriers for nanotechnology in drinking water treatment." *Environmental Science: Nano* no. 3:1241-1253.

White, Christopher M, Richard Banks, Ian Hamerton, and John F Watts. 2016. "Characterisation of commercially CVD grown multi-walled carbon nanotubes for paint applications." *Progress in Organic Coatings* no. 90:44-53.

Whitelam, Stephen, and Robert L Jack. 2015. "The statistical mechanics of dynamic pathways to self-assembly." *Annual Review of Physical Chemistry* no. 66:143-163.

Wind, Thorsten. 2007. "Detergent phosphates and their environmental relevance in future European perspectives." *Tenside Surfactants Detergents* no. 44:19-24.

Włodarczyk-Makuła, Maria, Ewa Wiśniowska, and Agnieszka Popenda. 2018. "Monitoring of Organic Micropollutants in Effluents as Crucial Tool in Sustainable Development." *Problemy Ekorozwoju* no. 13.

Wu, Donghai, Jingjing Yao, Guanghua Lu, Fuli Liu, Chao Zhou, Pei Zhang, and Matthew Nkoom. 2017. "Adsorptive removal of aqueous bezafibrate by magnetic ferrite modified carbon nanotubes." *RSC Advances* no. 7:39594-39603.

Wu, Hao, Xiaojun Niu, Jia Yang, Caihong Wang, and Meiqing Lu. 2016. "Retentions of bisphenol A and norfloxacin by three different ultrafiltration membranes in regard to drinking water treatment." *Chemical Engineering Journal* no. 294:410-416.

Wurendaodi, W, J Dujiya, S Zhao, H Wu, and S Asuha. 2017. "Thermal transformation of water-dispersible magnetite nanoparticles: Synthesis of

water-dispersible maghemite nanoparticles." *Journal of Thermal Analysis and Calorimetry* no. 130:681-688.

Xia, Mingfang, Aimin Li, Zhaolian Zhu, Qin Zhou, and Weiben Yang. 2013. "Factors influencing antibiotics adsorption onto engineered adsorbents." *Journal of Environmental Sciences* no. 25:1291-1299.

Xia, Qianshan, Zhichun Zhang, Yanju Liu, and Jinsong Leng. 2020. "Buckypaper and its composites for aeronautic applications." *Composites Part B: Engineering* no. 199:108231.

Xiong, Weiping, Guangming Zeng, Zhaohui Yang, Yaoyu Zhou, Chen Zhang, Min Cheng, Yang Liu, Liang Hu, Jia Wan, and Chengyun Zhou. 2018. "Adsorption of tetracycline antibiotics from aqueous solutions on nanocomposite multi-walled carbon nanotube functionalized MIL-53 (Fe) as new adsorbent." *Science of the Total Environment* no. 627:235-244.

Xu, Guanghui, Qiang Zhang, Weiping Zhou, Jiaqi Huang, and Fei Wei. 2008. "The feasibility of producing MWCNT paper and strong MWCNT film from VACNT array." *Applied Physics A* no. 92:531-539.

Xu, Rui, Wei Qin, Zeshen Tian, Yuan He, Xiaomao Wang, and Xianghua Wen. 2020. "Enhanced micropollutants removal by nanofiltration and their environmental risks in wastewater reclamation: A pilot-scale study." *Science of the Total Environment* no. 744:140954.

Xue, Xing-yan, Rong Cheng, Lei Shi, Zhong Ma, and Xiang Zheng. 2017. "Nanomaterials for water pollution monitoring and remediation." *Environmental Chemistry Letters* no. 15:23-27.

Yampolskii, Yu, N Belov, and A Alentiev. 2020. "Perfluorinated polymers as materials of membranes for gas and vapor separation." *Journal of Membrane Science* no. 598:117779.

Yan, Kang-Kang, Lei Jiao, Saisai Lin, Xiaosheng Ji, Yin Lu, and Lin Zhang. 2018. "Superhydrophobic electrospun nanofiber membrane coated by carbon nanotubes network for membrane distillation." *Desalination* no. 437:26-33.

Yan, Wentao, Mengqi Shi, Chenxi Dong, Lifen Liu, and Congjie Gao. 2020. "Applications of tannic acid in membrane technologies: A review." *Advances in Colloid and Interface Science* no. 284:102267.

Yañez-Macias, Roberto, Ernesto Hernandez-Hernandez, Carlos A Gallardo-Vega, Raquel Ledezma-Rodríguez, Ronald F Ziolo, Yucundo Mendoza-

Tolentino, Salvador Fernández-Tavizon, Carlos A Avila-Orta, Zureima Garcia-Hernandez, and Pablo Gonzalez-Morones. 2019. "Covalent grafting of unfunctionalized pristine MWCNT with Nylon-6 by microwave assist in-situ polymerization." *Polymer* no. 185:121946.

Yang, Gang, Zhanghong Wang, Qiming Xian, Fei Shen, Cheng Sun, Yanzong Zhang, and Jun Wu. 2015. "Effects of pyrolysis temperature on the physicochemical properties of biochar derived from vermicompost and its potential use as an environmental amendment." *RSC Advances* no. 5:40117-40125.

Yang, Jia-Ying, Xin-Yu Jiang, Fei-Peng Jiao, and Jin-Gang Yu. 2018. "The oxygen-rich pentaerythritol modified multi-walled carbon nanotube as an efficient adsorbent for aqueous removal of alizarin yellow R and alizarin red S." *Applied Surface Science* no. 436:198-206.

Yang, Jianlei, Yern Chee Ching, and Kiwao Kadokami. 2022. "Occurrence and exposure risk assessment of organic micropollutants in indoor dust from Malaysia." *Chemosphere* no. 287:132340.

Yang, Xiaoshuang, Jieun Lee, Lixiang Yuan, So-Ryong Chae, Vanessa K Peterson, Andrew I Minett, Yongbai Yin, and Andrew T Harris. 2013. "Removal of natural organic matter in water using functionalised carbon nanotube buckypaper." *Carbon* no. 59:160-166.

Yang, Yinjie, Zhongli Chen, Jialing Zhang, Siqi Wu, Li Yang, Lin Chen, and Ying Shao. 2021. "The challenge of micropollutants in surface water of the Yangtze River." *Science of the Total Environment* no. 780:146537.

Yang, Zhe, Peng-Fei Sun, Xianhui Li, Bowen Gan, Li Wang, Xiaoxiao Song, Hee-Deung Park, and Chuyang Y Tang. 2020. "A critical review on thin-film nanocomposite membranes with interlayered structure: mechanisms, recent developments, and environmental applications." *Environmental Science & Technology* no. 54:15563-15583.

Yashima, Eiji, Naoki Ousaka, Daisuke Taura, Kouhei Shimomura, Tomoyuki Ikai, and Katsuhiro Maeda. 2016. "Supramolecular helical systems: helical assemblies of small molecules, foldamers, and polymers with chiral amplification and their functions." *Chemical Reviews* no. 116:13752-13990.

Yee, Kian Fei, Yit Thai Ong, Abdul Rahman Mohamed, and Soon Huat Tan. 2014. "Novel MWCNT-buckypaper/polyvinyl alcohol asymmetric membrane

for dehydration of etherification reaction mixture: Fabrication, characterisation and application." *Journal of Membrane Science* no. 453:546-555.

Yee, Min Juey, NM Mubarak, Mohammad Khalid, EC Abdullah, and Priyanka Jagadish. 2018. "Synthesis of polyvinyl alcohol (PVA) infiltrated MWCNTs buckypaper for strain sensing application." *Scientific Reports* no. 8:17295.

Yi, Yunfeng, Ying Zhang, Yixiao Wang, Lihua Shen, Mengmeng Jia, Yu Huang, Zhenqing Hou, and Guohong Zhuang. 2014. "Ethylenediaminetetraacetic acid as capping ligands for highly water-dispersible iron oxide particles." *Nanoscale Research Letters* no. 9:1-7.

Younis, Sherif A, and Yasser M Moustafa. 2017. "Synthesis of urea-modified MnFe 2 O 4 for aromatic micro-pollutants adsorption from wastewater: Mechanism and modeling." *Clean Technologies and Environmental Policy* no. 19:527-540.

Yousefi, Mahmood, Mitra Gholami, Vahide Oskoei, Ali Akbar Mohammadi, Mansour Baziar, and Ali Esrafili. 2021. "Comparison of LSSVM and RSM in simulating the removal of ciprofloxacin from aqueous solutions using magnetization of functionalized multi-walled carbon nanotubes: Process optimization using GA and RSM techniques." *Journal of Environmental Chemical Engineering* no. 9:105677.

Yu, Chenfei, Qiang Chen, Anqi Wang, Xi Zhou, Shishan Wu, and Qianping Ran. 2015. "Improved dispersibility of multi-wall carbon nanotubes with reversible addition–fragmentation chain transfer polymer modification." *Polymer International* no. 64:1219-1224.

Yu, Fei, Junhong Chen, Lu Chen, Jing Huai, Wenyi Gong, Zhiwen Yuan, Jinhe Wang, and Jie Ma. 2012. "Magnetic carbon nanotubes synthesis by Fenton's reagent method and their potential application for removal of azo dye from aqueous solution." *Journal of Colloid and Interface Science* no. 378:175-183.

Yu, Fei, Sainan Sun, Sheng Han, Jie Zheng, and Jie Ma. 2016. "Adsorption removal of ciprofloxacin by multi-walled carbon nanotubes with different oxygen contents from aqueous solutions." *Chemical Engineering Journal* no. 285:588-595.

Yu, Wansong, Yiqun Huang, Lu Pei, Yuxia Fan, Xiaohui Wang, and Keqiang Lai. 2014. "Magnetic Fe 3 O 4/Ag hybrid nanoparticles as surface-enhanced

raman scattering substrate for trace analysis of furazolidone in fish feeds." *Journal of Nanomaterials* no. 2014:103-103.

Zaib, Qammer, Iftheker A Khan, Navid B Saleh, Joseph RV Flora, Yong-Gyun Park, and Yeomin Yoon. 2012. "Removal of Bisphenol A and 17β-Estradiol by single-walled carbon nanotubes in aqueous solution: Adsorption and molecular modeling." *Water, Air, & Soil Pollution* no. 223:3281-3293.

Zaib, Qammer, Bilal Mansoor, and Farrukh Ahmad. 2013. "Photo-regenerable multi-walled carbon nanotube membranes for the removal of pharmaceutical micropollutants from water." *Environmental Science: Processes & Impacts* no. 15:1582-1589.

Zamora-Ledezma, Camilo, Daniela Negrete-Bolagay, Freddy Figueroa, Ezequiel Zamora-Ledezma, Ming Ni, Frank Alexis, and Victor H Guerrero. 2021. "Heavy metal water pollution: A fresh look about hazards, novel and conventional remediation methods." *Environmental Technology & Innovation* no. 22:101504.

Zdarta, Agata, Wojciech Smułek, Zuzanna Bielan, Jakub Zdarta, Luong N Nguyen, Agnieszka Zgoła-Grześkowiak, Long D Nghiem, Teofil Jesionowski, and Ewa Kaczorek. 2021. "Significance of the presence of antibiotics on the microbial consortium in wastewater–The case of nitrofurantoin and furazolidone." *Bioresource Technology* no. 339:125577.

Zdarta, Jakub, Teofil Jesionowski, Manuel Pinelo, Anne S Meyer, Hafiz MN Iqbal, Muhammad Bilal, Luong N Nguyen, and Long D Nghiem. 2022. "Free and immobilized biocatalysts for removing micropollutants from water and wastewater: Recent progress and challenges." *Bioresource Technology* no. 344:126201.

Zehua, Qu, and Wang Guojian. 2012. "Effective chemical oxidation on the structure of multiwalled carbon nanotubes." *Journal of Nanoscience and Nanotechnology* no. 12:105-111.

Zhang, Di, Bo Pan, Min Wu, Bin Wang, Huang Zhang, Hongbo Peng, Di Wu, and Ping Ning. 2011. "Adsorption of sulfamethoxazole on functionalized carbon nanotubes as affected by cations and anions." *Environmental Pollution* no. 159:2616-2621.

Zhang, Lei, Georgia C Papaefthymiou, and Jackie Y Ying. 2001. "Synthesis and properties of γ-Fe2O3 nanoclusters within mesoporous aluminosilicate matrices." *The Journal of Physical Chemistry B* no. 105:7414-7423.

Zhang, Lei, Bin Zhao, Chuan Jiang, Junhe Yang, and Guangping Zheng. 2015. "Preparation and transport performances of high-density, aligned carbon nanotube membranes." *Nanoscale Research Letters* no. 10:1-8.

Zhang, Lin, Junling Chen, Yasun Wang, Fangming Ren, Wen Yu, and Linan Cheng. 2009. "Pregnancy outcome after levonorgestrel-only emergency contraception failure: a prospective cohort study." *Human Reproduction* no. 24:1605-1611.

Zhang, Songlin, Nam Nguyen, Branden Leonhardt, Claire Jolowsky, Ayou Hao, Jin Gyu Park, and Richard Liang. 2019. "Carbon-nanotube-based electrical conductors: fabrication, optimization, and applications." *Advanced Electronic Materials* no. 5:1800811.

Zhang, Xiang, Naiqin Zhao, and Chunnian He. 2020. "The superior mechanical and physical properties of nanocarbon reinforced bulk composites achieved by architecture design–a review." *Progress in Materials Science* no. 113:100672.

Zhao, Shuaifei, Zhipeng Liao, Anthony Fane, Jiansheng Li, Chuyang Tang, Chunmiao Zheng, Jiuyang Lin, and Lingxue Kong. 2021. "Engineering antifouling reverse osmosis membranes: A review." *Desalination* no. 499:114857.

Zhao, Tingkai, Xianglin Ji, Xinai Guo, Wenbo Jin, Alei Dang, Hao Li, and Tiehu Li. 2016. "Preparation and electrochemical property of Fe3O4/MWCNT nanocomposite." *Chemical Physics Letters* no. 653:202-206.

Zhao, Xia, Zhong-lin Chen, Xiao-chun Wang, Ji-min Shen, and Hao Xu. 2014. "PPCPs removal by aerobic granular sludge membrane bioreactor." *Applied Microbiology and Biotechnology* no. 98:9843-9848.

Zhen-Yuan, Zhao, and Xiong Zhen-Hu. 2015. "Removal of four nitrofurans drugs from aqueous solution by magnetic multi-wall carbon nanotubes." *Fullerenes, Nanotubes and Carbon Nanostructures* no. 23:640-648.

Zhou, Jian, Shuai Huang, and Yingui Qiu. 2022. "Optimization of random forest through the use of MVO, GWO and MFO in evaluating the stability of underground entry-type excavations." *Tunnelling and Underground Space Technology* no. 124:104494.

Zhou, Lincheng, Liqin Ji, Peng-Cheng Ma, Yanming Shao, He Zhang, Weijie Gao, and Yanfeng Li. 2014. "Development of carbon nanotubes/CoFe2O4 magnetic hybrid material for removal of tetrabromobisphenol A and Pb (II)." *Journal of Hazardous Materials* no. 265:104-114.

Zhou, Shengguo, Xiaobo Zhu, Liqiu Ma, Qingqing Yan, and Shuncai Wang. 2018. "Outstanding superhydrophobicity and corrosion resistance on carbon-based film surfaces coupled with multi-walled carbon nanotubes and nickel nano-particles." *Surface Science* no. 677:193-202.

Zhou, Shiqing, Yisheng Shao, Naiyun Gao, Jing Deng, and Chaoqun Tan. 2013. "Equilibrium, kinetic, and thermodynamic studies on the adsorption of triclosan onto multi-walled carbon nanotubes." *Clean–Soil, Air, Water* no. 41:539-547.

Zhou, YX, PX Wu, ZY Cheng, J Ingram, and S Jeelani. 2008. "Improvement in electrical, thermal and mechanical properties of epoxy by filling carbon nanotube." *Express Polymer Letters* no. 2:40-48.

Zhu, H-Y, R Jiang, S-H Huang, J Yao, F-Q Fu, and J-B Li. 2015. "Novel magnetic NiFe2O4/multi-walled carbon nanotubes hybrids: facile synthesis, characterization, and application to the treatment of dyeing wastewater." *Ceramics International* no. 41:11625-11631.

Zhu, Hongwei, and Bingqing Wei. 2008. "Assembly and applications of carbon nanotube thin films." *Journal of Materials Science & Technology* no. 24:447.

Zhu, Qiaohong, Qing Xu, Mengmeng Du, Xiaofei Zeng, Guofu Zhong, Bocheng Qiu, and Jinlong Zhang. 2022. "Recent progress of metal sulfide photocatalysts for solar energy conversion." *Advanced Materials* no. 34:2202929.

Zorita, Saioa, Lennart Mårtensson, and Lennart Mathiasson. 2009. "Occurrence and removal of pharmaceuticals in a municipal sewage treatment system in the south of Sweden." *Science of the Total Environment* no. 407:2760-2770.

COPYRIGHT MATERIAL

SUPPLEMENTARY DATA

APPENDIX A

Tab. A.1: Physicochemical properties of furazolidone

Generic Name
Furazolidone
Summary
It is a nitrofuran anti-microbial agent, generally used for the treatment of diarrhea/ enteritis caused by protozoan/ bacterial infections. Besides, it also possess anti-protozoal and anti-bacterial characteristics, thus also used for cholera and giardiasis treatment.
Structure
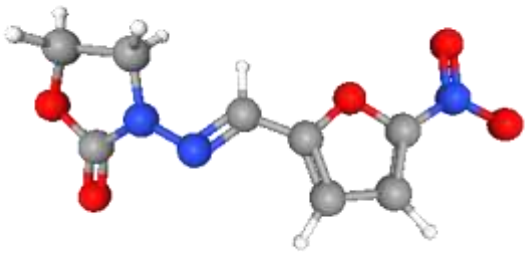
Chemical Formula
$C_8H_7N_3O_5$
International Union of Pure and Applied Chemistry (IUPAC) name
3-[(E)-[(5-Nitro-2-furyl) methylene] amino]-1, 3- oxazolidine-2-one
Synonym
Furazolidona, furazolidonum, nirofurazolidonium, nitrofuroxon
Weight
Average: 225.16 Mono-isotopic: 225.038570337
Physical Colour
Yellow odorless solid
Maximum absorption wavelength, λ_{max} (nm)
356
Solubility in water
40 mg/L at 25 ºC (pH 6)

Tab. A.2: FZD micropollutant concentration standard curve

Concentration of FZD micropollutant (mg/L)	**Average Absorbance λ_{max} (nm)**
0	0
5	0.15
10	0.29
15	0.43
20	0.605
25	0.765

APPENDIX B

Tab. B.1: Experimental design matrix for FZD removal efficiency

Run	Initial pH	Agitation speed (rpm)	Contact time (min.)	FZD removal efficiency (%)
1	4	200	20	35.82
2	8	200	20	56.71
3	6	150	185	87.6
4	4	100	350	92.59
5	8	200	350	87.99
6	6	150	350	89.3
7	4	100	20	31.62
8	8	150	185	73.14
9	6	100	185	81.68
10	8	100	350	86.54
11	4	100	20	44.59
12	8	100	350	89.12
13	6	200	350	98.74
14	4	200	20	45.95
15	4	150	185	49.36
16	8	200	20	63.97
17	4	200	350	87.07
18	6	200	185	86.41
19	8	100	20	76.43
20	8	100	20	77.56
21	6	150	20	68.41
22	8	200	350	87.99
23	4	200	350	89.49
24	4	100	350	92.59

APPENDIX C

Source codes, Functions and System Files

C.1: Training, Testing and Output Data

```
>>fuzzy
>>dataTraining= [];
```

Tab. C.1: ANFIS training data

pH	Agitation speed (rpm)	Time (min.)	Removal %
4	200	20	35.82
8	200	20	56.71
6	150	185	87.6
4	100	350	92.59
8	200	350	87.99
6	150	350	89.3
4	100	20	31.62
8	150	185	73.14
6	100	185	81.68
8	100	350	86.54
4	100	20	44.59
8	100	350	89.12
6	200	350	98.74
4	200	20	45.95
4	150	185	49.36
8	200	20	63.97
4	200	350	87.07
6	200	185	86.41
8	100	20	76.43
8	100	20	77.56
6	150	20	68.41
8	200	350	87.99
4	200	350	89.49
4	100	350	92.59
4	200	20	35.82
8	200	20	56.71
6	150	185	87.6
4	100	350	92.59

pH	Agitation speed (rpm)	Time (min.)	Removal %
8	200	350	87.99
6	150	350	89.3
4	100	20	31.62
8	150	185	73.14
6	100	185	81.68
8	100	350	86.54
4	100	20	44.59
8	100	350	89.12
6	200	350	98.74
4	200	20	45.95
4	150	185	49.36
8	200	20	63.97
4	200	350	87.07
6	200	185	86.41
8	100	20	76.43
8	100	20	77.56
6	150	20	68.41
8	200	350	87.99
4	200	350	89.49
4	100	350	92.59
4	200	20	35.82
8	200	20	56.71
6	150	185	87.6
4	100	350	92.59
8	200	350	87.99
6	150	350	89.3
4	100	20	31.62
8	150	185	73.14
6	100	185	81.68
8	100	350	86.54
4	100	20	44.59
8	100	350	89.12
6	200	350	98.74
4	200	20	45.95
4	150	185	49.36
8	200	20	63.97
4	200	350	87.07
6	200	185	86.41
8	100	20	76.43
8	100	20	77.56

pH	Agitation speed (rpm)	Time (min.)	Removal %
6	150	20	68.41
8	200	350	87.99
4	200	350	89.49
4	100	350	92.59
4	200	20	35.82
8	200	20	56.71
6	150	185	87.6
4	100	350	92.59
8	200	350	87.99
6	150	350	89.3
4	100	20	31.62
8	150	185	73.14
6	100	185	81.68
8	100	350	86.54
4	100	20	44.59
8	100	350	89.12
6	200	350	98.74
4	200	20	45.95
4	150	185	49.36
8	200	20	63.97
4	200	350	87.07
6	200	185	86.41
8	100	20	76.43
8	100	20	77.56
6	150	20	68.41
8	200	350	87.99
4	200	350	89.49
4	100	350	92.59
4	200	20	35.82
8	200	20	56.71
6	150	185	87.6
4	100	350	92.59
8	200	350	87.99
6	150	350	89.3
4	100	20	31.62
8	150	185	73.14
6	100	185	81.68
8	100	350	86.54
4	100	20	44.59
8	100	350	89.12

pH	Agitation speed (rpm)	Time (min.)	Removal %
6	200	350	98.74
4	200	20	45.95
4	150	185	49.36
8	200	20	63.97
4	200	350	87.07
6	200	185	86.41
8	100	20	76.43
8	100	20	77.56
6	150	20	68.41
8	200	350	87.99
4	200	350	89.49
4	100	350	92.59
4	200	20	35.82
8	200	20	56.71
6	150	185	87.6
4	100	350	92.59
8	200	350	87.99
6	150	350	89.3
4	100	20	31.62
8	150	185	73.14
6	100	185	81.68
8	100	350	86.54
4	100	20	44.59
8	100	350	89.12
6	200	350	98.74
4	200	20	45.95
4	150	185	49.36
8	200	20	63.97
4	200	350	87.07
6	200	185	86.41
8	100	20	76.43
8	100	20	77.56
6	150	20	68.41
8	200	350	87.99
4	200	350	89.49
4	100	350	92.59

```
>> dataTesting= [];
```

Tab. C.2: ANFIS testing data

pH	Agitation speed (rpm)	Time (min.)	Removal %
4	200	20	35.82
8	200	20	56.71
6	150	185	87.6
4	100	350	92.59
8	200	350	87.99
6	150	350	89.3
4	100	20	31.62
8	150	185	73.14
6	100	185	81.68
8	100	350	86.54
4	100	20	44.59
8	100	350	89.12
6	200	350	98.74
4	200	20	45.95
4	150	185	49.36
8	200	20	63.97
4	200	350	87.07
6	200	185	86.41
8	100	20	76.43
8	100	20	77.56
6	150	20	68.41
8	200	350	87.99
4	200	350	89.49
4	100	350	92.59
4	200	20	35.82
8	200	20	56.71
6	150	185	87.6
4	100	350	92.59
8	200	350	87.99
6	150	350	89.3
4	100	20	31.62
8	150	185	73.14
6	100	185	81.68
8	100	350	86.54
4	100	20	44.59
8	100	350	89.12
6	200	350	98.74
4	200	20	45.95

4	150	185	49.36
8	200	20	63.97
4	200	350	87.07
6	200	185	86.41
8	100	20	76.43
8	100	20	77.56
6	150	20	68.41
8	200	350	87.99
4	200	350	89.49
4	100	350	92.59
4	200	20	35.82
8	200	20	56.71
6	150	185	87.6
4	100	350	92.59
8	200	350	87.99
6	150	350	89.3
4	100	20	31.62
8	150	185	73.14
6	100	185	81.68
8	100	350	86.54
4	100	20	44.59
8	100	350	89.12
6	200	350	98.74
4	200	20	45.95
4	150	185	49.36
8	200	20	63.97
4	200	350	87.07
6	200	185	86.41
8	100	20	76.43
8	100	20	77.56
6	150	20	68.41
8	200	350	87.99
4	200	350	89.49
4	100	350	92.59
4	200	20	35.82
8	200	20	56.71
6	150	185	87.6
4	100	350	92.59
8	200	350	87.99
6	150	350	89.3
4	100	20	31.62
8	150	185	73.14

6	100	185	81.68
8	100	350	86.54
4	100	20	44.59
8	100	350	89.12
6	200	350	98.74
4	200	20	45.95
4	150	185	49.36
8	200	20	63.97
4	200	350	87.07
6	200	185	86.41
8	100	20	76.43
8	100	20	77.56
6	150	20	68.41
8	200	350	87.99
4	200	350	89.49
4	100	350	92.59

```
>>dataOutput= [];
```

Tab. C.3: ANFIS output data

pH	Agitation speed (rpm)	Time (min.)
4	200	20
8	200	20
6	150	185
4	100	350
8	200	350
6	150	350
4	100	20
8	150	185
6	100	185
8	100	350
4	100	20
8	100	350
6	200	350
4	200	20
4	150	185
8	200	20
4	200	350
6	200	185
8	100	20
8	100	20
6	150	20

pH	Agitation speed (rpm)	Time (min.)
8	200	350
4	200	350
4	100	350
4	200	20
8	200	20
6	150	185
4	100	350
8	200	350
6	150	350
4	100	20
8	150	185
6	100	185
8	100	350
4	100	20
8	100	350
6	200	350
4	200	20
4	150	185
8	200	20
4	200	350
6	200	185
8	100	20
8	100	20
6	150	20
8	200	350
4	200	350
4	100	350
4	200	20
8	200	20
6	150	185
4	100	350
8	200	350
6	150	350
4	100	20
8	150	185
6	100	185
8	100	350
4	100	20
8	100	350
6	200	350
4	200	20

pH	Agitation speed (rpm)	Time (min.)
4	150	185
8	200	20
4	200	350
6	200	185
8	100	20
8	100	20
6	150	20
8	200	350
4	200	350
4	100	350
4	200	20
8	200	20
6	150	185
4	100	350
8	200	350
6	150	350
4	100	20
8	150	185
6	100	185
8	100	350
4	100	20
8	100	350
6	200	350
4	200	20
4	150	185
8	200	20
4	200	350
6	200	185
8	100	20
8	100	20
6	150	20
8	200	350
4	200	350
4	100	350
4	200	20
8	200	20
6	150	185
4	100	350
8	200	350
6	150	350
4	100	20

pH	Agitation speed (rpm)	Time (min.)
8	150	185
6	100	185
8	100	350
4	100	20
8	100	350
6	200	350
4	200	20
4	150	185
8	200	20
4	200	350
6	200	185
8	100	20
8	100	20
6	150	20
8	200	350
4	200	350
4	100	350
4	200	20
8	200	20
6	150	185
4	100	350
8	200	350
6	150	350
4	100	20
8	150	185
6	100	185
8	100	350
4	100	20
8	100	350
6	200	350
4	200	20
4	150	185
8	200	20
4	200	350
6	200	185
8	100	20
8	100	20
6	150	20
8	200	350
4	200	350
4	100	350

pH	Agitation speed (rpm)	Time (min.)
4	200	20
8	200	20
6	150	185
4	100	350
8	200	350
6	150	350
4	100	20
8	150	185
6	100	185
8	100	350
4	100	20
8	100	350
6	200	350
4	200	20
4	150	185
8	200	20
4	200	350
6	200	185
8	100	20
8	100	20
8	200	350
4	200	350
4	100	350
4	200	20
8	200	20
6	150	185
4	100	350
8	200	350
6	150	350
4	100	20
8	150	185
6	100	185
8	100	350
4	100	20
8	100	350
6	200	350
4	200	20
4	150	185
8	200	20
4	200	350
6	200	185

pH	Agitation speed (rpm)	Time (min.)
8	100	20
8	100	20
6	150	20
8	200	350
4	200	350
4	100	350
4	200	20
8	200	20
6	150	185
4	100	350
8	200	350
6	150	350
4	100	20
8	150	185
6	100	185
8	100	350
4	100	20
8	100	350
6	200	350
4	200	20
4	150	185
8	200	20
4	200	350
6	200	185
8	100	20
8	100	20
6	150	20
8	200	350
4	200	350
4	100	350
4	200	20
8	200	20
6	150	185
4	100	350
8	200	350
6	150	350
4	100	20
8	150	185
6	100	185
8	100	350
4	100	20

pH	Agitation speed (rpm)	Time (min.)
8	100	350
6	200	350
4	200	20
4	150	185
8	200	20
4	200	350
6	200	185
8	100	20
8	100	20
6	150	20
8	200	350
4	200	350
4	100	350
4	200	20
8	200	20
6	150	185
4	100	350
8	200	350
6	150	350
4	100	20
8	150	185
6	100	185
8	100	350
4	100	20
8	150	185
6	100	185
8	100	350
4	100	20
8	100	350
6	200	350
4	200	20
4	150	185
8	200	20
4	200	350
4	100	350

C.2: Epoch for Train and Testing

1. If (input1 is in1mf1) and (input2 is in2mf1) and (input3 is in3mf1) then (output is out1mf1) (1)

2. If (input1 is in1mf1) and (input2 is in2mf1) and (input3 is in3mf2) then (output is out1mf2) (1)

3. If (input1 is in1mf1) and (input2 is in2mf1) and (input3 is in3mf3) then (output is out1mf3) (1)

4. If (input1 is in1mf1) and (input2 is in2mf2) and (input3 is in3mf1) then (output is out1mf4) (1)

5. If (input1 is in1mf1) and (input2 is in2mf2) and (input3 is in3mf2) then (output is out1mf5) (1)

6. If (input1 is in1mf1) and (input2 is in2mf2) and (input3 is in3mf3) then (output is out1mf6) (1)

7. If (input1 is in1mf1) and (input2 is in2mf3) and (input3 is in3mf1) then (output is out1mf7) (1)

8. If (input1 is in1mf1) and (input2 is in2mf3) and (input3 is in3mf2) then (output is out1mf8) (1)

9. If (input1 is in1mf1) and (input2 is in2mf3) and (input3 is in3mf3) then (output is out1mf9) (1)

10. If (input1 is in1mf2) and (input2 is in2mf1) and (input3 is in3mf1) then (output is out1mf10) (1)

11. If (input1 is in1mf2) and (input2 is in2mf1) and (input3 is in3mf2) then (output is out1mf11) (1)

12. If (input1 is in1mf2) and (input2 is in2mf1) and (input3 is in3mf3) then (output is out1mf12) (1)

13. If (input1 is in1mf2) and (input2 is in2mf2) and (input3 is in3mf1) then (output is out1mf13) (1)

14. If (input1 is in1mf2) and (input2 is in2mf2) and (input3 is in3mf2) then (output is out1mf14) (1)

15. If (input1 is in1mf2) and (input2 is in2mf2) and (input3 is in3mf3) then (output is out1mf15) (1)

16. If (input1 is in1mf2) and (input2 is in2mf3) and (input3 is in3mf1) then (output is out1mf16) (1)

17. If (input1 is in1mf2) and (input2 is in2mf3) and (input3 is in3mf2) then (output is out1mf17) (1)

18. If (input1 is in1mf2) and (input2 is in2mf3) and (input3 is in3mf3) then (output is out1mf18) (1)

19. If (input1 is in1mf3) and (input2 is in2mf1) and (input3 is in3mf1) then (output is out1mf19) (1)

20. If (input1 is in1mf3) and (input2 is in2mf1) and (input3 is in3mf2) then (output is out1mf20) (1)

21. If (input1 is in1mf3) and (input2 is in2mf1) and (input3 is in3mf3) then (output is out1mf21) (1)

22. If (input1 is in1mf3) and (input2 is in2mf2) and (input3 is in3mf1) then (output is out1mf22) (1)

23. If (input1 is in1mf3) and (input2 is in2mf2) and (input3 is in3mf2) then (output is out1mf23) (1)

24. If (input1 is in1mf3) and (input2 is in2mf2) and (input3 is in3mf3) then (output is out1mf24) (1)

25. If (input1 is in1mf3) and (input2 is in2mf3) and (input3 is in3mf1) then (output is out1mf25) (1)

26. If (input1 is in1mf3) and (input2 is in2mf3) and (input3 is in3mf2) then (output is out1mf26) (1)

27. If (input1 is in1mf3) and (input2 is in2mf3) and (input3 is in3mf3) then (output is out1mf27) (1)

C.3: ANFIS Train and Testing

Minimal training RMSE = 2.651003

ANFIS info:
Number of nodes: 78
Number of linear parameters: 27
Number of nonlinear parameters: 27
Total number of parameters: 54
Number of training data pairs: 144
Number of checking data pairs: 0
Number of fuzzy rules: 27

Start training ANFIS ...

1 2.651
2 2.651

Designated epoch number reached --> ANFIS training completed at epoch 2.

Minimal training RMSE = 2.651003

ANFIS info:
Number of nodes: 78
Number of linear parameters: 27
Number of nonlinear parameters: 27
Total number of parameters: 54
Number of training data pairs: 144
Number of checking data pairs: 0
Number of fuzzy rules: 27

Start training ANFIS ...

1 2.651
2 2.651

Designated epoch number reached --> ANFIS training completed at epoch 2.

Minimal training RMSE = 2.651003

ANFIS info:
Number of nodes: 78
Number of linear parameters: 27
Number of nonlinear parameters: 27
Total number of parameters: 54
Number of training data pairs: 144
Number of checking data pairs: 0
Number of fuzzy rules: 27

Start training ANFIS ...

1 2.651
2 2.651

Designated epoch number reached --> ANFIS training completed at epoch 2.

Minimal training RMSE = 2.651003

ANFIS info:
Number of nodes: 78
Number of linear parameters: 27
Number of nonlinear parameters: 27
Total number of parameters: 54
Number of training data pairs: 144
Number of checking data pairs: 0
Number of fuzzy rules: 27

Start training ANFIS ...

1 2.651
2 2.651

Designated epoch number reached --> ANFIS training completed at epoch 2.

Minimal training RMSE = 2.651003

ANFIS info:
Number of nodes: 78
Number of linear parameters: 27

Number of nonlinear parameters: 27

Total number of parameters: 54

Number of training data pairs: 144

Number of checking data pairs: 0

Number of fuzzy rules: 27

Start training ANFIS ...

1 2.651

2 2.651

Designated epoch number reached --> ANFIS training completed at epoch 2.

Minimal training RMSE = 2.651003

ANFIS info:

Number of nodes: 78

Number of linear parameters: 27

Number of nonlinear parameters: 27

Total number of parameters: 54

Number of training data pairs: 144

Number of checking data pairs: 0

Number of fuzzy rules: 27

Start training ANFIS ...

1 2.651

2 2.651

Designated epoch number reached --> ANFIS training completed at epoch 2.

Minimal training RMSE = 2.651003

ANFIS info:
Number of nodes: 78
Number of linear parameters: 27
Number of nonlinear parameters: 27
Total number of parameters: 54
Number of training data pairs: 144
Number of checking data pairs: 0
Number of fuzzy rules: 27

Start training ANFIS ...

1 2.651
2 2.651

Designated epoch number reached --> ANFIS training completed at epoch 2.

Minimal training RMSE = 2.651003

ANFIS info:
Number of nodes: 78
Number of linear parameters: 27
Number of nonlinear parameters: 27
Total number of parameters: 54
Number of training data pairs: 144
Number of checking data pairs: 0
Number of fuzzy rules: 27

Start training ANFIS ...

1 2.651

2 2.651

Designated epoch number reached --> ANFIS training completed at epoch 2.

Minimal training RMSE = 2.651003

ANFIS info:

Number of nodes: 78

Number of linear parameters: 27

Number of nonlinear parameters: 27

Total number of parameters: 54

Number of training data pairs: 144

Number of checking data pairs: 0

Number of fuzzy rules: 27

Start training ANFIS ...

1 2.651

2 2.651

Designated epoch number reached --> ANFIS training completed at epoch 2.

Minimal training RMSE = 2.651003

ANFIS info:

Number of nodes: 78

Number of linear parameters: 27

Number of nonlinear parameters: 27

Total number of parameters: 54

Number of training data pairs: 144
Number of checking data pairs: 0
Number of fuzzy rules: 27

Start training ANFIS ...

1 2.651
2 2.651

Designated epoch number reached --> ANFIS training completed at epoch 2.

Minimal training RMSE = 2.651003

ANFIS info:
Number of nodes: 78
Number of linear parameters: 27
Number of nonlinear parameters: 27
Total number of parameters: 54
Number of training data pairs: 144
Number of checking data pairs: 0
Number of fuzzy rules: 27

Start training ANFIS ...

1 2.651
2 2.651

Designated epoch number reached --> ANFIS training completed at epoch 2.

Minimal training RMSE = 2.651003

ANFIS info:
Number of nodes: 78
Number of linear parameters: 27
Number of nonlinear parameters: 27
Total number of parameters: 54
Number of training data pairs: 144
Number of checking data pairs: 0
Number of fuzzy rules: 27

Start training ANFIS ...

1 2.651
2 2.651

Designated epoch number reached --> ANFIS training completed at epoch 2.

Minimal training RMSE = 2.651003

ANFIS info:
Number of nodes: 78
Number of linear parameters: 27
Number of nonlinear parameters: 27
Total number of parameters: 54
Number of training data pairs: 144
Number of checking data pairs: 0
Number of fuzzy rules: 27

Start training ANFIS ...

1 2.651

2 2.651

Designated epoch number reached --> ANFIS training completed at epoch 2.

Minimal training RMSE = 2.651003

ANFIS info:
Number of nodes: 78
Number of linear parameters: 27
Number of nonlinear parameters: 27
Total number of parameters: 54
Number of training data pairs: 144
Number of checking data pairs: 0
Number of fuzzy rules: 27

Start training ANFIS ...

1 2.651
2 2.651

Designated epoch number reached --> ANFIS training completed at epoch 2.

Minimal training RMSE = 2.651003

ANFIS info:
Number of nodes: 78
Number of linear parameters: 27
Number of nonlinear parameters: 27
Total number of parameters: 54
Number of training data pairs: 144
Number of checking data pairs: 0

Number of fuzzy rules: 27

Start training ANFIS ...

1 2.651
2 2.651

Designated epoch number reached --> ANFIS training completed at epoch 2.

Minimal training RMSE = 2.651003

ANFIS info:
Number of nodes: 78
Number of linear parameters: 27
Number of nonlinear parameters: 27
Total number of parameters: 54
Number of training data pairs: 144
Number of checking data pairs: 0
Number of fuzzy rules: 27

Start training ANFIS ...

1 2.651
2 2.651

Designated epoch number reached --> ANFIS training completed at epoch 2.

Minimal training RMSE = 2.651003

ANFIS info:

Number of nodes: 78

Number of linear parameters: 27

Number of nonlinear parameters: 27

Total number of parameters: 54

Number of training data pairs: 144

Number of checking data pairs: 0

Number of fuzzy rules: 27

Start training ANFIS ...

1 2.651

2 2.651

Designated epoch number reached --> ANFIS training completed at epoch 2.

Minimal training RMSE = 2.651003

ANFIS info:

Number of nodes: 78

Number of linear parameters: 27

Number of nonlinear parameters: 27

Total number of parameters: 54

Number of training data pairs: 144

Number of checking data pairs: 0

Number of fuzzy rules: 27

Start training ANFIS ...

1 2.651

2 2.651

Designated epoch number reached --> ANFIS training completed at epoch 2.

Minimal training RMSE = 2.651003

ANFIS info:
Number of nodes: 78
Number of linear parameters: 27
Number of nonlinear parameters: 27
Total number of parameters: 54
Number of training data pairs: 144
Number of checking data pairs: 0
Number of fuzzy rules: 27

Start training ANFIS ...

1 2.651
2 2.651

Designated epoch number reached --> ANFIS training completed at epoch 2.

Minimal training RMSE = 2.651003

ANFIS info:
Number of nodes: 78
Number of linear parameters: 27
Number of nonlinear parameters: 27
Total number of parameters: 54
Number of training data pairs: 144
Number of checking data pairs: 0
Number of fuzzy rules: 27

Start training ANFIS ...

1 2.651
2 2.651

Designated epoch number reached --> ANFIS training completed at epoch 2.

Minimal training RMSE = 2.651003

ANFIS info:
Number of nodes: 78
Number of linear parameters: 27
Number of nonlinear parameters: 27
Total number of parameters: 54
Number of training data pairs: 144
Number of checking data pairs: 0
Number of fuzzy rules: 27

Start training ANFIS ...

1 2.651
2 2.651

Designated epoch number reached --> ANFIS training completed at epoch 2.

Minimal training RMSE = 2.651003

ANFIS info:
Number of nodes: 78
Number of linear parameters: 27

Number of nonlinear parameters: 27

Total number of parameters: 54

Number of training data pairs: 144

Number of checking data pairs: 0

Number of fuzzy rules: 27

Start training ANFIS ...

1 2.651

2 2.651

Designated epoch number reached --> ANFIS training completed at epoch 2.

Minimal training RMSE = 2.651003

ANFIS info:

Number of nodes: 78

Number of linear parameters: 27

Number of nonlinear parameters: 27

Total number of parameters: 54

Number of training data pairs: 144

Number of checking data pairs: 0

Number of fuzzy rules: 27

Start training ANFIS ...

1 2.651

2 2.651

Designated epoch number reached --> ANFIS training completed at epoch 2.

Minimal training RMSE = 2.651003

ANFIS info:
Number of nodes: 78
Number of linear parameters: 27
Number of nonlinear parameters: 27
Total number of parameters: 54
Number of training data pairs: 144
Number of checking data pairs: 0
Number of fuzzy rules: 27

Start training ANFIS ...

1 2.651
2 2.651

Designated epoch number reached --> ANFIS training completed at epoch 2.

Minimal training RMSE = 2.651003

ANFIS info:
Number of nodes: 78
Number of linear parameters: 27
Number of nonlinear parameters: 27
Total number of parameters: 54
Number of training data pairs: 144
Number of checking data pairs: 0
Number of fuzzy rules: 27

Start training ANFIS ...

1 2.651

2 2.651

Designated epoch number reached --> ANFIS training completed at epoch 2.

Minimal training RMSE = 2.651003

ANFIS info:

Number of nodes: 78

Number of linear parameters: 27

Number of nonlinear parameters: 27

Total number of parameters: 54

Number of training data pairs: 144

Number of checking data pairs: 0

Number of fuzzy rules: 27

Start training ANFIS ...

1 2.651

2 2.651

Designated epoch number reached --> ANFIS training completed at epoch 2.

Minimal training RMSE = 2.651003

ANFIS info:

Number of nodes: 78

Number of linear parameters: 27

Number of nonlinear parameters: 27

Total number of parameters: 54

Number of training data pairs: 144
Number of checking data pairs: 0
Number of fuzzy rules: 27

Start training ANFIS ...

1 2.651
2 2.651

Designated epoch number reached --> ANFIS training completed at epoch 2.

Minimal training RMSE = 2.651003

ANFIS info:
Number of nodes: 78
Number of linear parameters: 27
Number of nonlinear parameters: 27
Total number of parameters: 54
Number of training data pairs: 144
Number of checking data pairs: 0
Number of fuzzy rules: 27

Start training ANFIS ...

1 2.651
2 2.651

Designated epoch number reached --> ANFIS training completed at epoch 2.

Minimal training RMSE = 2.651003

ANFIS info:
Number of nodes: 78
Number of linear parameters: 27
Number of nonlinear parameters: 27
Total number of parameters: 54
Number of training data pairs: 144
Number of checking data pairs: 0
Number of fuzzy rules: 27

Start training ANFIS ...

1 2.651
2 2.651

Designated epoch number reached --> ANFIS training completed at epoch 2.

Minimal training RMSE = 2.651003

ANFIS info:
Number of nodes: 78
Number of linear parameters: 27
Number of nonlinear parameters: 27
Total number of parameters: 54
Number of training data pairs: 144
Number of checking data pairs: 0
Number of fuzzy rules: 27

Start training ANFIS ...

1 2.651

2 2.651

Designated epoch number reached --> ANFIS training completed at epoch 2.

Minimal training RMSE = 2.651003

ANFIS info:
Number of nodes: 78
Number of linear parameters: 27
Number of nonlinear parameters: 27
Total number of parameters: 54
Number of training data pairs: 144
Number of checking data pairs: 0
Number of fuzzy rules: 27

Start training ANFIS ...

1 2.651
2 2.651

Designated epoch number reached --> ANFIS training completed at epoch 2.

Minimal training RMSE = 2.651003

ANFIS info:
Number of nodes: 78
Number of linear parameters: 27
Number of nonlinear parameters: 27
Total number of parameters: 54
Number of training data pairs: 144
Number of checking data pairs: 0

Number of fuzzy rules: 27

Start training ANFIS ...

1 2.651
2 2.651

Designated epoch number reached --> ANFIS training completed at epoch 2.

Minimal training RMSE = 2.651003

ANFIS info:
Number of nodes: 78
Number of linear parameters: 27
Number of nonlinear parameters: 27
Total number of parameters: 54
Number of training data pairs: 144
Number of checking data pairs: 0
Number of fuzzy rules: 27

Start training ANFIS ...

1 2.651
2 2.651

Designated epoch number reached --> ANFIS training completed at epoch 2.

Minimal training RMSE = 2.651003

ANFIS info:

Number of nodes: 78

Number of linear parameters: 27

Number of nonlinear parameters: 27

Total number of parameters: 54

Number of training data pairs: 144

Number of checking data pairs: 0

Number of fuzzy rules: 27

Start training ANFIS ...

1 2.651

2 2.651

Designated epoch number reached --> ANFIS training completed at epoch 2.

Minimal training RMSE = 2.651003

ANFIS info:

Number of nodes: 78

Number of linear parameters: 27

Number of nonlinear parameters: 27

Total number of parameters: 54

Number of training data pairs: 144

Number of checking data pairs: 0

Number of fuzzy rules: 27

Start training ANFIS ...

1 2.651

2 2.651

Designated epoch number reached --> ANFIS training completed at epoch 2.

Minimal training RMSE = 2.651003

ANFIS info:
Number of nodes: 78
Number of linear parameters: 27
Number of nonlinear parameters: 27
Total number of parameters: 54
Number of training data pairs: 144
Number of checking data pairs: 0
Number of fuzzy rules: 27

Start training ANFIS ...

1 2.651
2 2.651

Designated epoch number reached --> ANFIS training completed at epoch 2.

Minimal training RMSE = 2.651003

ANFIS info:
Number of nodes: 78
Number of linear parameters: 27
Number of nonlinear parameters: 27
Total number of parameters: 54
Number of training data pairs: 144
Number of checking data pairs: 0
Number of fuzzy rules: 27

Start training ANFIS ...

1 2.651
2 2.651

Designated epoch number reached --> ANFIS training completed at epoch 2.

Minimal training RMSE = 2.651003

ANFIS info:
Number of nodes: 78
Number of linear parameters: 27
Number of nonlinear parameters: 27
Total number of parameters: 54
Number of training data pairs: 144
Number of checking data pairs: 0
Number of fuzzy rules: 27

Start training ANFIS ...

1 2.651
2 2.651

Designated epoch number reached --> ANFIS training completed at epoch 2.

Minimal training RMSE = 2.651003

ANFIS info:
Number of nodes: 78
Number of linear parameters: 27

Number of nonlinear parameters: 27

Total number of parameters: 54

Number of training data pairs: 144

Number of checking data pairs: 0

Number of fuzzy rules: 27

Start training ANFIS ...

1 2.651

2 2.651

Designated epoch number reached --> ANFIS training completed at epoch 2.

Minimal training RMSE = 2.651003

ANFIS info:

Number of nodes: 78

Number of linear parameters: 27

Number of nonlinear parameters: 27

Total number of parameters: 54

Number of training data pairs: 144

Number of checking data pairs: 0

Number of fuzzy rules: 27

Start training ANFIS ...

1 2.651

2 2.651

Designated epoch number reached --> ANFIS training completed at epoch 2.

Minimal training RMSE = 2.651003

ANFIS info:
Number of nodes: 78
Number of linear parameters: 27
Number of nonlinear parameters: 27
Total number of parameters: 54
Number of training data pairs: 144
Number of checking data pairs: 0
Number of fuzzy rules: 27

Start training ANFIS ...

1 2.651
2 2.651

Designated epoch number reached --> ANFIS training completed at epoch 2.

Minimal training RMSE = 2.651003

ANFIS info:
Number of nodes: 78
Number of linear parameters: 27
Number of nonlinear parameters: 27
Total number of parameters: 54
Number of training data pairs: 144
Number of checking data pairs: 0
Number of fuzzy rules: 27

Start training ANFIS ...

1 2.651

2 2.651

Designated epoch number reached --> ANFIS training completed at epoch 2.

Minimal training RMSE = 2.651003

ANFIS info:

Number of nodes: 78

Number of linear parameters: 27

Number of nonlinear parameters: 27

Total number of parameters: 54

Number of training data pairs: 144

Number of checking data pairs: 0

Number of fuzzy rules: 27

Start training ANFIS ...

1 2.651

2 2.651

Designated epoch number reached --> ANFIS training completed at epoch 2.

Minimal training RMSE = 2.651003

ANFIS info:

Number of nodes: 78

Number of linear parameters: 27

Number of nonlinear parameters: 27

Total number of parameters: 54

Number of training data pairs: 144
Number of checking data pairs: 0
Number of fuzzy rules: 27

Start training ANFIS ...

1 2.651
2 2.651

Designated epoch number reached --> ANFIS training completed at epoch 2.

Minimal training RMSE = 2.651003

ANFIS info:
Number of nodes: 78
Number of linear parameters: 27
Number of nonlinear parameters: 27
Total number of parameters: 54
Number of training data pairs: 144
Number of checking data pairs: 0
Number of fuzzy rules: 27

Start training ANFIS ...

1 2.651
2 2.651

Designated epoch number reached --> ANFIS training completed at epoch 2.

Minimal training RMSE = 2.651003

ANFIS info:
Number of nodes: 78
Number of linear parameters: 27
Number of nonlinear parameters: 27
Total number of parameters: 54
Number of training data pairs: 144
Number of checking data pairs: 0
Number of fuzzy rules: 27

Start training ANFIS ...

1 2.651
2 2.651

Designated epoch number reached --> ANFIS training completed at epoch 2.

Minimal training RMSE = 2.651003

ANFIS info:
Number of nodes: 78
Number of linear parameters: 27
Number of nonlinear parameters: 27
Total number of parameters: 54
Number of training data pairs: 144
Number of checking data pairs: 0
Number of fuzzy rules: 27

Start training ANFIS ...

1 2.651

2 2.651

Designated epoch number reached --> ANFIS training completed at epoch 2.

Minimal training RMSE = 2.651003

ANFIS info:
Number of nodes: 78
Number of linear parameters: 27
Number of nonlinear parameters: 27
Total number of parameters: 54
Number of training data pairs: 144
Number of checking data pairs: 0
Number of fuzzy rules: 27

Start training ANFIS ...

1 2.651
2 2.651

Designated epoch number reached --> ANFIS training completed at epoch 2.

Minimal training RMSE = 2.651003

ANFIS info:
Number of nodes: 78
Number of linear parameters: 27
Number of nonlinear parameters: 27
Total number of parameters: 54
Number of training data pairs: 144
Number of checking data pairs: 0

Number of fuzzy rules: 27

Start training ANFIS ...

1 2.651
2 2.651

Designated epoch number reached --> ANFIS training completed at epoch 2.

Minimal training RMSE = 2.651003

ANFIS info:
Number of nodes: 78
Number of linear parameters: 27
Number of nonlinear parameters: 27
Total number of parameters: 54
Number of training data pairs: 144
Number of checking data pairs: 0
Number of fuzzy rules: 27

Start training ANFIS ...

1 2.651
2 2.651

Designated epoch number reached --> ANFIS training completed at epoch 2.

Minimal training RMSE = 2.651003

ANFIS info:

Number of nodes: 78

Number of linear parameters: 27

Number of nonlinear parameters: 27

Total number of parameters: 54

Number of training data pairs: 144

Number of checking data pairs: 0

Number of fuzzy rules: 27

Start training ANFIS ...

1 2.651

2 2.651

Designated epoch number reached --> ANFIS training completed at epoch 2.

Minimal training RMSE = 2.651003

ANFIS info:

Number of nodes: 78

Number of linear parameters: 27

Number of nonlinear parameters: 27

Total number of parameters: 54

Number of training data pairs: 144

Number of checking data pairs: 0

Number of fuzzy rules: 27

Start training ANFIS ...

1 2.651

2 2.651

Designated epoch number reached --> ANFIS training completed at epoch 2.

Minimal training RMSE = 2.651003

ANFIS info:
Number of nodes: 78
Number of linear parameters: 27
Number of nonlinear parameters: 27
Total number of parameters: 54
Number of training data pairs: 144
Number of checking data pairs: 0
Number of fuzzy rules: 27

Start training ANFIS ...

1 2.651
2 2.651

Designated epoch number reached --> ANFIS training completed at epoch 2.

Minimal training RMSE = 2.651003

ANFIS info:
Number of nodes: 78
Number of linear parameters: 27
Number of nonlinear parameters: 27
Total number of parameters: 54
Number of training data pairs: 144
Number of checking data pairs: 0
Number of fuzzy rules: 27

Start training ANFIS ...

1 2.651
2 2.651

Designated epoch number reached --> ANFIS training completed at epoch 2.

Minimal training RMSE = 2.651003

ANFIS info:
Number of nodes: 78
Number of linear parameters: 27
Number of nonlinear parameters: 27
Total number of parameters: 54
Number of training data pairs: 144
Number of checking data pairs: 0
Number of fuzzy rules: 27

Start training ANFIS ...

1 2.651
2 2.651

Designated epoch number reached --> ANFIS training completed at epoch 2.

Minimal training RMSE = 2.651003

ANFIS info:
Number of nodes: 78
Number of linear parameters: 27

Number of nonlinear parameters: 27

Total number of parameters: 54

Number of training data pairs: 144

Number of checking data pairs: 0

Number of fuzzy rules: 27

Start training ANFIS ...

1 2.651

2 2.651

Designated epoch number reached --> ANFIS training completed at epoch 2.

Minimal training RMSE = 2.651003

ANFIS info:

Number of nodes: 78

Number of linear parameters: 27

Number of nonlinear parameters: 27

Total number of parameters: 54

Number of training data pairs: 144

Number of checking data pairs: 0

Number of fuzzy rules: 27

Start training ANFIS ...

1 2.651

2 2.651

Designated epoch number reached --> ANFIS training completed at epoch 2.

Minimal training RMSE = 2.651003

ANFIS info:
Number of nodes: 78
Number of linear parameters: 27
Number of nonlinear parameters: 27
Total number of parameters: 54
Number of training data pairs: 144
Number of checking data pairs: 0
Number of fuzzy rules: 27

Start training ANFIS ...

1 2.651
2 2.651

Designated epoch number reached --> ANFIS training completed at epoch 2.

Minimal training RMSE = 2.651003

ANFIS info:
Number of nodes: 78
Number of linear parameters: 27
Number of nonlinear parameters: 27
Total number of parameters: 54
Number of training data pairs: 144
Number of checking data pairs: 0
Number of fuzzy rules: 27

Start training ANFIS ...

1 2.651

2 2.651

Designated epoch number reached --> ANFIS training completed at epoch 2.

Minimal training RMSE = 2.651003

ANFIS info:

Number of nodes: 78

Number of linear parameters: 27

Number of nonlinear parameters: 27

Total number of parameters: 54

Number of training data pairs: 144

Number of checking data pairs: 0

Number of fuzzy rules: 27

Start training ANFIS ...

1 2.651

2 2.651

Designated epoch number reached --> ANFIS training completed at epoch 2.

Minimal training RMSE = 2.651003

ANFIS info:

Number of nodes: 78

Number of linear parameters: 27

Number of nonlinear parameters: 27

Total number of parameters: 54

Number of training data pairs: 144
Number of checking data pairs: 0
Number of fuzzy rules: 27

Start training ANFIS ...

1 2.651
2 2.651

Designated epoch number reached --> ANFIS training completed at epoch 2.

Minimal training RMSE = 2.651003

ANFIS info:
Number of nodes: 78
Number of linear parameters: 27
Number of nonlinear parameters: 27
Total number of parameters: 54
Number of training data pairs: 144
Number of checking data pairs: 0
Number of fuzzy rules: 27

Start training ANFIS ...

1 2.651
2 2.651

Designated epoch number reached --> ANFIS training completed at epoch 2.

Minimal training RMSE = 2.651003

ANFIS info:
Number of nodes: 78
Number of linear parameters: 27
Number of nonlinear parameters: 27
Total number of parameters: 54
Number of training data pairs: 144
Number of checking data pairs: 0
Number of fuzzy rules: 27

Start training ANFIS ...

1 2.651
2 2.651

Designated epoch number reached --> ANFIS training completed at epoch 2.

Minimal training RMSE = 2.651003

ANFIS info:
Number of nodes: 78
Number of linear parameters: 27
Number of nonlinear parameters: 27
Total number of parameters: 54
Number of training data pairs: 144
Number of checking data pairs: 0
Number of fuzzy rules: 27

Start training ANFIS ...

1 2.651

2 2.651

Designated epoch number reached --> ANFIS training completed at epoch 2.

Minimal training RMSE = 2.651003

ANFIS info:
Number of nodes: 78
Number of linear parameters: 27
Number of nonlinear parameters: 27
Total number of parameters: 54
Number of training data pairs: 144
Number of checking data pairs: 0
Number of fuzzy rules: 27

Start training ANFIS ...

1 2.651
2 2.651

Designated epoch number reached --> ANFIS training completed at epoch 2.

Minimal training RMSE = 2.651003

ANFIS info:
Number of nodes: 78
Number of linear parameters: 27
Number of nonlinear parameters: 27
Total number of parameters: 54
Number of training data pairs: 144
Number of checking data pairs: 0

Number of fuzzy rules: 27

Start training ANFIS ...

1 2.651
2 2.651

Designated epoch number reached --> ANFIS training completed at epoch 2.

Minimal training RMSE = 2.651003

ANFIS info:
Number of nodes: 78
Number of linear parameters: 27
Number of nonlinear parameters: 27
Total number of parameters: 54
Number of training data pairs: 144
Number of checking data pairs: 0
Number of fuzzy rules: 27

Start training ANFIS ...

1 2.651
2 2.651

Designated epoch number reached --> ANFIS training completed at epoch 2.

Minimal training RMSE = 2.651003

ANFIS info:

Number of nodes: 78

Number of linear parameters: 27

Number of nonlinear parameters: 27

Total number of parameters: 54

Number of training data pairs: 144

Number of checking data pairs: 0

Number of fuzzy rules: 27

Start training ANFIS ...

1 2.651

2 2.651

Designated epoch number reached --> ANFIS training completed at epoch 2.

Minimal training RMSE = 2.651003

ANFIS info:

Number of nodes: 78

Number of linear parameters: 27

Number of nonlinear parameters: 27

Total number of parameters: 54

Number of training data pairs: 144

Number of checking data pairs: 0

Number of fuzzy rules: 27

Start training ANFIS ...

1 2.651

2 2.651

Designated epoch number reached --> ANFIS training completed at epoch 2.

Minimal training RMSE = 2.651003

ANFIS info:
Number of nodes: 78
Number of linear parameters: 27
Number of nonlinear parameters: 27
Total number of parameters: 54
Number of training data pairs: 144
Number of checking data pairs: 0
Number of fuzzy rules: 27

Start training ANFIS ...

1 2.651
2 2.651

Designated epoch number reached --> ANFIS training completed at epoch 2.

Minimal training RMSE = 2.651003

ANFIS info:
Number of nodes: 78
Number of linear parameters: 27
Number of nonlinear parameters: 27
Total number of parameters: 54
Number of training data pairs: 144
Number of checking data pairs: 0
Number of fuzzy rules: 27

Start training ANFIS ...

1 2.651
2 2.651

Designated epoch number reached --> ANFIS training completed at epoch 2.

Minimal training RMSE = 2.651003

ANFIS info:
Number of nodes: 78
Number of linear parameters: 27
Number of nonlinear parameters: 27
Total number of parameters: 54
Number of training data pairs: 144
Number of checking data pairs: 0
Number of fuzzy rules: 27

Start training ANFIS ...

1 2.651
2 2.651

Designated epoch number reached --> ANFIS training completed at epoch 2.

Minimal training RMSE = 2.651003

ANFIS info:
Number of nodes: 78
Number of linear parameters: 27

Number of nonlinear parameters: 27

Total number of parameters: 54

Number of training data pairs: 144

Number of checking data pairs: 0

Number of fuzzy rules: 27

Start training ANFIS ...

1 2.651

2 2.651

Designated epoch number reached --> ANFIS training completed at epoch 2.

Minimal training RMSE = 2.651003

ANFIS info:

Number of nodes: 78

Number of linear parameters: 27

Number of nonlinear parameters: 27

Total number of parameters: 54

Number of training data pairs: 144

Number of checking data pairs: 0

Number of fuzzy rules: 27

Start training ANFIS ...

1 2.651

2 2.651

Designated epoch number reached --> ANFIS training completed at epoch 2.

Minimal training RMSE = 2.651003

ANFIS info:
Number of nodes: 78
Number of linear parameters: 27
Number of nonlinear parameters: 27
Total number of parameters: 54
Number of training data pairs: 144
Number of checking data pairs: 0
Number of fuzzy rules: 27

Start training ANFIS ...

1 2.651
2 2.651

Designated epoch number reached --> ANFIS training completed at epoch 2.

Minimal training RMSE = 2.651003

ANFIS info:
Number of nodes: 78
Number of linear parameters: 27
Number of nonlinear parameters: 27
Total number of parameters: 54
Number of training data pairs: 144
Number of checking data pairs: 0
Number of fuzzy rules: 27

Start training ANFIS ...

1 2.651

2 2.651

Designated epoch number reached --> ANFIS training completed at epoch 2.

Minimal training RMSE = 2.651003

ANFIS info:

Number of nodes: 78

Number of linear parameters: 27

Number of nonlinear parameters: 27

Total number of parameters: 54

Number of training data pairs: 144

Number of checking data pairs: 0

Number of fuzzy rules: 27

Start training ANFIS ...

1 2.651

2 2.651

Designated epoch number reached --> ANFIS training completed at epoch 2.

Minimal training RMSE = 2.651003

ANFIS info:

Number of nodes: 78

Number of linear parameters: 27

Number of nonlinear parameters: 27

Total number of parameters: 54

Number of training data pairs: 144
Number of checking data pairs: 0
Number of fuzzy rules: 27

Start training ANFIS ...

1 2.651
2 2.651

Designated epoch number reached --> ANFIS training completed at epoch 2.

Minimal training RMSE = 2.651003

ANFIS info:
Number of nodes: 78
Number of linear parameters: 27
Number of nonlinear parameters: 27
Total number of parameters: 54
Number of training data pairs: 144
Number of checking data pairs: 0
Number of fuzzy rules: 27

Start training ANFIS ...

1 2.651
2 2.651

Designated epoch number reached --> ANFIS training completed at epoch 2.

Minimal training RMSE = 2.651003

ANFIS info:
Number of nodes: 78
Number of linear parameters: 27
Number of nonlinear parameters: 27
Total number of parameters: 54
Number of training data pairs: 144
Number of checking data pairs: 0
Number of fuzzy rules: 27

Start training ANFIS ...

1 2.651
2 2.651

Designated epoch number reached --> ANFIS training completed at epoch 2.

Minimal training RMSE = 2.651003

ANFIS info:
Number of nodes: 78
Number of linear parameters: 27
Number of nonlinear parameters: 27
Total number of parameters: 54
Number of training data pairs: 144
Number of checking data pairs: 0
Number of fuzzy rules: 27

Start training ANFIS ...

1 2.651

2 2.651

Designated epoch number reached --> ANFIS training completed at epoch 2.

Minimal training RMSE = 2.651003

ANFIS info:
Number of nodes: 78
Number of linear parameters: 27
Number of nonlinear parameters: 27
Total number of parameters: 54
Number of training data pairs: 144
Number of checking data pairs: 0
Number of fuzzy rules: 27

Start training ANFIS ...

1 2.651
2 2.651

Designated epoch number reached --> ANFIS training completed at epoch 2.

Minimal training RMSE = 2.651003

ANFIS info:
Number of nodes: 78
Number of linear parameters: 27
Number of nonlinear parameters: 27
Total number of parameters: 54
Number of training data pairs: 144
Number of checking data pairs: 0

Number of fuzzy rules: 27

Start training ANFIS ...

1 2.651
2 2.651

Designated epoch number reached --> ANFIS training completed at epoch 2.

Minimal training RMSE = 2.651003

ANFIS info:
Number of nodes: 78
Number of linear parameters: 27
Number of nonlinear parameters: 27
Total number of parameters: 54
Number of training data pairs: 144
Number of checking data pairs: 0
Number of fuzzy rules: 27

Start training ANFIS ...

1 2.651
2 2.651

Designated epoch number reached --> ANFIS training completed at epoch 2.

Minimal training RMSE = 2.651003

ANFIS info:

Number of nodes: 78

Number of linear parameters: 27

Number of nonlinear parameters: 27

Total number of parameters: 54

Number of training data pairs: 144

Number of checking data pairs: 0

Number of fuzzy rules: 27

Start training ANFIS ...

1 2.651

2 2.651

Designated epoch number reached --> ANFIS training completed at epoch 2.

Minimal training RMSE = 2.651003

ANFIS info:

Number of nodes: 78

Number of linear parameters: 27

Number of nonlinear parameters: 27

Total number of parameters: 54

Number of training data pairs: 144

Number of checking data pairs: 0

Number of fuzzy rules: 27

Start training ANFIS ...

1 2.651

2 2.651

Designated epoch number reached --> ANFIS training completed at epoch 2.

Minimal training RMSE = 2.651003

ANFIS info:
Number of nodes: 78
Number of linear parameters: 27
Number of nonlinear parameters: 27
Total number of parameters: 54
Number of training data pairs: 144
Number of checking data pairs: 0
Number of fuzzy rules: 27

Start training ANFIS ...

1 2.651
2 2.651

Designated epoch number reached --> ANFIS training completed at epoch 2.

Minimal training RMSE = 2.651003

ANFIS info:
Number of nodes: 78
Number of linear parameters: 27
Number of nonlinear parameters: 27
Total number of parameters: 54
Number of training data pairs: 144
Number of checking data pairs: 0
Number of fuzzy rules: 27

Start training ANFIS ...

1 2.651
2 2.651

Designated epoch number reached --> ANFIS training completed at epoch 2.

Minimal training RMSE = 2.651003

ANFIS info:
Number of nodes: 78
Number of linear parameters: 27
Number of nonlinear parameters: 27
Total number of parameters: 54
Number of training data pairs: 144
Number of checking data pairs: 0
Number of fuzzy rules: 27

Start training ANFIS ...

1 2.651
2 2.651

Designated epoch number reached --> ANFIS training completed at epoch 2.

Minimal training RMSE = 2.651003

ANFIS info:
Number of nodes: 78
Number of linear parameters: 27

Number of nonlinear parameters: 27

Total number of parameters: 54

Number of training data pairs: 144

Number of checking data pairs: 0

Number of fuzzy rules: 27

Start training ANFIS ...

1 2.651

2 2.651

Designated epoch number reached --> ANFIS training completed at epoch 2.

Minimal training RMSE = 2.651003

ANFIS info:

Number of nodes: 78

Number of linear parameters: 27

Number of nonlinear parameters: 27

Total number of parameters: 54

Number of training data pairs: 144

Number of checking data pairs: 0

Number of fuzzy rules: 27

Start training ANFIS ...

1 2.651

2 2.651

Designated epoch number reached --> ANFIS training completed at epoch 2.

Minimal training RMSE = 2.651003

ANFIS info:
Number of nodes: 78
Number of linear parameters: 27
Number of nonlinear parameters: 27
Total number of parameters: 54
Number of training data pairs: 144
Number of checking data pairs: 0
Number of fuzzy rules: 27

Start training ANFIS ...

1 2.651
2 2.651

Designated epoch number reached --> ANFIS training completed at epoch 2.

Minimal training RMSE = 2.651003

ANFIS info:
Number of nodes: 78
Number of linear parameters: 27
Number of nonlinear parameters: 27
Total number of parameters: 54
Number of training data pairs: 144
Number of checking data pairs: 0
Number of fuzzy rules: 27

Start training ANFIS ...

1 2.651

2 2.651

Designated epoch number reached --> ANFIS training completed at epoch 2.

Minimal training RMSE = 2.651003

ANFIS info:

Number of nodes: 78

Number of linear parameters: 27

Number of nonlinear parameters: 27

Total number of parameters: 54

Number of training data pairs: 144

Number of checking data pairs: 0

Number of fuzzy rules: 27

Start training ANFIS ...

1 2.651

2 2.651

Designated epoch number reached --> ANFIS training completed at epoch 2.

Minimal training RMSE = 2.651003

ANFIS info:

Number of nodes: 78

Number of linear parameters: 27

Number of nonlinear parameters: 27

Total number of parameters: 54

Number of training data pairs: 144
Number of checking data pairs: 0
Number of fuzzy rules: 27

Start training ANFIS ...

1 2.651
2 2.651

Designated epoch number reached --> ANFIS training completed at epoch 2.

Minimal training RMSE = 2.651003

ANFIS info:
Number of nodes: 78
Number of linear parameters: 27
Number of nonlinear parameters: 27
Total number of parameters: 54
Number of training data pairs: 144
Number of checking data pairs: 0
Number of fuzzy rules: 27

Start training ANFIS ...

1 2.651
2 2.651

Designated epoch number reached --> ANFIS training completed at epoch 2.

Minimal training RMSE = 2.651003

ANFIS info:
Number of nodes: 78
Number of linear parameters: 27
Number of nonlinear parameters: 27
Total number of parameters: 54
Number of training data pairs: 144
Number of checking data pairs: 0
Number of fuzzy rules: 27

Start training ANFIS ...

1 2.651
2 2.651

Designated epoch number reached --> ANFIS training completed at epoch 2.

Minimal training RMSE = 2.651003

ANFIS info:
Number of nodes: 78
Number of linear parameters: 27
Number of nonlinear parameters: 27
Total number of parameters: 54
Number of training data pairs: 144
Number of checking data pairs: 0
Number of fuzzy rules: 27

Start training ANFIS ...

1 2.651

2 2.651

Designated epoch number reached --> ANFIS training completed at epoch 2.

Minimal training RMSE = 2.651003

ANFIS info:
Number of nodes: 78
Number of linear parameters: 27
Number of nonlinear parameters: 27
Total number of parameters: 54
Number of training data pairs: 144
Number of checking data pairs: 0
Number of fuzzy rules: 27

Start training ANFIS ...

1 2.651
2 2.651

Designated epoch number reached --> ANFIS training completed at epoch 2.

Minimal training RMSE = 2.651003

ANFIS info:
Number of nodes: 78
Number of linear parameters: 27
Number of nonlinear parameters: 27
Total number of parameters: 54
Number of training data pairs: 144
Number of checking data pairs: 0

Number of fuzzy rules: 27

Start training ANFIS ...

1 2.651
2 2.651

Designated epoch number reached --> ANFIS training completed at epoch 2.

Minimal training RMSE = 2.651003

ANFIS info:
Number of nodes: 78
Number of linear parameters: 27
Number of nonlinear parameters: 27
Total number of parameters: 54
Number of training data pairs: 144
Number of checking data pairs: 0
Number of fuzzy rules: 27

Start training ANFIS ...

1 2.651
2 2.651

Designated epoch number reached --> ANFIS training completed at epoch 2.

Minimal training RMSE = 2.651003

ANFIS info:

Number of nodes: 78

Number of linear parameters: 27

Number of nonlinear parameters: 27

Total number of parameters: 54

Number of training data pairs: 144

Number of checking data pairs: 0

Number of fuzzy rules: 27

Start training ANFIS ...

1 2.651

2 2.651

Designated epoch number reached --> ANFIS training completed at epoch 2.

Minimal training RMSE = 2.651003

ANFIS info:

Number of nodes: 78

Number of linear parameters: 27

Number of nonlinear parameters: 27

Total number of parameters: 54

Number of training data pairs: 144

Number of checking data pairs: 0

Number of fuzzy rules: 27

Start training ANFIS ...

1 2.651

2 2.651

Designated epoch number reached --> ANFIS training completed at epoch 2.

Minimal training RMSE = 2.651003

ANFIS info:
Number of nodes: 78
Number of linear parameters: 27
Number of nonlinear parameters: 27
Total number of parameters: 54
Number of training data pairs: 144
Number of checking data pairs: 0
Number of fuzzy rules: 27

Start training ANFIS ...

1 2.651
2 2.651

Designated epoch number reached --> ANFIS training completed at epoch 2.

Minimal training RMSE = 2.651003

ANFIS info:
Number of nodes: 78
Number of linear parameters: 27
Number of nonlinear parameters: 27
Total number of parameters: 54
Number of training data pairs: 144
Number of checking data pairs: 0
Number of fuzzy rules: 27

Start training ANFIS ...

1 2.651
2 2.651

Designated epoch number reached --> ANFIS training completed at epoch 2.

Minimal training RMSE = 2.651003

ANFIS info:
Number of nodes: 78
Number of linear parameters: 27
Number of nonlinear parameters: 27
Total number of parameters: 54
Number of training data pairs: 144
Number of checking data pairs: 0
Number of fuzzy rules: 27

Start training ANFIS ...

1 2.651
2 2.651

Designated epoch number reached --> ANFIS training completed at epoch 2.

Minimal training RMSE = 2.651003

ANFIS info:
Number of nodes: 78
Number of linear parameters: 27

Number of nonlinear parameters: 27

Total number of parameters: 54

Number of training data pairs: 144

Number of checking data pairs: 0

Number of fuzzy rules: 27

Start training ANFIS ...

1 2.651

2 2.651

Designated epoch number reached --> ANFIS training completed at epoch 2.

Minimal training RMSE = 2.651003

ANFIS info:

Number of nodes: 78

Number of linear parameters: 27

Number of nonlinear parameters: 27

Total number of parameters: 54

Number of training data pairs: 144

Number of checking data pairs: 0

Number of fuzzy rules: 27

Start training ANFIS ...

1 2.651

2 2.651

Designated epoch number reached --> ANFIS training completed at epoch 2.

Minimal training RMSE = 2.651003

ANFIS info:
Number of nodes: 78
Number of linear parameters: 27
Number of nonlinear parameters: 27
Total number of parameters: 54
Number of training data pairs: 144
Number of checking data pairs: 0
Number of fuzzy rules: 27

Start training ANFIS ...

1 2.651
2 2.651

Designated epoch number reached --> ANFIS training completed at epoch 2.

Minimal training RMSE = 2.651003

ANFIS info:
Number of nodes: 78
Number of linear parameters: 27
Number of nonlinear parameters: 27
Total number of parameters: 54
Number of training data pairs: 144
Number of checking data pairs: 0
Number of fuzzy rules: 27

Start training ANFIS ...

1 2.651

2 2.651

Designated epoch number reached --> ANFIS training completed at epoch 2.

Minimal training RMSE = 2.651003

ANFIS info:

Number of nodes: 78

Number of linear parameters: 27

Number of nonlinear parameters: 27

Total number of parameters: 54

Number of training data pairs: 144

Number of checking data pairs: 0

Number of fuzzy rules: 27

Start training ANFIS ...

1 2.651

2 2.651

Designated epoch number reached --> ANFIS training completed at epoch 2.

Minimal training RMSE = 2.651003

ANFIS info:

Number of nodes: 78

Number of linear parameters: 27

Number of nonlinear parameters: 27

Total number of parameters: 54

Number of training data pairs: 144
Number of checking data pairs: 0
Number of fuzzy rules: 27

Start training ANFIS ...

1 2.651
2 2.651

Designated epoch number reached --> ANFIS training completed at epoch 2.

Minimal training RMSE = 2.651003

ANFIS info:
Number of nodes: 78
Number of linear parameters: 27
Number of nonlinear parameters: 27
Total number of parameters: 54
Number of training data pairs: 144
Number of checking data pairs: 0
Number of fuzzy rules: 27

Start training ANFIS ...

1 2.651
2 2.651

Designated epoch number reached --> ANFIS training completed at epoch 2.

Minimal training RMSE = 2.651003

ANFIS info:
Number of nodes: 78
Number of linear parameters: 27
Number of nonlinear parameters: 27
Total number of parameters: 54
Number of training data pairs: 144
Number of checking data pairs: 0
Number of fuzzy rules: 27

Start training ANFIS ...

1 2.651
2 2.651

Designated epoch number reached --> ANFIS training completed at epoch 2.

Minimal training RMSE = 2.651003

ANFIS info:
Number of nodes: 78
Number of linear parameters: 27
Number of nonlinear parameters: 27
Total number of parameters: 54
Number of training data pairs: 144
Number of checking data pairs: 0
Number of fuzzy rules: 27

Start training ANFIS ...

1 2.651

2 2.651

Designated epoch number reached --> ANFIS training completed at epoch 2.

Minimal training RMSE = 2.651003

ANFIS info:
Number of nodes: 78
Number of linear parameters: 27
Number of nonlinear parameters: 27
Total number of parameters: 54
Number of training data pairs: 144
Number of checking data pairs: 0
Number of fuzzy rules: 27

Start training ANFIS ...

1 2.651
2 2.651

Designated epoch number reached --> ANFIS training completed at epoch 2.

Minimal training RMSE = 2.651003

ANFIS info:
Number of nodes: 78
Number of linear parameters: 27
Number of nonlinear parameters: 27
Total number of parameters: 54
Number of training data pairs: 144
Number of checking data pairs: 0

Number of fuzzy rules: 27

Start training ANFIS ...

1 2.651
2 2.651

Designated epoch number reached --> ANFIS training completed at epoch 2.

Minimal training RMSE = 2.651003

ANFIS info:
Number of nodes: 78
Number of linear parameters: 27
Number of nonlinear parameters: 27
Total number of parameters: 54
Number of training data pairs: 144
Number of checking data pairs: 0
Number of fuzzy rules: 27

Start training ANFIS ...

1 2.651
2 2.651

Designated epoch number reached --> ANFIS training completed at epoch 2.

Minimal training RMSE = 2.651003

ANFIS info:

Number of nodes: 78

Number of linear parameters: 27

Number of nonlinear parameters: 27

Total number of parameters: 54

Number of training data pairs: 144

Number of checking data pairs: 0

Number of fuzzy rules: 27

Start training ANFIS ...

1 2.651

2 2.651

Designated epoch number reached --> ANFIS training completed at epoch 2.

Minimal training RMSE = 2.651003

ANFIS info:

Number of nodes: 78

Number of linear parameters: 27

Number of nonlinear parameters: 27

Total number of parameters: 54

Number of training data pairs: 144

Number of checking data pairs: 0

Number of fuzzy rules: 27

Start training ANFIS ...

1 2.651

2 2.651

Designated epoch number reached --> ANFIS training completed at epoch 2.

Minimal training RMSE = 2.651003

ANFIS info:
Number of nodes: 78
Number of linear parameters: 27
Number of nonlinear parameters: 27
Total number of parameters: 54
Number of training data pairs: 144
Number of checking data pairs: 0
Number of fuzzy rules: 27

Start training ANFIS ...

1 2.651
2 2.651

Designated epoch number reached --> ANFIS training completed at epoch 2.

Minimal training RMSE = 2.651003

ANFIS info:
Number of nodes: 78
Number of linear parameters: 27
Number of nonlinear parameters: 27
Total number of parameters: 54
Number of training data pairs: 144
Number of checking data pairs: 0
Number of fuzzy rules: 27

Start training ANFIS ...

1 2.651
2 2.651

Designated epoch number reached --> ANFIS training completed at epoch 2.

Minimal training RMSE = 2.651003

ANFIS info:
Number of nodes: 78
Number of linear parameters: 27
Number of nonlinear parameters: 27
Total number of parameters: 54
Number of training data pairs: 144
Number of checking data pairs: 0
Number of fuzzy rules: 27

Start training ANFIS ...

1 2.651
2 2.651

Designated epoch number reached --> ANFIS training completed at epoch 2.

Minimal training RMSE = 2.651003

ANFIS info:
Number of nodes: 78
Number of linear parameters: 27

Number of nonlinear parameters: 27

Total number of parameters: 54

Number of training data pairs: 144

Number of checking data pairs: 0

Number of fuzzy rules: 27

Start training ANFIS ...

1 2.651

2 2.651

Designated epoch number reached --> ANFIS training completed at epoch 2.

Minimal training RMSE = 2.651003

ANFIS info:

Number of nodes: 78

Number of linear parameters: 27

Number of nonlinear parameters: 27

Total number of parameters: 54

Number of training data pairs: 144

Number of checking data pairs: 0

Number of fuzzy rules: 27

Start training ANFIS ...

1 2.651

2 2.651

Designated epoch number reached --> ANFIS training completed at epoch 2.

Minimal training RMSE = 2.651003

ANFIS info:
Number of nodes: 78
Number of linear parameters: 27
Number of nonlinear parameters: 27
Total number of parameters: 54
Number of training data pairs: 144
Number of checking data pairs: 0
Number of fuzzy rules: 27

Start training ANFIS ...

1 2.651
2 2.651

Designated epoch number reached --> ANFIS training completed at epoch 2.

Minimal training RMSE = 2.651003

ANFIS info:
Number of nodes: 78
Number of linear parameters: 27
Number of nonlinear parameters: 27
Total number of parameters: 54
Number of training data pairs: 144
Number of checking data pairs: 0
Number of fuzzy rules: 27

Start training ANFIS ...

1 2.651

2 2.651

Designated epoch number reached --> ANFIS training completed at epoch 2.

Minimal training RMSE = 2.651003

ANFIS info:

Number of nodes: 78

Number of linear parameters: 27

Number of nonlinear parameters: 27

Total number of parameters: 54

Number of training data pairs: 144

Number of checking data pairs: 0

Number of fuzzy rules: 27

Start training ANFIS ...

1 2.651

2 2.651

Designated epoch number reached --> ANFIS training completed at epoch 2.

Minimal training RMSE = 2.651003

ANFIS info:

Number of nodes: 78

Number of linear parameters: 27

Number of nonlinear parameters: 27

Total number of parameters: 54

Number of training data pairs: 144
Number of checking data pairs: 0
Number of fuzzy rules: 27

Start training ANFIS ...

1 2.651
2 2.651

Designated epoch number reached --> ANFIS training completed at epoch 2.

Minimal training RMSE = 2.651003

ANFIS info:
Number of nodes: 78
Number of linear parameters: 27
Number of nonlinear parameters: 27
Total number of parameters: 54
Number of training data pairs: 144
Number of checking data pairs: 0
Number of fuzzy rules: 27

Start training ANFIS ...

1 2.651
2 2.651

Designated epoch number reached --> ANFIS training completed at epoch 2.

Minimal training RMSE = 2.651003

ANFIS info:
Number of nodes: 78
Number of linear parameters: 27
Number of nonlinear parameters: 27
Total number of parameters: 54
Number of training data pairs: 144
Number of checking data pairs: 0
Number of fuzzy rules: 27

Start training ANFIS ...

1 2.651
2 2.651

Designated epoch number reached --> ANFIS training completed at epoch 2.

Minimal training RMSE = 2.651003

ANFIS info:
Number of nodes: 78
Number of linear parameters: 27
Number of nonlinear parameters: 27
Total number of parameters: 54
Number of training data pairs: 144
Number of checking data pairs: 0
Number of fuzzy rules: 27

Start training ANFIS ...

1 2.651

2 2.651

Designated epoch number reached --> ANFIS training completed at epoch 2.

Minimal training RMSE = 2.651003

ANFIS info:
Number of nodes: 78
Number of linear parameters: 27
Number of nonlinear parameters: 27
Total number of parameters: 54
Number of training data pairs: 144
Number of checking data pairs: 0
Number of fuzzy rules: 27

Start training ANFIS ...

1 2.651
2 2.651

Designated epoch number reached --> ANFIS training completed at epoch 2.

Minimal training RMSE = 2.651003

ANFIS info:
Number of nodes: 78
Number of linear parameters: 27
Number of nonlinear parameters: 27
Total number of parameters: 54
Number of training data pairs: 144
Number of checking data pairs: 0

Number of fuzzy rules: 27

Start training ANFIS ...

1 2.651
2 2.651

Designated epoch number reached --> ANFIS training completed at epoch 2.

Minimal training RMSE = 2.651003

ANFIS info:
Number of nodes: 78
Number of linear parameters: 27
Number of nonlinear parameters: 27
Total number of parameters: 54
Number of training data pairs: 144
Number of checking data pairs: 0
Number of fuzzy rules: 27

Start training ANFIS ...

1 2.651
2 2.651

Designated epoch number reached --> ANFIS training completed at epoch 2.

Minimal training RMSE = 2.651003

ANFIS info:

Number of nodes: 78

Number of linear parameters: 27

Number of nonlinear parameters: 27

Total number of parameters: 54

Number of training data pairs: 144

Number of checking data pairs: 0

Number of fuzzy rules: 27

Start training ANFIS ...

1 2.651

2 2.651

Designated epoch number reached --> ANFIS training completed at epoch 2.

Minimal training RMSE = 2.651003

ANFIS info:

Number of nodes: 78

Number of linear parameters: 27

Number of nonlinear parameters: 27

Total number of parameters: 54

Number of training data pairs: 144

Number of checking data pairs: 0

Number of fuzzy rules: 27

Start training ANFIS ...

1 2.651

2 2.651

Designated epoch number reached --> ANFIS training completed at epoch 2.

Minimal training RMSE = 2.651003

ANFIS info:
Number of nodes: 78
Number of linear parameters: 27
Number of nonlinear parameters: 27
Total number of parameters: 54
Number of training data pairs: 144
Number of checking data pairs: 0
Number of fuzzy rules: 27

Start training ANFIS ...

1 2.651
2 2.651

Designated epoch number reached --> ANFIS training completed at epoch 2.

Minimal training RMSE = 2.651003

ANFIS info:
Number of nodes: 78
Number of linear parameters: 27
Number of nonlinear parameters: 27
Total number of parameters: 54
Number of training data pairs: 144
Number of checking data pairs: 0
Number of fuzzy rules: 27

Start training ANFIS ...

1 2.651
2 2.651

Designated epoch number reached --> ANFIS training completed at epoch 2.

Minimal training RMSE = 2.651003

ANFIS info:
Number of nodes: 78
Number of linear parameters: 27
Number of nonlinear parameters: 27
Total number of parameters: 54
Number of training data pairs: 144
Number of checking data pairs: 0
Number of fuzzy rules: 27

Start training ANFIS ...

1 2.651
2 2.651

Designated epoch number reached --> ANFIS training completed at epoch 2.

Minimal training RMSE = 2.651003

ANFIS info:
Number of nodes: 78
Number of linear parameters: 27

Number of nonlinear parameters: 27

Total number of parameters: 54

Number of training data pairs: 144

Number of checking data pairs: 0

Number of fuzzy rules: 27

Start training ANFIS ...

1 2.651

2 2.651

Designated epoch number reached --> ANFIS training completed at epoch 2.

Minimal training RMSE = 2.651003

ANFIS info:

Number of nodes: 78

Number of linear parameters: 27

Number of nonlinear parameters: 27

Total number of parameters: 54

Number of training data pairs: 144

Number of checking data pairs: 0

Number of fuzzy rules: 27

Start training ANFIS ...

1 2.651

2 2.651

Designated epoch number reached --> ANFIS training completed at epoch 2.

Minimal training RMSE = 2.651003

ANFIS info:
Number of nodes: 78
Number of linear parameters: 27
Number of nonlinear parameters: 27
Total number of parameters: 54
Number of training data pairs: 144
Number of checking data pairs: 0
Number of fuzzy rules: 27

Start training ANFIS ...

1 2.651
2 2.651

Designated epoch number reached --> ANFIS training completed at epoch 2.

Minimal training RMSE = 2.651003

ANFIS info:
Number of nodes: 78
Number of linear parameters: 27
Number of nonlinear parameters: 27
Total number of parameters: 54
Number of training data pairs: 144
Number of checking data pairs: 0
Number of fuzzy rules: 27

Start training ANFIS ...

1 2.651

2 2.651

Designated epoch number reached --> ANFIS training completed at epoch 2.

Minimal training RMSE = 2.651003

ANFIS info:

Number of nodes: 78

Number of linear parameters: 27

Number of nonlinear parameters: 27

Total number of parameters: 54

Number of training data pairs: 144

Number of checking data pairs: 0

Number of fuzzy rules: 27

Start training ANFIS ...

1 2.651

2 2.651

Designated epoch number reached --> ANFIS training completed at epoch 2.

Minimal training RMSE = 2.651003

ANFIS info:

Number of nodes: 78

Number of linear parameters: 27

Number of nonlinear parameters: 27

Total number of parameters: 54

Number of training data pairs: 144
Number of checking data pairs: 0
Number of fuzzy rules: 27

Start training ANFIS ...

1 2.651
2 2.651

Designated epoch number reached --> ANFIS training completed at epoch 2.

Minimal training RMSE = 2.651003

ANFIS info:
Number of nodes: 78
Number of linear parameters: 27
Number of nonlinear parameters: 27
Total number of parameters: 54
Number of training data pairs: 144
Number of checking data pairs: 0
Number of fuzzy rules: 27

Start training ANFIS ...

1 2.651
2 2.651

Designated epoch number reached --> ANFIS training completed at epoch 2.

Minimal training RMSE = 2.651003

ANFIS info:
Number of nodes: 78
Number of linear parameters: 27
Number of nonlinear parameters: 27
Total number of parameters: 54
Number of training data pairs: 144
Number of checking data pairs: 0
Number of fuzzy rules: 27

Start training ANFIS ...

1 2.651
2 2.651

Designated epoch number reached --> ANFIS training completed at epoch 2.

Minimal training RMSE = 2.651003

ANFIS info:
Number of nodes: 78
Number of linear parameters: 27
Number of nonlinear parameters: 27
Total number of parameters: 54
Number of training data pairs: 144
Number of checking data pairs: 0
Number of fuzzy rules: 27

Start training ANFIS ...

1 2.651

2 2.651

Designated epoch number reached --> ANFIS training completed at epoch 2.

Minimal training RMSE = 2.651003

ANFIS info:
Number of nodes: 78
Number of linear parameters: 27
Number of nonlinear parameters: 27
Total number of parameters: 54
Number of training data pairs: 144
Number of checking data pairs: 0
Number of fuzzy rules: 27

Start training ANFIS ...

1 2.651
2 2.651

Designated epoch number reached --> ANFIS training completed at epoch 2.

Minimal training RMSE = 2.651003

ANFIS info:
Number of nodes: 78
Number of linear parameters: 27
Number of nonlinear parameters: 27
Total number of parameters: 54
Number of training data pairs: 144
Number of checking data pairs: 0

Number of fuzzy rules: 27

Start training ANFIS ...

1 2.651
2 2.651

Designated epoch number reached --> ANFIS training completed at epoch 2.

Minimal training RMSE = 2.651003

ANFIS info:
Number of nodes: 78
Number of linear parameters: 27
Number of nonlinear parameters: 27
Total number of parameters: 54
Number of training data pairs: 144
Number of checking data pairs: 0
Number of fuzzy rules: 27

Start training ANFIS ...

1 2.651
2 2.651

Designated epoch number reached --> ANFIS training completed at epoch 2.

Minimal training RMSE = 2.651003

ANFIS info:

Number of nodes: 78

Number of linear parameters: 27

Number of nonlinear parameters: 27

Total number of parameters: 54

Number of training data pairs: 144

Number of checking data pairs: 0

Number of fuzzy rules: 27

Start training ANFIS ...

1 2.651

2 2.651

Designated epoch number reached --> ANFIS training completed at epoch 2.

Minimal training RMSE = 2.651003

ANFIS info:

Number of nodes: 78

Number of linear parameters: 27

Number of nonlinear parameters: 27

Total number of parameters: 54

Number of training data pairs: 144

Number of checking data pairs: 0

Number of fuzzy rules: 27

Start training ANFIS ...

1 2.651

2 2.651

Designated epoch number reached --> ANFIS training completed at epoch 2.

Minimal training RMSE = 2.651003

ANFIS info:
Number of nodes: 78
Number of linear parameters: 27
Number of nonlinear parameters: 27
Total number of parameters: 54
Number of training data pairs: 144
Number of checking data pairs: 0
Number of fuzzy rules: 27

Start training ANFIS ...

1 2.651
2 2.651

Designated epoch number reached --> ANFIS training completed at epoch 2.

Minimal training RMSE = 2.651003

ANFIS info:
Number of nodes: 78
Number of linear parameters: 27
Number of nonlinear parameters: 27
Total number of parameters: 54
Number of training data pairs: 144
Number of checking data pairs: 0
Number of fuzzy rules: 27

Start training ANFIS ...

1 2.651
2 2.651

Designated epoch number reached --> ANFIS training completed at epoch 2.

Minimal training RMSE = 2.651003

ANFIS info:
Number of nodes: 78
Number of linear parameters: 27
Number of nonlinear parameters: 27
Total number of parameters: 54
Number of training data pairs: 144
Number of checking data pairs: 0
Number of fuzzy rules: 27

Start training ANFIS ...

1 2.651
2 2.651

Designated epoch number reached --> ANFIS training completed at epoch 2.

Minimal training RMSE = 2.651003

ANFIS info:
Number of nodes: 78
Number of linear parameters: 27

Number of nonlinear parameters: 27

Total number of parameters: 54

Number of training data pairs: 144

Number of checking data pairs: 0

Number of fuzzy rules: 27

Start training ANFIS ...

1 2.651

2 2.651

Designated epoch number reached --> ANFIS training completed at epoch 2.

Minimal training RMSE = 2.651003

ANFIS info:

Number of nodes: 78

Number of linear parameters: 27

Number of nonlinear parameters: 27

Total number of parameters: 54

Number of training data pairs: 144

Number of checking data pairs: 0

Number of fuzzy rules: 27

Start training ANFIS ...

1 2.651

2 2.651

Designated epoch number reached --> ANFIS training completed at epoch 2.

Minimal training RMSE = 2.651003

ANFIS info:
Number of nodes: 78
Number of linear parameters: 27
Number of nonlinear parameters: 27
Total number of parameters: 54
Number of training data pairs: 144
Number of checking data pairs: 0
Number of fuzzy rules: 27

Start training ANFIS ...

1 2.651
2 2.651

Designated epoch number reached --> ANFIS training completed at epoch 2.

Minimal training RMSE = 2.651003

ANFIS info:
Number of nodes: 78
Number of linear parameters: 27
Number of nonlinear parameters: 27
Total number of parameters: 54
Number of training data pairs: 144
Number of checking data pairs: 0
Number of fuzzy rules: 27

Start training ANFIS ...

1 2.651

2 2.651

Designated epoch number reached --> ANFIS training completed at epoch 2.

Minimal training RMSE = 2.651003

ANFIS info:

Number of nodes: 78

Number of linear parameters: 27

Number of nonlinear parameters: 27

Total number of parameters: 54

Number of training data pairs: 144

Number of checking data pairs: 0

Number of fuzzy rules: 27

Start training ANFIS ...

1 2.651

2 2.651

Designated epoch number reached --> ANFIS training completed at epoch 2.

Minimal training RMSE = 2.651003

ANFIS info:

Number of nodes: 78

Number of linear parameters: 27

Number of nonlinear parameters: 27

Total number of parameters: 54

Number of training data pairs: 144
Number of checking data pairs: 0
Number of fuzzy rules: 27

Start training ANFIS ...

1 2.651
2 2.651

Designated epoch number reached --> ANFIS training completed at epoch 2.

Minimal training RMSE = 2.651003

ANFIS info:
Number of nodes: 78
Number of linear parameters: 27
Number of nonlinear parameters: 27
Total number of parameters: 54
Number of training data pairs: 144
Number of checking data pairs: 0
Number of fuzzy rules: 27

Start training ANFIS ...

1 2.651
2 2.651

Designated epoch number reached --> ANFIS training completed at epoch 2.

Minimal training RMSE = 2.651003

ANFIS info:
Number of nodes: 78
Number of linear parameters: 27
Number of nonlinear parameters: 27
Total number of parameters: 54
Number of training data pairs: 144
Number of checking data pairs: 0
Number of fuzzy rules: 27

Start training ANFIS ...

1 2.651
2 2.651

Designated epoch number reached --> ANFIS training completed at epoch 2.

Minimal training RMSE = 2.651003

ANFIS info:
Number of nodes: 78
Number of linear parameters: 27
Number of nonlinear parameters: 27
Total number of parameters: 54
Number of training data pairs: 144
Number of checking data pairs: 0
Number of fuzzy rules: 27

Start training ANFIS ...

1 2.651

2 2.651

Designated epoch number reached --> ANFIS training completed at epoch 2.

Minimal training RMSE = 2.651003

ANFIS info:
Number of nodes: 78
Number of linear parameters: 27
Number of nonlinear parameters: 27
Total number of parameters: 54
Number of training data pairs: 144
Number of checking data pairs: 0
Number of fuzzy rules: 27

Start training ANFIS ...

1 2.651
2 2.651

Designated epoch number reached --> ANFIS training completed at epoch 2.

Minimal training RMSE = 2.651003

ANFIS info:
Number of nodes: 78
Number of linear parameters: 27
Number of nonlinear parameters: 27
Total number of parameters: 54
Number of training data pairs: 144
Number of checking data pairs: 0

Number of fuzzy rules: 27

Start training ANFIS ...

1 2.651
2 2.651

Designated epoch number reached --> ANFIS training completed at epoch 2.

Minimal training RMSE = 2.651003

ANFIS info:
Number of nodes: 78
Number of linear parameters: 27
Number of nonlinear parameters: 27
Total number of parameters: 54
Number of training data pairs: 144
Number of checking data pairs: 0
Number of fuzzy rules: 27

Start training ANFIS ...

1 2.651
2 2.651

Designated epoch number reached --> ANFIS training completed at epoch 2.

Minimal training RMSE = 2.651003

ANFIS info:

Number of nodes: 78

Number of linear parameters: 27

Number of nonlinear parameters: 27

Total number of parameters: 54

Number of training data pairs: 144

Number of checking data pairs: 0

Number of fuzzy rules: 27

Start training ANFIS ...

1 2.651

2 2.651

Designated epoch number reached --> ANFIS training completed at epoch 2.

Minimal training RMSE = 2.651003

ANFIS info:

Number of nodes: 78

Number of linear parameters: 27

Number of nonlinear parameters: 27

Total number of parameters: 54

Number of training data pairs: 144

Number of checking data pairs: 0

Number of fuzzy rules: 27

Start training ANFIS ...

1 2.651

2 2.651

Designated epoch number reached --> ANFIS training completed at epoch 2.

Minimal training RMSE = 2.651003

ANFIS info:
Number of nodes: 78
Number of linear parameters: 27
Number of nonlinear parameters: 27
Total number of parameters: 54
Number of training data pairs: 144
Number of checking data pairs: 0
Number of fuzzy rules: 27

Start training ANFIS ...

1 2.651
2 2.651

Designated epoch number reached --> ANFIS training completed at epoch 2.

Minimal training RMSE = 2.651003

ANFIS info:
Number of nodes: 78
Number of linear parameters: 27
Number of nonlinear parameters: 27
Total number of parameters: 54
Number of training data pairs: 144
Number of checking data pairs: 0
Number of fuzzy rules: 27

Start training ANFIS ...

1 2.651
2 2.651

Designated epoch number reached --> ANFIS training completed at epoch 2.

Minimal training RMSE = 2.651003

ANFIS info:
Number of nodes: 78
Number of linear parameters: 27
Number of nonlinear parameters: 27
Total number of parameters: 54
Number of training data pairs: 144
Number of checking data pairs: 0
Number of fuzzy rules: 27

Start training ANFIS ...

1 2.651
2 2.651

Designated epoch number reached --> ANFIS training completed at epoch 2.

Minimal training RMSE = 2.651003

ANFIS info:
Number of nodes: 78
Number of linear parameters: 27

Number of nonlinear parameters: 27

Total number of parameters: 54

Number of training data pairs: 144

Number of checking data pairs: 0

Number of fuzzy rules: 27

Start training ANFIS ...

1 2.651

2 2.651

Designated epoch number reached --> ANFIS training completed at epoch 2.

Minimal training RMSE = 2.651003

ANFIS info:

Number of nodes: 78

Number of linear parameters: 27

Number of nonlinear parameters: 27

Total number of parameters: 54

Number of training data pairs: 144

Number of checking data pairs: 0

Number of fuzzy rules: 27

Start training ANFIS ...

1 2.651

2 2.651

Designated epoch number reached --> ANFIS training completed at epoch 2.

Minimal training RMSE = 2.651003

ANFIS info:
Number of nodes: 78
Number of linear parameters: 27
Number of nonlinear parameters: 27
Total number of parameters: 54
Number of training data pairs: 144
Number of checking data pairs: 0
Number of fuzzy rules: 27

Start training ANFIS ...

1 2.651
2 2.651

Designated epoch number reached --> ANFIS training completed at epoch 2.

Minimal training RMSE = 2.651003

ANFIS info:
Number of nodes: 78
Number of linear parameters: 27
Number of nonlinear parameters: 27
Total number of parameters: 54
Number of training data pairs: 144
Number of checking data pairs: 0
Number of fuzzy rules: 27

Start training ANFIS ...

1 2.651

2 2.651

Designated epoch number reached --> ANFIS training completed at epoch 2.

Minimal training RMSE = 2.651003

ANFIS info:

Number of nodes: 78

Number of linear parameters: 27

Number of nonlinear parameters: 27

Total number of parameters: 54

Number of training data pairs: 144

Number of checking data pairs: 0

Number of fuzzy rules: 27

Start training ANFIS ...

1 2.651

2 2.651

Designated epoch number reached --> ANFIS training completed at epoch 2.

Minimal training RMSE = 2.651003

ANFIS info:

Number of nodes: 78

Number of linear parameters: 27

Number of nonlinear parameters: 27

Total number of parameters: 54

Number of training data pairs: 144
Number of checking data pairs: 0
Number of fuzzy rules: 27

Start training ANFIS ...

1 2.651
2 2.651

Designated epoch number reached --> ANFIS training completed at epoch 2.

Minimal training RMSE = 2.651003

ANFIS info:
Number of nodes: 78
Number of linear parameters: 27
Number of nonlinear parameters: 27
Total number of parameters: 54
Number of training data pairs: 144
Number of checking data pairs: 0
Number of fuzzy rules: 27

Start training ANFIS ...

1 2.651
2 2.651

Designated epoch number reached --> ANFIS training completed at epoch 2.

Minimal training RMSE = 2.651003

ANFIS info:
Number of nodes: 78
Number of linear parameters: 27
Number of nonlinear parameters: 27
Total number of parameters: 54
Number of training data pairs: 144
Number of checking data pairs: 0
Number of fuzzy rules: 27

Start training ANFIS ...

1 2.651
2 2.651

Designated epoch number reached --> ANFIS training completed at epoch 2.

Minimal training RMSE = 2.651003

ANFIS info:
Number of nodes: 78
Number of linear parameters: 27
Number of nonlinear parameters: 27
Total number of parameters: 54
Number of training data pairs: 144
Number of checking data pairs: 0
Number of fuzzy rules: 27

Start training ANFIS ...

1 2.651

2 2.651

Designated epoch number reached --> ANFIS training completed at epoch 2.

Minimal training RMSE = 2.651003

ANFIS info:
Number of nodes: 78
Number of linear parameters: 27
Number of nonlinear parameters: 27
Total number of parameters: 54
Number of training data pairs: 144
Number of checking data pairs: 0
Number of fuzzy rules: 27

Start training ANFIS ...

1 2.651
2 2.651

Designated epoch number reached --> ANFIS training completed at epoch 2.

Minimal training RMSE = 2.651003

ANFIS info:
Number of nodes: 78
Number of linear parameters: 27
Number of nonlinear parameters: 27
Total number of parameters: 54
Number of training data pairs: 144
Number of checking data pairs: 0

Number of fuzzy rules: 27

Start training ANFIS ...

1 2.651
2 2.651

Designated epoch number reached --> ANFIS training completed at epoch 2.

Minimal training RMSE = 2.651003

ANFIS info:
Number of nodes: 78
Number of linear parameters: 27
Number of nonlinear parameters: 27
Total number of parameters: 54
Number of training data pairs: 144
Number of checking data pairs: 0
Number of fuzzy rules: 27

Start training ANFIS ...

1 2.651
2 2.651

Designated epoch number reached --> ANFIS training completed at epoch 2.

Minimal training RMSE = 2.651003

ANFIS info:

Number of nodes: 78

Number of linear parameters: 27

Number of nonlinear parameters: 27

Total number of parameters: 54

Number of training data pairs: 144

Number of checking data pairs: 0

Number of fuzzy rules: 27

Start training ANFIS ...

1 2.651

2 2.651

Designated epoch number reached --> ANFIS training completed at epoch 2.

Minimal training RMSE = 2.651003

ANFIS info:

Number of nodes: 78

Number of linear parameters: 27

Number of nonlinear parameters: 27

Total number of parameters: 54

Number of training data pairs: 144

Number of checking data pairs: 0

Number of fuzzy rules: 27

Start training ANFIS ...

1 2.651

2 2.651

Designated epoch number reached --> ANFIS training completed at epoch 2.

Minimal training RMSE = 2.651003

ANFIS info:
Number of nodes: 78
Number of linear parameters: 27
Number of nonlinear parameters: 27
Total number of parameters: 54
Number of training data pairs: 144
Number of checking data pairs: 0
Number of fuzzy rules: 27

Start training ANFIS ...

1 2.651
2 2.651

Designated epoch number reached --> ANFIS training completed at epoch 2.

Minimal training RMSE = 2.651003

ANFIS info:
Number of nodes: 78
Number of linear parameters: 27
Number of nonlinear parameters: 27
Total number of parameters: 54
Number of training data pairs: 144
Number of checking data pairs: 0
Number of fuzzy rules: 27

Start training ANFIS ...

1 2.651
2 2.651

Designated epoch number reached --> ANFIS training completed at epoch 2.

Minimal training RMSE = 2.651003

ANFIS info:
Number of nodes: 78
Number of linear parameters: 27
Number of nonlinear parameters: 27
Total number of parameters: 54
Number of training data pairs: 144
Number of checking data pairs: 0
Number of fuzzy rules: 27

Start training ANFIS ...

1 2.651
2 2.651

Designated epoch number reached --> ANFIS training completed at epoch 2.

Minimal training RMSE = 2.651003

ANFIS info:
Number of nodes: 78
Number of linear parameters: 27

Number of nonlinear parameters: 27

Total number of parameters: 54

Number of training data pairs: 144

Number of checking data pairs: 0

Number of fuzzy rules: 27

Start training ANFIS ...

1 2.651

2 2.651

Designated epoch number reached --> ANFIS training completed at epoch 2.

Minimal training RMSE = 2.651003

ANFIS info:

Number of nodes: 78

Number of linear parameters: 27

Number of nonlinear parameters: 27

Total number of parameters: 54

Number of training data pairs: 144

Number of checking data pairs: 0

Number of fuzzy rules: 27

Start training ANFIS ...

1 2.651

2 2.651

Designated epoch number reached --> ANFIS training completed at epoch 2.

Minimal training RMSE = 2.651003

ANFIS info:
Number of nodes: 78
Number of linear parameters: 27
Number of nonlinear parameters: 27
Total number of parameters: 54
Number of training data pairs: 144
Number of checking data pairs: 0
Number of fuzzy rules: 27

Start training ANFIS ...

1 2.651
2 2.651

Designated epoch number reached --> ANFIS training completed at epoch 2.

Minimal training RMSE = 2.651003

ANFIS info:
Number of nodes: 78
Number of linear parameters: 27
Number of nonlinear parameters: 27
Total number of parameters: 54
Number of training data pairs: 144
Number of checking data pairs: 0
Number of fuzzy rules: 27

Start training ANFIS ...

1 2.651

2 2.651

Designated epoch number reached --> ANFIS training completed at epoch 2.

Minimal training RMSE = 2.651003

ANFIS info:

Number of nodes: 78

Number of linear parameters: 27

Number of nonlinear parameters: 27

Total number of parameters: 54

Number of training data pairs: 144

Number of checking data pairs: 0

Number of fuzzy rules: 27

Start training ANFIS ...

1 2.651

2 2.651

Designated epoch number reached --> ANFIS training completed at epoch 2.

Minimal training RMSE = 2.651003

ANFIS info:

Number of nodes: 78

Number of linear parameters: 27

Number of nonlinear parameters: 27

Total number of parameters: 54

Number of training data pairs: 144
Number of checking data pairs: 0
Number of fuzzy rules: 27

Start training ANFIS ...

1 2.651
2 2.651

Designated epoch number reached --> ANFIS training completed at epoch 2.

Minimal training RMSE = 2.651003

ANFIS info:
Number of nodes: 78
Number of linear parameters: 27
Number of nonlinear parameters: 27
Total number of parameters: 54
Number of training data pairs: 144
Number of checking data pairs: 0
Number of fuzzy rules: 27

Start training ANFIS ...

1 2.651
2 2.651

Designated epoch number reached --> ANFIS training completed at epoch 2.

Minimal training RMSE = 2.651003

ANFIS info:
Number of nodes: 78
Number of linear parameters: 27
Number of nonlinear parameters: 27
Total number of parameters: 54
Number of training data pairs: 144
Number of checking data pairs: 0
Number of fuzzy rules: 27

Start training ANFIS ...

1 2.651
2 2.651

Designated epoch number reached --> ANFIS training completed at epoch 2.

Minimal training RMSE = 2.651003

ANFIS info:
Number of nodes: 78
Number of linear parameters: 27
Number of nonlinear parameters: 27
Total number of parameters: 54
Number of training data pairs: 144
Number of checking data pairs: 0
Number of fuzzy rules: 27

Start training ANFIS ...

1 2.651

2 2.651

Designated epoch number reached --> ANFIS training completed at epoch 2.

Minimal training RMSE = 2.651003

ANFIS info:
Number of nodes: 78
Number of linear parameters: 27
Number of nonlinear parameters: 27
Total number of parameters: 54
Number of training data pairs: 144
Number of checking data pairs: 0
Number of fuzzy rules: 27

Start training ANFIS ...

1 2.651
2 2.651

Designated epoch number reached --> ANFIS training completed at epoch 2.

Minimal training RMSE = 2.651003

ANFIS info:
Number of nodes: 78
Number of linear parameters: 27
Number of nonlinear parameters: 27
Total number of parameters: 54
Number of training data pairs: 144
Number of checking data pairs: 0

Number of fuzzy rules: 27

Start training ANFIS ...

1 2.651
2 2.651

Designated epoch number reached --> ANFIS training completed at epoch 2.

Minimal training RMSE = 2.651003

ANFIS info:
Number of nodes: 78
Number of linear parameters: 27
Number of nonlinear parameters: 27
Total number of parameters: 54
Number of training data pairs: 144
Number of checking data pairs: 0
Number of fuzzy rules: 27

Start training ANFIS ...

1 2.651
2 2.651

Designated epoch number reached --> ANFIS training completed at epoch 2.

Minimal training RMSE = 2.651003

ANFIS info:

Number of nodes: 78

Number of linear parameters: 27

Number of nonlinear parameters: 27

Total number of parameters: 54

Number of training data pairs: 144

Number of checking data pairs: 0

Number of fuzzy rules: 27

Start training ANFIS ...

1 2.651

2 2.651

Designated epoch number reached --> ANFIS training completed at epoch 2.

Minimal training RMSE = 2.651003

ANFIS info:

Number of nodes: 78

Number of linear parameters: 27

Number of nonlinear parameters: 27

Total number of parameters: 54

Number of training data pairs: 144

Number of checking data pairs: 0

Number of fuzzy rules: 27

Start training ANFIS ...

1 2.651

2 2.651

Designated epoch number reached --> ANFIS training completed at epoch 2.

Minimal training RMSE = 2.651003

ANFIS info:
Number of nodes: 78
Number of linear parameters: 27
Number of nonlinear parameters: 27
Total number of parameters: 54
Number of training data pairs: 144
Number of checking data pairs: 0
Number of fuzzy rules: 27

Start training ANFIS ...

1 2.651
2 2.651

Designated epoch number reached --> ANFIS training completed at epoch 2.

Minimal training RMSE = 2.651003

ANFIS info:
Number of nodes: 78
Number of linear parameters: 27
Number of nonlinear parameters: 27
Total number of parameters: 54
Number of training data pairs: 144
Number of checking data pairs: 0
Number of fuzzy rules: 27

Start training ANFIS ...

1 2.651
2 2.651

Designated epoch number reached --> ANFIS training completed at epoch 2.

Minimal training RMSE = 2.651003

ANFIS info:
Number of nodes: 78
Number of linear parameters: 27
Number of nonlinear parameters: 27
Total number of parameters: 54
Number of training data pairs: 144
Number of checking data pairs: 0
Number of fuzzy rules: 27

Start training ANFIS ...

1 2.651
2 2.651

Designated epoch number reached --> ANFIS training completed at epoch 2.

Minimal training RMSE = 2.651003

ANFIS info:
Number of nodes: 78
Number of linear parameters: 27

Number of nonlinear parameters: 27

Total number of parameters: 54

Number of training data pairs: 144

Number of checking data pairs: 0

Number of fuzzy rules: 27

Start training ANFIS ...

1 2.651

2 2.651

Designated epoch number reached --> ANFIS training completed at epoch 2.

Minimal training RMSE = 2.651003

ANFIS info:

Number of nodes: 78

Number of linear parameters: 27

Number of nonlinear parameters: 27

Total number of parameters: 54

Number of training data pairs: 144

Number of checking data pairs: 0

Number of fuzzy rules: 27

Start training ANFIS ...

1 2.651

2 2.651

Designated epoch number reached --> ANFIS training completed at epoch 2.

Minimal training RMSE = 2.651003

ANFIS info:
Number of nodes: 78
Number of linear parameters: 27
Number of nonlinear parameters: 27
Total number of parameters: 54
Number of training data pairs: 144
Number of checking data pairs: 0
Number of fuzzy rules: 27

Start training ANFIS ...

1 2.651
2 2.651

Designated epoch number reached --> ANFIS training completed at epoch 2.

Minimal training RMSE = 2.651003

ANFIS info:
Number of nodes: 78
Number of linear parameters: 27
Number of nonlinear parameters: 27
Total number of parameters: 54
Number of training data pairs: 144
Number of checking data pairs: 0
Number of fuzzy rules: 27

Start training ANFIS ...

1 2.651

2 2.651

Designated epoch number reached --> ANFIS training completed at epoch 2.

Minimal training RMSE = 2.651003

ANFIS info:

Number of nodes: 78

Number of linear parameters: 27

Number of nonlinear parameters: 27

Total number of parameters: 54

Number of training data pairs: 144

Number of checking data pairs: 0

Number of fuzzy rules: 27

Start training ANFIS ...

1 2.651

2 2.651

Designated epoch number reached --> ANFIS training completed at epoch 2.

Minimal training RMSE = 2.651003

ANFIS info:

Number of nodes: 78

Number of linear parameters: 27

Number of nonlinear parameters: 27

Total number of parameters: 54

Number of training data pairs: 144
Number of checking data pairs: 0
Number of fuzzy rules: 27

Start training ANFIS ...

1 2.651
2 2.651

Designated epoch number reached --> ANFIS training completed at epoch 2.

Minimal training RMSE = 2.651003

ANFIS info:
Number of nodes: 78
Number of linear parameters: 27
Number of nonlinear parameters: 27
Total number of parameters: 54
Number of training data pairs: 144
Number of checking data pairs: 0
Number of fuzzy rules: 27

Start training ANFIS ...

1 2.651
2 2.651

Designated epoch number reached --> ANFIS training completed at epoch 2.

Minimal training RMSE = 2.651003

ANFIS info:
Number of nodes: 78
Number of linear parameters: 27
Number of nonlinear parameters: 27
Total number of parameters: 54
Number of training data pairs: 144
Number of checking data pairs: 0
Number of fuzzy rules: 27

Start training ANFIS ...

1 2.651
2 2.651

Designated epoch number reached --> ANFIS training completed at epoch 2.

Minimal training RMSE = 2.651003

ANFIS info:
Number of nodes: 78
Number of linear parameters: 27
Number of nonlinear parameters: 27
Total number of parameters: 54
Number of training data pairs: 144
Number of checking data pairs: 0
Number of fuzzy rules: 27

Start training ANFIS ...

1 2.651

2 2.651

Designated epoch number reached --> ANFIS training completed at epoch 2.

Minimal training RMSE = 2.651003

ANFIS info:
Number of nodes: 78
Number of linear parameters: 27
Number of nonlinear parameters: 27
Total number of parameters: 54
Number of training data pairs: 144
Number of checking data pairs: 0
Number of fuzzy rules: 27

Start training ANFIS ...

1 2.651
2 2.651

Designated epoch number reached --> ANFIS training completed at epoch 2.

Minimal training RMSE = 2.651003

ANFIS info:
Number of nodes: 78
Number of linear parameters: 27
Number of nonlinear parameters: 27
Total number of parameters: 54
Number of training data pairs: 144
Number of checking data pairs: 0

Number of fuzzy rules: 27

Start training ANFIS ...

1 2.651
2 2.651

Designated epoch number reached --> ANFIS training completed at epoch 2.

Minimal training RMSE = 2.651003

ANFIS info:
Number of nodes: 78
Number of linear parameters: 27
Number of nonlinear parameters: 27
Total number of parameters: 54
Number of training data pairs: 144
Number of checking data pairs: 0
Number of fuzzy rules: 27

Start training ANFIS ...

1 2.651
2 2.651

Designated epoch number reached --> ANFIS training completed at epoch 2.

Minimal training RMSE = 2.651003

ANFIS info:

Number of nodes: 78

Number of linear parameters: 27

Number of nonlinear parameters: 27

Total number of parameters: 54

Number of training data pairs: 144

Number of checking data pairs: 0

Number of fuzzy rules: 27

Start training ANFIS ...

1 2.651

2 2.651

Designated epoch number reached --> ANFIS training completed at epoch 2.

Minimal training RMSE = 2.651003

ANFIS info:

Number of nodes: 78

Number of linear parameters: 27

Number of nonlinear parameters: 27

Total number of parameters: 54

Number of training data pairs: 144

Number of checking data pairs: 0

Number of fuzzy rules: 27

Start training ANFIS ...

1 2.651

2 2.651

Designated epoch number reached --> ANFIS training completed at epoch 2.

Minimal training RMSE = 2.651003

ANFIS info:
Number of nodes: 78
Number of linear parameters: 27
Number of nonlinear parameters: 27
Total number of parameters: 54
Number of training data pairs: 144
Number of checking data pairs: 0
Number of fuzzy rules: 27

Start training ANFIS ...

1 2.651
2 2.651

Designated epoch number reached --> ANFIS training completed at epoch 2.

Minimal training RMSE = 2.651003

ANFIS info:
Number of nodes: 78
Number of linear parameters: 27
Number of nonlinear parameters: 27
Total number of parameters: 54
Number of training data pairs: 144
Number of checking data pairs: 0
Number of fuzzy rules: 27

Start training ANFIS ...

1 2.651
2 2.651

Designated epoch number reached --> ANFIS training completed at epoch 2.

Minimal training RMSE = 2.651003

ANFIS info:
Number of nodes: 78
Number of linear parameters: 27
Number of nonlinear parameters: 27
Total number of parameters: 54
Number of training data pairs: 144
Number of checking data pairs: 0
Number of fuzzy rules: 27

Start training ANFIS ...

1 2.651
2 2.651

Designated epoch number reached --> ANFIS training completed at epoch 2.

Minimal training RMSE = 2.651003

ANFIS info:
Number of nodes: 78
Number of linear parameters: 27

Number of nonlinear parameters: 27

Total number of parameters: 54

Number of training data pairs: 144

Number of checking data pairs: 0

Number of fuzzy rules: 27

Start training ANFIS ...

1 2.651

2 2.651

Designated epoch number reached --> ANFIS training completed at epoch 2.

Minimal training RMSE = 2.651003

ANFIS info:

Number of nodes: 78

Number of linear parameters: 27

Number of nonlinear parameters: 27

Total number of parameters: 54

Number of training data pairs: 144

Number of checking data pairs: 0

Number of fuzzy rules: 27

Start training ANFIS ...

1 2.651

2 2.651

Designated epoch number reached --> ANFIS training completed at epoch 2.

Minimal training RMSE = 2.651003

ANFIS info:
Number of nodes: 78
Number of linear parameters: 27
Number of nonlinear parameters: 27
Total number of parameters: 54
Number of training data pairs: 144
Number of checking data pairs: 0
Number of fuzzy rules: 27

Start training ANFIS ...

1 2.651
2 2.651

Designated epoch number reached --> ANFIS training completed at epoch 2.

Minimal training RMSE = 2.651003

ANFIS info:
Number of nodes: 78
Number of linear parameters: 27
Number of nonlinear parameters: 27
Total number of parameters: 54
Number of training data pairs: 144
Number of checking data pairs: 0
Number of fuzzy rules: 27

Start training ANFIS ...

1 2.651

2 2.651

Designated epoch number reached --> ANFIS training completed at epoch 2.

Minimal training RMSE = 2.651003

ANFIS info:

Number of nodes: 78

Number of linear parameters: 27

Number of nonlinear parameters: 27

Total number of parameters: 54

Number of training data pairs: 144

Number of checking data pairs: 0

Number of fuzzy rules: 27

Start training ANFIS ...

1 2.651

2 2.651

Designated epoch number reached --> ANFIS training completed at epoch 2.

Minimal training RMSE = 2.651003

ANFIS info:

Number of nodes: 78

Number of linear parameters: 27

Number of nonlinear parameters: 27

Total number of parameters: 54

Number of training data pairs: 144
Number of checking data pairs: 0
Number of fuzzy rules: 27

Start training ANFIS ...

1 2.651
2 2.651

Designated epoch number reached --> ANFIS training completed at epoch 2.

Minimal training RMSE = 2.651003

ANFIS info:
Number of nodes: 78
Number of linear parameters: 27
Number of nonlinear parameters: 27
Total number of parameters: 54
Number of training data pairs: 144
Number of checking data pairs: 0
Number of fuzzy rules: 27

Start training ANFIS ...

1 2.651
2 2.651

Designated epoch number reached --> ANFIS training completed at epoch 2.

Minimal training RMSE = 2.651003

ANFIS info:
Number of nodes: 78
Number of linear parameters: 27
Number of nonlinear parameters: 27
Total number of parameters: 54
Number of training data pairs: 144
Number of checking data pairs: 0
Number of fuzzy rules: 27

Start training ANFIS ...

1 2.651
2 2.651

Designated epoch number reached --> ANFIS training completed at epoch 2.

Minimal training RMSE = 2.651003

ANFIS info:
Number of nodes: 78
Number of linear parameters: 27
Number of nonlinear parameters: 27
Total number of parameters: 54
Number of training data pairs: 144
Number of checking data pairs: 0
Number of fuzzy rules: 27

Start training ANFIS ...

1 2.651

2 2.651

Designated epoch number reached --> ANFIS training completed at epoch 2.

Minimal training RMSE = 2.651003

ANFIS info:
Number of nodes: 78
Number of linear parameters: 27
Number of nonlinear parameters: 27
Total number of parameters: 54
Number of training data pairs: 144
Number of checking data pairs: 0
Number of fuzzy rules: 27

Start training ANFIS ...

1 2.651
2 2.651

Designated epoch number reached --> ANFIS training completed at epoch 2.

Minimal training RMSE = 2.651003

ANFIS info:
Number of nodes: 78
Number of linear parameters: 27
Number of nonlinear parameters: 27
Total number of parameters: 54
Number of training data pairs: 144
Number of checking data pairs: 0

Number of fuzzy rules: 27

Start training ANFIS ...

1 2.651
2 2.651

Designated epoch number reached --> ANFIS training completed at epoch 2.

Minimal training RMSE = 2.651003

ANFIS info:
Number of nodes: 78
Number of linear parameters: 27
Number of nonlinear parameters: 27
Total number of parameters: 54
Number of training data pairs: 144
Number of checking data pairs: 0
Number of fuzzy rules: 27

Start training ANFIS ...

1 2.651
2 2.651

Designated epoch number reached --> ANFIS training completed at epoch 2.

Minimal training RMSE = 2.651003

ANFIS info:

Number of nodes: 78

Number of linear parameters: 27

Number of nonlinear parameters: 27

Total number of parameters: 54

Number of training data pairs: 144

Number of checking data pairs: 0

Number of fuzzy rules: 27

Start training ANFIS ...

1 2.651

2 2.651

Designated epoch number reached --> ANFIS training completed at epoch 2.

Minimal training RMSE = 2.651003

ANFIS info:

Number of nodes: 78

Number of linear parameters: 27

Number of nonlinear parameters: 27

Total number of parameters: 54

Number of training data pairs: 144

Number of checking data pairs: 0

Number of fuzzy rules: 27

Start training ANFIS ...

1 2.651

2 2.651

Designated epoch number reached --> ANFIS training completed at epoch 2.

Minimal training RMSE = 2.651003

ANFIS info:
Number of nodes: 78
Number of linear parameters: 27
Number of nonlinear parameters: 27
Total number of parameters: 54
Number of training data pairs: 144
Number of checking data pairs: 0
Number of fuzzy rules: 27

Start training ANFIS ...

1 2.651
2 2.651

Designated epoch number reached --> ANFIS training completed at epoch 2.

Minimal training RMSE = 2.651003

ANFIS info:
Number of nodes: 78
Number of linear parameters: 27
Number of nonlinear parameters: 27
Total number of parameters: 54
Number of training data pairs: 144
Number of checking data pairs: 0
Number of fuzzy rules: 27

Start training ANFIS ...

1 2.651
2 2.651

Designated epoch number reached --> ANFIS training completed at epoch 2.

Minimal training RMSE = 2.651003

ANFIS info:
Number of nodes: 78
Number of linear parameters: 27
Number of nonlinear parameters: 27
Total number of parameters: 54
Number of training data pairs: 144
Number of checking data pairs: 0
Number of fuzzy rules: 27

Start training ANFIS ...

1 2.651
2 2.651

Designated epoch number reached --> ANFIS training completed at epoch 2.

Minimal training RMSE = 2.651003

ANFIS info:
Number of nodes: 78
Number of linear parameters: 27

Number of nonlinear parameters: 27

Total number of parameters: 54

Number of training data pairs: 144

Number of checking data pairs: 0

Number of fuzzy rules: 27

Start training ANFIS ...

1 2.651

2 2.651

Designated epoch number reached --> ANFIS training completed at epoch 2.

Minimal training RMSE = 2.651003

ANFIS info:

Number of nodes: 78

Number of linear parameters: 27

Number of nonlinear parameters: 27

Total number of parameters: 54

Number of training data pairs: 144

Number of checking data pairs: 0

Number of fuzzy rules: 27

Start training ANFIS ...

1 2.651

2 2.651

Designated epoch number reached --> ANFIS training completed at epoch 2.

Minimal training RMSE = 2.651003

ANFIS info:
Number of nodes: 78
Number of linear parameters: 27
Number of nonlinear parameters: 27
Total number of parameters: 54
Number of training data pairs: 144
Number of checking data pairs: 0
Number of fuzzy rules: 27

Start training ANFIS ...

1 2.651
2 2.651

Designated epoch number reached --> ANFIS training completed at epoch 2.

Minimal training RMSE = 2.651003

ANFIS info:
Number of nodes: 78
Number of linear parameters: 27
Number of nonlinear parameters: 27
Total number of parameters: 54
Number of training data pairs: 144
Number of checking data pairs: 0
Number of fuzzy rules: 27

Start training ANFIS ...

1 2.651

2 2.651

Designated epoch number reached --> ANFIS training completed at epoch 2.

Minimal training RMSE = 2.651003

ANFIS info:

Number of nodes: 78

Number of linear parameters: 27

Number of nonlinear parameters: 27

Total number of parameters: 54

Number of training data pairs: 144

Number of checking data pairs: 0

Number of fuzzy rules: 27

Start training ANFIS ...

1 2.651

2 2.651

Designated epoch number reached --> ANFIS training completed at epoch 2.

Minimal training RMSE = 2.651003

ANFIS info:

Number of nodes: 78

Number of linear parameters: 27

Number of nonlinear parameters: 27

Total number of parameters: 54

Number of training data pairs: 144
Number of checking data pairs: 0
Number of fuzzy rules: 27

Start training ANFIS ...

1 2.651
2 2.651

Designated epoch number reached --> ANFIS training completed at epoch 2.

Minimal training RMSE = 2.651003

ANFIS info:
Number of nodes: 78
Number of linear parameters: 27
Number of nonlinear parameters: 27
Total number of parameters: 54
Number of training data pairs: 144
Number of checking data pairs: 0
Number of fuzzy rules: 27

Start training ANFIS ...

1 2.651
2 2.651

Designated epoch number reached --> ANFIS training completed at epoch 2.

Minimal training RMSE = 2.651003

ANFIS info:
Number of nodes: 78
Number of linear parameters: 27
Number of nonlinear parameters: 27
Total number of parameters: 54
Number of training data pairs: 144
Number of checking data pairs: 0
Number of fuzzy rules: 27

Start training ANFIS ...

1 2.651
2 2.651

Designated epoch number reached --> ANFIS training completed at epoch 2.

Minimal training RMSE = 2.651003

ANFIS info:
Number of nodes: 78
Number of linear parameters: 27
Number of nonlinear parameters: 27
Total number of parameters: 54
Number of training data pairs: 144
Number of checking data pairs: 0
Number of fuzzy rules: 27

Start training ANFIS ...

1 2.651

2 2.651

Designated epoch number reached --> ANFIS training completed at epoch 2.

Minimal training RMSE = 2.651003

ANFIS info:
Number of nodes: 78
Number of linear parameters: 27
Number of nonlinear parameters: 27
Total number of parameters: 54
Number of training data pairs: 144
Number of checking data pairs: 0
Number of fuzzy rules: 27

Start training ANFIS ...

1 2.651
2 2.651

Designated epoch number reached --> ANFIS training completed at epoch 2.

Minimal training RMSE = 2.651003

ANFIS info:
Number of nodes: 78
Number of linear parameters: 27
Number of nonlinear parameters: 27
Total number of parameters: 54
Number of training data pairs: 144
Number of checking data pairs: 0

Number of fuzzy rules: 27

Start training ANFIS ...

1 2.651
2 2.651

Designated epoch number reached --> ANFIS training completed at epoch 2.

Minimal training RMSE = 2.651003

ANFIS info:
Number of nodes: 78
Number of linear parameters: 27
Number of nonlinear parameters: 27
Total number of parameters: 54
Number of training data pairs: 144
Number of checking data pairs: 0
Number of fuzzy rules: 27

Start training ANFIS ...

1 2.651
2 2.651

Designated epoch number reached --> ANFIS training completed at epoch 2.

Minimal training RMSE = 2.651003

ANFIS info:

Number of nodes: 78

Number of linear parameters: 27

Number of nonlinear parameters: 27

Total number of parameters: 54

Number of training data pairs: 144

Number of checking data pairs: 0

Number of fuzzy rules: 27

Start training ANFIS ...

1 2.651

2 2.651

Designated epoch number reached --> ANFIS training completed at epoch 2.

Minimal training RMSE = 2.651003

ANFIS info:

Number of nodes: 78

Number of linear parameters: 27

Number of nonlinear parameters: 27

Total number of parameters: 54

Number of training data pairs: 144

Number of checking data pairs: 0

Number of fuzzy rules: 27

Start training ANFIS ...

1 2.651

2 2.651

Designated epoch number reached --> ANFIS training completed at epoch 2.

Minimal training RMSE = 2.651003

ANFIS info:
Number of nodes: 78
Number of linear parameters: 27
Number of nonlinear parameters: 27
Total number of parameters: 54
Number of training data pairs: 144
Number of checking data pairs: 0
Number of fuzzy rules: 27

Start training ANFIS ...

1 2.651
2 2.651

Designated epoch number reached --> ANFIS training completed at epoch 2.

Minimal training RMSE = 2.651003

ANFIS info:
Number of nodes: 78
Number of linear parameters: 27
Number of nonlinear parameters: 27
Total number of parameters: 54
Number of training data pairs: 144
Number of checking data pairs: 0
Number of fuzzy rules: 27

Start training ANFIS ...

1 2.651
2 2.651

Designated epoch number reached --> ANFIS training completed at epoch 2.

Minimal training RMSE = 2.651003

ANFIS info:
Number of nodes: 78
Number of linear parameters: 27
Number of nonlinear parameters: 27
Total number of parameters: 54
Number of training data pairs: 144
Number of checking data pairs: 0
Number of fuzzy rules: 27

Start training ANFIS ...

1 2.651
2 2.651

Designated epoch number reached --> ANFIS training completed at epoch 2.

Minimal training RMSE = 2.651003

ANFIS info:
Number of nodes: 78
Number of linear parameters: 27

Number of nonlinear parameters: 27

Total number of parameters: 54

Number of training data pairs: 144

Number of checking data pairs: 0

Number of fuzzy rules: 27

Start training ANFIS ...

1 2.651

2 2.651

Designated epoch number reached --> ANFIS training completed at epoch 2.

Minimal training RMSE = 2.651003

ANFIS info:

Number of nodes: 78

Number of linear parameters: 27

Number of nonlinear parameters: 27

Total number of parameters: 54

Number of training data pairs: 144

Number of checking data pairs: 0

Number of fuzzy rules: 27

Start training ANFIS ...

1 2.651

2 2.651

Designated epoch number reached --> ANFIS training completed at epoch 2.

Minimal training RMSE = 2.651003

ANFIS info:
Number of nodes: 78
Number of linear parameters: 27
Number of nonlinear parameters: 27
Total number of parameters: 54
Number of training data pairs: 144
Number of checking data pairs: 0
Number of fuzzy rules: 27

Start training ANFIS ...

1 2.651
2 2.651

Designated epoch number reached --> ANFIS training completed at epoch 2.

Minimal training RMSE = 2.651003

ANFIS info:
Number of nodes: 78
Number of linear parameters: 27
Number of nonlinear parameters: 27
Total number of parameters: 54
Number of training data pairs: 144
Number of checking data pairs: 0
Number of fuzzy rules: 27

Start training ANFIS ...

1 2.651

2 2.651

Designated epoch number reached --> ANFIS training completed at epoch 2.

Minimal training RMSE = 2.651003

ANFIS info:

Number of nodes: 78

Number of linear parameters: 27

Number of nonlinear parameters: 27

Total number of parameters: 54

Number of training data pairs: 144

Number of checking data pairs: 0

Number of fuzzy rules: 27

Start training ANFIS ...

1 2.651

2 2.651

Designated epoch number reached --> ANFIS training completed at epoch 2.

Minimal training RMSE = 2.651003

ANFIS info:

Number of nodes: 78

Number of linear parameters: 27

Number of nonlinear parameters: 27

Total number of parameters: 54

Number of training data pairs: 144
Number of checking data pairs: 0
Number of fuzzy rules: 27

Start training ANFIS ...

1 2.651
2 2.651

Designated epoch number reached --> ANFIS training completed at epoch 2.

Minimal training RMSE = 2.651003

ANFIS info:
Number of nodes: 78
Number of linear parameters: 27
Number of nonlinear parameters: 27
Total number of parameters: 54
Number of training data pairs: 144
Number of checking data pairs: 0
Number of fuzzy rules: 27

Start training ANFIS ...

1 2.651
2 2.651

Designated epoch number reached --> ANFIS training completed at epoch 2.

Minimal training RMSE = 2.651003

ANFIS info:
Number of nodes: 78
Number of linear parameters: 27
Number of nonlinear parameters: 27
Total number of parameters: 54
Number of training data pairs: 144
Number of checking data pairs: 0
Number of fuzzy rules: 27

Start training ANFIS ...

1 2.651
2 2.651

Designated epoch number reached --> ANFIS training completed at epoch 2.

Minimal training RMSE = 2.651003

ANFIS info:
Number of nodes: 78
Number of linear parameters: 27
Number of nonlinear parameters: 27
Total number of parameters: 54
Number of training data pairs: 144
Number of checking data pairs: 0
Number of fuzzy rules: 27

Start training ANFIS ...

1 2.651

2 2.651

Designated epoch number reached --> ANFIS training completed at epoch 2.

Minimal training RMSE = 2.651003

ANFIS info:
Number of nodes: 78
Number of linear parameters: 27
Number of nonlinear parameters: 27
Total number of parameters: 54
Number of training data pairs: 144
Number of checking data pairs: 0
Number of fuzzy rules: 27

Start training ANFIS ...

1 2.651
2 2.651

Designated epoch number reached --> ANFIS training completed at epoch 2.

Minimal training RMSE = 2.651003

ANFIS info:
Number of nodes: 78
Number of linear parameters: 27
Number of nonlinear parameters: 27
Total number of parameters: 54
Number of training data pairs: 144
Number of checking data pairs: 0

Number of fuzzy rules: 27

Start training ANFIS ...

1 2.651
2 2.651

Designated epoch number reached --> ANFIS training completed at epoch 2.

Minimal training RMSE = 2.651003

ANFIS info:
Number of nodes: 78
Number of linear parameters: 27
Number of nonlinear parameters: 27
Total number of parameters: 54
Number of training data pairs: 144
Number of checking data pairs: 0
Number of fuzzy rules: 27

Start training ANFIS ...

1 2.651
2 2.651

Designated epoch number reached --> ANFIS training completed at epoch 2.

Minimal training RMSE = 2.651003

ANFIS info:

Number of nodes: 78

Number of linear parameters: 27

Number of nonlinear parameters: 27

Total number of parameters: 54

Number of training data pairs: 144

Number of checking data pairs: 0

Number of fuzzy rules: 27

Start training ANFIS ...

1 2.651

2 2.651

Designated epoch number reached --> ANFIS training completed at epoch 2.

Minimal training RMSE = 2.651003

ANFIS info:

Number of nodes: 78

Number of linear parameters: 27

Number of nonlinear parameters: 27

Total number of parameters: 54

Number of training data pairs: 144

Number of checking data pairs: 0

Number of fuzzy rules: 27

Start training ANFIS ...

1 2.651

2 2.651

Designated epoch number reached --> ANFIS training completed at epoch 2.

Minimal training RMSE = 2.651003

APPENDIX D

Tab. D.1: ANFIS models

Process Parameters			Removal efficiency (%)	
pH	**Agitation speed (rpm)**	**Contact time (min.)**	**Experiment**	**ANFIS prediction**
4	200	20	35.82	40.86
8	200	20	56.71	60.34
6	150	185	87.6	87.60
4	100	350	92.59	92.59
8	200	350	87.99	87.99
6	150	350	89.3	89.30
4	100	20	31.62	38.11
8	150	185	73.14	73.14
6	100	185	81.68	81.68
8	100	350	86.54	87.83
4	100	20	44.59	38.11
8	100	350	89.12	87.83
6	200	350	98.74	98.74
4	200	20	45.95	40.86
4	150	185	49.36	49.36
8	200	20	63.97	60.34
4	200	350	87.07	88.28
6	200	185	86.41	86.41
8	100	20	76.43	76.99
8	100	20	77.56	76.99
6	150	20	68.41	68.41
8	200	350	87.99	87.99
4	200	350	89.49	88.28
4	100	350	92.59	92.59

Tab. D.2: Comparison of RSM and ANFIS model

Process Parameters			Removal efficiency (%)			Residuals	
			Exp.	Model prediction (%)			
pH	Agitation speed (rpm)	Contact time (min.)		RSM	ANFIS	RSM	ANFIS
4	200	20	35.82	38.46	40.86	-2.64	-5.065
8	200	20	56.71	65.05	60.34	-8.34	-3.629
6	150	185	87.6	79.19	87.60	8.41	0.001
4	100	350	92.59	87.56	92.59	5.03	0.001
8	200	350	87.99	84.38	87.99	3.61	0.001
6	150	350	89.3	96.73	89.30	-7.43	0.001
4	100	20	31.62	40.58	38.11	-8.96	-6.485
8	150	185	73.14	71.4	73.14	1.74	0.001
6	100	185	81.68	87.26	81.68	-5.58	0.001
8	100	350	86.54	89.94	87.83	-3.4	-1.289
4	100	20	44.59	40.58	38.11	4.01	6.485
8	100	350	89.12	89.94	87.83	-0.82	1.291
6	200	350	98.74	99.69	98.74	-0.95	0.001
4	200	20	45.95	38.46	40.86	7.49	5.065
4	150	185	49.36	56.92	49.36	-7.56	0.001
8	200	20	63.97	65.05	60.34	-1.08	3.631
4	200	350	87.07	89.49	88.28	-2.42	-1.209
6	200	185	86.41	83.42	86.41	2.99	0.001
8	100	20	76.43	74.66	76.99	1.77	-0.565
8	100	20	77.56	74.66	76.99	2.9	0.565
6	150	20	68.41	63.57	68.41	4.84	0.0002
8	200	350	87.99	84.38	87.99	3.61	0.001
4	200	350	89.49	89.491	88.28	-0.001	1.211
4	100	350	92.59	87.56	92.59	5.03	0.001

Thesis

ORIGINALITY REPORT

24%	22%	15%	15%
SIMILARITY INDEX	INTERNET SOURCES	PUBLICATIONS	STUDENT PAPERS

PRIMARY SOURCES

1	journals.scholarpublishing.org Internet Source	17%
2	qdoc.tips Internet Source	4%
3	Submitted to Curtin University of Technology Student Paper	1%
4	Zhu, Futao, Zhongmin Deng, and Junfeng Zhang. "An integrated approach for structural damage identification using wavelet neuro-fuzzy model", Expert Systems with Applications, 2013. Publication	1%
5	infoscience.epfl.ch Internet Source	1%
6	Submitted to IIT Delhi Student Paper	<1%
7	tailieu.vn Internet Source	<1%